

EBERHARD KARLS UNIVERSITÄT TÜBINGEN

THEORETICAL ASTROPHYSICS

UNIVERSITEIT UTRECHT

INSTITUTE FOR THEORETICAL PHYSICS

MASTER THESIS

Nonradial neutron star oscillations



EBERHARD KARLS
UNIVERSITÄT
TÜBINGEN



Date:

November 7, 2014

Author:

Pablo GREGORIAN

Supervisors:

Prof. Dr. Konstantinos KOKKOTAS

Dr. Tomislav PROKOPEC

Abstract

The aim of this study is to introduce a formulation of the equations of motion for nonradial neutron star oscillations originally used in the context of terrestrial global seismology. The main advantage of this formulation is that it opens the way for faster and more accurate calculations of neutron star oscillation spectra.

Using this formulation of the equations of motion, nonrelativistic and Cowling-approximated relativistic oscillation spectra for polytropic neutron stars with and without a crust are calculated. Existing results for the oscillation spectra of neutron stars are reproduced to show the validity of the equations of motion in the new formulation. New spectra for polytropic neutron star models with a crust are calculated. A comparison is made between the Cowling-approximated and exact nonrelativistic spectra of neutron star models with a crust.

It is found that the new formulation of the equations of motion is applicable to neutron star seismology in both nonrelativistic and Cowling-approximated relativistic calculations. Further, it is shown that the nonrelativistic Cowling approximation has very little effect on crustal s -modes.

Acknowledgements

Many people have helped me to stay on the right track in writing this thesis. I would like to thank Prof. Dr. Kokkotas for his invaluable guidance and advice and I would like to thank Dr. Prokopec for supervising this thesis.

During my stay at the institute for theoretical astrophysics in Tübingen, I had the privilege of discussing neutron star seismology with many fantastic astrophysicists. Many thanks to Dr. Kostas Glampedakis, Dr. Sam Lander, Patrick Dürr, Dr. Tanja Bode, Dr. Daniela Doneva, Marlene Herbrink and Pantelis Pnigouras! A very special thanks to Heike Fricke for being so exceptionally welcoming.

I have also had very helpful discussions with terrestrial seismologists. I would like to thank Dr. David Al-Attar for illuminating me on various topics in terrestrial global seismology.

Finally, I would like to thank Anne van der Meer for keeping me motivated to finish my thesis by sharing incredible amounts of coffee in the university library.

In the course of this thesis I have used many valuable sources to get a grasp of the historical and theoretical aspects of oscillations of spherical objects. For writing the historical overview of terrestrial seismology, the book on global terrestrial seismology by Dahlen and Tromp (1998) was particularly useful. I have used the lecture notes by Woodhouse (1978) to give an overview of the nonrelativistic oscillation theory in this thesis. For the analytical solution due to Love for uniform spherical models, the review article (Martinec, 1984) was of great use. Without these sources, it would have been much harder to give a comprehensive theoretical review.

The book ‘Numerical Recipes’ by Press et. al. (1992) was very helpful in the process of tackling the numerical questions encountered in this study.

Contents

1	Introduction	5
1.1	Neutron stars and neutron star oscillations	5
1.2	History of stellar and terrestrial oscillation research	6
1.2.1	Terrestrial global seismology	7
1.2.2	Stellar seismology	8
1.3	Problem statement	9
1.4	Significance of this study	10
1.5	Thesis outline	11
2	Theory	12
2.1	Dynamic equilibrium of neutron stars	12
2.1.1	The neutron star as a Fermi gas	13
2.1.2	Newtonian polytropic stellar models	16
2.1.3	Relativistic polytropic stellar models	18
2.1.4	Adiabatic approximation	24
2.1.5	Elastic properties of neutron star crust	26
2.2	Oscillation spectrum of an incompressible, uniform fluid sphere .	26
2.3	Linearized Newtonian equations of motion for linearly elastic and perfect fluid stellar models	32
2.3.1	Equations of motion in spherical coordinates	35
2.3.2	Spherical harmonic expansion of the equations of motion .	37
2.3.3	Oscillations of uniform stellar models	42
2.3.4	Symmetric formulation of the equations of motion	49
2.3.4.1	Linearly elastic stellar models	49
2.3.4.2	Perfect fluid stellar models	51
2.3.5	Boundary conditions	53
2.3.5.1	Regularity conditions at the center of the model	53
2.3.5.2	Internal boundary conditions	56
2.3.6	Boundary conditions for the free surface	57

2.4	Symmetric formulation of the equations of motion of a relativistic, perfect fluid stellar model in the Cowling approximation	58
2.5	Symmetric formulation of the equations of motion of a relativistic linearly elastic stellar model in the Cowling approximation	69
2.6	Boundary conditions for relativistic stellar oscillations	77
2.6.1	Regularity conditions at the center of the model	77
2.6.1.1	Internal boundary conditions	79
2.6.2	Boundary conditions for the free surface	79
2.7	Nondimensionalization of equations and boundary conditions	79
2.7.1	Nonrelativistic perfect fluid	80
2.7.2	Nonrelativistic perfect fluid in the Cowling approximation	81
2.7.3	Relativistic perfect fluid in the Cowling approximation	82
2.7.4	Elastic solid	83
2.7.5	Elastic solid in the Cowling approximation	84
2.7.6	Relativistic elastic solid in the Cowling approximation	85
3	Numerical methods	86
3.1	Numerical analysis of first order ordinary differential equations	87
3.1.1	Initial value problems	87
3.1.2	Boundary value problems	88
3.2	Calculation of eigenfrequencies	88
3.3	Calculation of eigenfunctions	90
4	Results	92
4.1	The equilibrium model	93
4.1.1	Solutions of the Newtonian Lane-Emden equation	94
4.1.2	Solutions of the relativistic Lane-Emden equations	96
4.2	Oscillation spectra of polytropic fluid stellar models	97
4.2.1	Benchmarks of the numerical algorithm	97
4.2.2	Oscillation spectra in Newtonian gravity	97
4.2.3	Spectra in the relativistic Cowling approximation	99
4.3	Oscillation of fluid star models with a solid crust	102
4.3.1	Benchmarks of the numerical algorithm	102
4.3.2	Oscillation spectra in Newtonian gravity	103
4.3.3	Spectra in Cowling-approximated general relativity	114
5	Discussion and conclusion	127
	Bibliography	132

A	Vector calculus	137
A.1	Identities	137
A.2	Spherical coordinates	138
B	Spherical harmonics	140
C	Solutions to some differential equations	142
D	Eulerian and Lagrangian perturbations	144
E	Gravity	146
E.1	Newtonian gravity	146
E.2	General relativity	147
E.2.1	World lines and proper time	147
E.2.2	Four-velocity	147
E.2.3	Covariant derivative	147
E.2.4	Curvature and Einstein field equations	148
E.2.5	Spherically symmetric metric	149
E.2.6	Conservation of energy-momentum	149
F	Fluid mechanics	150
F.1	Nonrelativistic fluid mechanics	150
F.1.1	Material derivative	151
F.1.2	Reynolds' transport theorem	152
F.1.3	Mass conservation and incompressibility	153
F.1.4	Alternate form of Reynolds' transport theorem	153
F.1.5	Momentum equation	154
F.2	Relativistic fluid mechanics	155
F.2.1	Law of Baryon conservation	155
F.2.2	Relativistic Euler equation	155
G	Elasticity	157
G.1	Nonrelativistic elasticity	157
G.1.1	Deformation	157
G.1.2	Deformation gradient	160
G.1.3	Strain	162
G.1.4	Stress	163
G.1.5	Momentum equation for an elastic solid	164
G.1.6	Isotropic linear elasticity	165
G.2	Relativistic elasticity	166

Chapter 1

Introduction

1.1 Neutron stars and neutron star oscillations

Neutron stars are remnants of high mass stars that collapse under their own weight due to the disappearance of radiation pressure, once nuclear fusion in the stellar core stops. If during the collapse the gravitational force on the stellar core is strong enough to overcome the electron degeneracy pressure that arises due to the Pauli exclusion principle, which does not allow two electrons (fermions) to occupy the same state, protons and electrons combine to form neutrons and neutrinos. While the neutrinos escape, neutrons are packed more closely until the density of the star is equal to the density of an atomic nucleus. Since neutrons are also fermionic particles, neutron degeneracy pressure halts further compression of the star. In case the gravitational force is even stronger than the neutron degeneracy pressure, further collapse will occur eventually and a black hole will form. Otherwise, the neutron degeneracy pressure prevents further collapse and a neutron star is formed.

Neutron stars are the tiniest and densest stars observed in the universe. The density of neutron stars is approximately 10^{17} kg/m³, the density you would get if you would squeeze the entire human race into a sugarcube. Because neutron stars are formed during a collapse, they rotate very fast due to angular momentum conservation and they have very strong magnetic fields due to conservation of magnetic flux. As a consequence, neutron stars have rotation periods of less than a second and magnetic field strengths 10^{12} times that of the Earth.

Because of their extreme nature, neutron stars are invaluable laboratories for theoretical physics. Insight in the internal structure of neutron stars would provide important new information regarding gravity, condensed matter physics, particle physics and superfluidity in extreme and unprobed circumstances.

A special type of neutron star exists with even stronger magnetic fields, but slightly longer rotation periods of about 10 seconds. This type of neutron star is called a magnetar. Starquakes on the surface of a magnetar may lead to disturbances in the magnetic field, which may be the source of strong gamma ray flare emissions that have been observed on Earth on March 5th 1979 (Mazets et. al., 1979a), August 27th 1998 (Hurley et. al., 1999) and December 27th 2004 (Hurley et. al., 2005). In the tails of these emissions, oscillations are detected (Mazets et. al., 1979b), (Israel et. al., 2005). These oscillations might be related to normal mode oscillations of neutron stars: when out of dynamical equilibrium, gravitational and thermodynamical restoring forces set up neutron star oscillations. These type of oscillations are not unique for neutron stars, but occur in our daily life: when a string is plucked, or a bell is rung, sound with a distinct pitch and characteristic overtones is produced, originating from the oscillations of the object. Similarly, neutron stars have an oscillation spectrum, which, when known in sufficient detail, comprises a very important set of data about the otherwise inaccessible internal structure of neutron stars. In the field of *asteroseismology*, this oscillation spectrum is used as input for the inverse problem of determining the internal structure and composition of stellar objects. Although this oscillation spectrum is currently only accessible only through oscillations in the tail of gamma ray flare emissions from magnetars, it is expected that in the future, oscillations will be observed in gravitational radiation induced by neutron star oscillations (Andersson and Kokkotas, 1998).

Before an inverse calculation of the internal structure of a neutron star from a given oscillation spectrum is possible, the calculation of an oscillation spectrum from a given neutron star model must be well understood. The calculation of oscillation spectra of neutron stars is, in the broadest sense, the subject of this study.

1.2 History of stellar and terrestrial oscillation research

The study of the oscillation frequencies of spherical bodies has a long history, both in the context of terrestrial and stellar seismology. Although the two fields are related, their historical development is best explained for both fields separately.

1.2.1 Terrestrial global seismology

The first steps towards the determination of a realistic oscillation spectrum for spherical bodies were taken in the context of the development of *continuum mechanics*, in the 19th century. Continuum mechanics deals with the analysis of the mechanical behaviour of continuous materials, rather than the kinematics and dynamics of discrete particles. It was Poisson (1829) who determined the frequencies of purely radial oscillations of a homogeneous, linearly elastic solid sphere, without taking into account gravitational effects. His analysis later proved to be incomplete, and only valid in a special case.

Thomson, perhaps better known as Lord Kelvin, calculated the spectrum of a homogeneous, incompressible fluid sphere (Thomson, 1863), taking into account gravitational effects. He did his calculations to challenge the view that the interior of the Earth was completely molten. Unfortunately, Lord Kelvin did not have means to measure the eigenfrequencies of the Earth, but his calculation is well worth repeating as an introduction in the study of normal mode calculation for spherical objects, since it has all characteristics of spectrum calculations for more complex spherical objects such as neutron stars, but no numerical analysis is needed: it has an analytical solution. His analysis is reformulated in section 2.2.

The first general theoretical investigation of oscillations of a compressible, linearly elastic, non-gravitating solid sphere was undertaken by Lamb (1882). He was the first to make the clear distinction between toroidal and spheroidal oscillations: two independent types of oscillation that occur in elastic spherical bodies. Surprisingly, Lamb did his analysis in Cartesian coordinates. Solving the same problem taking into account gravitation proved to be much more difficult. After incorrect, but important tries of Jeans, Rayleigh and Love, it was Love (1911) who corrected his own mistake and found the correct oscillation frequencies of a homogeneous and elastic Earth model with gravitational effects included. Although his calculation was for a homogeneous model, the equations for a radially variable model are implicit in his analysis. Love's analysis is covered in section 2.3.3.

The advent of the computer finally allowed for the calculation of oscillation spectra of realistic Earth models. The first solution for the spectrum of oscillations of an Earth model with radially variable parameters, a fluid mantle and an elastic crust was found by Alterman, Jarosch and Pekeris (1959). They were the first to write the problem in terms of coupled first order linear ordinary differential equations, making numerical integration of the differential equations realizable. The differential equations they used still form the basis of terrestrial normal mode seismology.

1.2.2 Stellar seismology

In the beginning of the 20th century, oscillations of spherical objects were studied not only in terrestrial seismology, but also in astrophysics. Stellar oscillations were studied in the context of stability of stellar configurations, the tidal distortion of binary systems and the oscillation of RR Lyrae and cepheids that are used to measure galactic and extragalactic distances. The oscillations of a heterogeneous spherical stellar model consisting of a perfect fluid were studied theoretically by Pekeris (1938). He found an analytical solution to his equations for a model with constant density. Cowling (1941) has studied the oscillation of heterogeneous stellar models assuming an unperturbed background gravitational force. This appropriately named *Cowling approximation* is still often used.

The first numerical calculations for realistic fluid stellar models were performed by Hurley, Roberts and Wright (1966) and Robe (1968). The first numerical solutions for the oscillations spectrum of realistic Newtonian neutron star models with an elastic crust were found by McDermott, Van Horn and Hansen (1988). Their calculation makes use of the Cowling approximation.

For the analysis of normal mode oscillations of stars, the Newtonian theory of gravity is usually sufficiently accurate. Due to their extreme compact nature, in neutron star seismology general relativistic effects are nonnegligible. To this end, equations of motion for the relativistic oscillations of fluid stars consisting of a perfect fluid have been derived by Thorne and Campolattaro (1967). The first numerical integration of these equations was performed by Lindblom and Detweiler (1983). Later, they found a more suitable formulation of the differential equations and improved their calculation (Detweiler and Lindblom, 1985).

It was soon discovered that the relativistic effects on the oscillations of neutron stars were not merely corrections to the Newtonian results. An entirely new category of gravitational wave (*w*-) modes emerges in the spectrum of fluid stars. Kokkotas and Schutz (1986) suggested the existence of these modes through a model problem. Their results were numerically verified by Kojima (1988) and extended and corrected by Kokkotas and Schutz (1992).

Meanwhile, the exact relativistic equations of motion for a linearly elastic solid were derived partly by Schumaker and Thorne (1983) and by Finn (1990). Schumaker and Thorne found the equations for the toroidal oscillations a relativistic neutron star crust. Finn found the equations for the spheroidal oscillations. The exact relativistic toroidal equations have been solved numerically for realistic neutron star models with a crust by Leins (1994).

The Cowling approximation can also be applied in the relativistic theory of stellar oscillations, by neglecting the perturbation in relativistic gravity. This simplifies the problem at the cost of an inconsistency in the equations, which luckily leads to qualitatively correct results. The relativistic Cowling approximation has been introduced by McDermott, Van Horn and Scholl (1983) for a fluid stellar model. Calculations for the spectrum of a neutron star model with a linearly elastic solid crust, using the relativistic Cowling approximation, were calculated for the first time by Yoshida and Lee (2002).

1.3 Problem statement

Whereas effects of rotation, magnetic fields and non-adiabaticity will be neglected in this work, one important aspect of more advanced neutron star models cannot be ignored in the context of neutron star oscillations: the presence of an elastic crust. Although the crust only represents a very small part of the neutron star mass, it is crucial for neutron star oscillations. It is likely that neutron star oscillations originate from brittle deformation of the crust. The presence of a crust also adds entirely new types of oscillations to the oscillation spectrum that are confined in the crust. Since starquakes most likely occur in the crustal part of a neutron star, these crustal modes are excited in particular.

Crustal oscillations are grouped in spheroidal and toroidal oscillations. Toroidal oscillations take place in the crust only and are characterized by motion perpendicular to the radius and are hence uninfluenced by gravitational forces. Spheroidal oscillations are further divided into radial and nonradial oscillations, of which radial oscillations involve radial movement only and nonradial oscillations are characterized by both radial and tangential motion. The nonradial oscillations, which are the topic of this study, pose the biggest challenge, since they are associated with a system of six coupled first order differential equations, whereas the radial and toroidal modes are governed by a system of two coupled differential equations.

In neutron star seismology, nonradial crustal normal modes pose a computational challenge: firstly, the oscillation spectrum contains closely and irregularly spaced eigenfrequencies. Therefore, it is difficult to know whether all eigenfrequencies in a given frequency interval have been found. Secondly, the effect of the Cowling approximation on crustal nonradial oscillations is not quantified yet. Thirdly, the current formulation of the equations of motion for an elastic neutron star crust may give rise to numerical instabilities at moderately high oscillation frequencies, since this is the case in terrestrial seismology (Gilbert and Backus, 1966).

Because the sciences of terrestrial and asteroseismology are related, advances in one field are sometimes applicable in the other. For oscillation spectrum calculations in the context of terrestrial seismology, it is known (Chapman and Woodhouse, 1981) that the equations of motion that govern small oscillations of a spherically symmetric, non-rotating, linearly elastic body can be given as a set of coupled first order differential equations:

$$\frac{d\mathbf{y}(r)}{dr} = \mathbf{A}(\omega, r)\mathbf{y}(r), \quad (1.1)$$

in which \mathbf{y} is a vector containing functions describing the perturbations of the model, r is the radial coordinate and ω is the frequency of oscillation.

The matrix \mathbf{A} contains functions dependent on ω and equilibrium model parameters and has the form of a Hamiltonian matrix:

$$\mathbf{A} = \begin{pmatrix} \mathbf{T} & \mathbf{K} \\ \mathbf{S} & -\mathbf{T}^T \end{pmatrix}, \quad (1.2)$$

where \mathbf{T} , \mathbf{K} and \mathbf{S} are matrices, and \mathbf{K} and \mathbf{S} are symmetric. Since the Hamiltonian matrices are the generators of the symplectic group, the equations are sometimes referred to as having a symplectic structure (Al-Attar and Woodhouse, 2008). Writing the equations in this particular form has a couple of advantages. Firstly, it makes the numerical algorithm more efficient, since less matrix elements need to be calculated. Secondly, Woodhouse (1988) has found a way to use the symplectic structure in the differential equations together with the ‘minors’ method, discovered by Gilbert and Backus (1966) and (1969), to determine the number of eigenfrequencies in a given frequency interval. This makes it possible to check whether all eigenfrequencies in a given frequency interval have been found, without resorting to very high resolution searches for eigenfrequencies. The ‘minors’ formulation of the differential equations uses vector cross product representations of \mathbf{y} are used as functions in the differential equations rather than \mathbf{y} itself, which has the further advantage that it is numerically stable at high frequencies, which is not the case for the equations in the original formulation in the context of terrestrial seismology.

The questions this thesis addresses are firstly whether the symmetric formulation (1.1, 1.2) of the equations of motion is applicable in neutron star oscillation theory and in particular whether the relativistic equations of motion for fluid and linearly elastic neutron star models can also be formulated in this symmetric way. Secondly, the question of how much of an effect the Cowling approximation has on crustal modes will be addressed.

1.4 Significance of this study

This study brings the fields of terrestrial and stellar seismology a little bit closer together by introducing the concept of the symplectic formulation (1.1, 1.2) of the equations of motion that was found in the context of terrestrial seismology in relativistic neutron star seismology. This enables the application of the ‘minors’ method in relativistic stellar seismology, allowing for an efficient calculation of the full oscillation spectrum of a neutron star up to high frequencies. Additionally, this study gives insight in the effect of the Cowling approximation on the spectrum of crustal neutron star oscillations.

1.5 Thesis outline

The remainder of this work starts with a theoretical review on the equations of motion and boundary conditions of Newtonian and relativistic oscillations of spherical solid and fluid bodies. The neutron star models that are used in this study are discussed in section 2.1. As an introduction to oscillations of spherical objects in general, the analytical solution for the oscillation spectrum of Lord Kelvin’s incompressible, homogenous fluid Earth model is discussed in section 2.2. A discussion of the Newtonian equations of motion and boundary conditions in the symplectic formulation (1.1, 1.2) for fluid and solid spherical models is given in section 2.3. In subsection 2.3.3 the analytical solution for a uniform model due to Love is given. In the remainder of the sections of chapter 2, the development of the symplectic formulation (1.1, 1.2) of the relativistic equations of motion and boundary conditions for fluid and solid models is given.

Chapter 3 covers the numerical methods used to solve the differential equations that govern neutron star oscillations.

Chapter 4 contains the results. Equilibrium neutron star models in equilibrium that are given in section 4.1, oscillation spectra for various Newtonian and relativistic fluid neutron star models are given in section 4.2 and section 4.3 contains the oscillation spectra for Newtonian and relativistic neutron star models with a crust.

Chapter 5 contains the discussion and conclusion.

The bibliography is included right after the conclusion. The thesis has an appendix, containing general theoretical concepts needed throughout the thesis.

Chapter 2

Theory

In this chapter a review of theory on neutron star oscillations will be given. In section 2.1 the configuration of a neutron star in nonrelativistic and relativistic dynamic equilibrium is discussed. The concept of a polytropic equation of state will be introduced and the properties of adiabatic oscillations and neutron star crusts will be reviewed. In section 2.2 the solution of Lord Kelvin (Thomson, 1863) for the oscillation spectrum of an incompressible fluid sphere will be discussed as an example. The central part of this chapter is the review on the nonrelativistic (section 2.3) and relativistic (section 2.4 - 2.6) differential equations that govern neutron star oscillations. The equations of motion and boundary conditions are worked out in spherical polar coordinates, the dynamical variables are expanded into (vector) spherical harmonics and the differential equations are presented in the formulation with symplectic structure (1.1, 1.2). In subsection 2.3.3 an analytical solution for a uniform model due to Love (1911) is given that will serve as a benchmark for the algorithm that is used to calculate oscillation spectra. The chapter is concluded in section 2.7 with the nondimensionalization of the differential equations to facilitate the implementation of numerical methods to solve them.

2.1 Dynamic equilibrium of neutron stars

The density distribution of a neutron star is a crucial part of information that is needed to calculate the oscillation spectrum of neutron stars. To find the density distribution an equation of state, which relates density ϱ and pressure P in the material, is needed for neutron star matter.

A neutron star mainly consists of neutrons. Since neutron stars are cool, the neutrons tend to occupy the lowest energy state. A neutron star is very dense, but since it consists of fermions, the Pauli exclusion principle forbids two neutrons to occupy the same quantum state. This generates a form of pressure referred to as the Fermi pressure or, in the case of neutrons, neutron degeneracy pressure, a quantum mechanical repelling 'force' between the densely packed neutrons in a neutron star.

Since the neutrons exclude each other, they can be thought of as occupying a volume with a characteristic wavelength $\lambda \sim R/N^{1/3}$ of the wave function with R the radius of the neutron star and N the total number of neutrons.

The de Broglie equation relates this characteristic wavelength to a momentum $p \sim \hbar/\lambda \sim \hbar N^{1/3}/R$, where \hbar is the reduced Planck constant. If the radius of the star shrinks, the characteristic momentum increases, which causes an increase in pressure, decelerating the collapse. Hence the existence of neutron degeneracy pressure in a neutron star allows for a situation of dynamical equilibrium.

2.1.1 The neutron star as a Fermi gas

The simplest realistic equation of state for a neutron star is obtained by assuming that neutrons form an ideal gas. In this section, expressions for the density, mean energy density and pressure will be derived for such an ideal gas.

Classically, there is no limit on the number of particles that are allowed to occupy a certain energy level. However, if a quantum mechanical gas of N neutrons with mass m in a box with volume $V = L^3$ is considered, the collective wavefunction $\psi(\mathbf{r}) = Ce^{i\mathbf{k}\cdot\mathbf{r}}$, where \mathbf{k} is the wave vector and \mathbf{r} is the position, must satisfy boundary conditions at the edge of the box.

This leads to the constraint that the wave vector \mathbf{k} is equal to $2\pi\mathbf{n}/L$, and $\mathbf{n} = (n_x, n_y, n_z)$ is a vector with integer components, labeling distinct states. Hence not all values of \mathbf{k} lead to wavefunctions that satisfy the boundary conditions. Each volume $(2\pi/L)^3$ in \mathbf{k} -space contains one allowed state.

Since the momentum $\mathbf{p} = \hbar\mathbf{k}$, the number of states of the neutron gas per unit volume $g(p)$ available between momentum p and $p + dp$ is given by:

$$g(p) dp = 2 \cdot \frac{d^3p}{(2\pi\hbar)^3} = \frac{8\pi p^2 dp}{(2\pi\hbar)^3}, \quad (2.1)$$

where the factor 2 arises because neutrons can be either spin up or down.

Since neutrons are fermions, the ideal gas is described by Fermi-Dirac statistics, with an energy distribution function $g(\epsilon)$ given by:

$$g(\epsilon) = \frac{1}{e^{(\epsilon-\mu)/kT} + 1}, \quad (2.2)$$

where ϵ is the energy of a particular state, μ is the total chemical potential, k is the Boltzmann constant and T is the absolute temperature.

To find an equation of state, i.e. a relationship between the pressure and density of the neutron gas, first an expression for the density must be found. At zero temperature, all energy levels will be filled up to a limit, which is called the Fermi energy E_F . Hence for $T \rightarrow 0$:

$$g(E) = \begin{cases} 1 & \text{if } E \leq E_F \\ 0 & \text{if } E > E_F. \end{cases} \quad (2.3)$$

This means that there is a maximum momentum $p_F = \sqrt{2mE_F}/\hbar$ that is occupied. This enables the calculation of the neutron density $\varrho(p_F)$:

$$\varrho(p_F) = m \int_0^{p_F} \frac{8\pi p^2 dp}{(2\pi\hbar)^3} = \frac{mp_F^3}{3\pi^2\hbar^3} = \frac{m^4 c^3 x^3}{3\pi^2\hbar^3}, \quad (2.4)$$

where $x = p_F/mc$ is the dimensionless Fermi momentum and c is the speed of light. To find an expression for the pressure, the mean energy density $\epsilon(p_F)$ must be calculated first, since from the expression for $\epsilon(p_F)$, the pressure P is calculated using the thermodynamic relation

$$P = - \left. \frac{\partial U}{\partial V} \right|_{T=0} = \varrho^2 \frac{\partial(\epsilon/\varrho)}{\partial \varrho}. \quad (2.5)$$

The mean energy density $\epsilon(p_F)$ is found by integrating the product of the number of states for a given momentum p with the energy corresponding to p :

$$\epsilon(p_F) = \int_0^{p_F} g(p)E(p)dp, \quad (2.6)$$

where $E(p) = \sqrt{p^2c^2 + m^2c^4}$ is the relativistic energy of a neutron.

The outcome of this integral is:

$$\epsilon(p_F) = \frac{8\pi}{(2\pi\hbar)^3} \int_0^{p_F} p^2 \sqrt{p^2 c^2 + m^2 c^4} dp \quad (2.7)$$

$$= \frac{m^4 c^5}{\pi^2 \hbar^3} \int_0^{p_F/mc} u^2 \sqrt{u^2 + 1} du \quad (2.8)$$

$$= \frac{m^4 c^5}{3\pi^2 \hbar^3} \left[x^3 \sqrt{x^2 + 1} - \int_0^x \frac{u^4}{\sqrt{u^2 + 1}} \right] \quad (2.9)$$

$$= \frac{m^4 c^5}{8\pi^2 \hbar^3} \left[(2x^3 + x) \sqrt{1 + x^2} - \operatorname{arcsinh}(x) \right]. \quad (2.10)$$

The pressure follows from equation (2.5), with the use of equations (2.4) and (2.9):

$$P(p_F) = n^2 \frac{\partial(\epsilon/n)}{\partial n} = -\epsilon + \varrho \frac{\partial \epsilon}{\partial \varrho} \quad (2.11)$$

$$= \frac{m^4 c^5}{3\pi^2 \hbar^3} \int_0^x \frac{u^4 du}{\sqrt{u^2 + 1}} \quad (2.12)$$

$$= \frac{m^4 c^5}{24\pi^2 \hbar^3} \left[(2x^3 - 3x) \sqrt{1 + x^2} + 3 \operatorname{arcsinh}(x) \right]. \quad (2.13)$$

This expression for the pressure has no simple relationship to the density ϱ . Nonetheless, it turns out that two limiting cases do. First consider the relativistic limit, i.e. $p_F \gg mc$. This limit of equation (2.12) for the pressure is:

$$P(p_F) = \frac{m^4 c^5}{3\pi^2 \hbar^3} \int_0^x u^3 du \quad (2.14)$$

$$= \frac{m^4 c^5 x^4}{12\pi^2 \hbar^3} \quad (2.15)$$

$$= K_{\text{rel}} \varrho^{4/3}, \quad (2.16)$$

where K_{rel} is a constant. In the same way, the nonrelativistic limit $p_F \ll mc$ yields:

$$P(p_F) = \frac{m^4 c^5}{3\pi^2 \hbar^3} \int_0^x u^4 du \quad (2.17)$$

$$= K_{\text{nonrel}} \varrho^{5/3}, \quad (2.18)$$

where K_{nonrel} is a constant. Expressions (2.16) and (2.18) for the relativistic and nonrelativistic limit of the identity for the pressure are examples of a polytropic equation of state, which is defined as:

$$P(\varrho) = K \varrho^{1+1/n}, \quad (2.19)$$

where P is the pressure, K is a constant, ϱ is the density and n is the polytropic index. It is referred to as a polytropic equation of state since it can accurately describe many (hence the words *poly*, meaning many in ancient Greek) different thermodynamic processes by varying the polytropic index n . Hence a relativistic neutron gas behaves like a polytrope with polytropic index $n = 3$. A nonrelativistic neutron gas behaves like a polytrope with index $n = 3/2$.

2.1.2 Newtonian polytropic stellar models

If, for simplicity, a neutron star is assumed to have a polytropic equation of state (2.19) with a fixed polytropic index, this equation of state gives enough information to find an equilibrium model where the density of the material is known as a function of the radial coordinate. To find the equilibrium model, the Poisson equation (E.2)

$$\nabla^2 \varphi_0 = 4\pi G \varrho_0, \quad (2.20)$$

and the momentum equation (F.15) with $\mathbf{v} = 0$ for a fluid at rest

$$\nabla P_0 = -\varrho_0 \nabla \varphi_0, \quad (2.21)$$

are used, where φ_0 is the Newtonian gravitational potential, G is the gravitational constant, ϱ_0 is the density and P_0 is the pressure. The subscript zero indicates that these are equilibrium model parameters. When the momentum equation (2.21) is substituted in the Poisson equation (2.20) it is found:

$$\frac{1}{r^2} \frac{d}{dr} \left(\frac{r^2}{\varrho_0} \frac{dP_0}{dr} \right) + 4\pi G \varrho_0 = 0, \quad (2.22)$$

where r is the radial distance from the center. To nondimensionalize this equation, the density ϱ_0 is parametrized with a dimensionless function ϑ , where

$$\varrho_0 = \varrho_c \vartheta^n, \quad (2.23)$$

and ϱ_c is the central density. The polytropic equation of state (2.19) then dictates that $P_0 = K \varrho_c^{1+1/n} \vartheta^{n+1}$. This yields, when substituted in equation (2.22):

$$\frac{1}{r^2} \frac{d}{dr} \left(r^2 K \varrho_c^{1/n} (n+1) \frac{d\vartheta}{dr} \right) + 4\pi G \varrho_c \vartheta^n = 0. \quad (2.24)$$

This is the *Lane-Emden equation*. By defining $\alpha^2 = (n+1)K \varrho_c^{1/n-1} / 4\pi G$ and substituting

$$r = \alpha \xi, \quad (2.25)$$

the dimensionless form of the Lane-Emden equation is obtained:

$$\frac{1}{\xi^2} \frac{d}{d\xi} \left(\xi^2 \frac{d\vartheta}{d\xi} \right) + \vartheta^n = 0. \quad (2.26)$$

The boundary conditions for the differential equation are given by

$$\vartheta(0) = 1, \quad \left. \frac{d\vartheta}{dr} \right|_{r=0} = 0, \quad (2.27)$$

which state that the density in the center is equal to the central density ϱ_c and that the derivative of the density distribution in the center is zero. The free surface is represented by the first zero of the function ϑ at $\xi = \xi_1$. Analytical solutions for the Lane-Emden equation (2.26) exist for $n = 0, 1$ and 5 . A detailed account of these analytical solutions is found in Chandrasekhar (1957). For numerical solutions available for general n , the Lane-Emden equation (2.26) is restated as a set of two coupled first order differential equations to allow for a straightforward numerical solution.

$$\frac{d\vartheta}{d\xi} = -\frac{v}{\xi^2}, \quad (2.28)$$

$$\frac{dv}{d\xi} = \vartheta^n \xi^2, \quad (2.29)$$

with boundary conditions

$$\vartheta(0) = 1, \quad v(0) = 0. \quad (2.30)$$

Assuming that the solution for ϑ has been found, all relevant model parameters follow. An identity which relates the constant K to the radius R follows from equation (2.25):

$$R = \alpha \xi_1 = \sqrt{\frac{(n+1)K}{4\pi G}} \varrho_c^{(1-n)/2n} \xi_1. \quad (2.31)$$

The mass enclosed within ξ is given by:

$$M(\xi) = \int_0^{\alpha\xi} 4\pi \varrho_0 r^2 dr = 4\pi \alpha^3 \varrho_c \int_0^\xi \xi'^2 \vartheta^n d\xi', \quad (2.32)$$

or, by using the Lane-Emden equation (2.26),

$$M(\xi) = -4\pi \alpha^3 \varrho_c \int_0^\xi \frac{d}{d\xi'} \left(\xi'^2 \frac{d\vartheta}{d\xi'} \right) d\xi', \quad (2.33)$$

which implies that

$$M(\xi) = -4\pi \alpha^3 \varrho_c \xi^2 \frac{d\vartheta}{d\xi}. \quad (2.34)$$

From equations (2.31), (2.34) and the polytropic relation (2.19) it follows:

$$P_0 = \frac{4\pi GR^2 \varrho_c^2}{(n+1)\xi_1^2} \vartheta^{(n+1)}, \quad (2.35)$$

$$g_0 = -\frac{4\pi GR \varrho_c}{\xi_1} \frac{d\vartheta}{d\xi}. \quad (2.36)$$

For a Newtonian polytrope of index n the relationship between the central density ϱ_c and the average density $\bar{\varrho}_0(\xi)$ of the matter inside ξ is given by

$$\bar{\varrho}_0 = \frac{M(\xi)}{\frac{4}{3}\pi\alpha^3\xi^3} = -\frac{3}{\xi} \left(\frac{d\vartheta}{d\xi} \right) \varrho_c, \quad (2.37)$$

or, for the average density of the whole neutron star:

$$\frac{\varrho_c}{\bar{\varrho}_0} = - \left[\frac{\xi}{3} \left(\frac{d\vartheta}{d\xi} \right)^{-1} \right]_{\xi=\xi_1}. \quad (2.38)$$

All equilibrium model parameters that are needed to calculate the nonrelativistic oscillation spectrum of polytropic neutron star models are now found. Analytical and numerical solutions for these parameters are presented in section 4.1.1.

2.1.3 Relativistic polytropic stellar models

General relativistic equations of motion for polytropic stellar models follow from the Einstein field equations (E.11)

$$R_{\alpha\beta} - \frac{1}{2}g_{\alpha\beta}R = \frac{8\pi G}{c^4}T_{\alpha\beta}, \quad (2.39)$$

which are a set of differential equations that govern the behaviour of the metric $g_{\alpha\beta}$, which defines the length of a line element. In this equation, $R_{\alpha\beta}$ is the Ricci curvature tensor (E.12)

$$R_{\alpha\beta} = \sum_{\chi} \left[\partial_{\chi} \Gamma_{\beta\alpha}^{\chi} - \partial_{\beta} \Gamma_{\chi\alpha}^{\chi} \right] + \sum_{\chi,\lambda} \left[\Gamma_{\chi\lambda}^{\chi} \Gamma_{\beta\alpha}^{\lambda} - \Gamma_{\beta\lambda}^{\chi} \Gamma_{\chi\alpha}^{\lambda} \right], \quad (2.40)$$

where $\Gamma_{\beta\gamma}^{\alpha}$ are the Christoffel symbols (E.7) determined by the metric $g_{\alpha\beta}$:

$$\Gamma_{\beta\gamma}^{\alpha} = \frac{1}{2} \sum_{\sigma} g^{\alpha\sigma} \left(\frac{\partial g_{\sigma\beta}}{\partial x^{\gamma}} + \frac{\partial g_{\sigma\gamma}}{\partial x^{\beta}} - \frac{\partial g_{\beta\gamma}}{\partial x^{\sigma}} \right), \quad (2.41)$$

R is the scalar curvature (E.13)

$$R = \sum_{\alpha,\beta} g^{\alpha\beta} R_{\alpha\beta}, \quad (2.42)$$

where $g^{\alpha\beta}$ is the inverse metric. $T_{\alpha\beta}$ is the stress-energy tensor, that describes the density and flux of energy in spacetime. It is, in the case of a neutron star, determined by the properties of the matter of which the neutron star model consists. A general relativistic polytropic model consisting of a perfect fluid, has a stress-energy tensor $T_{\alpha\beta}$ given by (F.17):

$$T_{\alpha\beta} = \left(\rho_0 + \frac{P_0}{c^2}\right) u_\alpha u_\beta - P_0 g_{\alpha\beta}. \quad (2.43)$$

Since a spherically symmetric polytropic neutron star model is assumed, the most general spherically symmetric metric (E.14) is chosen:

$$ds^2 = \sum_{\alpha,\beta} g_{\alpha\beta} dx^\alpha dx^\beta = e^{2\nu} c^2 dt^2 - e^{2\lambda} dr^2 - r^2 (d\theta^2 + \sin^2 \theta d\phi^2). \quad (2.44)$$

The Christoffel symbols (2.41) for this metric are given by:

$$\Gamma_{rt}^t = \Gamma_{tr}^t = \frac{d\nu}{dr}, \quad (2.45)$$

$$\Gamma_{tt}^r = c^2 \frac{d\nu}{dr} e^{2(\nu-\lambda)}, \quad \Gamma_{\theta\theta}^r = -r e^{-2\lambda}, \quad \Gamma_{rr}^r = \frac{d\lambda}{dr}, \quad \Gamma_{\phi\phi}^r = -r \sin^2 \theta e^{-2\lambda}, \quad (2.46)$$

$$\Gamma_{r\theta}^\theta = \Gamma_{\theta r}^\theta = \frac{1}{r}, \quad \Gamma_{\phi\phi}^\theta = -\sin \theta \cos \theta, \quad (2.47)$$

$$\Gamma_{r\phi}^\phi = \Gamma_{\phi r}^\phi = \frac{1}{r}, \quad \Gamma_{\theta\phi}^\phi = \Gamma_{\phi\theta}^\phi = \cot \theta. \quad (2.48)$$

The equations governing the equilibrium configuration now follow from the Einstein field equations (2.39). Using the expressions for the Christoffel symbols, the Einstein field equations reduce to:

$$e^{-2\lambda} \left(\frac{2}{r} \frac{d\nu}{dr} + \frac{1}{r^2} \right) - \frac{1}{r^2} = \frac{8\pi G}{c^4} P_0, \quad (2.49)$$

$$e^{-2\lambda} \left(\frac{2}{r} \frac{d\lambda}{dr} - \frac{1}{r^2} \right) + \frac{1}{r^2} = \frac{8\pi G}{c^2} \rho_0, \quad (2.50)$$

$$e^{-2\lambda} \left(\frac{d^2\nu}{dr^2} + \left(\frac{d\nu}{dr} - \frac{d\lambda}{dr} \right) \left(\frac{d\nu}{dr} + \frac{1}{r} \right) \right) = \frac{8\pi G}{c^4} P_0. \quad (2.51)$$

An additional relation is obtained by using the conservation law (E.16)

$$\sum_{\alpha} T_{\beta;\alpha}^{\alpha} = 0, \quad (2.52)$$

where a semicolon denotes the covariant derivative (E.10). This yields:

$$\frac{dP_0}{dr} + (P_0 + \varrho_0 c^2) \frac{d\nu}{dr} = 0. \quad (2.53)$$

The relativistic Lane-Emden equations are now derived from a combination of equations (2.49) – (2.51), (2.53) and the polytropic equation of state (2.19). Define the dimensionless variable u :

$$u = \frac{c^2 r}{2GM} (1 - e^{-2\lambda}). \quad (2.54)$$

This implies that

$$e^{-2\lambda} = 1 - \frac{2GMu}{c^2 r}. \quad (2.55)$$

In terms of this definition, equation (2.50) becomes:

$$M \frac{du}{dr} = 4\pi r^2 \varrho_0. \quad (2.56)$$

The total mass $M(r)$ within a sphere of radius r is given by $M(r) = Mu(r)$. Outside the star, the solution should match with the Schwarzschild metric (E.15), which is the solution of the Einstein field equations (2.39) outside a spherical mass. This implies that $u(R) = 1$.

Since a polytropic equation of state is assumed,

$$P_0 = K \varrho_0^{1+1/n} \quad (2.57)$$

where n is the polytropic index and K is a constant. Just like in the case of a Newtonian polytrope, the differential equations are nondimensionalized. Write, analogously to the Newtonian case:

$$\varrho_0 = \varrho_c \vartheta^n \quad (2.58)$$

then it follows that

$$P_0 = K \varrho_c^{1+1/n} \vartheta^{n+1}. \quad (2.59)$$

Equation (2.56) connects u and ϑ . Restating this equation in terms of the dimensionless variables u and ϑ yields:

$$M \frac{du}{dr} = 4\pi r^2 \varrho_c \vartheta^n. \quad (2.60)$$

Equation (2.53) becomes, in terms of the dimensionless parameter ϑ :

$$\frac{d\nu}{dr} + \frac{\sigma(n+1)}{1+\sigma\vartheta} \frac{d\vartheta}{dr} = 0, \quad (2.61)$$

with $\sigma = K \varrho_c^{1/n} = P_c / \varrho_c c^2$. This equation is integrated to find:

$$e^{2\nu} = e^{2\nu_c} \left(\frac{1+\sigma}{1+\sigma\vartheta} \right)^{2(n+1)}. \quad (2.62)$$

To find $e^{2\nu_c}$, the solution should match with the Schwarzschild solution (E.15) at $r = R$. This gives:

$$e^{2\nu} = (1+\sigma\vartheta)^{-2(n+1)} \left(1 - \frac{2GM}{c^2 R} \right). \quad (2.63)$$

After substituting equation (2.55) and (2.61) into equation (2.49), it becomes, in terms of σ , u and ϑ :

$$\frac{\sigma(n+1)}{1+\sigma\vartheta} r \frac{d\vartheta}{dr} \left(1 - \frac{2GMu}{c^2 r} \right) + \frac{GMu}{c^2 r} + \frac{GM}{c^2} \sigma \vartheta \frac{du}{dr} = 0. \quad (2.64)$$

The system of equations (2.60) and (2.64) is to be solved with initial conditions $\vartheta(0) = 1$ and $u(0) = 0$, which fixes the density at $r = 0$ to ϱ_c .

To put these two differential equations in dimensionless form, a change of variables is performed. Define:

$$\xi = Ar, \quad (2.65)$$

$$w(\xi) = \frac{A^3 GM}{4\pi \varrho_c c^2} u(r), \quad (2.66)$$

with A defined as

$$A = \left(\frac{4\pi \varrho_c}{(n+1)\sigma} \right)^{1/2}. \quad (2.67)$$

In terms of the new dimensionless variables, the relativistic Lane-Emden equations are found:

$$\xi^2 \frac{d\vartheta}{d\xi} \frac{1-2\sigma(n+1)w/\xi}{1+\sigma\vartheta} + w + \sigma \xi \vartheta \frac{dw}{d\xi} = 0, \quad (2.68)$$

$$\frac{dw}{d\xi} = \xi^2 \vartheta^n, \quad (2.69)$$

with boundary conditions

$$\vartheta(0) = 1, \quad w(0) = 0. \quad (2.70)$$

The free surface of the sphere is represented by the first zero ξ_1 of the function ϑ ,

$$\vartheta(\xi_1) = 0. \quad (2.71)$$

The function $w(\xi)$ is restated using (2.65) and (2.67), to find an expression for $\frac{GM}{c^2 r}$ in terms of dimensionless variables:

$$w(\xi) = \frac{Mu(r)}{4\pi\rho_c} \frac{\xi A^2}{r} = \frac{M(r)}{\sigma(n+1)} \frac{\xi}{r}. \quad (2.72)$$

When $r = R$, $\xi = \xi_1$ and $u(R) = 1$. Therefore

$$\frac{GM}{c^2 R} = \frac{\sigma(n+1)w_1}{\xi_1}, \quad (2.73)$$

when $w_1 = w(\xi_1)$. Combining equations (2.72) and (2.73), it is found that

$$\frac{M(r)}{M} = \frac{w}{w_1}. \quad (2.74)$$

From equation (2.72) it also follows that

$$w_1 = \frac{M\xi_1^3}{4\pi\rho_c R^3} = \frac{\xi_1^3 \bar{\rho}_0}{3\rho_c}, \quad (2.75)$$

where $\bar{\rho}_0$ is the average density. This identity gives the ratio between the central and average density:

$$\frac{\rho_c}{\bar{\rho}_0} = \frac{\xi_1^3}{3w_1}. \quad (2.76)$$

This allows a reformulation of equation (2.73):

$$\frac{\pi G \bar{\rho}_0 R^2}{c^2} = \frac{3 GM}{4 c^2 R} = \frac{3\sigma(n+1)w_1}{4\xi_1}. \quad (2.77)$$

The metric components $e^{2\lambda}$, given in equation (2.55) and $e^{2\nu}$ from equation (2.63) are, in terms of the dimensionless variables:

$$e^{-2\lambda} = 1 - 2\sigma(n+1)w(\xi)/\xi, \quad (2.78)$$

$$e^{2\nu} = (1 + \sigma\vartheta)^{-2(n+1)} \left(1 - \frac{2\sigma(n+1)w_1}{\xi_1} \right). \quad (2.79)$$

Using equations (2.58), (2.59) and the derivatives of equations (2.55) and (2.63) and the use of the relativistic Lane-Emden equations (2.68, 2.69), the following

relations for model parameters as a function of $x = \xi/\xi_1$, with $\vartheta = \vartheta(x)$ and $w = w(x)$ are found:

$$\frac{\varrho_0 c^2 + P_0}{\varrho_c c^2} = (1 + \sigma\vartheta) \vartheta^n, \quad (2.80)$$

$$\frac{P_0(x)}{P_c} = \vartheta^{n+1}, \quad (2.81)$$

$$\frac{1}{\sigma} \frac{d\nu}{dx} = \frac{\xi_1(n+1)(w + \sigma\xi^3\vartheta^{n+1})}{\xi^2(1 - 2\sigma(n+1)w/\xi)}, \quad (2.82)$$

$$\frac{1}{\sigma} \frac{d^2\nu}{dx^2} = \xi_1(n+1) \left\{ \frac{\vartheta^n \xi_1 (1 + 3\sigma\vartheta)}{1 - 2\sigma(n+1)w/\xi} - \right. \quad (2.83)$$

$$\left. \frac{\xi_1(w + \sigma\xi^3\vartheta^{n+1})}{\xi^2(\xi - 2\sigma(n+1)w)^2} \times \right. \quad (2.84)$$

$$\left. \times [2\xi - \sigma(n+1)(2w + \xi^3\vartheta^n(1 - \sigma\vartheta))] \right\}, \quad (2.85)$$

$$\frac{d\lambda}{dx} = \frac{\sigma(n+1)\xi_1(\xi\vartheta^n - w/\xi^2)}{1 - 2\sigma(n+1)w\xi}. \quad (2.86)$$

In the center, the initial conditions are used to calculate the limiting values of these parameters. These are:

$$\frac{\varrho_0 c^2 + P_0}{\varrho_c c^2} = 1 + \sigma, \quad (2.87)$$

$$e^{2\nu}(x) = \frac{1 - 2\sigma(n+1)w_1/\xi_1}{(1 + \sigma)^{2(n+1)}}, \quad (2.88)$$

$$yF \frac{1}{\sigma} \frac{d^2\nu}{dx^2} = \xi_1^2(n+1) \left(\frac{1}{3} + \sigma \right), \quad (2.89)$$

$$\frac{P_0(x)}{P_c} = e^{2\lambda}(x) = 1, \quad (2.90)$$

$$\frac{d\lambda}{dx} = \frac{M(r)}{M} = \frac{1}{\sigma} \frac{d\nu}{dx} = 0. \quad (2.91)$$

At the free surface, the density and pressure are zero, and $M(r)/M = 1$. The metric at the free surface is the same as the Schwarzschild metric. This gives, for $\xi \geq \xi_1$:

$$e^{2\nu} = e^{-2\lambda} = 1 - 2\sigma(n+1)w_1/\xi, \quad (2.92)$$

$$\frac{1}{\sigma} \frac{d\nu}{dx} = \frac{(n+1)w_1\xi_1}{\xi^2(1 - 2\sigma(n+1)w_1/\xi)}, \quad (2.93)$$

$$\frac{1}{\sigma} \frac{d^2 \nu}{dx^2} = \frac{2(n+1)w_1 \xi_1^2}{\xi^3 \left(1 - \frac{2(n+1)w_1 \sigma}{\xi}\right)^2} \left(\frac{\sigma(n+1)w_1}{\xi} - 1 \right), \quad (2.94)$$

$$\frac{d\lambda}{dx} = \frac{\sigma(n+1)w_1 \xi_1}{\xi^2(1 - 2\sigma(n+1)w_1/\xi)}. \quad (2.95)$$

In the nonrelativistic limit $c \rightarrow \infty$ or $\sigma \rightarrow 0$, the relativistic Lane-Emden equations (2.68) and (2.69) reduce to their Newtonian counterparts (2.28, 2.29). The relativistic Lane-Emden equations have an analytical solution for $n = 0$ due to Schwarzschild (1916). Unfortunately, no other analytical solutions to these equations have been found.

Numerical solutions were first found by Tooper (1964) and serve as a benchmark for the numerical solutions to the relativistic Lane-Emden equations used in this study. Solutions that are used in this study are presented in section 4.1.2.

2.1.4 Adiabatic approximation

In neutron stars, it is reasonable to assume adiabaticity during oscillations, since the thermal relaxation time within the star is much larger than the periods of oscillation. Put otherwise, neutron star matter has such a high heat capacity that heat exchange between parcels of the neutron star matter is small during oscillations. This means that it is reasonable to assume entropy S is conserved during an oscillation. This assumption is often called the *adiabatic approximation*. From the first law of thermodynamics, it follows that the relation between the Lagrangian pressure perturbation ΔP and a Lagrangian density perturbation $\Delta \varrho$ is related by the adiabatic index Γ_1 :

$$\frac{\varrho_0}{P_0} \frac{\Delta P}{\Delta \varrho} = \Gamma_1, \quad (2.96)$$

where the adiabatic index Γ_1 is defined as:

$$\Gamma_1 = \left(\frac{\partial(\ln P)}{\partial(\ln \varrho)} \right)_S, \quad (2.97)$$

and the Lagrangian pressure perturbation is defined in appendix D. This implies that the bulk modulus κ is given by:

$$\kappa = \varrho_0 \frac{\Delta p}{\Delta \varrho} = \Gamma_1 P_0. \quad (2.98)$$

If it is assumed that the relationship between P_0 and ϱ_0 is polytropic,

$$P_0 = K \varrho_0^{1+1/N}, \quad (2.99)$$

then it follows from definition (2.97) that Γ_1 is:

$$\Gamma_1 \equiv 1 + \frac{1}{N}, \quad (2.100)$$

in which the polytropic index N is not necessarily the same as the polytropic index n that is used for the equilibrium model, for example because neutron star matter might behave differently on the shorter timescales involved with neutron star oscillations compared to the time available for an equilibrium configuration to form.

For a relativistic adiabatic stellar model, the definition of the adiabatic index is slightly different:

$$\frac{\varrho_0 + P_0/c^2}{P_0} \frac{\Delta P}{\Delta \varrho} = \Gamma_1, \quad (2.101)$$

where the relativistic adiabatic index is defined by:

$$\Gamma_1 = \left(\frac{\varrho + P/c^2}{P} \frac{\partial P}{\partial \varrho} \right)_S. \quad (2.102)$$

The bulk modulus κ is given by

$$\kappa = n_0 \frac{\Delta P}{\Delta n}, \quad (2.103)$$

where n_0 is the equilibrium baryon number density. It will be shown in section 2.4, equation (2.388) that the relationship between Δn and $\Delta \varrho$ is given by:

$$\Delta \varrho = \frac{\Delta n}{n_0} \left(\varrho_0 + \frac{P_0}{c^2} \right). \quad (2.104)$$

This leads to the relation

$$\kappa = n_0 \frac{\Delta p}{\Delta n} = \Gamma_1 P_0. \quad (2.105)$$

If it is assumed that the relationship between P_0 and ϱ_0 is polytropic,

$$P_0 = K \varrho_0^{1+1/N}, \quad (2.106)$$

then it follows that Γ_1 is, using (2.80):

$$\Gamma_1 \equiv \left(1 + \frac{1}{N} \right) \left(1 + \frac{P_0}{\varrho_0 c^2} \right) = \left(1 + \frac{1}{N} \right) (1 + \sigma \vartheta). \quad (2.107)$$

Unlike in the Newtonian case, the adiabatic index is not a constant throughout the model for a polytropic neutron star model.

If the adiabatic oscillation is used and a fluid model is assumed, the equilibrium model is completely described through the model parameters described in the previous sections and the bulk modulus κ . In case a solid crust is assumed, an additional parameter is needed, which will be discussed in the next section.

2.1.5 Elastic properties of neutron star crust

For neutron star oscillations, the elastic behaviour of the neutron star crust is relevant, because it determines the reaction of the crust on deformations set up by the oscillations. This, in turn, has influence on the oscillation spectrum.

The main difference between an elastic material and a fluid is the fact that an elastic material can withstand shear forces. In other words: it has a nonzero shear modulus μ , whereas a fluid is characterized by $\mu = 0$. In order to model crustal oscillations correctly, a reasonable model for the shear modulus μ in a neutron star crust is needed. It is beyond the scope of this thesis to give a full account of the details of neutron star crusts. It turns out (Ogata and Ichimaru, 1990), (Haensel, Potekhin and Yakovlev, 2007) that it is a reasonable approximation to assume an isotropic crust, where the ratio between the shear modulus μ and bulk modulus κ in a neutron star crust is modeled as:

$$\frac{\mu}{\kappa} = 0.016(Z/26)^{2/3} \frac{P_e}{\gamma P}, \quad (2.108)$$

where Z is the ion number density, for which $Z \approx 40$ holds for neutron star crusts (Negele and Vautherin, 1973), P_e is the ultra-relativistic electron degeneracy pressure of the electrons in the crust, γ is the adiabatic index of the crustal matter, which is equal to $1 + \frac{1}{n}$ for a polytropic equation of state, and P is the pressure. Throughout the crust, $P \simeq P_e$ holds.

From this result, it is learned that throughout the neutron star crust $\mu \ll \kappa$. Further, it is reasonable to assume that throughout the crust, the factor $\frac{P_e}{\gamma P}$ is constant, which implies $\mu \propto \kappa$. In this study, crustal neutron star models with $\mu \propto \kappa$ will be used with various proportionality constants.

2.2 Oscillation spectrum of an incompressible, uniform fluid sphere

One of the first steps towards a determination of the spectrum of normal mode oscillations for spherical objects was made by Thomson (1863), better known as Lord Kelvin. Thomson intended to find an estimate for the frequency of the fundamental oscillatory mode of the Earth, but his theory can be used equally well to estimate the oscillation spectra of other spherical objects, such as (neutron) stars.

His calculations assume a homogeneous, incompressible and self-gravitating fluid sphere, with density ϱ_0 and radius R . The analysis of the oscillation spectrum

for this model illustrates the general features of the problem of determining the oscillation spectrum for more general spherical star models wonderfully, yet no numerical methods are needed and an elegant analytical result for the oscillation spectrum exists. Therefore it serves as a good introduction to the calculations for more complicated (yet more realistic) stellar models, that are to be discussed later.

To solve the problem, a good understanding of the equilibrium model is needed. The equations (2.20) and (2.21)

$$\nabla P_0 = -\varrho_0 \nabla \varphi_0, \quad (2.109)$$

$$\nabla^2 \varphi_0 = 4\pi G \varrho_0, \quad (2.110)$$

that relate the pressure $P_0 = P_0(r)$, density $\varrho_0 = \varrho_0(r)$ and gravitational potential $\varphi_0 = \varphi_0(r)$ have already been discussed in section 2.1.2 in the context of a polytropic neutron star model.

For constant density, it is checked by using (A.10) and (A.11) that the solutions of these equations are, for $r \leq R$:

$$\varphi_0 = \frac{2}{3}\pi G r^2 \varrho_0, \quad (2.111)$$

$$P_0 = \frac{2}{3}\pi \varrho_0^2 G (R^2 - r^2). \quad (2.112)$$

An incompressible material is characterized by expression (F.9):

$$\nabla \cdot \mathbf{v} = 0. \quad (2.113)$$

To find the oscillation spectrum for Thomson's model, the momentum equation (F.15), Poisson equation (E.2) and continuity equation (F.7)

$$\varrho \left(\frac{\partial \mathbf{v}}{\partial t} + (\mathbf{v} \cdot \nabla) \mathbf{v} \right) = -\nabla p - \varrho \nabla \varphi, \quad (2.114)$$

$$\nabla^2 \varphi = 4\pi G \varrho, \quad (2.115)$$

$$\frac{\partial \varrho}{\partial t} + \nabla \cdot (\varrho \mathbf{v}) = 0. \quad (2.116)$$

need to be solved simultaneously for a model that is out of equilibrium.

Since the oscillations are considered to be small, first order perturbation theory is used and all terms of second order or higher in the perturbations are neglected. If material particles are moved from their equilibrium position \mathbf{x}_0 by a *displacement*

$\mathbf{s}(\mathbf{x}_0, t)$ to the position $\mathbf{x}(\mathbf{x}_0, t)$:

$$\mathbf{x}(\mathbf{x}_0, t) = \mathbf{x}_0 + \mathbf{s}(\mathbf{x}_0, t), \quad (2.117)$$

the dynamical variables such as density, pressure and gravitational potential are written as a sum of their value in equilibrium and an Eulerian perturbation (D.1):

$$\varrho(\mathbf{r}, t) = \varrho_0(\mathbf{r}) + \delta\varrho(\mathbf{r}, t), \quad (2.118)$$

$$p(\mathbf{r}, t) = P_0(\mathbf{r}) + \delta p(\mathbf{r}, t), \quad (2.119)$$

$$\varphi(\mathbf{r}, t) = \varphi_0(\mathbf{r}) + \delta\varphi(\mathbf{r}, t), \quad (2.120)$$

where \mathbf{r} is a position. To simplify notation, the dependencies of the dynamical variables on position and time are understood in the remainder of this section.

First order perturbation theory is used to linearize the momentum and Poisson equation. The velocity is also considered to be a first order perturbation. Therefore the second term on the left hand side of the momentum equation is neglected. Likewise, all products of perturbations (not necessarily the same quantity), including the velocity, are neglected.

Then, by using the equation of hydrostatic equilibrium (2.109), the linearized momentum equation and linearized Poisson equation are obtained:

$$\varrho_0 \frac{\partial^2 \mathbf{s}}{\partial t^2} = -\nabla \delta p - \varrho_0 \nabla \delta \varphi - \delta \varrho \nabla \varphi_0, \quad (2.121)$$

$$\nabla^2 \delta \varphi = 4\pi G \delta \varrho. \quad (2.122)$$

The continuity equation (2.116) in integrated form expresses the density perturbation in terms of the equilibrium density ϱ_0 and the displacement \mathbf{s} :

$$\delta \varrho = -\nabla \cdot (\varrho_0 \mathbf{s}) = -\mathbf{s} \cdot \nabla \varrho_0, \quad (2.123)$$

where the last step can be made because the model is considered to be incompressible, hence (2.113) holds, which implies that $\nabla \cdot \mathbf{s} = 0$.

Since the model has constant density, yet the density jumps discontinuously from ϱ_0 to zero at $r = R$, expression (2.123) can be simplified even further:

$$\nabla \varrho_0 = -\varrho_0 \delta(r - R) \hat{r}, \quad (2.124)$$

where $\delta(r - R)$ is the Dirac delta function and \hat{r} is a unit vector in outward radial direction.

It is explained in appendix B, that (vector) spherical harmonics can be used to represent a (vector valued) function on a sphere. Since spherical harmonics are solutions to the angular part of the Laplace equation, they are greatly facilitating the solution of wavelike phenomena in systems possessing spherical symmetry in general. Therefore, at this point the best way to proceed is to expand all scalar variables in spherical harmonics and all vector variables in vector spherical harmonics. Hence, define:

$$\delta\varphi = \sum_{\ell=0}^{\infty} \sum_{m=-\ell}^{\ell} \Phi_{\ell}^m(r) Y_{\ell}^m(\theta, \phi) e^{i\omega t}, \quad (2.125)$$

$$\delta p = \sum_{\ell=0}^{\infty} \sum_{m=-\ell}^{\ell} R_{\ell}^m(r) Y_{\ell}^m(\theta, \phi) e^{i\omega t}. \quad (2.126)$$

The angular part of the functions $\delta\varphi$ and δp is expanded as a sum over spherical harmonic functions Y_{ℓ}^m with radially dependent *eigenfunctions* Φ_{ℓ}^m and R_{ℓ}^m for each pair of indices (ℓ, m) . The temporal part is expanded in modes with frequency $\omega \equiv \omega_{\ell, m}$, where the frequency can be different for different indices (ℓ, m) .

Likewise, the displacement \mathbf{s} is expanded in vector spherical harmonics:

$$\mathbf{s} = \hat{r} U + \hat{\nabla}_1 V - \hat{r} \times \hat{\nabla}_1 W, \quad (2.127)$$

where $\hat{\nabla}_1$ is the tangential derivative operator on the unit sphere:

$$\hat{\nabla}_1 = \hat{\theta} \partial_{\theta} + \hat{\phi} \csc \theta \partial_{\phi}, \quad (2.128)$$

and U, V and W are given by:

$$U = \sum_{\ell=0}^{\infty} \sum_{m=-\ell}^{\ell} U_{\ell}^m(r) Y_{\ell}^m(\theta, \phi) e^{i\omega t}, \quad (2.129)$$

$$V = \sum_{\ell=0}^{\infty} \sum_{m=-\ell}^{\ell} V_{\ell}^m(r) Y_{\ell}^m(\theta, \phi) e^{i\omega t}, \quad (2.130)$$

$$W = \sum_{\ell=0}^{\infty} \sum_{m=-\ell}^{\ell} W_{\ell}^m(r) Y_{\ell}^m(\theta, \phi) e^{i\omega t}. \quad (2.131)$$

In spherical coordinates, this leads to:

$$s_r = U, \quad (2.132)$$

$$s_{\theta} = \partial_{\theta} V + \frac{1}{\sin \theta} \partial_{\phi} W, \quad (2.133)$$

$$s_{\phi} = \frac{1}{\sin \theta} \partial_{\phi} V - \partial_{\theta} W. \quad (2.134)$$

First the case $r < R$ is considered. Note that in this case $\delta Q = 0$, hence the linearized Poisson equation (2.122) has a zero right hand side. Taking the divergence of the linearized momentum equation (2.121) and using incompressibility (2.113), two equations hold:

$$\nabla^2 \delta \varphi = 0, \quad (2.135)$$

$$\nabla^2 \delta p = 0. \quad (2.136)$$

Both equations are an example of the *Laplace equation*. Because the spherical harmonics are solutions to the angular part of this equation, only the radial part of the Laplace equation is left to be solved for each eigenfunction. This boils down to the following two equations:

$$\frac{d}{dr} \left(r^2 \frac{d\Phi_\ell^m}{dr} \right) = \ell(\ell + 1) \Phi_\ell^m, \quad (2.137)$$

$$\frac{d}{dr} \left(r^2 \frac{dR_\ell^m}{dr} \right) = \ell(\ell + 1) R_\ell^m. \quad (2.138)$$

The solution of these equations in spherical coordinates is derived in appendix C, and stated in equation (C.2). This gives:

$$\Phi_\ell^m(r) = Ar^\ell + Cr^{-\ell-1}, \quad (2.139)$$

$$R_\ell^m(r) = Br^\ell + Dr^{-\ell-1}, \quad (2.140)$$

where A , B , C and D are arbitrary real constants. Because of the regularity of the perturbations at the origin, $C = D = 0$. The constant B can be determined from the boundary condition that the pressure at the surface of the sphere is zero. Since the surface has moved because of the perturbation, the boundary condition gives, to first order:

$$\left[\delta p + s_r \frac{\partial P_0}{\partial r} \right]_{r=R} = 0. \quad (2.141)$$

The derivative of equation (2.112) for the equilibrium pressure in combination with some algebraic manipulation yields the value of the constant B :

$$B = \frac{4\pi GR \varrho_0^2 U_\ell^m(R)}{3R^{\ell-1}} \quad (2.142)$$

Now the case $r > R$ is considered. The solution for the gravitational potential perturbation is the same:

$$\Phi_\ell^m(r) = Kr^\ell + Lr^{-\ell-1}, \quad (2.143)$$

where K and L are constants. There is no pressure perturbation outside the spherical model. Now $K = 0$, because of regularity of the perturbation at infinity. To determine the remaining constants A and L , the continuity of the gravitational potential perturbation and a condition for its derivative, related to the jump in density at $r = R$, are used. Continuity of the potential gives:

$$\frac{L}{R^{\ell+1}} = AR^{\ell}, \quad (2.144)$$

hence

$$L = AR^{2\ell+1}. \quad (2.145)$$

By integrating equation (2.122) over a thin spherical shell containing the spherical surface with radius R and by using Gauss' theorem on the left hand side of the equation and integrating out the Dirac delta function on the right hand side, a constraint on the derivative of the potential is found:

$$\left. \frac{\partial \delta \varphi}{\partial r} \right|_{r \downarrow R} - \left. \frac{\partial \delta \varphi}{\partial r} \right|_{r \uparrow R} = 4\pi G \varrho_0 s_r. \quad (2.146)$$

This equation gives for A :

$$A = -\frac{4\pi G \varrho_0 U_{\ell}^m(R)}{(2\ell + 1) R^{\ell-1}}. \quad (2.147)$$

All constants are now fixed. The radial component of the linearized momentum equation (2.121) at $r = R$ gives the eigenfrequencies. By plugging in results (2.139) and (2.140) with the appropriate constants in this equation and observing that $\partial_t^2 \mathbf{s} = -\omega^2 \mathbf{s}$ it turns out that the linearized momentum equation only holds for a discrete set of frequencies, which form the oscillation spectrum of Thomson's spherical model:

$$\omega^2 = \frac{GM}{R^3} \frac{2\ell(\ell-1)}{2\ell+1}. \quad (2.148)$$

Three lessons can be learned from this result. Firstly, the eigenfrequency scales with the square root of the density. This is no coincidence and will remain to be true for the more advanced stellar models to be discussed next. Secondly, the spectrum is independent of m , which will be true for all oscillation spectra of spherically symmetric bodies. Thirdly, the large ℓ limit of this result is:

$$\omega^2 = \frac{GM\ell}{R^3}. \quad (2.149)$$

This result is also obtained for the eigenfrequencies of the model, if the perturbation of the gravitational potential is neglected in the linearized momentum equation

(2.121). This means that for higher ℓ , the gravitational potential perturbation has an increasingly weaker effect on the oscillations. The approximation in which the gravitational potential perturbation is neglected is called the *Cowling approximation*, after Thomas Cowling, who used this approximation in his paper on oscillations of polytropic stars (Cowling, 1941). This approximation is used very often in literature on neutron star oscillations since, because it simplifies the equations considerably, yet it has a relatively small influence on the solutions, especially for high ℓ . Hence it is a good way to get approximate, yet qualitatively correct results. The increasing accuracy of (2.149) for high ℓ illustrates this fact.

2.3 Linearized Newtonian equations of motion for linearly elastic and perfect fluid stellar models

In a pioneering paper, Alterman, Jarosch and Pekeris (1959) were the first to find the oscillation spectrum for small oscillations of a realistic Earth model in hydrostatic equilibrium, with an elastic crust and a core consisting of a perfect fluid, using numerical methods. Although relativistic effects are neglected, their method is useful to get a qualitative picture of the spectrum of neutron star models with an elastic crust. Therefore, a derivation of their equations and boundary conditions from first principles will be given in this section. Additionally, the equations of motion in the Cowling approximation follow as a limit of zero perturbation in the gravitational potential in the equations. The presence of a symplectic structure of the form (1.1, 1.2) in the equations of motion will also be shown.

The starting point of the most easily accessible derivation of the equations of motion is Newton's second law (G.45) for a continuous, solid medium, often called the momentum equation. It describes the change of velocity \mathbf{v} of a material particle with density ϱ , at time t , as a consequence of: 1. mechanical stress applied at the material particle boundary, described by the stress tensor \mathbf{t} , and 2. gravity, governed by the gravitational potential φ , acting on the material particle:

$$\varrho \left(\frac{\partial \mathbf{v}}{\partial t} + (\mathbf{v} \cdot \nabla) \mathbf{v} \right) = -\nabla \cdot \mathbf{t} - \varrho \nabla \varphi. \quad (2.150)$$

Along with this equation comes the notion of mass conservation in a parcel of continuous matter, which leads to the continuity equation (F.7):

$$\frac{\partial \varrho}{\partial t} + \nabla \cdot (\varrho \mathbf{v}) = 0. \quad (2.151)$$

Since the gravitational field couples to the oscillations, the Poisson equation (E.2) that governs the behaviour of the gravitational field, is needed:

$$\nabla^2 \varphi = 4\pi G \varrho. \quad (2.152)$$

The momentum equation is non-linear, but for small oscillations it is linearizable. If material particles are moved from their equilibrium position \mathbf{x}_0 by $\mathbf{s}(\mathbf{x}_0, t)$ to the position $\mathbf{x}(\mathbf{x}_0, t)$:

$$\mathbf{x}(\mathbf{x}_0, t) = \mathbf{x}_0 + \mathbf{s}(\mathbf{x}_0, t), \quad (2.153)$$

the dynamical variables are written as a sum of their value in equilibrium and an Eulerian perturbation (D.1) just like in the analysis of Lord Kelvin's model in section 2.2:

$$\mathbf{t} = \mathbf{t}_0 + \delta \mathbf{t}, \quad (2.154)$$

$$\varrho = \varrho_0 + \delta \varrho, \quad (2.155)$$

$$\varphi = \varphi_0 + \delta \varphi. \quad (2.156)$$

The equation for dynamical equilibrium, that is obtained by setting $\mathbf{v} = 0$ in equation (2.150) is:

$$\nabla \cdot \mathbf{t}_0 = -\varrho_0 \nabla \varphi_0. \quad (2.157)$$

The equation of motion (2.150) is linearized in the perturbations by plugging in (2.154) – (2.156). When equation (2.157) is used to subtract the equilibrium terms, the linearized momentum equation is found:

$$\varrho_0 \frac{\partial \mathbf{v}}{\partial t} = \varrho_0 \frac{\partial^2 \mathbf{s}}{\partial t^2} = \nabla \cdot \delta \mathbf{t} - \delta \varrho \nabla \varphi_0 - \varrho_0 \nabla \delta \varphi. \quad (2.158)$$

In the remainder of this chapter, the equations of motion for small oscillations of a linearly and isotropically elastic material will be derived. Isotropic elasticity means that the material in consideration has no preferential direction of deformation. As is given in appendix G.1.6, for small oscillations of an isotropic elastic material, the Lagrangian perturbation (D.8) of stress $\Delta \mathbf{t}$ is related to the displacement \mathbf{s} through the strain tensor \mathbf{e} :

$$\Delta \mathbf{t} = 2\mu \mathbf{e} + \left(\kappa - \frac{2\mu}{3} \right) \Theta \mathbf{I}, \quad (2.159)$$

where \mathbf{I} is the identity matrix and $\Theta \equiv \nabla \cdot \mathbf{s}$ is the dilation, which is the volume change per unit volume. This relation is the generalization of Hooke's law for a continuous, isotropic medium.

The linearized strain tensor \mathbf{e} is found by linearizing (G.39) and is given by:

$$\mathbf{e} = \frac{1}{2} (\nabla \mathbf{s} + (\nabla \mathbf{s})^T). \quad (2.160)$$

In a three dimensional isotropic medium, two parameters determine the behaviour of the material: the bulk modulus κ and shear modulus μ . The bulk modulus measures the resistance of a material against uniform compression, the shear modulus measures resistance against transverse internal forces.

To enable the use of Hooke's law (2.159), the linearized momentum equation (2.158) must be formulated in terms of the Lagrangian stress perturbation $\Delta \mathbf{t}$ instead of the Eulerian perturbation $\delta \mathbf{t}$. The relation between the Lagrangian and Eulerian stress perturbation (D.8) is given by:

$$\Delta \mathbf{t} = \delta \mathbf{t} - \mathbf{s} \cdot \nabla P_0 \mathbf{l} = \delta \mathbf{t} + \varrho_0 (\mathbf{s} \cdot \nabla \varphi_0) \mathbf{l}, \quad (2.161)$$

since the equilibrium stress of the material is hydrostatic: $\mathbf{t}_0 = -P_0 \mathbf{l}$, with \mathbf{l} the identity tensor and equation (2.20) holds for the equilibrium parameter P_0 . This leads to the following formulation of the linearized momentum equation:

$$\varrho_0 \frac{\partial^2 \mathbf{s}}{\partial t^2} = \nabla \cdot \Delta \mathbf{t} - \nabla (\varrho_0 (\mathbf{s} \cdot \nabla \varphi_0)) - \delta \varrho \nabla \varphi_0 - \varrho_0 \nabla \delta \varphi. \quad (2.162)$$

Likewise, φ and ϱ in Poisson equation (2.152) are expressed as a sum of their value in dynamical equilibrium plus a perturbation. Since the Poisson equation is already linear, this directly leads to two equations: one for the equilibrium variables ϱ_0 and $g_0 = \partial_r \varphi_0$, and one for $\delta \varrho$ and $\delta \varphi$:

$$\nabla^2 \varphi_0 = \partial_r g_0 + \frac{2}{r} g_0 = 4\pi G \varrho_0, \quad (2.163)$$

$$\nabla^2 \delta \varphi = 4\pi G \delta \varrho. \quad (2.164)$$

The time-integrated and linearized version of the continuity equation (2.151)

$$\delta \varrho = -\nabla \cdot (\varrho_0 \mathbf{s}). \quad (2.165)$$

is useful because it allows the elimination of $\delta \varrho$ from the equations of motion. Equation (2.162) is hence, in terms of \mathbf{s} , $\delta \varphi$ and equilibrium model parameters:

$$\varrho_0 \frac{\partial^2 \mathbf{s}}{\partial t^2} = \nabla \cdot \Delta \mathbf{t} - \nabla (\varrho_0 (\mathbf{s} \cdot \nabla \varphi_0)) + \nabla \cdot (\varrho_0 \mathbf{s}) \nabla \varphi_0 - \varrho_0 \nabla \delta \varphi, \quad (2.166)$$

Since ϱ_0 and φ_0 depend on r only, equation (2.166) is equivalent to:

$$\varrho_0 \left(\frac{\partial^2 \mathbf{s}}{\partial t^2} + \nabla (\mathbf{s} \cdot \nabla \varphi_0) - (\nabla \cdot \mathbf{s}) \nabla \varphi_0 + \nabla \delta \varphi \right) = \nabla \cdot \Delta \mathbf{t}. \quad (2.167)$$

With the help of equation (2.165), equation (2.164) is restated as:

$$\nabla \cdot (\nabla \delta \varphi + 4\pi G \rho_0 \mathbf{s}) = 0. \quad (2.168)$$

Equations (2.167) and (2.168) are the differential equations for small oscillations of a linearly and isotropically elastic solid. The equations for a perfect fluid are a special case of these equations. Since a perfect fluid does not have internal shear strength, it is equivalent to an isotropically elastic material with zero shear modulus. Hence by using the general formulation (2.159) as a relationship between stress and displacement, the equations for a perfect fluid model are simply derived by taking the limit $\mu \rightarrow 0$ in the resulting equations of motion for an isotropically elastic material.

In the next section, equations (2.167) and (2.168) are worked out in spherical coordinates.

2.3.1 Equations of motion in spherical coordinates

Since the neutron star models considered in this thesis all possess spherical symmetry, the set of equations (2.167, 2.168) are most straightforwardly solved in spherical coordinates r , θ and ϕ , in which r is the radial coordinate, θ is the colatitude and ϕ is the azimuthal angle. For this, all components of the equations must be worked out in spherical coordinates, starting with the divergence of the Lagrangian stress perturbation $\nabla \cdot \Delta \mathbf{t}$. To do this, first the strain tensor $\mathbf{e} = \frac{1}{2} (\nabla \mathbf{s} + (\nabla \mathbf{s})^T)$ and the dilation Θ , which is the trace of the strain tensor, are worked out in terms of the vector components of \mathbf{s} in spherical coordinates. To this end, the expression in spherical coordinates for the gradient (A.15) of a vector field, given in appendix A.2, is used to find an expression for the symmetric strain tensor \mathbf{e} :

$$\mathbf{e}_{ij} = \begin{pmatrix} e_{rr} & e_{r\theta} & e_{r\phi} \\ e_{r\theta} & e_{\theta\theta} & e_{\theta\phi} \\ e_{r\phi} & e_{\theta\phi} & e_{\phi\phi} \end{pmatrix}, \quad (2.169)$$

with the components of \mathbf{e} given by:

$$e_{rr} = \partial_r s_r, \quad (2.170)$$

$$e_{r\theta} = \frac{1}{2} \left(\partial_r s_\theta + \frac{1}{r} \partial_\theta s_r - \frac{s_\theta}{r} \right), \quad (2.171)$$

$$e_{r\phi} = \frac{1}{2} \left(\partial_r s_\phi + \frac{1}{r \sin \theta} \partial_\phi s_r - \frac{s_\phi}{r} \right), \quad (2.172)$$

$$e_{\theta\theta} = \frac{1}{r} (\partial_\theta s_\theta + s_r), \quad (2.173)$$

$$e_{\theta\phi} = \frac{1}{2r} \left(\partial_{\theta} s_{\phi} + \frac{1}{\sin\theta} \partial_{\phi} s_{\theta} - \cot\theta s_{\phi} \right), \quad (2.174)$$

$$e_{\phi\phi} = \frac{1}{r} \left(\csc\theta \partial_{\phi} s_{\phi} + s_r + \cot\theta s_{\theta} \right). \quad (2.175)$$

The dilation $\Theta \equiv \nabla \cdot \mathbf{s}$, given by the trace of the strain tensor, is:

$$\Theta = \partial_r s_r + \frac{1}{r} \left(\partial_{\theta} s_{\theta} + 2s_r + \csc\theta \partial_{\phi} s_{\phi} + \cot\theta s_{\theta} \right). \quad (2.176)$$

The Lagrangian stress perturbation, given in equation (2.159) is, restated in spherical coordinates:

$$\Delta t_{rr} = 2\mu e_{rr} + \left(\kappa - \frac{2}{3}\mu \right) \Theta, \quad \Delta t_{\theta\phi} = 2\mu e_{\theta\phi}, \quad (2.177)$$

$$\Delta t_{\theta\theta} = 2\mu e_{\theta\theta} + \left(\kappa - \frac{2}{3}\mu \right) \Theta, \quad \Delta t_{r\phi} = 2\mu e_{r\phi}, \quad (2.178)$$

$$\Delta t_{\phi\phi} = 2\mu e_{\phi\phi} + \left(\kappa - \frac{2}{3}\mu \right) \Theta, \quad \Delta t_{r\theta} = 2\mu e_{r\theta}. \quad (2.179)$$

To find out what the divergence in spherical coordinates of the Lagrangian stress perturbation is, the general expression for the divergence of a second order tensor in spherical coordinates (A.16) – (A.18) from appendix A.2 is used. Since the Lagrangian perturbation $\Delta \mathbf{t}$ of the stress tensor is symmetric, this expression is reduced to:

$$\begin{aligned} (\nabla \cdot \Delta \mathbf{t})_r &= \partial_r \Delta t_{rr} + \\ &+ \frac{1}{r} \left(\partial_{\theta} \Delta t_{r\theta} + \csc\theta \partial_{\phi} \Delta t_{r\phi} + 2\Delta t_{rr} + \cot\theta \Delta t_{r\theta} - \Delta t_{\theta\theta} - \Delta t_{\phi\phi} \right), \end{aligned} \quad (2.180)$$

$$\begin{aligned} (\nabla \cdot \Delta \mathbf{t})_{\theta} &= \partial_r \Delta t_{r\theta} + \\ &+ \frac{1}{r} \left(\partial_{\theta} \Delta t_{\theta\theta} + \csc\theta \partial_{\phi} \Delta t_{\theta\phi} + 3\Delta t_{r\theta} + \cot\theta \left(\Delta t_{\theta\theta} - \Delta t_{\phi\phi} \right) \right), \end{aligned} \quad (2.181)$$

$$\begin{aligned} (\nabla \cdot \Delta \mathbf{t})_{\phi} &= \partial_r \Delta t_{r\phi} + \\ &+ \frac{1}{r} \left(\partial_{\theta} \Delta t_{\theta\phi} + \csc\theta \partial_{\phi} \Delta t_{\phi\phi} + 3\Delta t_{r\phi} + 2\cot\theta \Delta t_{\theta\phi} \right). \end{aligned} \quad (2.182)$$

The momentum equation in spherical coordinates then becomes:

$$\begin{aligned} \varrho_0 \frac{\partial^2 s_r}{\partial t^2} &= \varrho_0 [g_0 \Theta - \partial_r \delta\varphi - \partial_r (g_0 s_r)] + \partial_r \left[\left(\kappa - \frac{2\mu}{3} \right) \Theta + 2\mu e_{rr} \right] + \\ &+ \frac{2\mu}{r} \left(\partial_{\theta} e_{\theta r} + 2e_{rr} - e_{\theta\theta} - e_{\phi\phi} + \cot\theta e_{\theta r} \right) + \frac{2\mu}{r \sin\theta} \partial_{\phi} e_{\phi r}, \end{aligned} \quad (2.183)$$

$$\begin{aligned} \varrho_0 \frac{\partial^2 s_{\theta}}{\partial t^2} &= -\frac{\varrho_0}{r} \partial_{\theta} \delta\varphi + \frac{1}{r} \partial_{\theta} \left[2\mu e_{\theta\theta} + \left(\kappa - \frac{2\mu}{3} \right) \Theta - \varrho_0 g_0 s_r \right] + \partial_r (2\mu e_{r\theta}) \\ &+ \frac{2\mu}{r} \left[\left(e_{\theta\theta} - e_{\phi\phi} \right) \cot\theta + 3e_{r\theta} \right] + \frac{2\mu}{r \sin\theta} \partial_{\phi} e_{\phi\theta}, \end{aligned} \quad (2.184)$$

$$\begin{aligned} \varrho_0 \frac{\partial^2 s_\phi}{\partial t^2} = & -\frac{\varrho_0}{r \sin \theta} \partial_\phi \delta\varphi + \frac{1}{r \sin \theta} \partial_\phi \left[2\mu e_{\phi\phi} + \left(\kappa - \frac{2\mu}{3} \right) \Theta - \varrho_0 g_0 s_r \right] + \\ & + \partial_r (2\mu e_{r\phi}) + \frac{2\mu}{r} \partial_\theta e_{\theta\phi} + \frac{2\mu}{r} (3e_{r\phi} + 2 \cot \theta e_{\theta\phi}). \end{aligned} \quad (2.185)$$

It will turn out that the spherical symmetry of the equilibrium model will allow for further simplification of the differential equations. In the next section, (vector) spherical harmonics will help to formulate the differential equations in a one-dimensional version, where the equations depend on the radial coordinate r only.

2.3.2 Spherical harmonic expansion of the equations of motion

Like in the case of Lord Kelvin's incompressible fluid stellar model, the gravitational potential perturbation $\delta\varphi$ is expanded in spherical harmonics and the displacement \mathbf{s} is expanded in vector spherical harmonics, as defined in appendix B:

$$\Phi \equiv \delta\varphi = \sum_{n=0}^{\infty} \sum_{\ell=0}^{\infty} \sum_{m=-\ell}^{\ell} {}_n\Phi_\ell^m(r) Y_\ell^m(\theta, \phi) e^{i\omega_\ell n t}, \quad (2.186)$$

$$\mathbf{s} = \hat{r}U + \hat{\nabla}_1 V - \hat{r} \times \hat{\nabla}_1 W, \quad (2.187)$$

where $\hat{\nabla}_1$ is the tangential derivative operator on the unit sphere:

$$\hat{\nabla}_1 = \hat{\theta} \partial_\theta + \hat{\phi} \csc \theta \partial_\phi, \quad (2.188)$$

and U , V and W are given by:

$$U = \sum_{n=0}^{\infty} \sum_{\ell=0}^{\infty} \sum_{m=-\ell}^{\ell} {}_nU_\ell^m(r) Y_\ell^m(\theta, \phi) e^{i\omega_\ell n t}, \quad (2.189)$$

$$V = \sum_{n=0}^{\infty} \sum_{\ell=0}^{\infty} \sum_{m=-\ell}^{\ell} {}_nV_\ell^m(r) Y_\ell^m(\theta, \phi) e^{i\omega_\ell n t}, \quad (2.190)$$

$$W = \sum_{n=0}^{\infty} \sum_{\ell=0}^{\infty} \sum_{m=-\ell}^{\ell} {}_nW_\ell^m(r) Y_\ell^m(\theta, \phi) e^{i\omega_\ell n t}. \quad (2.191)$$

In spherical coordinates, this leads to:

$$s_r = U, \quad (2.192)$$

$$s_\theta = \partial_\theta V + \frac{1}{\sin \theta} \partial_\phi W, \quad (2.193)$$

$$s_\phi = \frac{1}{\sin \theta} \partial_\phi V - \partial_\theta W. \quad (2.194)$$

The main difference with the spherical harmonic expansion used in the case of Lord Kelvin's model is the appearance of an extra index n . In the case of Lord Kelvin's model, there was only one eigenfrequency for each index ℓ . This is not in general the case, since usually there are more modes associated with a given index ℓ , of which the one with the lowest frequency is called the fundamental mode and the other modes are called overtones. The new index n labels these modes.

The eigenfrequencies $\omega_{\ell,n} \equiv {}_n\omega_{\ell}^m$ could in principle vary for different values of m , but it will turn out that this is not the case. To express the differential equations (2.183), (2.184) and (2.185) in terms of spherical harmonics, the components of the strain tensor \mathbf{e} are first represented in terms of U , V and W :

$$e_{rr} = \partial_r U, \quad (2.195)$$

$$e_{r\theta} = \frac{1}{2} \left(\partial_{\theta} \partial_r V + \csc \theta \partial_{\phi} \partial_r W + \frac{1}{r} \left[\partial_{\theta} (U - V) - \csc \theta \partial_{\phi} W \right] \right), \quad (2.196)$$

$$e_{r\phi} = \frac{1}{2} \left(\csc \theta \partial_{\phi} \partial_r V + \partial_{\theta} \partial_r W + \frac{1}{r} \left[\csc \theta \partial_{\phi} (U - V) + \partial_{\theta} W \right] \right), \quad (2.197)$$

$$e_{\theta\theta} = \frac{1}{r} \left(\partial_{\theta}^2 V - \cot \theta \csc \theta \partial_{\phi} W + \csc \theta \partial_{\phi} \partial_{\theta} W + U \right), \quad (2.198)$$

$$e_{\theta\phi} = \frac{1}{r} \left(\csc \theta \partial_{\phi} ((\partial_{\theta} - \cot \theta) V) + \frac{1}{2} \left(\csc^2 \theta \partial_{\phi}^2 + \cot \theta \partial_{\theta} - \partial_{\theta}^2 \right) W \right), \quad (2.199)$$

$$e_{\phi\phi} = \frac{1}{r} \left(\csc^2 \theta \partial_{\phi}^2 V - \csc \theta \partial_{\phi} \partial_{\theta} W + U + \cot \theta \partial_{\theta} V + \cot \theta \csc \theta \partial_{\phi} W \right). \quad (2.200)$$

Likewise, the dilation $\Theta \equiv \nabla \cdot \mathbf{s}$ is represented by:

$$\Theta = \partial_r U + \frac{1}{r} \left(\hat{\nabla}_1^2 V + 2U \right), \quad (2.201)$$

where

$$\hat{\nabla}_1^2 = \partial_{\theta}^2 + \cot \theta \partial_{\theta} + \csc^2 \theta \partial_{\phi}^2, \quad (2.202)$$

is the surface Laplacian on the unit sphere. Substitution of the expressions for the strain tensor (2.195) - (2.200) and dilation (2.201) into the equations of motion (2.183), (2.184) and (2.185) yields:

$$\begin{aligned} & -\varrho_0 \partial_t^2 U + \varrho_0 (\Theta g_0 - \partial_r \Phi - \partial_r (g_0 U)) + \partial_r \left(\left(\kappa - \frac{2}{3} \mu \right) \Theta + 2\mu \partial_r U \right) \\ & + \frac{\mu}{r^2} \left(r \hat{\nabla}_1^2 \partial_r V + \hat{\nabla}_1^2 U + 4r \partial_r U - 4U - 3\hat{\nabla}_1^2 V \right) = 0, \end{aligned} \quad (2.203)$$

$$\begin{aligned} & \hat{\nabla}_1 \left[-\varrho_0 \partial_t^2 V + \frac{1}{r} \left(\left(\kappa - 2\mu/3 \right) \Theta - \varrho_0 \Phi - \varrho_0 g_0 U \right) + \partial_r \left\{ \mu \left(\partial_r V - \frac{V-U}{r} \right) \right\} + \right. \\ & \quad \left. + \frac{\mu}{r^2} \left\{ 2\hat{\nabla}_1^2 V + 5U - V + 3r \partial_r V \right\} \right] \\ & - \hat{r} \times \hat{\nabla}_1 \left[-\varrho_0 \partial_t^2 W + \partial_r \left\{ \mu \left(\partial_r W - \frac{W}{r} \right) \right\} + \right. \\ & \quad \left. + \frac{\mu}{r^2} \left\{ \hat{\nabla}_1^2 W + 3r \partial_r W - W \right\} \right] = 0. \end{aligned} \quad (2.204)$$

Since for spherical harmonics, identity (B.4) holds:

$$\hat{\nabla}_1^2 Y_\ell^m(\theta, \phi) = -\ell(\ell + 1)Y_\ell^m(\theta, \phi), \quad (2.205)$$

it follows that equation (2.203) is a sum over spherical harmonics. Similarly, equation (2.204) is a sum over vector spherical harmonics. Because the sums are equal to zero and the (vector) spherical harmonic representation is unique, the coefficients of the sums are zero. Using $\partial_t^2 = -\omega_{\ell,n}^2$, it follows that:

$$\begin{aligned} & \partial_r \left\{ \left(\kappa - \frac{2\mu}{3} \right) {}_n\Theta_\ell^m + 2\mu \partial_r \left({}_nU_\ell^m \right) \right\} = \\ & = \varrho_0 \left(4\pi G \varrho_0 - \frac{2g_0}{r} - \omega_{\ell,n}^2 \right) {}_nU_\ell^m + \varrho_0 \left(g_0 \partial_r \left({}_nU_\ell^m \right) + \partial_r \left({}_n\Phi_\ell^m \right) - {}_n\Theta_\ell^m g_0 \right) + \\ & \quad + \frac{\mu}{r^2} \left\{ (4 + \ell(\ell + 1)) {}_nU_\ell^m - 3\ell(\ell + 1) {}_nV_\ell^m - 4r \partial_r \left({}_nU_\ell^m \right) + \right. \\ & \quad \left. + \ell(\ell + 1)r \partial_r \left({}_nV_\ell^m \right) \right\}, \quad (2.206) \end{aligned}$$

$$\begin{aligned} & \partial_r \left\{ \mu \left(\partial_r \left({}_nV_\ell^m \right) + \frac{1}{r} \left({}_nU_\ell^m - {}_nV_\ell^m \right) \right) \right\} = \\ & = \varrho_0 \left(\frac{g_0}{r} {}_nU_\ell^m + \frac{1}{r} {}_n\Phi_\ell^m - \omega_{\ell,n}^2 \left({}_nV_\ell^m \right) \right) - \frac{1}{r} \left(\kappa - \frac{2\mu}{3} \right) {}_n\Theta_\ell^m + \\ & \quad + \frac{\mu}{r^2} \left\{ {}_nV_\ell^m - 5 {}_nU_\ell^m - 3r \partial_r \left({}_nV_\ell^m \right) + 2\ell(\ell + 1) {}_nV_\ell^m \right\}, \quad (2.207) \end{aligned}$$

$$\begin{aligned} & \partial_r \left\{ \mu \left(\partial_r \left({}_nW_\ell^m \right) - \frac{{}_nW_\ell^m}{r} \right) \right\} = \\ & = -\varrho_0 \omega_{\ell,n}^2 \left({}_nW_\ell^m \right) + \frac{\mu}{r^2} \left\{ {}_nW_\ell^m - 3r \partial_r \left({}_nW_\ell^m \right) + \ell(\ell + 1) {}_nW_\ell^m \right\}, \quad (2.208) \end{aligned}$$

where the Poisson equation (2.163) for the equilibrium model parameters,

$$\partial_r g_0 + \frac{2}{r} g_0 = 4\pi G \varrho_0, \quad (2.209)$$

has been used to remove the derivative of g_0 and where

$${}_n\Theta_\ell^m = \partial_r \left({}_nU_\ell^m \right) + \frac{2}{r} \left({}_nU_\ell^m - \frac{\ell(\ell+1)}{2} {}_nV_\ell^m \right). \quad (2.210)$$

To complete the set of differential equations that govern the oscillations of the neutron star model, consider the perturbed Poisson equation (2.168):

$$\nabla \cdot (\nabla \delta\varphi + 4\pi G \varrho_0 \mathbf{s}) = 0. \quad (2.211)$$

The gradient is split up in its angular and radial part. This yields:

$$\left(\hat{r} \partial_r + \frac{1}{r} \nabla_1 \right) \cdot \left(\hat{r} \partial_r \delta\varphi + \frac{1}{r} \nabla_1 \delta\varphi + 4\pi G \varrho_0 \mathbf{s} \right) = 0. \quad (2.212)$$

Using the identity (2.201) for Θ and the identity (2.205) for the surface Laplacian the following relation between U , V and Φ is obtained:

$$\partial_r (\partial_r \Phi + 4\pi G \varrho_0 U) + \frac{2}{r} \partial_r \Phi + \frac{4\pi G \varrho_0}{r} (2U - \ell(\ell+1)V) - \frac{\ell(\ell+1)}{r^2} \Phi = 0. \quad (2.213)$$

Again, the left hand side of this equation is a sum over spherical harmonics, identical to zero. Because of uniqueness of the spherical harmonic representation, this leads to the following equation for the expansion coefficient functions:

$$\begin{aligned} \partial_r \left(\partial_r \left({}_n \Phi_\ell^m \right) + 4\pi G \varrho_0 {}_n U_\ell^m \right) + \frac{2}{r} \partial_r \left({}_n \Phi_\ell^m \right) + \\ + \frac{8\pi G \varrho_0}{r} \left({}_n U_\ell^m - \frac{\ell(\ell+1)}{2} {}_n V_\ell^m \right) - \frac{\ell(\ell+1)}{r^2} {}_n \Phi_\ell^m = 0. \end{aligned} \quad (2.214)$$

The differential equations (2.206), (2.207), (2.208) and (2.214) for the coefficients ${}_n U_\ell^m$, ${}_n V_\ell^m$, ${}_n W_\ell^m$ and ${}_n \Phi_\ell^m$ and their derivatives also contain derivatives of the equilibrium model parameters ϱ_0 , κ and μ . In the case of terrestrial seismology, the derivatives of the equilibrium model parameters are less well known than the model parameters themselves. An elegant way to get rid of the model parameter derivatives exists, which makes a succinct formulation of the boundary conditions possible as an extra bonus. This is achieved by reformulating the differential equations in terms of the traction vector $\boldsymbol{\tau}$ on radial surfaces:

$$\boldsymbol{\tau} = (\Delta T)_{rr} \hat{r} + (\Delta T)_{r\theta} \hat{\theta} + (\Delta T)_{r\phi} \hat{\phi}. \quad (2.215)$$

The traction vector is also expanded into vector spherical harmonics:

$$\boldsymbol{\tau} = \hat{r} R + \hat{\nabla}_1 S - \hat{r} \times \hat{\nabla}_1 T, \quad (2.216)$$

where R , S and T are given by:

$$R = \sum_{n=0}^{\infty} \sum_{\ell=0}^{\infty} \sum_{m=-\ell}^{\ell} {}_n R_\ell^m (r) Y_\ell^m (\theta, \phi) e^{i\omega_\ell n t}, \quad (2.217)$$

$$S = \sum_{n=0}^{\infty} \sum_{\ell=0}^{\infty} \sum_{m=-\ell}^{\ell} S_\ell^m (r) Y_\ell^m (\theta, \phi) e^{i\omega_\ell n t}, \quad (2.218)$$

$$T = \sum_{n=0}^{\infty} \sum_{\ell=0}^{\infty} \sum_{m=-\ell}^{\ell} T_\ell^m (r) Y_\ell^m (\theta, \phi) e^{i\omega_\ell n t}. \quad (2.219)$$

In spherical coordinates, this leads to:

$$\tau_r = (\Delta T)_{rr} = R, \quad (2.220)$$

$$\tau_\theta = (\Delta T)_{r\theta} = \partial_\theta S + \frac{1}{\sin\theta} \partial_\phi T, \quad (2.221)$$

$$\tau_\phi = (\Delta T)_{r\phi} = \frac{1}{\sin\theta} \partial_\phi S - \partial_\theta T. \quad (2.222)$$

It follows from the stress tensor components (2.177), (2.179) and (2.178) combined with the expressions for the strain tensor (2.195) - (2.200):

$${}_n R_\ell^m = \left(\kappa - \frac{2\mu}{3}\right) {}_n \Theta_\ell^m + 2\mu \partial_r ({}_n U_\ell^m), \quad (2.223)$$

$${}_n S_\ell^m = \mu \left(\partial_r ({}_n V_\ell^m) + \frac{1}{r} ({}_n U_\ell^m - {}_n V_\ell^m) \right), \quad (2.224)$$

$${}_n T_\ell^m = \mu \left(\partial_r ({}_n W_\ell^m) - \frac{1}{r} {}_n W_\ell^m \right). \quad (2.225)$$

For notational simplicity, the sub- and superscripts n , ℓ and m are understood for the variables ω , U , V , W , Φ , R , S and T in the remainder of this work. Hence, for example, $U \equiv {}_n U_\ell^m$. This is possible, because in the differential equations, each mode (n, l, m) is decoupled from the other modes.

To write the equations in terms of R , S and T rather than the derivatives of U , V and W , these derivatives are replaced by using equations (2.223) – (2.225):

$$\partial_r U = \left(\kappa + \frac{4\mu}{3}\right)^{-1} R + \frac{1}{r} \frac{\kappa - 2\mu/3}{\kappa + 4\mu/3} (\ell(\ell + 1)V - 2U), \quad (2.226)$$

$$\partial_r V = \frac{1}{\mu} S + \frac{1}{r} (V - U), \quad (2.227)$$

$$\partial_r W = \frac{1}{\mu} T + \frac{1}{r} W. \quad (2.228)$$

Likewise, for the derivative of Φ an auxiliary variable is introduced, of which the practical use will become clear in section 2.3.6 on the boundary conditions on the outer surface:

$$\Psi = \partial_r \Phi + (\ell + 1) \frac{\Phi}{r} + 4\pi G \varrho_0 U, \quad (2.229)$$

where $\Psi \equiv {}_n \Psi_l^m$. This gives, for the derivative of Φ :

$$\partial_r \Phi = \Psi - (\ell + 1) \frac{\Phi}{r} - 4\pi G \varrho_0 U. \quad (2.230)$$

Restating equations (2.206), (2.207), (2.208) and (2.213) in terms of the auxiliary variables R , S , T and Ψ yields:

$$\begin{aligned} \partial_r R = & \left[-\varrho_0 \omega^2 + \frac{4}{r} \left(\frac{\gamma}{r} - \varrho_0 g_0 \right) \right] U + \frac{\ell(\ell+1)}{r} \left(\varrho_0 g_0 - \frac{2\gamma}{r} \right) V \\ & - \frac{4}{r} \frac{\mu}{\kappa + 4\mu/3} R + \frac{\ell(\ell+1)}{r} S - \frac{\varrho_0(\ell+1)}{r} \Phi + \varrho_0 \Psi, \end{aligned} \quad (2.231)$$

$$\begin{aligned} \partial_r S = & \frac{1}{r} \left(\varrho_0 g_0 - \frac{2\gamma}{r} \right) U + \left\{ \frac{1}{r^2} [\ell(\ell + 1) (\gamma + \mu) - 2\mu] - \varrho_0 \omega^2 \right\} V \\ & - \frac{1}{r} \frac{\kappa - 2\mu/3}{\kappa + 4\mu/3} R - \frac{3}{r} S + \frac{\varrho_0}{r} \Phi, \end{aligned} \quad (2.232)$$

$$\partial_r T = \left(\frac{\mu}{r^2} (\ell - 1)(\ell + 2) - \varrho_0 \omega^2 \right) W - \frac{3}{r} T, \quad (2.233)$$

$$\partial_r \Psi = -4\pi G \varrho_0 \frac{\ell+1}{r} U + 4\pi G \varrho_0 \frac{\ell(\ell+1)}{r} V + \frac{\ell-1}{r} \Psi, \quad (2.234)$$

where $\gamma = 3\mu\kappa\left(\kappa + \frac{4\mu}{3}\right)^{-1}$ is introduced for notational simplicity. Equations (2.226) – (2.228), (2.230) and (2.231) – (2.234) are equivalent to the equations derived by Alterman, Jarosch and Pekeris (1959) used by them to determine the oscillation spectrum of the Earth.

Three important conclusions are drawn from these equations. Firstly, the equations for U , V and Φ are completely decoupled from the equations for W . Secondly, every component (n, ℓ, m) is completely decoupled from every other. Finally, m does not appear in the equations of motion, hence solutions are independent of m .

These three observations allow for a classification of different types of oscillation. The first type of oscillation are the *toroidal modes*, characterized by angular motion only: $U = V = \Phi = 0$. The displacement \mathbf{s} for a particular mode (n, ℓ, m) is governed by the solution for W only:

$$\mathbf{s} = -W(r) \left(\hat{\mathbf{r}} \times \hat{\mathbf{V}}_1 \right) Y_\ell^m(\theta, \phi) e^{i\omega t}. \quad (2.235)$$

The second type of oscillation are the *spheroidal modes*, characterized by $W = 0$. The displacement is now governed by the solutions for U and V :

$$\mathbf{s} = \left[U(r) \hat{\mathbf{r}} Y_\ell^m(\theta, \phi) + V(r) \hat{\mathbf{V}}_1 Y_\ell^m(\theta, \phi) \right] e^{i\omega t}. \quad (2.236)$$

For each mode with distinct (n, ℓ) there will be different eigenfunctions $U = {}_n U_\ell$, $V = {}_n V_\ell$ and $W = {}_n W_\ell$ and eigenfrequencies $\omega = \omega_{\ell, n}$. The indices n and ℓ are understood for the eigenfunctions and eigenfrequency in (2.235) and (2.236).

The next section will be on analytical solutions for the equations derived in this chapter for the special case of a uniform sphere.

2.3.3 Oscillations of uniform stellar models

The first successful calculation of the fundamental mode frequency of a homogeneous and elastic solid sphere taking into account gravitation was made by Love (1911). Love was, like Thomson, primarily interested in estimating the frequency of the fundamental mode of oscillation of the Earth. His calculations assume a homogeneous, elastic and isotropic solid sphere, with density ϱ_0 , bulk modulus κ , shear modulus μ and radius R .

If the shear modulus μ is set to zero, this model reduces to a homogeneous sphere consisting of a perfect fluid, which is a more general case of Thomson's model, since it is compressible.

Unlike Thomson's model, the spectrum of normal mode oscillations of these models cannot be put in an explicit, analytical form. However, analytical solutions for the eigenfunctions of these oscillations exist. Therefore, the solutions for Love's model are an excellent benchmark for the numerical methods that are needed for the more general case, where models with radially dependent model parameters ϱ_0 , κ and μ are analyzed.

Since the model considered by Love is uniform, all model parameters are constant. This leads to significantly more tractable equations of motion compared to the more general equations that have been derived in the previous section for radially variable models. The starting point is the linearized momentum equation for a spherically symmetric elastic object (2.167):

$$\varrho_0 \left(\frac{\partial^2 \mathbf{s}}{\partial t^2} + \nabla (\mathbf{s} \cdot \nabla \varphi_0) - (\nabla \cdot \mathbf{s}) \nabla \varphi_0 + \nabla \delta \varphi \right) = \nabla \cdot \Delta \mathbf{t}. \quad (2.237)$$

For constant model parameters, using the identities (A.3), (A.4) and (A.6), the divergence of the Lagrangian perturbation of the stress tensor $\nabla \cdot \Delta \mathbf{t}$ reduces to:

$$\nabla \cdot \Delta \mathbf{t} = \left(\kappa + \frac{4\mu}{3} \right) \nabla (\nabla \cdot \mathbf{s}) - \mu \nabla \times \nabla \times \mathbf{s}. \quad (2.238)$$

Hence, for a uniform elastic sphere, the linearized momentum equation is:

$$\begin{aligned} \varrho_0 \left(\frac{\partial^2 \mathbf{s}}{\partial t^2} + \nabla (\mathbf{s} \cdot \nabla \varphi_0) - (\nabla \cdot \mathbf{s}) \nabla \varphi_0 + \nabla \delta \varphi \right) &= \\ &= \left(\kappa + \frac{4\mu}{3} \right) \nabla (\nabla \cdot \mathbf{s}) - \mu \nabla \times \nabla \times \mathbf{s}. \end{aligned} \quad (2.239)$$

To proceed, the curl and divergence of this equation are taken. Because the curl and divergence of the displacement \mathbf{s} have convenient expressions in terms of the spherical harmonic expansion (2.187), this will lead to a straightforward solution of the equations of motion.

By taking the curl of the linearized momentum equation (2.239) and using the identities (A.1) and (A.8), the following relation is found:

$$\frac{\partial^2 (\nabla \times \mathbf{s})}{\partial t^2} + \nabla \varphi_0 \times \nabla (\nabla \cdot \mathbf{s}) = -\frac{\mu}{\varrho_0} \nabla \times \nabla \times (\nabla \times \mathbf{s}). \quad (2.240)$$

Using identities (A.2), (A.7) and definition (A.9), the divergence of equation (2.239) yields:

$$\begin{aligned} \frac{\partial^2 (\nabla \cdot \mathbf{s})}{\partial t^2} + \nabla^2 (\mathbf{s} \cdot \nabla \varphi_0) - \left((\nabla \cdot \mathbf{s}) \nabla^2 \varphi_0 + \nabla (\nabla \cdot \mathbf{s}) \cdot \nabla \varphi_0 \right) + \nabla^2 \delta \varphi &= \\ &= \frac{1}{\varrho_0} \left(\kappa + \frac{4\mu}{3} \right) \nabla^2 (\nabla \cdot \mathbf{s}). \end{aligned} \quad (2.241)$$

Using spherical harmonic expansion (2.187) for spheroidal modes (hence $W = 0$), and using identity (A.12) for the curl in spherical coordinates, $\nabla \times \mathbf{s}$ is expressed as:

$$\nabla \times \mathbf{s} = H \begin{pmatrix} 0 \\ \frac{-1}{\sin \theta} \frac{\partial}{\partial \phi} \\ \frac{\partial}{\partial \theta} \end{pmatrix} Y_\ell^m(\theta, \phi) e^{i\omega t}, \quad (2.242)$$

where

$$H = H(r) = \frac{dV}{dr} + \frac{V}{r} - \frac{U}{r}, \quad (2.243)$$

and again the indices are understood, hence $H = {}_n H_\ell^m(r)$ and $\omega = \omega_{\ell, n}$. Similarly, by using identity (A.13) for the divergence in spherical coordinates, $\nabla \cdot \mathbf{s}$ is found:

$$\nabla \cdot \mathbf{s} = X Y_\ell^m(\theta, \phi) e^{i\omega t}, \quad (2.244)$$

where

$$X = X(r) = \frac{dU}{dr} + \frac{2U}{r} - \frac{\ell(\ell+1)V}{r}. \quad (2.245)$$

Equations (2.240) and (2.241) for the curl and divergence of \mathbf{s} are now worked out in terms of H and X . A convenient expression for the right hand side of the differential equation (2.240) for the curl of \mathbf{s} exists. Using identities (A.4), (A.14), (A.13) and (A.10) on (2.242), it follows:

$$\nabla \times \nabla \times (\nabla \times \mathbf{s}) = -\mathcal{L}^2 (\nabla \times \mathbf{s}), \quad (2.246)$$

where

$$\mathcal{L}^2 = \frac{d^2}{dr^2} + \frac{2}{r} \frac{d}{dr} - \frac{\ell(\ell+1)}{r^2}. \quad (2.247)$$

The second term, $\nabla \varphi_0 \times \nabla (\nabla \cdot \mathbf{s})$, on the left hand side of the differential equation (2.240) also has an expression in terms of $\nabla \times \mathbf{s}$. Using expression (A.10), it is found:

$$\nabla \varphi_0 \times \nabla (\nabla \cdot \mathbf{s}) = \frac{\gamma X}{H} (\nabla \times \mathbf{s}), \quad (2.248)$$

where $\gamma = \frac{4}{3}\pi G \varrho_0$ follows from expression (2.111) for φ_0 for a uniform sphere.

Using the two convenient expressions (2.246) and (2.248) in equation (2.240) for the curl of \mathbf{s} yields, using $\partial_t^2 H = -\omega^2 H$:

$$\frac{\mu}{\varrho_0} \mathcal{L}^2 H + \omega^2 H = \gamma X. \quad (2.249)$$

Now equation (2.241) for the divergence of \mathbf{s} is worked out. By using the identities (A.5), (A.13), (A.7) and (A.14), applying identity (B.4) for the surface Laplacian of $Y_\ell^m(\theta, \phi)$, and by using the expressions (2.243), (2.245) for H and X and the corresponding expression for $\frac{dX}{dr}$, the second term of the left hand side of equation (2.241) reduces to:

$$\nabla^2 (\mathbf{s} \cdot \nabla \varphi_0) = \gamma \left(2X + r \frac{dX}{dr} + \ell(\ell + 1)H \right) Y_\ell^m(\theta, \phi) e^{i\omega t}. \quad (2.250)$$

By using the Poisson equations (2.163) and (2.164) for dynamical equilibrium and perturbations respectively, using expression (2.111) for φ_0 for a uniform sphere again and by observing that

$$\nabla^2 (\nabla \cdot \mathbf{s}) = \mathcal{L}^2 (\nabla \cdot \mathbf{s}), \quad (2.251)$$

it follows that

$$\frac{1}{\varrho_0} \left(\kappa + \frac{4\mu}{3} \right) \mathcal{L}^2 X + (\omega^2 + 4\gamma) X = \gamma \ell(\ell + 1)H. \quad (2.252)$$

A differential equation for X is derived by applying the operator $(\mu/\varrho_0) \mathcal{L}^2 + \omega^2$ to equation (2.252) and by then using equation (2.249). This leads to:

$$\left(\frac{\mu}{\varrho_0} \mathcal{L}^2 + \omega^2 \right) \left[\frac{1}{\varrho_0} \left(\kappa + \frac{4\mu}{3} \right) \mathcal{L}^2 X + (\omega^2 + 4\gamma) X \right] = \gamma^2 \ell(\ell + 1)X. \quad (2.253)$$

It turns out that a similar equation also holds for H . This is seen by applying the operator $\left[\left(\kappa + \frac{4}{3}\mu \right) / \varrho_0 \right] \mathcal{L}^2 + \omega^2 + 4\gamma$ to equation (2.249). Then, equation (2.252) is used to obtain:

$$\left(\frac{\mu}{\varrho_0} \mathcal{L}^2 + \omega^2 \right) \left[\frac{1}{\varrho_0} \left(\kappa + \frac{4\mu}{3} \right) \mathcal{L}^2 H + (\omega^2 + 4\gamma) H \right] = \gamma^2 \ell(\ell + 1)H. \quad (2.254)$$

Equation (2.253) can be put in a more tractable form:

$$(\mathcal{L}^2 + k_1^2) (\mathcal{L}^2 + k_2^2) X = 0, \quad (2.255)$$

where, using the sound and shear wave velocities $\alpha^2 = \left(\kappa + \frac{4\mu}{3} \right) / \varrho_0$ and $\beta^2 = \mu / \varrho_0$, k_1 and k_2 are given by:

$$k_{1,2}^2 = \frac{1}{2} \left\{ \frac{\omega^2 + 4\gamma}{\alpha^2} + \frac{\omega^2}{\beta^2} \pm \sqrt{\left(\frac{\omega^2 + 4\gamma}{\alpha^2} - \frac{\omega^2}{\beta^2} \right)^2 + \frac{4\ell(\ell + 1)\gamma^2}{\alpha^2 \beta^2}} \right\}. \quad (2.256)$$

The general solution of equation (2.255) is found by taking a linear combination of the solutions (C.10) denoted by $f_\ell(kr)$ of the spherical Bessel equation

$$\left(\mathcal{L}^2 + k^2\right) f_\ell(kr) = 0, \quad (2.257)$$

as discussed in appendix C and given in equation (C.16). Hence:

$$X = A_1 f_\ell(k_1 r) + A_2 f_\ell(k_2 r), \quad (2.258)$$

where A_1 and A_2 are constants. From equation (2.249), it directly follows from equation (2.257) for $k = k_1$ and $k = k_2$, that

$$H = -\frac{A_1}{q_1} f_\ell(k_1 r) - \frac{A_2}{q_2} f_\ell(k_2 r), \quad (2.259)$$

where

$$q_{1,2} = \frac{1}{\gamma} \left(\beta^2 k_{1,2}^2 - \omega_n^2 \right). \quad (2.260)$$

The definitions of H and X , given in equations (2.243) and (2.245), are used to obtain two first order differential equations for U and V :

$$\frac{dU}{dr} + \frac{2U}{r} - \frac{\ell(\ell+1)V}{r} = A_1 f_\ell(k_1 r) + A_2 f_\ell(k_2 r), \quad (2.261)$$

$$\frac{dV}{dr} + \frac{V}{r} - \frac{U}{r} = -\frac{A_1}{q_1} f_\ell(k_1 r) - \frac{A_2}{q_2} f_\ell(k_2 r) \quad (2.262)$$

The solution of these differential equations will be presented as a linear combination of three different solutions. The homogeneous solution to the equations above is one of them. The other two solutions are found by seeking a particular solution using the method of variation of parameters.

First consider the homogeneous solution $U^{(1)}$, $V^{(1)}$ to the set of homogeneous differential equations, which is obtained by setting the right hand side of equations (2.261) and (2.262) to zero. These are the oscillations where $X = H = 0$ and hence for which $\nabla \cdot \mathbf{s} = 0$ and $\nabla \times \mathbf{s} = 0$. The homogeneous solution is obtained by substituting $r = e^t$ and by working out the resulting system of coupled differential equations:

$$\frac{d}{dt} \begin{bmatrix} U^{(1)} \\ V^{(1)} \end{bmatrix} = \begin{bmatrix} -2 & \ell(\ell+1) \\ 1 & -1 \end{bmatrix} \begin{bmatrix} U^{(1)} \\ V^{(1)} \end{bmatrix}. \quad (2.263)$$

The characteristic equation $(2 + \lambda)(1 + \lambda) = \ell(\ell + 1)$ for the eigenvalues λ of this system leads to the solutions

$$U^{(1)}(r) = B_1 \ell r^{\ell-1} + B_2 (\ell + 1) r^{-\ell-2}, \quad (2.264)$$

$$V^{(1)}(r) = B_1 r^{\ell-1} - B_2 r^{-\ell-2}. \quad (2.265)$$

The other two solutions are found by setting *one* of the constants $\{A_1, A_2\}$ to zero in equations (2.258) and (2.259). This will lead to two solutions: one for the choice $\{A_1 = A, A_2 = 0\}$ and one for $\{A_1 = 0, A_2 = A\}$ by using the method of variation of constants.

The method of variation of constants works by making the constants $B_1 = B_1(r)$, $B_2 = B_2(r)$ dependent on r . A particular solution is then obtained by using the recurrent formulae (C.11) – (C.14) that hold for f_ℓ . To simplify notation further, k and q will represent k_1, k_2 and q_1, q_2 . This leads to the solutions

$$U^{(2,3)} = \ell hr^{-1} f_\ell(kr) - qk f_{\ell+1}(kr), \quad (2.266)$$

$$V^{(2,3)} = hr^{-1} f_\ell(kr) + k f_{\ell+1}(kr), \quad (2.267)$$

where

$$h = q - (\ell + 1). \quad (2.268)$$

By plugging this solution into definition (2.245) for X and by applying the recurrent formulae (C.11) – (C.14), it follows that

$$X^{(2,3)} = -k^2 q f_\ell(kr). \quad (2.269)$$

Now the homogeneous part $\Phi^{(1)}$ of the solution for Φ is determined from the angular part of equation (2.240). Since for the homogeneous solution, $\nabla \cdot \mathbf{s} = 0$ and $\nabla \times \mathbf{s} = 0$, this leads to:

$$\Phi^{(1)} = \omega^2 V^{(1)} r - \gamma U^{(1)} r. \quad (2.270)$$

Using the homogeneous solutions (2.264) and (2.265), it now follows that

$$\Phi^{(1)} = B_1 (\omega^2 - \ell\gamma) r^\ell - B_2 (\omega^2 + (\ell + 1)\gamma) r^{-\ell-1}. \quad (2.271)$$

The inhomogeneous part $\Phi^{(2,3)}$ is most easily found by considering the perturbed Poisson equation (2.168) for constant density:

$$\mathcal{L}^2 \Phi^{(2,3)} = -3\gamma X^{(2,3)}. \quad (2.272)$$

By assuming $\Phi^{(2,3)} = CX^{(2,3)}$ in equation (2.272), with C a constant, a solution is found:

$$\mathcal{L}^2 X^{(2,3)} + \frac{3\gamma}{C} X^{(2,3)} = 0. \quad (2.273)$$

Since $X^{(2,3)}$ obeys the spherical Bessel equation, it follows that $k^2 = \frac{3\gamma}{C}$, and:

$$\Phi^{(2,3)} = -3\gamma q f_\ell(kr). \quad (2.274)$$

Now all three solutions for U , V and Φ are found. The corresponding solutions for R , S and T are found by applying definitions (2.223), (2.225) and (2.229).

At this stage it is convenient to introduce the condition that the solution must be regular at the origin. This implies that $B_2 = 0$ and that f_ℓ reduces to the spherical Bessel function of the first kind j_ℓ , as defined in equation (C.7), which is the only solution to the spherical Bessel equation that is regular at the origin.

It follows that the most general solution of the problem that satisfies the regularity conditions at the origin, is given by a linear combination of the following three solutions:

$$U^{(1)} = \ell r^{\ell-1}, \quad (2.275)$$

$$V^{(1)} = r^{\ell-1}, \quad (2.276)$$

$$\Phi^{(1)} = (\omega^2 - \ell\gamma)r^\ell, \quad (2.277)$$

$$R^{(1)} = 2\mu\ell(\ell-1)r^{\ell-2}, \quad (2.278)$$

$$S^{(1)} = 2\mu(\ell-1)r^{\ell-2}, \quad (2.279)$$

$$\Psi^{(1)} = \left[(2\ell+1)\omega^2 - 2\ell(\ell-1)\gamma \right] r^{\ell-1}, \quad (2.280)$$

$$U^{(2,3)} = \ell hr^{-1} f_\ell(kr) - qk j_{\ell+1}(kr), \quad (2.281)$$

$$V^{(2,3)} = hr^{-1} f_\ell(kr) + k j_{\ell+1}(kr), \quad (2.282)$$

$$\Phi^{(2,3)} = -3\gamma q j_\ell(kr), \quad (2.283)$$

$$R^{(2,3)} = \left[2\mu\ell(\ell-1)hr^{-2} - \left(\kappa + \frac{4\mu}{3} \right) qk^2 \right] j_\ell(kr) + 2\mu(2q + l(l+1))kr^{-1}j_{\ell+1}(kr), \quad (2.284)$$

$$S^{(2,3)} = -2\mu(q+1)kr^{-1}j_{\ell+1}(kr) + \mu \left[k^2 + 2(l-1)hr^{-2} \right] j_\ell(kr) \quad (2.285)$$

$$\Psi^{(2,3)} = -3\gamma r^{-1} [l(l+1) + (l+1)q] j_\ell(kr), \quad (2.286)$$

where the solution with superscript (2, 3) represents two solutions since two values for k exist: $k = k_1, k_2$.

As will be explained in more detail in section 2.3.6, the eigenfrequencies of oscillation are found by demanding that boundary conditions $R = S = \Psi = 0$ hold at the outer radius of the model. As will be explained in 3.2, it follows that the

determinant function

$$D(\omega) = \begin{vmatrix} R^{(1)} & R^{(2)} & R^{(3)} \\ S^{(1)} & S^{(2)} & S^{(3)} \\ \Psi^{(1)} & \Psi^{(2)} & \Psi^{(3)} \end{vmatrix}, \quad (2.287)$$

must be zero at the free surface. If $\mu = 0$, one of solutions represented by (2.281) – (2.286) vanishes and the two remaining solutions have

$$k^2 = \frac{1}{\alpha^2} \left[\omega_n^2 + 4\gamma - \frac{\ell(\ell+1)\gamma^2}{\omega_n^2} \right], \quad q = -\omega_n^2/\gamma, \quad h = q - (\ell + 1). \quad (2.288)$$

The eigenfrequencies for the uniform, perfect fluid sphere are found by seeking the roots of the determinant function

$$D(\omega) = \begin{vmatrix} R^{(1)} & R^{(2)} \\ \Psi^{(1)} & \Psi^{(2)} \end{vmatrix}, \quad (2.289)$$

at the edge of the sphere. The analytical solutions now obtained for the oscillations of a uniform sphere are very important results, since they allow for a check of the algorithms used to find solutions to radially variable models. However, to be able to determine oscillation spectra numerically, the differential equations for oscillations of radially variable models must first be put in a form that is suitable for numerical integration. A first step toward this goal is taken in the next section, where the differential equations for radially variable models will be put in the form (1.1, 1.2) with symplectic structure.

2.3.4 Symmetric formulation of the equations of motion

It turns out that the equations of motion for neutron star oscillations derived in section 2.3.2 have additional symmetry, if a smart choice of variables is made. In this section, the equations with additional symmetry for spheroidal modes of a linearly elastic model will be derived first. The equations for a perfect fluid follow from the equations for a linearly elastic solid in the limit $\mu \rightarrow 0$. The equations of motion in the Cowling approximation are obtained by taking the limit of zero gravitational potential perturbation: $\Phi \rightarrow 0$ and consequently $\Psi \rightarrow 4\pi G \varrho_0 U$.

2.3.4.1 Linearly elastic stellar models

Consider the equations (2.226) – (2.227), (2.230) – (2.232) and (2.234) that govern the spheroidal oscillations of a linearly elastic model. These equations together

form a set of six linear coupled ordinary differential equations. This type of differential equations can be represented in matrix form in the following way:

$$\frac{d\mathbf{y}}{dr} = \mathbf{A}\mathbf{y}, \quad (2.290)$$

with \mathbf{y} a vector containing representations of the unknown functions U, V, Φ, R, S and Ψ and \mathbf{A} a 6×6 matrix containing model parameter functions. Generally, the matrix \mathbf{A} has 36 different components, but if a smart choice for \mathbf{y} is made, \mathbf{A} will become more symmetric, reducing its independent nonzero components to 14.

If for \mathbf{y} the vector

$$\mathbf{y} = \begin{pmatrix} rU \\ rV \sqrt{\ell(\ell+1)} \\ r\Phi_1 \\ rR \\ rS \sqrt{\ell(\ell+1)} \\ r\Psi_1/4\pi G \end{pmatrix}, \quad (2.291)$$

is chosen, the matrix \mathbf{A} takes the following form:

$$\mathbf{A} = \begin{pmatrix} \mathbf{T} & \mathbf{K} \\ \mathbf{S} & -\mathbf{T}^T \end{pmatrix}, \quad (2.292)$$

where \mathbf{T} , \mathbf{K} and \mathbf{S} are 3×3 matrices given by

$$\mathbf{T} = \begin{pmatrix} \frac{1}{r} \frac{8\mu-3\kappa}{3\kappa+4\mu} & \frac{\sqrt{\ell(\ell+1)}}{r} \frac{3\kappa-2\mu}{3\kappa+4\mu} & 0 \\ -\frac{\sqrt{\ell(\ell+1)}}{r} & \frac{2}{r} & 0 \\ -4\pi G \varrho_0 & 0 & -\frac{\ell}{r} \end{pmatrix}, \quad (2.293)$$

$$\mathbf{K} = \begin{pmatrix} \left(\kappa + \frac{4\mu}{3}\right)^{-1} & 0 & 0 \\ 0 & \mu^{-1} & 0 \\ 0 & 0 & 4\pi G \end{pmatrix}, \quad (2.294)$$

$$\mathbf{S} = \begin{pmatrix} \frac{4}{r^2} \gamma - \frac{4\varrho_0 g_0}{r} - \varrho_0 \omega^2 & S_{21} & S_{31} \\ \frac{\sqrt{\ell(\ell+1)}}{r^2} (\varrho_0 g_0 r - 2\gamma) & \frac{\ell(\ell+1)}{r^2} (\gamma + \mu) - \frac{2\mu}{r^2} - \varrho_0 \omega^2 & S_{32} \\ -\frac{\varrho_0(\ell+1)}{r} & \frac{\varrho_0 \sqrt{\ell(\ell+1)}}{r} & 0 \end{pmatrix}, \quad (2.295)$$

and \mathbf{S} is symmetric. Hence the equations are reduced to a form which contains the symplectic structure (1.1, 1.2) mentioned in the introduction. To obtain the

same type of equations for the case where the Cowling approximation is applied, let $\Phi \rightarrow 0$ and consequently $\Psi \rightarrow 4\pi G \varrho_0 U$. This leads to the equations:

$$\frac{d\mathbf{y}}{dr} = \mathbf{A}\mathbf{y}, \quad (2.296)$$

with

$$\mathbf{y} = \begin{pmatrix} y_1 \\ y_2 \\ y_4 \\ y_5 \end{pmatrix} = \begin{pmatrix} rU \\ rV \sqrt{\ell(\ell+1)} \\ rR \\ rS \sqrt{\ell(\ell+1)} \end{pmatrix}, \quad (2.297)$$

and

$$\mathbf{A} = \begin{pmatrix} \mathbf{T} & \mathbf{K} \\ \mathbf{S} & -\mathbf{T}^T \end{pmatrix}, \quad (2.298)$$

where \mathbf{T} , \mathbf{K} and \mathbf{S} are matrices given by

$$\mathbf{T} = \begin{pmatrix} \frac{1}{r} \frac{8\mu-3\kappa}{4\mu+3\kappa} & \frac{\sqrt{\ell(\ell+1)}}{r} \frac{3\kappa-2\mu}{3\kappa+4\mu} \\ -\frac{\sqrt{\ell(\ell+1)}}{r} & \frac{2}{r} \end{pmatrix}, \quad (2.299)$$

$$\mathbf{K} = \begin{pmatrix} \left(\kappa + \frac{4\mu}{3}\right)^{-1} & 0 \\ 0 & \mu^{-1} \end{pmatrix}, \quad (2.300)$$

$$\mathbf{S} = \begin{pmatrix} \frac{4(\gamma-\varrho_0 g_0 r)}{r^2} - \varrho_0 \omega^2 + 4\pi G \varrho_0^2 & S_{21} \\ \frac{\sqrt{\ell(\ell+1)}}{r^2} (\varrho_0 g_0 r - 2\gamma) & \frac{\ell(\ell+1)(\gamma+\mu)-2\mu}{r^2} - \varrho_0 \omega^2 \end{pmatrix}. \quad (2.301)$$

Hence the Cowling approximation does not have an effect on the symmetry that is present in the equations.

2.3.4.2 Perfect fluid stellar models

To find the differential equations that govern the oscillations of a perfect fluid, the limit $\mu \rightarrow 0$ has to be taken in equation (2.290). Then, it follows from equation (2.232) that:

$$V = \frac{g_0}{\omega^2 r} U + \frac{1}{\omega^2 r} \Phi - \frac{1}{\varrho_0 \omega^2 r} R. \quad (2.302)$$

This equation is used in the remaining four differential equations (2.226), (2.230), (2.231) and (2.234) to eliminate V . The resulting equations are written in the form:

$$\frac{d\mathbf{y}}{dr} = \mathbf{A}\mathbf{y}, \quad (2.303)$$

with

$$\mathbf{y} = \begin{pmatrix} y_1 \\ y_3 \\ y_4 \\ y_6 \end{pmatrix} = \begin{pmatrix} rU \\ r\Phi \\ rR \\ r\Psi/4\pi G \end{pmatrix}, \quad (2.304)$$

and

$$\mathbf{A} = \begin{pmatrix} \mathbf{T} & \mathbf{K} \\ \mathbf{S} & -\mathbf{T}^T \end{pmatrix}, \quad (2.305)$$

where \mathbf{T} , \mathbf{K} and \mathbf{S} are matrices given by

$$\mathbf{T} = \begin{pmatrix} \frac{\ell(\ell+1)g_0}{\omega^2 r^2} - \frac{1}{r} & \frac{\ell(\ell+1)}{\omega^2 r^2} \\ -4\pi G \varrho_0 & -l/r \end{pmatrix}, \quad (2.306)$$

$$\mathbf{K} = \begin{pmatrix} \frac{1}{\kappa} - \frac{\ell(\ell+1)}{\varrho_0 \omega^2 r^2} & 0 \\ 0 & 4\pi G \end{pmatrix}, \quad (2.307)$$

$$\mathbf{S} = \varrho_0 \begin{pmatrix} \frac{\ell(\ell+1)g_0^2}{\omega^2 r^2} - \omega^2 - \frac{4g_0}{r} & S_{21} \\ \frac{\ell(\ell+1)g_0}{\omega^2 r^2} - \frac{\ell+1}{r} & \frac{\ell(\ell+1)}{\omega^2 r^2} \end{pmatrix}, \quad (2.308)$$

and \mathbf{S} is symmetric.

In case the Cowling approximation is used, the number of equations in the set of coupled differential equations governing the oscillations, is reduced to two because $\Phi \rightarrow 0$ and $\Psi \rightarrow 4\pi G \varrho_0 U$. The nondimensionalized differential equations are:

$$\frac{d\mathbf{y}}{dr} = \mathbf{A}\mathbf{y}, \quad (2.309)$$

where the vector \mathbf{y} is given by:

$$\mathbf{y} = \begin{pmatrix} y_1 \\ y_4 \end{pmatrix} = \begin{pmatrix} rU \\ rR \end{pmatrix}, \quad (2.310)$$

and

$$\mathbf{A} = \begin{pmatrix} T & K \\ S & -T \end{pmatrix}, \quad (2.311)$$

where

$$T = \frac{\ell(\ell+1)g_0}{\omega^2 r^2} - \frac{1}{r}, \quad (2.312)$$

$$K = \frac{1}{\kappa} - \frac{\ell(\ell+1)}{\varrho_0 \omega^2 r^2}, \quad (2.313)$$

$$S = \varrho_0 \left(\frac{\ell(\ell+1)g_0^2}{\omega^2 r^2} - \omega^2 - \frac{4g_0}{r} + 4\varrho_0 \right). \quad (2.314)$$

Again, the Cowling approximation does not affect the symmetry present in the equations. The differential equations governing small oscillations in a linearly elastic solid and a perfect fluid have now been derived in exact and Cowling-approximated form. To solve the differential equations, boundary conditions are needed, which will be discussed in the next section.

2.3.5 Boundary conditions

The differential equations discussed in the previous section have an infinite number of solutions for any frequency ω , as long as boundary conditions are not specified. Boundary conditions force the oscillation to be of a certain frequency and are the reason for the discrete oscillation spectrum.

The boundary conditions consist of two different types: regularity conditions at the center of the model and continuity conditions on boundaries in the model and the free surface.

It will turn out that the regularity conditions at the origin of a fluid core will lead to two linearly independent starting solutions $\mathbf{y}^{(1)}(r_1)$ and $\mathbf{y}^{(2)}(r_1)$ at a very small radius r_1 very close to the center of the model, that satisfy the regularity conditions. Using the numerical techniques that are described in chapter 3, the starting solutions will be integrated for a given frequency ω from the center of the model to the free surface. In case the model is entirely fluid, this integration will lead to two linearly independent solutions $\mathbf{y}^{(1)}(R)$ and $\mathbf{y}^{(2)}(R)$ at the surface $r = R$. If the frequency ω is an eigenfrequency, a linear combination of $\mathbf{y}^{(1)}(R)$ and $\mathbf{y}^{(2)}(R)$ will satisfy the boundary conditions on the free surface. In case the model has a solid crust, an extra starting value $\mathbf{y}^{(3)}(r_{CCB})$ will be added at the core-crust boundary located at r_{CCB} . The resulting three linearly independent solutions will be integrated to the free surface and a linear combination of the three solutions $\mathbf{y}^{(1)}(R)$, $\mathbf{y}^{(2)}(R)$ and $\mathbf{y}^{(3)}(R)$ will satisfy the boundary conditions there when ω is an eigenfrequency.

In the following sections the details of the boundary conditions at the center and on interfaces and the free surface will be discussed.

2.3.5.1 Regularity conditions at the center of the model

It turns out that the differential equations allow for solutions that are singular in the center of the model. Such solutions do not represent actual oscillations of stars,

since these oscillations will have regular displacements and stress perturbations. Hence boundary conditions follow from the constraint that all dynamical variables and consequently the eigenfunctions such as U , R , Φ and Ψ are regular.

These regularity conditions will now be derived for a perfect fluid core, since in this study the cores in all models that are considered are fluid. Analogous conditions also hold for elastic cores, which are studied in the context of terrestrial seismology. Power series solutions that lead to boundary conditions at the center of linearly elastic cores have been studied by Crossley (1975) and worked out in more detail by Martinec (1984).

To derive relations between the variables U , R , Φ and Ψ at the center $r = 0$, equations (2.214), (2.226), (2.230) and (2.231) are considered for a fluid, by setting $\mu = 0$. This yields:

$$\frac{d^2\Phi}{dr^2} = \frac{\ell(\ell+1)}{r^2}\Phi - 4\pi G \frac{d}{dr}(\varrho_0 U) - \frac{2}{r} \frac{d\Phi}{dr} - \frac{4\pi G \varrho_0}{r} (2U - \ell(\ell+1)V), \quad (2.315)$$

$$\frac{dU}{dr} = \frac{1}{\kappa} R + \frac{1}{r} [\ell(\ell+1)V - 2U], \quad (2.316)$$

$$\frac{d\Phi}{dr} = \Psi - (\ell+1) \frac{\Phi}{r} - 4\pi G \varrho_0 U. \quad (2.317)$$

$$\frac{1}{\varrho_0} \frac{dR}{dr} = -\left(\omega^2 + \frac{4g_0}{r}\right) U + \frac{\ell(\ell+1)}{r} g_0 V - \frac{\ell+1}{r} \Phi + \Psi. \quad (2.318)$$

A combination of equations (2.315) and (2.316) yields:

$$\frac{d}{dr} \left(r^2 \frac{d\Phi}{dr} \right) + 4\pi G r^2 \left(\frac{d\varrho_0}{dr} U - \frac{\varrho_0}{\kappa} R \right) = \ell(\ell+1) \Phi. \quad (2.319)$$

Using equations (2.316), (2.317) and (2.318), while using (2.163) to get rid of the derivative of g_0 , the left hand side of the following expression reduces to:

$$\frac{1}{\varrho_0} \frac{d}{dr} (R - \varrho_0 g_0 U - \varrho_0 \Phi) = \left(-\omega^2 - \frac{g_0}{\varrho_0} \frac{d\varrho_0}{dr} \right) U - \frac{g_0}{\kappa} R - \frac{1}{\varrho_0} \frac{d\varrho_0}{dr} \Phi. \quad (2.320)$$

Equation (2.316) is restated as:

$$\frac{d}{dr} (r^2 U) = -\frac{\ell(\ell+1)}{\varrho_0 \omega^2} [R - \varrho_0 g_0 U - \varrho_0 \Phi] + \frac{r^2}{\kappa} R. \quad (2.321)$$

Now the limit $r \rightarrow 0$ is taken in equation (2.321), noting that for $r \ll 1$ the gravitational acceleration $g_0 \sim r$ and demanding the regularity of the dynamical variables U , R , Φ and Ψ at $r = 0$. Subsequently, the derivative of equation (2.321) is taken and using (2.320), this leads to the following two equations in the limit $r \rightarrow 0$:

$$\frac{d^2}{dr^2} (r^2 U) = \ell(\ell+1) U, \quad (2.322)$$

$$\frac{d}{dr} \left(r^2 \frac{d\Phi}{dr} \right) = \ell(\ell+1) \Phi. \quad (2.323)$$

The solution to equation (2.322) is given in appendix C by (C.4):

$$U = Ar^{-\ell-2} + Br^{\ell-1}, \quad (2.324)$$

and the solution to equation (2.323) is given by (C.2):

$$\Phi = Cr^{-\ell-1} + Dr^{\ell}, \quad (2.325)$$

where A , B , C and D are constants. Because U and Φ must be regular at the origin, $A = C = 0$. Hence:

$$U \sim r^{\ell-1}, \quad (2.326)$$

$$\Phi \sim r^{\ell}. \quad (2.327)$$

Now two relations between U , V , Φ and Ψ at $r = 0$ are found. Equation (2.327) leads to the relation:

$$\frac{d\Phi}{dr} = \frac{\ell\Phi}{r} = \Psi - (\ell + 1)\frac{\Phi}{r} - 4\pi G\varrho_0 U, \quad (2.328)$$

where equation (2.317) is used. Equation (2.326) is used in the left hand side of equation (2.321) to obtain:

$$U = \frac{\ell}{\varrho_0\omega^2 r} (\varrho_0 g_0 U + \varrho_0 \Phi - R). \quad (2.329)$$

The two relations (2.328) and (2.329) are equivalent to the following two relations between the variables y_1 , y_3 , y_4 and y_6 from the definition (2.291) of \mathbf{y} for $r \rightarrow 0$:

$$\varrho_0 y_1 + \frac{2l+1}{4\pi G r} y_3 - y_6 = 0, \quad (2.330)$$

$$y_1 \left(\frac{\omega^2 r}{l} - g_0 \right) - y_3 + \frac{y_4}{\varrho_0} = 0. \quad (2.331)$$

In practice these boundary conditions at the center of the model are implemented by choosing two linearly independent starting values $\mathbf{y}^{(1)}(r_1)$ and $\mathbf{y}^{(2)}(r_1)$ for integration of the differential equations, that satisfy equations (2.330) and (2.331) at a very small value $r = r_1$.

Starting value $\mathbf{y}^{(1)}(r_1)$ corresponds to the choice that at $r = r_1$, $\Psi = 0$ and $U = 1$. This is quite an arbitrary choice, as long as the choice for the second starting value is linearly independent from this choice, everything is fine. This leads to:

$$\mathbf{y}^{(1)}(r_1) = \begin{pmatrix} y_1^{(2)}(r_1) \\ y_3^{(2)}(r_1) \\ y_4^{(2)}(r_1) \\ y_6^{(2)}(r_1) \end{pmatrix} = \begin{pmatrix} r_1 \\ -\frac{4\pi G\varrho_0 r_1^2}{2l+1} \\ \varrho_0 r_1^2 \left(\frac{8}{3} \frac{\ell-1}{2l+1} \pi G \varrho_0 - \frac{\omega^2}{l} \right) \\ 0 \end{pmatrix}. \quad (2.332)$$

The second starting value $\mathbf{y}^{(2)}(r_1)$ corresponds to the choice $\Psi = 1$ and $U = 0$ at $r = r_1$. This is indeed a choice that is linearly independent from the first one. The gravitational acceleration g_0 is represented by a power series in the center:

$$g_0 = \frac{4}{3}\pi G \varrho_0 r + O(r^2), \quad (2.333)$$

where the constant term in the power series in r vanishes, because the gravitational acceleration is zero for $r = 0$. Now the following values are found for starting vector $\mathbf{y}^{(2)}(r_1)$:

$$\mathbf{y}^{(2)}(r_1) = \begin{pmatrix} y_1^{(1)}(r_1) \\ y_3^{(1)}(r_1) \\ y_4^{(1)}(r_1) \\ y_6^{(1)}(r_1) \end{pmatrix} = \begin{pmatrix} 0 \\ \frac{r_1^2}{2l+1} \\ \frac{\varrho_0 r_1^2}{2l+1} \\ \frac{r_1}{4\pi G} \end{pmatrix}. \quad (2.334)$$

When the Cowling approximation is applied, only one starting vector remains, and follows from equation (2.331) with $y_3 = 0$:

$$\mathbf{y}^{(1)}(r_1) = \begin{pmatrix} y_1^{(1)}(r_1) \\ y_4^{(1)}(r_1) \end{pmatrix} = \begin{pmatrix} r_1 \\ \varrho_0 r_1^2 \left(\frac{4}{3}\pi G \varrho_0 - \frac{\omega^2}{l} \right) \end{pmatrix}. \quad (2.335)$$

2.3.5.2 Internal boundary conditions

Internal discontinuities in a neutron star model, such as the boundary between the neutron star fluid core and solid crust, are subject to boundary conditions. Firstly, when effects of surface tension on the discontinuity are neglected, the stress tensor is continuous across discontinuities. This is shown by considering the integral form of Newton's second law for a continuum (G.42):

$$\frac{d}{dt} \int_{V(t)} \varrho \mathbf{v} dV = \int_{\partial V(t)} \mathbf{T}_{(\mathbf{n})} dS - \int_{V(t)} \varrho \nabla \varphi dV, \quad (2.336)$$

where $\mathbf{T}_{(\mathbf{n})} = \mathbf{T} \cdot \mathbf{n}$ is the stress vector on a surface with normal \mathbf{n} and $V(t)$ is an arbitrary (time dependent) volume in the continuum and $\partial V(t)$ is its boundary. If for $V(t)$ an arbitrarily oriented infinitesimal cylindrical volume is chosen and the limit of zero height of the cylinder is taken, the terms proportional to the volume in equation (2.336) are zero in this limit. Then it follows that the stress tensor \mathbf{T} must be continuous because the identity

$$\int_{\partial V(t)} \mathbf{T}_{(\mathbf{n})} dS = 0, \quad (2.337)$$

must hold in the limit of zero thickness of the cylinder. This implies that the traction vector on radial surfaces (2.216) is continuous across a boundary in the model and hence R , S and T must be continuous.

Secondly, an expression regarding the behaviour of Ψ and Φ across boundaries is obtained by considering the integration of equation (2.168) over a cylinder with top and bottom located on the two sides of the boundary. This leads to the continuity of

$$\frac{d\Phi}{dr} + 4\pi G \rho_0 U, \quad (2.338)$$

across boundaries. Since Φ must be continuous throughout the model, because its derivative gives the magnitude of gravitational acceleration perturbation, which is finite, the continuity of (2.338) implies continuity of Ψ .

Thirdly, across a boundary between two solid materials, the displacement must be continuous, because the connection between the two different materials at the boundary must remain intact. Hence U , V and W must be continuous. However, when the boundary is between a liquid and a solid, like in the case of a neutron star, the radial component of displacement U must be continuous, but the tangential component represented by V and W does not need to be continuous. Because the fluid cannot withhold shear stress, the solid can move freely parallel to the fluid-solid boundary.

In the case of the nonradial oscillations of a neutron star, the core is fluid and the crust is solid and the freedom of tangential movement of the solid crust is represented by a third independent starting vector $\mathbf{y}^{(3)}$ for integration at the core-crust boundary, with all components zero except

$$y_2^{(3)}(r_{CCB}) = C, \quad (2.339)$$

where C is an arbitrary constant.

Exactly the same conditions hold on internal boundaries in the case the Cowling approximation is applied, although of course conditions on the gravitational potential are no longer applicable, since they are neglected.

2.3.6 Boundary conditions for the free surface

On the outer or free surface of a neutron star model, the same conditions hold as on an internal boundary. Since outside the neutron star stress is assumed to be zero, this leads to the conditions that $R = S = T = 0$ on the free surface.

It follows from equation (2.164) that the Laplace equation is satisfied by the gravitational potential Φ , since the density perturbation is zero outside of the neutron star. Because Φ has to be regular at $r \rightarrow \infty$, outside the model, $\Phi \sim r^{-\ell-1}$. Using this fact in combination with $\varrho_0 = 0$ outside the neutron star, it follows from identity (2.229)

$$\Psi = \partial_r \Phi + (\ell + 1) \frac{\Phi}{r} + 4\pi G \varrho_0 U, \quad (2.340)$$

that $\Psi = 0$ at the free surface. This convenient formulation of the boundary condition on the free surface is the reason Ψ is defined as it is. This section finishes the review on Newtonian oscillations of spherically symmetric stellar models. The next sections will develop a similar theory of relativistic oscillations of neutron stars.

2.4 Symmetric formulation of the equations of motion of a relativistic, perfect fluid stellar model in the Cowling approximation

In general relativity, the equilibrium configuration of a spherically symmetric neutron star model with a given equation of state is found by finding the solution of the Einstein field equations (E.11) for the most general spherically symmetric metric (E.14). If a polytropic equation of state (2.19) is chosen, this leads to the relativistic Lane-Emden equations (2.68, 2.69), which allow for a solution for the equilibrium configuration of a polytropic neutron star, as is described in section 2.1.3. When it is assumed that the neutron star model consists of a perfect fluid, the perturbations of such a neutron star model are governed by the change of the stress-energy tensor (F.17) for a perfect fluid and the metric (E.14). The time-evolution of the perturbations is found by studying the perturbed Einstein field equations that follow from the perturbed metric and stress-energy tensor:

$$\delta G_{\alpha\beta} = \frac{8\pi G}{c^4} \delta T_{\alpha\beta}, \quad (2.341)$$

where $G_{\alpha\beta} = R_{\alpha\beta} - \frac{1}{2}g_{\alpha\beta}R$ is the Einstein tensor. By linearizing this equation in the perturbations, differential equations for the perturbed metric components and stress energy tensor components are obtained.

As mentioned in the historical introduction, this approach has been worked out theoretically by Thorne and Campolattaro (1967) for a perfect fluid and by Schumaker and Thorne (1983) and Finn (1990) for a model with an elastic crust. Calculations

on the spectrum of a star that arise from these equations have first been done by Lindblom and Detweiler (1983) for a purely fluid model and by Leins (1994) for the toroidal oscillations in a neutron star model with a crust. A type of purely gravitational modes, named *w*-modes, has been discovered by Kokkotas and Schutz (1992) in a study on the oscillations of a fluid neutron star model.

In this study however, the relativistic Cowling approximation will be applied, in which perturbations in the metric are neglected. The relativistic Cowling approximation was introduced by McDermott, Van Horn and Scholl (1983). The simplification of the equations of motion that follows comes at the price of an inconsistency: it will be shown in this section that if the metric perturbations are neglected, it follows from the diagonal components of the perturbed Einstein equations (2.341) that the perturbations in pressure and density are zero as well, which would lead to no oscillations at all. Instead, the inconsistent assumption is made that the metric perturbations are zero, but the perturbation in pressure is nonzero. It turns out that this inconsistency does not have a qualitative influence on the results and leads to significantly more simple equations of motion. Because the metric is not perturbed, it remains the spherically symmetric metric (E.14):

$$ds^2 = \sum_{\alpha,\beta} g_{\alpha\beta} dx^\alpha dx^\beta = e^{2\nu} c^2 dt^2 - e^{2\lambda} dr^2 - r^2 (d\theta^2 + \sin^2 \theta d\phi^2). \quad (2.342)$$

The Christoffel symbols associated with this metric are given by equations (2.45) – (2.48).

Just like in the Newtonian case, equations of motion will be derived from the relativistic analogue of the momentum equation and continuity equation. The relativistic analogue of the momentum equation is given by the relativistic Euler equation (F.21)

$$\sum_{\mu} \left(\varrho + \frac{P}{c^2} \right) u^\mu u_{\nu;\mu} = \partial_\nu P - \sum_{\mu} \frac{u_\nu u^\mu}{c^2} (\partial_\mu P), \quad (2.343)$$

which follows from the Einstein field equations for a perfect fluid.

In the Newtonian case, the continuity equation (F.7) follows from the conservation of mass. In general relativity, mass is no longer a conserved quantity. This means that the continuity equation does not hold. However, an analogous relation exists: the number of baryons in a given parcel of fluid is conserved. From this fact, the law of baryon conservation (F.16) follows:

$$\frac{dn}{d\tau} = -n \sum_{\mu} u^\mu{}_{;\mu}, \quad (2.344)$$

where \mathbf{u} is the four-velocity (E.4), D is the covariant derivative (E.6) and n is the baryon number density.

The equations will be considered in spherical coordinates and will be expanded in (vector) spherical harmonics. Unlike in the analysis for the Newtonian equations, presented in the preceding chapters, the analysis will be done for spherical harmonic components with $m = 0$, following Thorne and Campolattaro (1967), to simplify the equations. Due to the spherical symmetry of the problem, the radial part of the solution of the equations of motion will not depend on m and oscillations for $m \neq 0$ are obtained by suitable rotations about the center of the neutron star model.

The position (t, r, θ, ϕ) of a fluid element in spacetime as a function of proper time τ (see definition E.3), is indicated by the position four-vector ξ ,

$$\xi(\tau) = \begin{pmatrix} \xi^t \\ \xi^r \\ \xi^\theta \\ \xi^\phi \end{pmatrix}. \quad (2.345)$$

At this point it is insightful to note that the position four-vector ξ has a different character than the position vector \mathbf{x} in the Newtonian analysis. Apart from the extra coordinate time component present in ξ , the angular components of the vector are given as angles, whereas the angular components of \mathbf{x} are given in terms of a length unit. This has to be taken into account when the relativistic equations of motion are compared to their Newtonian analogues.

When a fluid element located at ξ_0 in dynamical equilibrium moves to

$$\xi(\xi_0, \tau) = \xi_0 + \varsigma(\xi_0, \tau), \quad (2.346)$$

with ς the displacement, a perturbation in pressure P , density ϱ , and number of baryons n at a given position occurs.

Hence

$$P = P_0 + \delta p, \quad (2.347)$$

$$\varrho = \varrho_0 + \delta \varrho, \quad (2.348)$$

$$n = n_0 + \delta n. \quad (2.349)$$

The way to derive equations of motion for small perturbations is to linearize the relativistic Euler equations (2.343) in the perturbations. To do this, the four-velocity (E.4) of the fluid elements

$$\mathbf{u} = \frac{d\xi}{d\tau} = \frac{d\varsigma}{d\tau}, \quad (2.350)$$

is needed, to first order in the perturbations. The components of the four-velocity are found by using identity (E.5)

$$\sum_{\mu} u_{\mu} u^{\mu} = c^2, \quad (2.351)$$

which leads to:

$$c^2 e^{2\nu} (u^t)^2 - e^{2\lambda} (u^r)^2 - r^2 (u^{\theta})^2 - r^2 \sin^2 \theta (u^{\phi})^2 = c^2. \quad (2.352)$$

Since $(u^r)^2$, $(u^{\theta})^2$ and $(u^{\phi})^2$ are all of second order in the perturbations, they are neglected. Hence:

$$u^t = \frac{d\zeta^t}{d\tau} = \frac{dt}{d\tau} = e^{-\nu}, \quad (2.353)$$

where ζ^t is denoted as t for clarity. The other components of the four-velocity now follow:

$$u^r = \frac{d\zeta^r}{d\tau} = \frac{d\zeta^r}{dt} \frac{dt}{d\tau} = e^{-\nu} \frac{d\zeta^r}{dt}, \quad (2.354)$$

$$u^{\theta} = \frac{d\zeta^{\theta}}{d\tau} = \frac{d\zeta^{\theta}}{dt} \frac{dt}{d\tau} = e^{-\nu} \frac{d\zeta^{\theta}}{dt}, \quad (2.355)$$

$$u^{\phi} = \frac{d\zeta^{\phi}}{d\tau} = \frac{d\zeta^{\phi}}{dt} \frac{dt}{d\tau} = e^{-\nu} \frac{d\zeta^{\phi}}{dt}. \quad (2.356)$$

The way to proceed is to expand all variables in (vector) spherical harmonics. As already mentioned, the equations of motion for modes with $m = 0$ will be derived. The vector spherical harmonic expansion $Y_{\ell}^0(\theta, \phi)$ of the displacement of a particular spheroidal mode ($\ell, m = 0$) is, following McDermott, Van Horn and Scholl (1983), defined to be:

$$\zeta^r = \frac{e^{-\lambda}}{r^2} Q(r, t) P_{\ell}(\cos \theta), \quad (2.357)$$

$$\zeta^{\theta} = -\frac{1}{r^2} Z(r, t) \frac{\partial P_{\ell}(\cos \theta)}{\partial \theta}, \quad (2.358)$$

$$\zeta^{\phi} = 0, \quad (2.359)$$

where, just like in the newtonian case, the dependency of the eigenfunctions on the index ℓ is omitted. The relativistic Euler equation (F.21) will now be linearized and expressed in the spherical harmonic expansion. Using the metric (2.342) on the components of the velocity (2.353) – (2.356), the covariant components of the 4-velocity are found to be

$$u_t = c^2 e^{\nu}, \quad u_{\theta} = -r^2 e^{-\nu} \frac{\partial \zeta^{\theta}}{\partial t}, \quad (2.360)$$

$$u_r = -e^{2\lambda - \nu} \frac{\partial \zeta^r}{\partial t}, \quad u_{\phi} = 0. \quad (2.361)$$

First the left hand side of the $\nu = t$ component of the relativistic Euler equation is expressed in terms of the spherical harmonic expansion.

$$\sum_{\mu} u^{\mu} u_{t;\mu} = u^t \left(\partial_t u_t - \sum_{\alpha} \Gamma_{tt}^{\alpha} u_{\alpha} \right) + u^r \left(\partial_r u_t - \sum_{\alpha} \Gamma_{rt}^{\alpha} u_{\alpha} \right). \quad (2.362)$$

Using the expressions for the Christoffel symbols (2.45) – (2.48) for the spherically symmetric metric, it is found that

$$\sum_{\alpha} \Gamma_{tt}^{\alpha} u_{\alpha} = c^2 \frac{d\nu}{dr} e^{2(\nu-\lambda)} u_r, \quad \sum_{\alpha} \Gamma_{rt}^{\alpha} u_{\alpha} = \frac{d\nu}{dr} u_t. \quad (2.363)$$

After a line of algebra it follows that

$$\sum_{\mu} u^{\mu} u_{t;\mu} = c^2 \frac{d\nu}{dr} \frac{\partial \mathcal{S}^r}{\partial t}, \quad (2.364)$$

while the right hand side of the relativistic Euler equation (F.21) is equal to

$$\partial_t \delta P - \frac{u_t}{c^2} \left(u^t \partial_t \delta P + u^r \partial_r P_0 \right) = -\frac{\partial \mathcal{S}^r}{\partial t} \partial_r P_0. \quad (2.365)$$

Hence the $\nu = t$ component of the relativistic Euler equation yields

$$\frac{dP_0}{dr} + \frac{d\nu}{dr} (\rho_0 c^2 + P_0) = 0. \quad (2.366)$$

The radial component of the relativistic Euler equation yields another differential equation. The left hand side is found from

$$\begin{aligned} \sum_{\mu} u^{\mu} u_{r;\mu} = u^t \left(\partial_t u_r - \sum_{\alpha} \Gamma_{tr}^{\alpha} u_{\alpha} \right) + u^r \left(\partial_r u_r - \sum_{\alpha} \Gamma_{rr}^{\alpha} u_{\alpha} \right) + \\ + u^{\theta} \left(\partial_{\theta} u_r - \sum_{\alpha} \Gamma_{\theta r}^{\alpha} u_{\alpha} \right). \end{aligned} \quad (2.367)$$

Again the expressions for the Christoffel symbols (2.45) – (2.48) are used to derive:

$$\sum_{\alpha} \Gamma_{tr}^{\alpha} u_{\alpha} = c^2 \frac{d\nu}{dr} e^{\nu}, \quad \sum_{\alpha} \Gamma_{rr}^{\alpha} u_{\alpha} = -\frac{d\lambda}{dr} e^{2\lambda-\nu} \frac{\partial \mathcal{S}^r}{\partial t}, \quad (2.368)$$

$$\sum_{\alpha} \Gamma_{\theta r}^{\alpha} u_{\alpha} = -r e^{-\nu} \frac{d\mathcal{S}^{\theta}}{dt}. \quad (2.369)$$

To first order in the displacement, the left hand side of the Euler equation becomes

$$\sum_{\mu} u^{\mu} u_{r;\mu} = u^t \left(\partial_t u_r - \sum_{\alpha} \Gamma_{tr}^{\alpha} u_{\alpha} \right) = -e^{2(\lambda-\nu)} \frac{\partial^2 \mathcal{S}^r}{\partial t^2} - c^2 \frac{d\nu}{dr}. \quad (2.370)$$

Using the $\nu = t$ component (2.366) of the relativistic Euler equation, the radial component becomes, linearized in the displacement:

$$\left(\varrho_0 + \frac{P_0}{c^2} \right) e^{2(\lambda-\nu)} \frac{\partial^2 \mathcal{S}^r}{\partial t^2} + (\delta P + c^2 \delta \varrho) \frac{d\nu}{dr} + \partial_r \delta P = 0. \quad (2.371)$$

The azimuthal component of the left hand side relativistic Euler equation is found from the following expression, when linearized in the displacement:

$$\sum_{\mu} u^{\mu} u_{\theta;\mu} = u^t \partial_t u_{\theta} = -e^{-2\nu} r^2 \frac{\partial^2 \mathcal{S}^{\theta}}{\partial t^2}. \quad (2.372)$$

The corresponding relativistic Euler equation component is:

$$\left(\varrho_0 + \frac{P_0}{c^2} \right) e^{-2\nu} r^2 \frac{\partial^2 \mathcal{S}^{\theta}}{\partial t^2} + \partial_{\theta} \delta P = 0. \quad (2.373)$$

Now the baryon conservation law (2.344) is linearized and expressed in terms of the $(\ell, m = 0)$ mode of the spherical harmonic expansion. To do this, first the divergence of the velocity (E.9) $\sum_{\mu} u^{\mu}{}_{;\mu}$ is calculated:

$$\sum_{\mu} (u^{\mu}{}_{;\mu}) = \frac{1}{\sqrt{-\|g\|}} \partial_{\mu} \left(\sqrt{-\|g\|} u^{\mu} \right), \quad (2.374)$$

where $\|g\|$ is the metric determinant, which reduces to

$$\sqrt{-\|g\|} = c e^{\lambda+\nu} r^2 \sin \theta, \quad (2.375)$$

in the Cowling approximation. The divergence of the velocity \mathbf{u} is:

$$\sum_{\mu} (u^{\mu}{}_{;\mu}) = \partial_r u^r + \frac{\partial_r \sqrt{-\|g\|}}{\sqrt{-\|g\|}} u^r + \partial_{\theta} u^{\theta} + \frac{\partial_{\theta} \sqrt{-\|g\|}}{\sqrt{-\|g\|}} u^{\theta} \quad (2.376)$$

$$= \partial_r u^r + \partial_{\theta} u^{\theta} + \left(\frac{2}{r} + \frac{d\nu}{dr} + \frac{d\lambda}{dr} \right) u^r + \cot \theta u^{\theta}. \quad (2.377)$$

For the $(l, m = 0)$ mode, the first two terms are:

$$\partial_r u^r = - \left(\frac{2}{r} + \frac{d\nu}{dr} + \frac{d\lambda}{dr} \right) u^r + \frac{1}{r^2} e^{-(\nu+\lambda)} \frac{\partial^2 Q}{\partial r \partial t} P_l(\cos \theta), \quad (2.378)$$

$$\partial_{\theta} u^{\theta} = - \frac{1}{r^2} e^{-\nu} \frac{\partial Z}{\partial t} \partial_{\theta}^2 P_l(\cos \theta). \quad (2.379)$$

If identity (B.4) is considered for $m = 0$, it directly follows that

$$(\partial_\theta^2 + \cot \theta \partial_\theta) P_\ell(\cos \theta) = -\ell(\ell + 1) P_\ell(\cos \theta), \quad (2.380)$$

which implies that

$$\partial_\theta u^\theta + \cot \theta u^\theta = \frac{e^{-\nu}}{r^2} \ell(\ell + 1) \frac{\partial Z}{\partial t}. \quad (2.381)$$

The divergence of the four-velocity \mathbf{u} is hence given by:

$$\sum_\mu u^\mu{}_{;\mu} = \frac{1}{r^2} e^{-(\nu+\lambda)} \frac{\partial^2 Q}{\partial r \partial t} P_\ell(\cos \theta) + \frac{e^{-\nu}}{r^2} \ell(\ell + 1) \frac{\partial Z}{\partial t}. \quad (2.382)$$

The baryon conservation law is, in terms of the spherical harmonic expansion:

$$\frac{dn}{d\tau} = -\frac{n}{r^2} \left(e^{-(\nu+\lambda)} \frac{\partial^2 Q}{\partial r \partial t} + e^{-\nu} \ell(\ell + 1) \frac{\partial Z}{\partial t} \right) P_\ell(\cos \theta). \quad (2.383)$$

Since the proper time derivative is taken along a fluid worldline of a fluid parcel, it measures the change of n at the fluid parcel, hence it is in fact the change of the Lagrangian perturbation Δn , as explained in appendix D. Hence $\frac{dn}{d\tau} = \frac{d\Delta n}{d\tau}$. Integrating with respect to τ gives, to first order in perturbations:

$$\frac{\Delta n}{n_0} = -\frac{1}{r^2} \left(e^{-(\nu+\lambda)} \frac{\partial Q}{\partial r} \frac{\partial \tau}{\partial t} + e^{-\nu} \ell(\ell + 1) Z \frac{\partial \tau}{\partial t} \right) P_\ell(\cos \theta) \quad (2.384)$$

$$= -\frac{1}{r^2} \left(e^{-\lambda} \frac{\partial Q}{\partial r} + \ell(\ell + 1) Z \right) P_\ell(\cos \theta). \quad (2.385)$$

In the two components (2.371) and (2.372) of the relativistic Euler equation, perturbations in density and pressure occur. To express these perturbations in terms of the spherical harmonic expansion (hence in terms of the functions Q and Z), the component of the relativistic Euler equation (F.20) parallel to the four-velocity \mathbf{u} is used to express the density perturbation in terms of a perturbation of the baryon number. The bulk modulus κ of the fluid is introduced to find an equation for the pressure perturbation in terms of the perturbation of the baryon number.

Equation (2.385) is then used to express the perturbation in baryon number in terms of Q and Z . Since the density and pressure perturbation are written in terms of the perturbation in baryon number, this allows the density and pressure perturbation to be written in terms of Q and Z as well.

The Baryon number density n is related to the density ϱ by the component of the relativistic Euler equation (F.20) parallel to the four-velocity \mathbf{u} :

$$\left(\varrho + \frac{P}{c^2} \right) \sum_\mu (u^\mu{}_{;\mu}) + \frac{\partial \varrho}{\partial \tau} = 0. \quad (2.386)$$

This equation, combined with the baryon conservation law (2.344), gives

$$\frac{1}{n} \left(\varrho + \frac{P}{c^2} \right) \frac{dn}{d\tau} = \frac{d\varrho}{d\tau}. \quad (2.387)$$

Again, since $d/d\tau$ is a derivative along a fluid worldline, the changes in density ϱ and baryon number density n are changes of their Lagrangian perturbations. Linearizing and integrating with respect to τ yields:

$$\Delta\varrho = \frac{\Delta n}{n_0} \left(\varrho_0 + \frac{P_0}{c^2} \right). \quad (2.388)$$

Invoking relationship (D.8) between Lagrangian and Eulerian perturbations yields:

$$\begin{aligned} \delta\varrho &= \Delta\varrho - \frac{d\varrho_0}{dr} \zeta^r & (2.389) \\ &= - \left\{ \left(\varrho_0 + \frac{P_0}{c^2} \right) \frac{1}{r^2} \left(e^{-\lambda} \frac{dQ}{dr} + \ell(\ell+1)Z \right) + \frac{d\varrho_0}{dr} \frac{e^{-\lambda}}{r^2} Q \right\} P_\ell(\cos\theta). & (2.390) \end{aligned}$$

Since adiabatic oscillations are assumed, the pressure perturbation in terms of Δn is found by using the bulk modulus of the fluid, which measures the resistance of the fluid to uniform compression:

$$\kappa = n \frac{\Delta P}{\Delta n} = \Gamma_1 P. \quad (2.391)$$

The Eulerian perturbation in pressure is, by using (D.8):

$$\begin{aligned} \delta P &= \Delta P - \frac{dP_0}{dr} \zeta^r & (2.392) \\ &= - \left\{ \frac{\kappa}{r^2} \left(e^{-\lambda} \frac{dQ}{dr} + \ell(\ell+1)Z \right) + \frac{dP_0}{dr} \frac{e^{-\lambda}}{r^2} Q \right\} P_\ell(\cos\theta). & (2.393) \end{aligned}$$

As mentioned in the beginning of this section, as a consequence of the relativistic Cowling approximation in which metric perturbations in the perturbed Einstein field equations (2.341) are neglected, both the density and pressure perturbation are vanishing. To illustrate this, consider the component of the perturbed Einstein field equations with $\alpha = \beta = t$:

$$\delta G_t^t = \frac{8\pi G}{c^4} \delta T_t^t = \frac{8\pi G}{c^2} \delta\varrho. \quad (2.394)$$

If the metric perturbations are neglected, the left hand side of this equation vanishes and $\delta\varrho = 0$. Similarly, the component with $\alpha = \beta = r$ gives, to first order in the perturbations:

$$\delta G_r^r = \frac{8\pi G}{c^4} \delta T_r^r = -\frac{8\pi G}{c^4} \delta P. \quad (2.395)$$

The relativistic Cowling approximation implies $\delta G_r^r = 0$ and hence $\delta P = 0$. This means that neglecting the metric perturbations leads to no oscillations at all, since both the density and pressure are left unperturbed. Instead, the metric perturbations are neglected and the density perturbation $\delta \varrho$ is set to zero, but inconsistently the pressure perturbation δP is *not* set to zero. McDermott, Van Horn and Scholl (1983) have found that this inconsistent approach leads to qualitative correct results.

Hence in the Cowling approximation, the pressure perturbation $\delta \varrho = 0$ leads to an additional equation for the spherical harmonic expansion functions Q and Z . Using equations (2.390) and (2.393) with $\delta \varrho = 0$ in the radial component of the relativistic Euler equation (2.371), yields:

$$\begin{aligned} - \left(\varrho_0 + \frac{P_0}{c^2} \right) \frac{e^{\lambda-2\nu}}{r^2} \frac{\partial^2 Q}{\partial t^2} + \frac{d\nu}{dr} \left\{ \frac{\kappa}{r^2} \left(e^{-\lambda} \frac{\partial Q}{\partial r} + \ell(\ell+1)Z \right) + \frac{dP_0}{dr} \frac{e^{-\lambda}}{r^2} Q \right\} + \\ + \frac{d}{dr} \left\{ \frac{\kappa}{r^2} \left(e^{-\lambda} \frac{\partial Q}{\partial r} + \ell(\ell+1)Z \right) + \frac{dP_0}{dr} \frac{e^{-\lambda}}{r^2} Q \right\} = 0. \end{aligned} \quad (2.396)$$

The last term of the left hand side of the equation is:

$$\frac{d}{dr} \left(\frac{dP_0}{dr} \frac{e^{-\lambda}}{r^2} Q \right) = -\frac{d}{dr} \left[(P_0 + \varrho_0 c^2) \frac{d\nu}{dr} \frac{e^{-\lambda}}{r^2} Q \right] \quad (2.397)$$

$$\begin{aligned} &= - \left(\frac{dP_0}{dr} + c^2 \frac{d\varrho_0}{dr} \right) \frac{d\nu}{dr} \frac{e^{-\lambda}}{r^2} Q \\ &\quad - (P_0 + \varrho_0 c^2) \left\{ \frac{d\nu}{dr} \frac{e^{-\lambda}}{r^2} \frac{\partial Q}{\partial r} + \frac{d}{dr} \left(\frac{d\nu}{dr} \frac{e^{-\lambda}}{r^2} \right) Q \right\} \end{aligned} \quad (2.398)$$

$$\begin{aligned} &= - (P_0 + \varrho_0 c^2) \frac{d}{dr} \left(\frac{d\nu}{dr} \frac{e^{-\lambda}}{r^2} \right) Q - \frac{dP_0}{dr} \frac{d\nu}{dr} \frac{e^{-\lambda}}{r^2} Q + \\ &\quad + \frac{1}{r^2} \frac{d\nu}{dr} (P_0 + \varrho_0 c^2) \ell(\ell+1)Z. \end{aligned} \quad (2.399)$$

In the first step, equation (2.366) is used and in the last step, the equation $\delta \varrho = 0$ is used. Assuming a normal mode solution, the variables Q and Z are assumed to have time dependence of the form $e^{i\omega t}$ with ω the frequency of the mode. Hence the double time derivative is replaced by $-\omega^2$. Equation (2.399), used in the radial component of the relativistic Euler equation (2.396) then yields:

$$\begin{aligned} \left(\varrho_0 + \frac{P_0}{c^2} \right) \frac{e^{\lambda-2\nu}}{r^2} \omega^2 Q + \frac{d\nu}{dr} \frac{\kappa}{r^2} \left(e^{-\lambda} \frac{dQ}{dr} + \ell(\ell+1)Z \right) + \\ + \frac{d}{dr} \left\{ \frac{\kappa}{r^2} \left(e^{-\lambda} \frac{dQ}{dr} + \ell(\ell+1)Z \right) \right\} - (P_0 + \varrho_0 c^2) \frac{d}{dr} \left(\frac{e^{-\lambda}}{r^2} \frac{d\nu}{dr} \right) Q + \\ + \frac{1}{r^2} \frac{d\nu}{dr} (P_0 + \varrho_0 c^2) \ell(\ell+1)Z = 0. \end{aligned} \quad (2.400)$$

Multiplying the equation with $-e^\nu$ and incorporating the second term into the third by inserting a factor e^ν inside the derivative of the third term yields:

$$\begin{aligned} \frac{d}{dr} \left\{ \frac{\kappa}{r^2} \left(e^{-\lambda} \frac{dQ}{dr} + \ell(\ell+1)Z \right) e^\nu \right\} &= e^\nu (\varrho_0 c^2 + P_0) \frac{d}{dr} \left(\frac{e^{-\lambda}}{r^2} \frac{d\nu}{dr} \right) Q \\ &- \omega^2 \frac{e^{\lambda-\nu}}{r^2} \left(\varrho_0 + \frac{P_0}{c^2} \right) Q - \ell(\ell+1) (\varrho_0 c^2 + P_0) \frac{de^\nu}{dr} \frac{Z}{r^2}. \end{aligned} \quad (2.401)$$

This equation is identical to equation (3a) in (McDermott, Van Horn and Scholl, 1983), up to a definition difference of factor two in the parameters ν and λ . The azimuthal component of the relativistic Euler equations (2.373) in terms of the spherical harmonic expansion is:

$$\omega^2 \left(\varrho_0 + \frac{P_0}{c^2} \right) e^{-2\nu} Z - \left\{ \frac{\kappa}{r^2} \left(e^{-\lambda} \frac{dQ}{dr} + \ell(\ell+1)Z \right) + \frac{dP_0}{dr} \frac{e^{-\lambda}}{r^2} Q \right\} = 0. \quad (2.402)$$

This equation is identical to equation (3b) in (McDermott, Van Horn and Scholl, 1983), up to an overall minus sign and the definition difference of factor two in the parameters ν and λ .

To put equations (2.401) and (2.402) in a form exactly analogous to the Newtonian equations, call:

$$R(r) = \frac{\kappa}{r^2} \left(e^{-\lambda} \frac{dQ}{dr} + \ell(\ell+1)Z \right), \quad (2.403)$$

$$U(r) = \frac{e^{-\lambda}}{r^2} Q. \quad (2.404)$$

Comparing with equation (2.393), it is clear that R is minus the Lagrangian perturbation of pressure, which is the Lagrangian perturbation of radial traction, because the positive direction of radial traction (outward radial direction) is opposite to the direction of positive pressure (inward direction). Hence R is defined just as in the Newtonian case (2.217). Similarly, U is defined as in the Newtonian case, which is verified by comparing the Newtonian expression (2.192) and the corresponding relativistic expression (2.357) for the radial displacement. Consequently,

$$\frac{dQ}{dr} = \frac{d}{dr} (r^2 e^\lambda U) = \left(2r + \frac{d\lambda}{dr} r^2 \right) e^\lambda U + r^2 e^\lambda \frac{dU}{dr}, \quad (2.405)$$

$$Z = \frac{r^2}{\ell(\ell+1)} \left(\frac{R}{\kappa} - \frac{e^{-\lambda}}{r^2} \frac{dQ}{dr} \right) \quad (2.406)$$

$$= \frac{r^2}{\ell(\ell+1)} \left(\frac{R}{\kappa} - \frac{dU}{dr} - \left(\frac{2}{r} + \frac{d\lambda}{dr} \right) U \right). \quad (2.407)$$

In terms of the new variables, equation (2.401) and (2.402) become, respectively,

$$e^\nu \frac{dR}{dr} + \frac{d\nu}{dr} R e^\nu = (P_0 + \varrho_0 c^2) r^2 e^{\lambda+\nu} \frac{d}{dr} \left(\frac{e^{-\lambda}}{r^2} \frac{d\nu}{dr} \right) U - \omega^2 e^{2\lambda-\nu} \left(\frac{P_0}{c^2} + \varrho_0 \right) U + \\ + (P_0 + \varrho_0 c^2) \frac{de^\nu}{dr} \left(\frac{dU}{dr} + \left(\frac{2}{r} + \frac{d\lambda}{dr} \right) U - \frac{R}{\kappa} \right), \quad (2.408)$$

$$\omega^2 \left(\varrho_0 + \frac{P_0}{c^2} \right) e^{-2\nu} \frac{r^2}{\ell(\ell+1)} \left(\frac{dU}{dr} + \left(\frac{2}{r} + \frac{d\lambda}{dr} \right) U - \frac{R}{\kappa} \right) + \frac{dP_0}{dr} U + R = 0. \quad (2.409)$$

The last equation is, with the help of equation (2.366), restated as,

$$\frac{dU}{dr} = \left(\frac{c^2 e^{2\nu} \frac{d\nu}{dr} \ell(\ell+1)}{\omega^2 r^2} - \frac{2}{r} - \frac{d\lambda}{dr} \right) U + \left(\frac{1}{\kappa} - \frac{c^2 e^{2\nu} \ell(\ell+1)}{\omega^2 (P_0 + \varrho_0 c^2) r^2} \right) R. \quad (2.410)$$

This equation is useful to get rid of the factor dU/dr in equation (2.408). Eliminating dU/dr yields, by also using equation (2.366):

$$\frac{dR}{dr} = (P_0 + \varrho_0 c^2) \left(\frac{c^2 e^{2\nu} \left(\frac{d\nu}{dr} \right)^2 \ell(\ell+1)}{\omega^2 r^2} - \frac{\omega^2 e^{2(\lambda-\nu)}}{c^2} + r^2 e^\lambda \frac{d}{dr} \left(\frac{e^{-\lambda}}{r^2} \frac{d\nu}{dr} \right) \right) U \\ - \left\{ \frac{d\nu}{dr} + \frac{c^2 e^{2\nu} \frac{d\nu}{dr} \ell(\ell+1)}{\omega^2 r^2} \right\} R. \quad (2.411)$$

Equations (2.410) and (2.411) for U and R have been derived for a spherical harmonic with $m = 0$. Since, because of spherical symmetry of the equilibrium model, the radial part of the differential equations governing the oscillations does not depend on m , as has been demonstrated in the various Newtonian models that were discussed in the previous sections, the equations for U and R derived in this section hold for any m . Like in the Newtonian case, these equations are put in the form (1.1, 1.2):

$$\frac{d\mathbf{y}}{dr} = \mathbf{A}\mathbf{y}, \quad (2.412)$$

with

$$\mathbf{y} = \begin{pmatrix} e^\lambda U r \\ e^\nu R r \end{pmatrix}, \quad (2.413)$$

and

$$\mathbf{A} = \begin{pmatrix} T & K \\ S & -T \end{pmatrix}, \quad (2.414)$$

where T , K and S are given by:

$$T = \frac{c^2 e^{2\nu} \frac{d\nu}{dr} \ell(\ell+1)}{\omega^2 r^2} - \frac{1}{r}, \quad (2.415)$$

$$K = e^{\lambda-\nu} \left(\frac{1}{\kappa} - \frac{c^2 e^{2\nu} \ell(\ell+1)}{(P_0 + \varrho_0 c^2) \omega^2 r^2} \right), \quad (2.416)$$

$$S = (P_0 + \varrho_0 c^2) \left(\frac{c^2 e^{\nu-\lambda} e^{2\nu} \ell(\ell+1)}{\omega^2 r^2} \left(\frac{d\nu}{dr} \right)^2 - \frac{\omega^2 e^{\lambda-\nu}}{c^2} + r^2 e^\nu \frac{d}{dr} \left(\frac{e^{-\lambda}}{r^2} \frac{d\nu}{dr} \right) \right). \quad (2.417)$$

Note that, if Poisson equation (2.163) for the equilibrium model parameters ϱ_0 and g_0 is used, the Newtonian limit $\{e^\lambda, e^\nu\} \rightarrow 1$, $c^2 \rightarrow \infty$ and $c^2 \frac{d\nu}{dr} \rightarrow g_0$ of the set of matrices (2.415) – (2.417) gives the Cowling approximated Newtonian equations of motion (2.309) – (2.314).

This section demonstrates that the symplectic structure that is present in the Newtonian equations of motion also occurs in the Cowling approximated relativistic equations of motion in the case of a perfect fluid neutron star model. It will soon turn out that this is no coincidence: in the next section, the equations of motion for an elastic crust will be determined and these equations will turn out to have the same symplectic structure.

2.5 Symmetric formulation of the equations of motion of a relativistic linearly elastic stellar model in the Cowling approximation

When it is assumed that a neutron star model has an elastic crust, this is incorporated in the general relativistic framework by adding a shear stress component $2\mu\Sigma$ to the stress-energy tensor (F.17) of a perfect fluid. This leads to the stress-energy tensor for an elastic solid (G.50)

$$T_{\alpha\beta} = \left(\varrho_0 + \frac{P_0}{c^2} \right) u_\alpha u_\beta - P_0 g_{\alpha\beta} + 2\mu \Sigma_{\alpha\beta}. \quad (2.418)$$

This adds an extra term to the relativistic Euler equation, which becomes of the form (G.54)

$$\sum_\alpha (\varrho + p) u^\alpha u_{\nu;\alpha} = \partial_\nu p - \sum_\alpha u_\nu u^\alpha (\partial_\alpha p) - \sum_\alpha (2\mu \Sigma_\nu^\alpha{}_{;\alpha}). \quad (2.419)$$

Since the Cowling approximation is applied, this equation is worked out by using the expressions for the velocity (2.353) – (2.356), (2.360), (2.361) and metric

(2.342) used the fluid case. The displacement ζ is again expanded in spherical harmonics with $m = 0$, just like in the previous section:

$$\zeta^r = U(r, t)P_l(\cos \theta), \quad (2.420)$$

$$\zeta^\theta = \frac{1}{r}V(r, t)\frac{\partial P_l(\cos \theta)}{\partial \theta}, \quad (2.421)$$

$$\zeta^\phi = 0, \quad (2.422)$$

where the definitions for the eigenfunctions U and V are such that they coincide with their Newtonian counterparts in the Newtonian limit of the equations. When compared to the expression (2.193) for \mathbf{s}_θ , the extra factor of $\frac{1}{r}$ arising in equation (2.421) for the azimuthal equation occurs because ζ^θ is the angular displacement in radians, whereas \mathbf{s}_θ is the displacement in length units. As explained in appendix G.2, the projection tensor \mathbf{P} as defined in equation (G.53)

$$P_{\alpha\beta} = g_{\alpha\beta} - u_\alpha u_\beta / c^2. \quad (2.423)$$

and the rate of shear $\boldsymbol{\sigma}$ as defined in equation (G.52)

$$\sigma_{\mu\nu} = \frac{1}{2} \sum_\alpha \left[(P_\mu^\alpha D_\alpha u_\nu + P_\nu^\alpha D_\alpha u_\mu) - \frac{1}{3} P_{\mu\nu} D_\alpha u^\alpha \right], \quad (2.424)$$

need to be calculated and then integrated to find the shear tensor $\boldsymbol{\Sigma}$, which is defined in (G.51):

$$\Sigma_{\alpha\beta} = e^\nu \int_0^t \sigma_{\alpha\beta} dt'. \quad (2.425)$$

The projection tensor \mathbf{P} is, to first order in the displacement:

$$P_{\alpha\beta} = \frac{1}{c^2} \begin{pmatrix} 0 & -u_t u_r & -u_t u_\theta & -u_t u_\phi \\ -u_t u_r & g_{rr} c^2 & 0 & 0 \\ -u_t u_\theta & 0 & g_{\theta\theta} c^2 & 0 \\ -u_t u_\phi & 0 & 0 & g_{\phi\phi} c^2 \end{pmatrix}. \quad (2.426)$$

The relevant, nonzero components of the rate of shear are σ_r^r , σ_θ^r , σ_θ^θ and σ_ϕ^ϕ . Using equation (2.424), the Christoffel symbols (2.45) – (2.48) and the expressions for the four-velocity and -displacement components, the linearized rate of shear is calculated, beginning with σ_r^r :

$$\sigma_r^r = \frac{1}{2} \sum_\alpha \left[(P_r^\alpha u^r{}_{;\alpha} + P^{\alpha r} u_{r;\alpha}) - \frac{1}{3} P_r^r u^\alpha{}_{;\alpha} \right] \quad (2.427)$$

$$= \sum_\alpha \left[P_r^\alpha u^r{}_{;\alpha} - \frac{1}{3} u^\alpha{}_{;\alpha} \right], \quad (2.428)$$

$$= P_r^t u^r ;_t + u^r ;_r - \frac{1}{3} \sum_{\alpha} u^{\alpha} ;_{\alpha} \quad (2.429)$$

$$= -u^t u_r \left(\partial_t u^r + \sum_{\alpha} \Gamma_{t\alpha}^r u^{\alpha} \right) + \partial_r u^r + \sum_{\alpha} \Gamma_{r\alpha}^r u^{\alpha} - \frac{1}{3} \sum_{\alpha} u^{\alpha} ;_{\alpha} \quad (2.430)$$

$$= e^{-\nu} \left(\partial_r \frac{\partial U}{\partial t} + \frac{d\lambda}{dr} \frac{\partial U}{\partial t} \right) P_l(\cos \theta) - \frac{1}{3} \sum_{\alpha} u^{\alpha} ;_{\alpha} \quad (2.431)$$

$$= e^{-\nu} \left(\frac{2}{3} \partial_r \frac{\partial U}{\partial t} + \frac{2}{3} (\partial_r \lambda) \frac{\partial U}{\partial t} + \frac{1}{3} \frac{\ell(\ell+1)}{r} \frac{\partial V}{\partial t} - \frac{2}{3r} \frac{\partial U}{\partial t} \right) P_l(\cos \theta), \quad (2.432)$$

where in the last step, equation (2.382) for the divergence of the velocity has been used. The linearized component σ_{θ}^r is:

$$\sigma_{\theta}^r = \frac{1}{2} \sum_{\alpha} \left(P_{\theta}^{\alpha} u^r ;_{\alpha} + P^{\alpha r} u_{\theta ; \alpha} \right) \quad (2.433)$$

$$= \frac{1}{2} \left(-u^r u^t u_{\theta ; t} + g^{rr} u_{\theta ; r} - u_{\theta} u^t u^r ;_t + u^r ;_{\theta} \right) \quad (2.434)$$

$$= \frac{1}{2} \left(\left(\partial_r u_{\theta} - \frac{u_{\theta}}{r} \right) g^{rr} - (u^t)^2 u_{\theta} c^2 \frac{dv}{dr} e^{2(\nu-\lambda)} + \partial_{\theta} u^r - r e^{-2\lambda} u^{\theta} \right) \quad (2.435)$$

$$= \frac{1}{2} \left(e^{-2\lambda-\nu} \partial_r \left(r \frac{\partial V}{\partial t} \right) - 2e^{-2\lambda} e^{-\nu} \frac{\partial V}{\partial t} + e^{-\nu} \frac{\partial U}{\partial t} \right) \partial_{\theta} P_l(\cos \theta) \quad (2.436)$$

$$= \frac{1}{2} \left(e^{-\nu} \frac{\partial U}{\partial t} + r^2 e^{-2\lambda-\nu} \partial_r \left(\frac{1}{r} \frac{\partial V}{\partial t} \right) \right) \partial_{\theta} P_l(\cos \theta). \quad (2.437)$$

The linearized component σ_{θ}^{θ} is:

$$\sigma_{\theta}^{\theta} = \frac{1}{2} \sum_{\alpha} \left(P_{\theta}^{\alpha} u^{\theta} ;_{\alpha} + P^{\alpha \theta} u_{\theta ; \alpha} \right) - \sum_{\alpha} \frac{1}{3} P_{\theta}^{\theta} u^{\alpha} ;_{\alpha} \quad (2.438)$$

$$= \sum_{\alpha} \left(P^{\alpha \theta} u_{\theta ; \alpha} - \frac{1}{3} \sum_{\alpha} u^{\alpha} ;_{\alpha} \right), \quad (2.439)$$

$$= u^{\theta} ;_{\theta} - \frac{1}{3} \sum_{\alpha} u^{\alpha} ;_{\alpha}, \quad (2.440)$$

$$= \frac{e^{-\nu}}{r} \frac{\partial V}{\partial t} \partial_{\theta}^2 P_l(\cos \theta) + \frac{e^{-\nu}}{r} \frac{\partial U}{\partial t} P_l(\cos \theta) - \frac{1}{3} \sum_{\alpha} u^{\alpha} ;_{\alpha}, \quad (2.441)$$

$$= e^{-\nu} \left\{ \frac{1}{3} \left[\left(\frac{1}{r} - \frac{d\lambda}{dr} - \partial_r \right) \frac{\partial U}{\partial t} + \frac{\ell(\ell+1)}{r} \frac{\partial V}{\partial t} \right] + \frac{1}{r} \frac{\partial V}{\partial t} \partial_{\theta}^2 \right\} P_l(\cos \theta). \quad (2.442)$$

The linearized component σ_{ϕ}^{ϕ} is:

$$\sigma_{\phi}^{\phi} = P^{\alpha \phi} u_{\phi ; \alpha} - \frac{1}{3} \sum_{\alpha} u^{\alpha} ;_{\alpha} \quad (2.443)$$

$$= u^{\phi} ;_{\phi} - \frac{1}{3} \sum_{\alpha} u^{\alpha} ;_{\alpha} \quad (2.444)$$

$$= \frac{e^{-\nu}}{r} \frac{\partial U}{\partial t} P_l(\cos \theta) + \frac{e^{-\nu}}{r} \frac{\partial V}{\partial t} \cot \theta \partial_{\theta} P_l(\cos \theta) - \frac{1}{3} \sum_{\alpha} u^{\alpha} ;_{\alpha} \quad (2.445)$$

$$= e^{-\nu} \left\{ \frac{1}{3} \left[\left(\frac{1}{r} - \frac{d\lambda}{dr} - \partial_r \right) \frac{\partial U}{\partial t} + \frac{\ell(\ell+1)}{r} \frac{\partial V}{\partial t} \right] + \frac{\cot \theta}{r} \frac{\partial V}{\partial t} \partial_{\theta} \right\} P_l(\cos \theta). \quad (2.446)$$

The shear tensor components are found by using equation (2.425):

$$\Sigma_r^r = \frac{1}{3} \left(2r e^{-\lambda} \frac{d}{dr} \left(\frac{e^\lambda U}{r} \right) + \frac{\ell(\ell+1)V}{r} \right) P_l(\cos \theta) \quad (2.447)$$

$$= \left\{ e^{-\lambda} \frac{d}{dr} \left(e^\lambda U \right) + \frac{1}{3r} \left(\ell(\ell+1)V - \frac{e^{-\lambda}}{r} \frac{d}{dr} \left(r^2 e^\lambda U \right) \right) \right\} P_l(\cos \theta) \quad (2.448)$$

$$\Sigma_\theta^r = \frac{1}{2} \left(U + r^2 e^{-2\lambda} \partial_r \left(\frac{V}{r} \right) \right) \partial_\theta P_l(\cos \theta) \quad (2.449)$$

$$\Sigma_\theta^\theta = \left\{ \frac{1}{3} \left[\left(\frac{1}{r} - \frac{d\lambda}{dr} \right) U - \frac{\partial U}{\partial r} + \frac{\ell(\ell+1)}{r} V \right] + \frac{V}{r} \partial_\theta^2 \right\} P_l(\cos \theta) \quad (2.450)$$

$$\Sigma_\phi^\phi = \left\{ \frac{1}{3} \left[\left(\frac{1}{r} - \frac{d\lambda}{dr} \right) U - \frac{\partial U}{\partial r} + \frac{\ell(\ell+1)}{r} V \right] + \frac{\cot \theta}{r} V \partial_\theta \right\} P_l(\cos \theta). \quad (2.451)$$

Now the elastic term $\sum_\alpha D_\alpha (2\mu \Sigma_\nu^\alpha)$ in the relativistic Euler equations (G.54) follows. The $\nu = r$ component is:

$$\begin{aligned} \sum_\alpha (2\mu \Sigma_r^\alpha{}_{;\alpha}) &= \sum_{\alpha,\beta} \left[\partial_\alpha (2\mu \Sigma_r^\alpha) + 2\mu \left(\Gamma_{\alpha\beta}^\alpha \Sigma_r^\beta - \Gamma_{\alpha r}^\beta \Sigma_\beta^\alpha \right) \right], \quad (2.452) \\ &= \partial_r (2\mu \Sigma_r^r) + \\ &\quad + 2\mu \left\{ \partial_\theta \Sigma_r^\theta + \left(\Gamma_{tr}^t + \Gamma_{rr}^r + \Gamma_{\theta r}^\theta + \Gamma_{\phi r}^\phi \right) \Sigma_r^r + \right. \\ &\quad \left. + \Gamma_{\phi\theta}^\phi \Sigma_r^\theta - \Gamma_{rr}^r \Sigma_r^r - \Gamma_{\theta r}^\theta \Sigma_\theta^\theta - \Gamma_{\phi r}^\phi \Sigma_\phi^\phi \right\}. \quad (2.453) \end{aligned}$$

This equation is now further worked out using expressions (2.45) – (2.48) for the Christoffel symbols and the shear tensor components (2.447) – (2.451):

$$\begin{aligned} \sum_\alpha (2\mu \Sigma_r^\alpha{}_{;\alpha}) &= \partial_r \left\{ 2\mu e^{-\lambda} \frac{d}{dr} \left(e^\lambda U \right) + \right. \\ &\quad + \frac{2\mu}{3r} \left[\ell(\ell+1)V - \frac{e^{-\lambda}}{r} \frac{d}{dr} \left(r^2 e^\lambda U \right) \right] \left. \right\} P_l(\cos \theta) \\ &\quad + 2\mu \left\{ g^{\theta\theta} g_{rr} \frac{1}{2} \left(U + r^2 e^{-2\lambda} \partial_r \left(\frac{V}{r} \right) \right) \partial_\theta^2 P_l(\cos \theta) \right. \\ &\quad + \left(\frac{dV}{dr} + \frac{2}{r} V \right) \left(e^{-\lambda} \frac{d}{dr} \left(e^\lambda U \right) \right) \\ &\quad + \frac{1}{3r} \left(\ell(\ell+1)V - \frac{e^{-\lambda}}{r} \frac{d}{dr} \left(r^2 e^\lambda U \right) \right) \left. \right\} P_l(\cos \theta) \\ &\quad + g^{\theta\theta} g_{rr} \frac{1}{2} \left(U + r^2 e^{-2\lambda} \partial_r \left(\frac{V}{r} \right) \right) \cot \theta \partial_\theta P_l(\cos \theta) \\ &\quad - \frac{1}{r} \left[\frac{V}{r} \partial_\theta^2 P_l(\cos \theta) + \frac{V}{r} \cot \theta \partial_\theta P_l(\cos \theta) \right. \\ &\quad \left. + \frac{2}{3} \left(\frac{U}{r} + \frac{\ell(\ell+1)V}{r} - \frac{d\lambda}{dr} U - \frac{dU}{dr} \right) P_l(\cos \theta) \right] \left. \right\}, \quad (2.454) \\ &= \partial_r \left\{ 2\mu e^{-\lambda} \frac{d}{dr} \left(e^\lambda U \right) \right. \\ &\quad + \frac{2\mu}{3r} \left[\ell(\ell+1)V - \frac{e^{-\lambda}}{r} \frac{d}{dr} \left(r^2 e^\lambda U \right) \right] \left. \right\} P_l(\cos \theta) \\ &\quad + 2\mu \left\{ - \frac{\ell(\ell+1)e^{2\lambda}}{2r^2} \left(U + r^2 e^{-2\lambda} \partial_r \left(\frac{V}{r} \right) \right) + \frac{\ell(\ell+1)V}{r^2} \right. \\ &\quad + \left(\frac{dV}{dr} + \frac{2}{r} V \right) \left(e^{-\lambda} \frac{d}{dr} \left(e^\lambda U \right) \right) + \frac{1}{3r} \left(\ell(\ell+1)V \right. \\ &\quad \left. - e^{-\lambda} \frac{d}{dr} \left(r^2 e^\lambda U \right) \right) - \frac{2}{3r^2} \left(3U - \frac{e^{-\lambda}}{r} \frac{d}{dr} \left(r^2 e^\lambda U \right) \right. \\ &\quad \left. + \ell(\ell+1)V \right\} P_l(\cos \theta), \quad (2.455) \end{aligned}$$

$$\begin{aligned}
&= \partial_r \left\{ 2\mu e^{-\lambda} \frac{d}{dr} (e^\lambda U) \right. \\
&\quad + \frac{2\mu}{3r} \left[\ell(\ell+1)V - \frac{e^{-\lambda}}{r} \frac{d}{dr} (r^2 e^\lambda U) \right] \left. \right\} P_l(\cos \theta) \\
&\quad + 2\mu \left\{ -\frac{\ell(\ell+1)e^{2\lambda}}{2r^2} \left(U + r^2 e^{-2\lambda} \partial_r \left(\frac{V}{r} \right) \right) + \frac{\ell(\ell+1)V}{r^2} \right. \\
&\quad + \frac{dv}{dr} \left(e^{-\lambda} \frac{d}{dr} (e^\lambda U) \right) + \frac{1}{3r} \left(\ell(\ell+1)V - \frac{e^{-\lambda}}{r} \frac{d}{dr} (r^2 e^\lambda U) \right) \left. \right\} \\
&\quad + \frac{2}{r} \left(e^{-\lambda} \frac{d}{dr} (e^\lambda U) \right) - \frac{2U}{r^2} \left. \right\} P_l(\cos \theta). \tag{2.456}
\end{aligned}$$

In the second step, the identity (2.380)

$$\left(\partial_\theta^2 + \cot \theta \partial_\theta \right) P_l(\cos \theta) = -\ell(\ell+1)P_l(\cos \theta), \tag{2.457}$$

is used. Likewise, the $\nu = \theta$ component is:

$$\sum_\alpha (2\mu \Sigma_\theta^\alpha{}_{;\alpha}) = \sum_{\alpha,\beta} \left[\partial_\alpha (2\mu \Sigma_\theta^\alpha) + 2\mu \left(\Gamma_{\alpha\beta}^\alpha \Sigma_\theta^\beta - \Gamma_{\alpha\theta}^\beta \Sigma_\beta^\alpha \right) \right], \tag{2.458}$$

$$= \partial_r (2\mu \Sigma_\theta^r) + \tag{2.459}$$

$$\begin{aligned}
&+ 2\mu \left\{ \partial_\theta \Sigma_\theta^\theta + \left(\Gamma_{tr}^t + \Gamma_{rr}^r + \Gamma_{\theta r}^\theta + \Gamma_{\phi r}^\phi \right) \Sigma_\theta^r + \right. \\
&\quad \left. + \Gamma_{\phi\theta}^\phi \Sigma_\theta^\theta - \Gamma_{r\theta}^\theta \Sigma_\theta^r - \Gamma_{\theta\theta}^r \Sigma_r^\theta - \Gamma_{\phi\theta}^\phi \Sigma_\phi^\phi \right\} \tag{2.460}
\end{aligned}$$

$$\begin{aligned}
&= \partial_r (2\mu \Sigma_\theta^r) + 2\mu \left\{ \partial_\theta \Sigma_\theta^\theta + \left(\Gamma_{tr}^t + \Gamma_{rr}^r + \Gamma_{\phi r}^\phi \right. \right. \\
&\quad \left. \left. - g^{\theta\theta} g_{rr} \Gamma_{\theta\theta}^r \right) \Sigma_\theta^r + \Gamma_{\phi\theta}^\phi \left(\Sigma_\theta^\theta - \Sigma_\phi^\phi \right) \right\}. \tag{2.461}
\end{aligned}$$

In the third step it is used that $\Sigma_r^\theta = g^{\theta\theta} g_{rr} \Sigma_\theta^r$ to first order in the perturbations. The derivative of equation (2.457)

$$\left[\partial_\theta^3 + \cot \theta \partial_\theta^2 P_l - \cot^2 \theta \partial_\theta \right] P_l(\cos \theta) = [1 - \ell(\ell+1)] \partial_\theta P_l(\cos \theta), \tag{2.462}$$

is used to work out the $\nu = \theta$ component of the relativistic Euler equation:

$$\begin{aligned}
\sum_\alpha (2\mu \Sigma_\theta^\alpha{}_{;\alpha}) &= \partial_r \left(\mu \left(U + r^2 e^{-2\lambda} \partial_r \left(\frac{V}{r} \right) \right) \right) \partial_\theta P_l(\cos \theta) + \frac{2\mu V}{r} \partial_\theta^3 P_l(\cos \theta) \\
&\quad + \frac{2\mu}{3} \left(\frac{U}{r} + \frac{\ell(\ell+1)V}{r} - \frac{d\lambda}{dr} U - \frac{dU}{dr} \right) \partial_\theta P_l(\cos \theta) \\
&\quad + \left(\frac{dv}{dr} + \frac{d\lambda}{dr} + \frac{2}{r} \right) \mu \left(U + r^2 e^{-2\lambda} \partial_r \left(\frac{V}{r} \right) \right) \partial_\theta P_l(\cos \theta) \\
&\quad + 2\mu \cot \theta \left(\frac{V}{r} \partial_\theta^2 P_l(\cos \theta) - \frac{\cot \theta}{r} V \partial_\theta P_l(\cos \theta) \right) \tag{2.463} \\
&= \partial_r \left(\mu \left(U + r^2 e^{-2\lambda} \partial_r \left(\frac{V}{r} \right) \right) \right) \partial_\theta P_l(\cos \theta) \\
&\quad - \frac{2\mu}{3r} \left(\frac{e^{-\lambda}}{r} \frac{d}{dr} (r^2 e^\lambda U) - \ell(\ell+1)V - 3U \right) \partial_\theta P_l(\cos \theta) \\
&\quad + \left(\frac{dv}{dr} + \frac{d\lambda}{dr} + \frac{2}{r} \right) \mu \left(U + r^2 e^{-2\lambda} \partial_r \left(\frac{V}{r} \right) \right) \partial_\theta P_l(\cos \theta) \\
&\quad - [\ell(\ell+1) - 1] \frac{2\mu V}{r} \partial_\theta P_l(\cos \theta). \tag{2.464}
\end{aligned}$$

The equations of motion now follow by adding the elastic part $\sum_{\alpha} (2\mu\Sigma_{\beta}^{\alpha};\alpha)$ to the previously derived Euler equations for the perturbation of a perfect fluid sphere. For the radial component, take equation (2.400). The relativistic Euler equations for an elastic solid indicate that the right hand side of this equation is not zero, but equal to $\sum_{\alpha} D_{\alpha} (2\mu\Sigma_r^{\alpha})$. For the radial component, this leads to:

$$\begin{aligned}
& \left(\varrho_0 + \frac{P_0}{c^2} \right) e^{2(\lambda-\nu)} \omega^2 U + \frac{d\nu}{dr} \frac{\kappa}{r} \left(\frac{e^{-\lambda}}{r} \frac{d}{dr} (e^{\lambda} r^2 U) - l(l+1)V \right) + \\
& + \frac{d}{dr} \left\{ \frac{\kappa}{r} \left(\frac{e^{-\lambda}}{r} \frac{d}{dr} (e^{\lambda} r^2 U) - \ell(\ell+1)V \right) \right\} - (P_0 + \varrho_0 c^2) \frac{d}{dr} \left(\frac{e^{-\lambda}}{r^2} \frac{d\nu}{dr} \right) e^{\lambda} r^2 U \\
& - \frac{1}{r} \frac{d\nu}{dr} (P_0 + \varrho_0 c^2) \ell(\ell+1)V + \partial_r \left\{ 2\mu e^{-\lambda} \frac{d}{dr} (e^{\lambda} U) + \right. \\
& \quad \left. + \frac{2\mu}{3r} \left[\ell(\ell+1)V - \frac{e^{-\lambda}}{r} \frac{d}{dr} (r^2 e^{\lambda} U) \right] \right\} + \\
& + 2\mu \left\{ - \frac{\ell(\ell+1)e^{2\lambda}}{2r^2} \left(U + r^2 e^{-2\lambda} \partial_r \left(\frac{V}{r} \right) \right) + \frac{\ell(\ell+1)V}{r^2} + \right. \\
& + \frac{d\nu}{dr} \left(e^{-\lambda} \frac{d}{dr} (e^{\lambda} U) + \frac{1}{3r} \left(\ell(\ell+1)V - \frac{e^{-\lambda}}{r} \frac{d}{dr} (r^2 e^{\lambda} U) \right) \right) \left. \right\} + \\
& + \frac{2}{r} \left(e^{-\lambda} \frac{d}{dr} (e^{\lambda} U) \right) - \frac{2U}{r^2} \Big\} = 0. \quad (2.465)
\end{aligned}$$

Just like in the Newtonian case, the equations are more conveniently expressed in terms of the radial and azimuthal Lagrangian stress perturbations. These are given by Δt_r^r and $\frac{1}{r} \Delta t_r^{\theta}$. This leads to the following definitions for radial stress R and azimuthal stress S :

$$R = \frac{1}{r} \left(\kappa - \frac{2\mu}{3} \right) \left[\frac{e^{-\lambda}}{r} \frac{d}{dr} (r^2 e^{\lambda} U) - l(l+1)V \right] + 2\mu e^{-\lambda} \frac{d}{dr} (e^{\lambda} U) \quad (2.466)$$

$$= \left(\kappa + \frac{4\mu}{3} \right) e^{-\lambda} \frac{d}{dr} (e^{\lambda} U) + \left(\kappa - \frac{2\mu}{3} \right) \left(\frac{2U}{r} - \frac{l(l+1)V}{r} \right), \quad (2.467)$$

$$S = \frac{\mu}{r} \left(U + r^2 e^{-2\lambda} \frac{d}{dr} \left(\frac{V}{r} \right) \right). \quad (2.468)$$

Note that the Newtonian limit of these expressions coincides with the Newtonian definitions (2.223) and (2.225). Note that the following helpful identity follows from these definitions:

$$e^{-\lambda} \frac{d}{dr} (e^{\lambda} U) = \left(\kappa + \frac{4\mu}{3} \right)^{-1} R - \frac{\kappa - 2\mu/3}{\kappa + 4\mu/3} \left(\frac{2U}{r} - \frac{l(l+1)V}{r} \right). \quad (2.469)$$

This identity used in equation (2.465) leads to the following equation for the derivative of the radial stress component R :

$$\begin{aligned}
\frac{dR}{dr} = & \left\{ \frac{12\mu\kappa}{r^2} \left(\kappa + \frac{4\mu}{3} \right)^{-1} + (P_0 + \varrho_0 c^2) \left[e^{\lambda} r^2 \frac{d}{dr} \left(\frac{e^{-\lambda}}{r^2} \frac{d\nu}{dr} \right) - e^{2(\lambda-\nu)} \frac{\omega^2}{c^2} \right] \right\} U + \\
& + \left\{ \frac{d\nu}{dr} (P_0 + \varrho_0 c^2) - \frac{6\mu\kappa}{r} \left(\kappa + \frac{4\mu}{3} \right)^{-1} \right\} V - \left\{ \frac{d\nu}{dr} + \frac{4\mu}{r} \left(\kappa + \frac{4\mu}{3} \right)^{-1} \right\} R \\
& - \frac{l(l+1)}{r} e^{2\lambda} S. \quad (2.470)
\end{aligned}$$

For the azimuthal component of the differential equations, the azimuthal component (2.402) of the relativistic Euler equation for a perfect fluid is taken and for the right hand side $\sum_{\alpha} D_{\alpha} (2\mu\Sigma_{\theta}^{\alpha})$ is chosen instead of zero. This leads to:

$$\begin{aligned} & -\frac{\omega^2}{c^2} (P_0 + \varrho_0 c^2) e^{-2\nu} V r - \left\{ \frac{\kappa}{r} \left(\frac{e^{-\lambda}}{r} \frac{d}{dr} (r^2 e^{\lambda} U) - \ell(\ell+1)V \right) - \frac{d\nu}{dr} (P_0 + \varrho_0 c^2) U \right\} \\ & - \frac{d}{dr} (rS) + \frac{2\mu}{3r} \left(\frac{e^{-\lambda}}{r} \frac{d}{dr} (r^2 e^{\lambda} U) - \ell(\ell+1)V - 3U \right) \\ & - \left(\frac{d\nu}{dr} + \frac{d\lambda}{dr} + \frac{2}{r} \right) rS + [\ell(\ell+1) - 1] \frac{2\mu}{r} V = 0. \quad (2.471) \end{aligned}$$

Using the definition of R , it is recognized that

$$\begin{aligned} & -\frac{\kappa}{r} \left(\frac{e^{-\lambda}}{r} \frac{d}{dr} (r^2 e^{\lambda} U) - \ell(\ell+1)V \right) + \frac{2\mu}{3r} \left(\frac{e^{-\lambda}}{r} \frac{d}{dr} (r^2 e^{\lambda} U) - \ell(\ell+1)V \right) = \\ & = -R + 2\mu e^{-\lambda} \frac{d}{dr} (e^{\lambda} U). \quad (2.472) \end{aligned}$$

This leads to the following equation for the derivative of S :

$$\begin{aligned} \frac{d}{dr} (Sr) &= \left\{ \frac{d\nu}{dr} (P_0 + \varrho_0 c^2) - \frac{12\mu\kappa}{r} \left(\kappa + \frac{4\mu}{3} \right)^{-1} \right\} U + \\ &+ \left\{ \frac{2\mu}{r} \left[\ell(\ell+1) \left(1 + \frac{\kappa-2\mu/3}{\kappa+4\mu/3} \right) - 1 \right] \right\} V + \\ &+ \frac{2\mu/3-\kappa}{4\mu/3+\kappa} R - \left\{ \frac{d\nu}{dr} + \frac{d\lambda}{dr} + \frac{2}{r} \right\} Sr. \quad (2.473) \end{aligned}$$

Now the differential equations governing the Cowling-approximated relativistic crust are reduced to a set of four coupled first order differential equations. Like in all other cases, these equations are put in the form (1.1, 1.2) with symplectic structure.

The equations in symplectic form are:

$$\frac{d\mathbf{y}}{dr} = \mathbf{A}\mathbf{y}, \quad (2.474)$$

with

$$\mathbf{y} = \begin{pmatrix} e^{\lambda} U r \\ e^{\lambda} V r \sqrt{\ell(\ell+1)} \\ e^{\nu} R r \\ e^{\nu} S r \sqrt{\ell(\ell+1)} \end{pmatrix}, \quad (2.475)$$

and

$$\mathbf{A} = \begin{pmatrix} \mathbf{T} & \mathbf{K} \\ \mathbf{S} & -\mathbf{T}^T \end{pmatrix}, \quad (2.476)$$

where \mathbf{T} , \mathbf{K} and \mathbf{S} are matrices given by

$$\mathbf{T} = \begin{pmatrix} \frac{1}{r} \frac{8\mu-3\kappa}{4\mu+3\kappa} & \frac{\sqrt{\ell(\ell+1)}}{r} \frac{3\kappa-2\mu}{3\kappa+4\mu} \\ -e^{2\lambda} \frac{\sqrt{\ell(\ell+1)}}{r} & \frac{d\lambda}{dr} + \frac{2}{r} \end{pmatrix}, \quad (2.477)$$

$$\mathbf{K} = \begin{pmatrix} e^{\lambda-\nu} \left(\kappa + \frac{4\mu}{3}\right)^{-1} & 0 \\ 0 & e^{3\lambda-\nu} \mu^{-1} \end{pmatrix}, \quad (2.478)$$

$$\mathbf{S} = \begin{pmatrix} S_{11} & S_{21} \\ S_{21} & S_{22} \end{pmatrix}, \quad (2.479)$$

and \mathbf{S} is symmetric, with components:

$$S_{11} = \frac{4\gamma e^{\nu-\lambda}}{r^2} + \left(\varrho_0 c^2 + P_0\right) \left(r^2 e^\nu \frac{d}{dr} \left(\frac{e^{-\lambda}}{r^2} \frac{d\nu}{dr}\right) - \frac{e^{\lambda-\nu} \omega^2}{c^2}\right), \quad (2.480)$$

$$S_{21} = \frac{e^{\nu-\lambda} \sqrt{\ell(\ell+1)}}{r} \left(\frac{d\nu}{dr} \left(\varrho_0 c^2 + P_0\right) - \frac{2\gamma}{r}\right), \quad (2.481)$$

$$S_{22} = ((\gamma + \mu)\ell(\ell + 1) - 2\mu) \frac{e^{\nu-\lambda}}{r^2} - \left(\varrho_0 c^2 + P_0\right) \frac{e^{-(\nu+\lambda)} \omega^2}{c^2}, \quad (2.482)$$

where $\gamma = 3\mu\kappa \left(\kappa + \frac{4\mu}{3}\right)^{-1}$. Note that, if Poisson equation (2.163) for the equilibrium model parameters ϱ_0 and g_0 is used, the Newtonian limit $\{e^\lambda, e^\nu\} \rightarrow 1$, $c^2 \rightarrow \infty$ and $c^2 \frac{d\nu}{dr} \rightarrow g_0$ of the set of matrices (2.477) – (2.482) gives the Cowling approximated Newtonian equations of motion (2.296) – (2.301).

The limit $\mu \rightarrow 0$ for a perfect fluid should lead to the previously derived equations of motion for a perfect relativistic fluid in the relativistic Cowling approximation. Indeed, the following equation for y_2 is found from the fact that $y_5 = 0$:

$$y_2 = (T_{12}y_4 - S_{12}y_1) / S_{22}, \quad (2.483)$$

which leads to the equations

$$\frac{dy_1}{dr} = \left(T_{11} - \frac{T_{12}S_{21}}{S_{22}}\right) y_1 + \left(\frac{T_{12}^2}{S_{22}} + K_{11}\right) y_4, \quad (2.484)$$

$$\frac{dy_4}{dr} = \left(S_{11} - \frac{S_{21}^2}{S_{22}}\right) y_1 + \left(\frac{S_{12}T_{12}}{S_{22}} - T_{11}\right) y_4. \quad (2.485)$$

These equations reduce to the relativistic equations (2.412) – (2.417) for a perfect fluid in the $\mu \rightarrow 0$ limit.

This shows that the symplectic structure present in all oscillation equations thus far is also present when a relativistic elastic crust is added to the model. This section concludes the theoretical review on the relativistic equations of motion in the Cowling approximation for fluids and solids. In the next section, boundary conditions that hold for neutron stars will be discussed. With the help of this boundary conditions, it will be possible to calculate the oscillation spectrum of neutron stars.

2.6 Boundary conditions for relativistic stellar oscillations

Like in the case of the Newtonian equations of motion, boundary conditions are needed to find the spectrum of oscillations. This section is ordered in exactly the same way as the section on boundary conditions of the Newtonian equations of motion. First the conditions that follow from regularity of the oscillations in the core will be discussed. Then the conditions on internal boundaries will be given and the conditions on the free surface will be discussed.

Because the Cowling-approximation is used, the regularity conditions will lead to one starting solution $\mathbf{y}^{(1)}(r_1)$ at a small radius r_1 that satisfies the regularity conditions, instead of two in the exact case. In case the model has a solid crust, an extra starting value $\mathbf{y}^{(3)}(r_{CCB})$ is added at the core-crust boundary located at r_{CCB} .

In the following sections the details of the boundary conditions at the center and on interfaces and the free surface are derived.

2.6.1 Regularity conditions at the center of the model

The differential equations for relativistic oscillations allow for unwanted solutions that are singular at the center of the model. Since the core of the relativistic neutron star models considered in this study is fluid, the conditions for regularity of the solution will be derived for a fluid core. From equations (2.410) and (2.411), it follows that

$$\begin{aligned} \left(\frac{P_0}{c^2} + \varrho_0\right)^{-1} \frac{d}{dr} \left(R - c^2 \frac{d\nu}{dr} \left[\frac{P_0}{c^2} + \varrho_0 \right] U \right) = -c^2 \frac{d\nu}{dr} \left\{ \frac{1}{\kappa} + \left(\frac{P_0}{c^2} + \varrho_0 \right)^{-1} \right\} R + \\ + \left\{ -\omega^2 e^{2(\lambda-\nu)} + c^2 \left(\frac{d\nu}{dr} \right)^2 - c^2 \left(\frac{P_0}{c^2} + \varrho_0 \right)^{-1} \frac{d\nu}{dr} \frac{d\varrho_0}{dr} \right\} U. \quad (2.486) \end{aligned}$$

From equation (2.410) it follows that

$$\frac{d}{dr} (r^2 U) = -\frac{\ell(\ell+1)e^{2\nu}}{\omega^2} \left(\frac{P_0}{c^2} + \varrho_0 \right)^{-1} \left(R - c^2 \frac{d\nu}{dr} \left[\frac{P_0}{c^2} + \varrho_0 \right] U \right) + \frac{r^2}{\kappa} R - r^2 \frac{d\lambda}{dr} U. \quad (2.487)$$

To derive the conditions that follow from regularity of the solutions, take the limit $r \rightarrow 0$. The two previous equations become:

$$\left(\frac{P_0}{c^2} + \varrho_0 \right)^{-1} \frac{d}{dr} \left(R - c^2 \frac{d\nu}{dr} \left[\frac{P_0}{c^2} + \varrho_0 \right] U \right) = -\omega^2 e^{2(\lambda-\nu)} U, \quad (2.488)$$

$$\frac{d}{dr} (r^2 U) = -\frac{\ell(\ell+1)e^{2\nu}}{\omega^2} \left(\frac{P_0}{c^2} + \varrho_0 \right)^{-1} \left(R - c^2 \frac{d\nu}{dr} \left[\frac{P_0}{c^2} + \varrho_0 \right] U \right). \quad (2.489)$$

The derivative of equation (2.489) is used and equation (2.488) is used to get

$$\frac{d^2}{dr^2} (r^2 U) = \ell(\ell+1) e^{2\lambda} U. \quad (2.490)$$

At $r = 0$, it follows from (2.55) and (2.56) that $e^{2\lambda} = 1$ at the center of the model. Hence:

$$U = Ar^{-\ell-2} + Br^{\ell-1}, \quad (2.491)$$

where A and B are constants. Because U must be regular at the origin, $A = 0$. Hence:

$$U \sim r^{\ell-1}, \quad (2.492)$$

Now a relation between U , R at $r = 0$ is found. Equation (2.492) is used in the left hand side of equation (2.487) to obtain:

$$U = \frac{\ell e^{2\nu}}{\omega^2 r} \left(\frac{P_0}{c^2} + \varrho_0 \right)^{-1} \left(c^2 \frac{d\nu}{dr} \left(\frac{P_0}{c^2} + \varrho_0 \right) U - R \right). \quad (2.493)$$

The relation (2.493) is equivalent to the following relation between the variables y_1 and y_4 from definition (2.413) of \mathbf{y} :

$$y_1 \left(\frac{\omega^2 r}{\ell e^{2\nu}} - c^2 \frac{d\nu}{dr} \right) + y_4 \left(\frac{P_0}{c^2} + \varrho_0 \right)^{-1} e^{\lambda-\nu} = 0. \quad (2.494)$$

In practice this condition is implemented by choosing a starting value $\mathbf{y}^{(1)}(r_1)$ for integration of the differential equations, that satisfy equations (2.494) at a very small value $r = r_1$. Such a starting value is found by assuming $U = 1$ at $r = r_1$ and hence $y_1 = r_1$ and by using equation (2.494) to find out what the corresponding value for y_4 is. This leads to:

$$\mathbf{y}^{(1)}(r_1) = \begin{pmatrix} y_1^{(1)}(r_1) \\ y_4^{(1)}(r_1) \end{pmatrix} = \begin{pmatrix} r_1 \\ \left(\frac{P_0}{c^2} + \varrho_0 \right) e^{\nu-\lambda} \left(c^2 \frac{d\nu}{dr} - \frac{\omega^2 r_1}{\ell e^{2\nu}} \right) r_1 \end{pmatrix}. \quad (2.495)$$

2.6.1.1 Internal boundary conditions

As starting solution (2.495) is integrated upwards, internal discontinuities such as the boundary between the neutron star fluid core and solid crust, occur. On these discontinuities, the stress-energy tensor is continuous. This implies that the traction vector on radial surfaces is continuous across a boundary in the model and hence R and S must be continuous.

Across a boundary between two solid materials, the displacement must be continuous, because the connection between the two different materials at the boundary must remain intact. Hence U and V must be continuous.

However, when the boundary is between a liquid and a solid, the azimuthal displacement represented by V does not need to be continuous. In the case of the nonradial oscillations of a neutron star, the core is fluid and the crust is solid and the freedom of tangential movement of the solid crust is represented by a third independent starting vector $\mathbf{y}^{(3)}$ for integration at the core-crust boundary, with all components zero except

$$y_2^{(3)}(r_{CCB}) = C, \quad (2.496)$$

where C is an arbitrary constant.

2.6.2 Boundary conditions for the free surface

On the outer or free surface of a neutron star model, stress is assumed to be zero. Because the stress-energy tensor must also be continuous on the outer boundary, it follows that $R = S = 0$ on the free surface.

2.7 Nondimensionalization of equations and boundary conditions

The differential equations of the form

$$\frac{d\mathbf{y}(r)}{dr} = \mathbf{A}(\omega, r)\mathbf{y}(r) \quad (2.497)$$

and starting solutions $\mathbf{y}^{(1)}$, $\mathbf{y}^{(2)}$ and $\mathbf{y}^{(3)}$ that were found in the previous sections are in principle enough to find the oscillation spectrum of neutron stars using numerical methods. In practice, the large numbers associated with the model parameters and

variables in the equations lead to numerical problems. To make the problem more tractable for numerical analysis, nondimensional equations are introduced. The vector \mathbf{y} is replaced by a nondimensional vector $\boldsymbol{\eta}$ of the form:

$$\boldsymbol{\eta} = \begin{pmatrix} y_1/R^2 \\ y_2/R^2 \\ y_3/\pi G \bar{\rho}_0 R^3 \\ y_4/\pi G \bar{\rho}_0^2 R^3 \\ y_5/\pi G \bar{\rho}_0^2 R^3 \\ y_6/\bar{\rho}_0 R^2 \end{pmatrix}, \quad (2.498)$$

where $\bar{\rho}_0$ is the average density, G is the gravitational constant and R is the stellar radius. The frequency ω is replaced by a nondimensional frequency $\Omega = \omega/\sqrt{\pi G \bar{\rho}_0}$. The matrix \mathbf{A} is replaced by a nondimensional matrix $\tilde{\mathbf{A}}$ of the form

$$\tilde{\mathbf{A}} = \begin{pmatrix} \tilde{\mathbf{T}} & \tilde{\mathbf{K}} \\ \tilde{\mathbf{S}} & -\tilde{\mathbf{T}}^T \end{pmatrix}. \quad (2.499)$$

This results in a set of nondimensionalized differential equations of the form

$$\frac{d\boldsymbol{\eta}(x)}{dx} = \tilde{\mathbf{A}}(\Omega, x)\boldsymbol{\eta}(x), \quad (2.500)$$

where $x = r/R$ is the nondimensionalized radial coordinate. In the following two sections, the form of the matrices $\tilde{\mathbf{T}}$, $\tilde{\mathbf{K}}$, $\tilde{\mathbf{S}}$ and starting solutions $\boldsymbol{\eta}^{(1)}$, $\boldsymbol{\eta}^{(2)}$ and $\boldsymbol{\eta}^{(3)}$ will be given for the equations of motion for a perfect fluid and an elastic solid. In each section, both the Newtonian and relativistic versions will be given, as well as the Cowling approximated equations.

2.7.1 Nonrelativistic perfect fluid

Since for a fluid, $\eta_5 = 0$ and η_2 is no longer an independent variable, the following nondimensional vector $\boldsymbol{\eta}$ is used:

$$\boldsymbol{\eta} = \begin{pmatrix} \eta_1 \\ \eta_3 \\ \eta_4 \\ \eta_6 \end{pmatrix} = \begin{pmatrix} y_1/R^2 \\ y_3/\pi G \bar{\rho}_0 R^3 \\ y_4/\pi G \bar{\rho}_0^2 R^3 \\ y_6/\bar{\rho}_0 R^2 \end{pmatrix}. \quad (2.501)$$

In the case a polytropic equation of state is used, the average density $\bar{\rho}_0$ follows from equation (2.38). It now follows that matrices \mathbf{T} , \mathbf{K} and \mathbf{S} given in equations

(2.306) – (2.308) take the following nondimensional from:

$$\tilde{\mathbf{T}} = \begin{pmatrix} \frac{\ell(\ell+1)g_0}{\pi G R \bar{\rho}_0 \Omega^2 x^2} - \frac{1}{x} & \frac{\ell(\ell+1)}{\Omega^2 x^2} \\ -4\rho_0/\bar{\rho}_0 & -l/x \end{pmatrix}, \quad (2.502)$$

$$\tilde{\mathbf{K}} = \begin{pmatrix} \frac{\pi G \bar{\rho}_0^2 R^2}{\kappa} - \frac{\ell(\ell+1)\bar{\rho}_0}{\rho_0 \Omega^2 x^2} & 0 \\ 0 & 4 \end{pmatrix}, \quad (2.503)$$

$$\tilde{\mathbf{S}} = \begin{pmatrix} \frac{\rho_0}{\bar{\rho}_0} \left(\frac{\ell(\ell+1)g_0^2}{(\pi \bar{\rho}_0 G R \Omega x)^2} - \Omega^2 - \frac{4g_0}{\pi G \bar{\rho}_0 R x} \right) & \tilde{S}_{21} \\ \frac{\rho_0}{\bar{\rho}_0} \left(\frac{\ell(\ell+1)g_0}{\pi G \bar{\rho}_0 R \Omega^2 x^2} - \frac{\ell+1}{x} \right) & \frac{\rho_0 \ell(\ell+1)}{\bar{\rho}_0 \Omega^2 x^2} \end{pmatrix}, \quad (2.504)$$

and $\tilde{\mathbf{S}}$ is symmetric. The starting values for integration at the center $\boldsymbol{\eta}^{(1)}(\varepsilon)$ at $x = \varepsilon$ with $\varepsilon \ll 1$ are obtained by nondimensionalizing the starting conditions (2.332) and (2.334). This gives for $\boldsymbol{\eta}^{(1)}(\varepsilon)$:

$$\begin{pmatrix} \eta_1^{(1)} \\ \eta_3^{(1)} \\ \eta_4^{(1)} \\ \eta_6^{(1)} \end{pmatrix} = \begin{pmatrix} \varepsilon \\ -\frac{4\rho_0(\varepsilon)}{\bar{\rho}_0} \frac{\varepsilon^2}{2\ell+1} \\ \frac{\rho_0(\varepsilon)}{\bar{\rho}_0} \left(\frac{8}{3} \frac{\rho_0(\varepsilon)}{\bar{\rho}_0} \frac{\ell-1}{2\ell+1} - \frac{\Omega^2}{\ell} \right) \varepsilon^2 \\ 0 \end{pmatrix}. \quad (2.505)$$

and $\boldsymbol{\eta}^{(2)}(\varepsilon)$:

$$\begin{pmatrix} \eta_1^{(2)} \\ \eta_3^{(2)} \\ \eta_4^{(2)} \\ \eta_6^{(2)} \end{pmatrix} = \begin{pmatrix} 0 \\ \frac{\varepsilon^2}{2\ell+1} \\ \frac{\rho_0(\varepsilon)}{\bar{\rho}_0} \frac{\varepsilon^2}{2\ell+1} \\ \frac{1}{4}\varepsilon \end{pmatrix}, \quad (2.506)$$

At the free surface $x = 1$ it follows from section 2.3.6 that $\eta_4 = \eta_6 = 0$.

2.7.2 Nonrelativistic perfect fluid in the Cowling approximation

The number of independent variables is reduced to two, since $\eta_3 = \eta_5 = 0$ and η_2 and η_6 are no longer independent variables. The nondimensionalized vector $\boldsymbol{\eta}$ is given by:

$$\boldsymbol{\eta} = \begin{pmatrix} \eta_1 \\ \eta_4 \end{pmatrix} = \begin{pmatrix} y_1/R^2 \\ y_4/\pi G \bar{\rho}_0^2 R^3 \end{pmatrix}, \quad (2.507)$$

and the nondimensionalized version of the functions T , K and S given in equations (2.312) – (2.314) is:

$$\tilde{T} = \frac{\ell(\ell+1)g_0}{\pi G R \bar{\varrho}_0 \Omega^2 x^2} - \frac{1}{x}, \quad (2.508)$$

$$\tilde{K} = \frac{\pi G \bar{\varrho}_0^2 R^2}{\kappa}, \quad (2.509)$$

$$\tilde{S} = \frac{\varrho_0}{\bar{\varrho}_0} \left(\frac{\ell(\ell+1)g_0^2}{(\pi \bar{\varrho}_0 G R \Omega x)^2} - \Omega^2 - \frac{4g_0}{\pi G \bar{\varrho}_0 R x} + 4 \frac{\varrho_0}{\bar{\varrho}_0} \right). \quad (2.510)$$

In the case a polytropic equation of state is used, the average density $\bar{\varrho}_0$ follows from equation (2.38). One starting value for integration exists when the Cowling approximation is applied. This starting value vector is:

$$\boldsymbol{\eta}^{(1)}(\varepsilon) = \begin{pmatrix} \eta_1^{(1)} \\ \eta_4^{(1)} \end{pmatrix} = \begin{pmatrix} \varepsilon \\ \frac{\varrho_0}{\bar{\varrho}_0} \varepsilon^2 \left(\frac{4}{3} \frac{\varrho_0}{\bar{\varrho}_0} - \frac{\Omega^2}{I} \right) \end{pmatrix}. \quad (2.511)$$

At the free surface $x = 1$ it follows from section 2.3.6 that $\eta_4 = 0$.

2.7.3 Relativistic perfect fluid in the Cowling approximation

To nondimensionalize the equations, the following nondimensional vector is used:

$$\boldsymbol{\eta} = \begin{pmatrix} \eta_1 \\ \eta_4 \end{pmatrix} = \begin{pmatrix} y_1/R^2 \\ y_4/\pi G \bar{\varrho}_0^2 R^3 \end{pmatrix}, \quad (2.512)$$

analogous to the Cowling-approximated Newtonian definition (2.507). The nondimensionalized versions of the functions T , K and S , as defined in equations (2.415) – (2.417), are given by:

$$\tilde{T} = \frac{c^2}{\pi G \bar{\varrho}_0 R^2} \frac{e^{2\nu} \frac{d\nu}{dx} \ell(\ell+1)}{\Omega^2 x^2} - \frac{1}{x}, \quad (2.513)$$

$$\tilde{K} = e^{\lambda-\nu} \left(\frac{\pi G \bar{\varrho}_0^2 R^2}{\kappa} - \frac{\bar{\varrho}_0 c^2}{P_0 + \varrho_0 c^2} \frac{e^{2\nu} \ell(\ell+1)}{\Omega^2 x^2} \right), \quad (2.514)$$

$$\begin{aligned} \tilde{S} = \frac{P_0 + \varrho_0 c^2}{\pi G \bar{\varrho}_0^2 R^2} \left(\frac{e^{\nu-\lambda} \ell(\ell+1) c^2}{\pi G \bar{\varrho}_0 R^2} \frac{e^{2\nu}}{\Omega^2 x^2} \left(\frac{d\nu}{dx} \right)^2 - \frac{\pi G \bar{\varrho}_0 R^2}{c^2} \Omega^2 e^{\lambda-\nu} + \right. \\ \left. + x^2 e^\nu \frac{d}{dx} \left(\frac{e^{-\lambda}}{x^2} \frac{d\nu}{dx} \right) \right). \quad (2.515) \end{aligned}$$

In case a polytropic equation of state is used, equations (2.76) and (2.77) are useful expressions to calculate parameters such as $\frac{\pi G \bar{\rho}_0 R^2}{c^2}$. The nondimensionalized starting value (2.495) for integration at the center $x = \varepsilon$ with $\varepsilon \ll 1$ is:

$$\boldsymbol{\eta}^{(1)}(\varepsilon) = \begin{pmatrix} \eta_1^{(1)} \\ \eta_4^{(1)} \end{pmatrix} = \begin{pmatrix} \varepsilon \\ \frac{P_0 + \rho_0 c^2}{\pi G \bar{\rho}_0^2 R^2} \left\{ e^{\nu - \lambda} \frac{d\nu}{dx} - \frac{\pi G \bar{\rho}_0 R^2}{c^2} \frac{\Omega^2 \varepsilon}{\ell} e^{-(\nu + \lambda)} \right\} \varepsilon \end{pmatrix}. \quad (2.516)$$

At the free surface $x = 1$ it follows from section 2.6.2 that $\eta_4 = 0$.

2.7.4 Elastic solid

To nondimensionalize equations (2.290) – (2.295), the following nondimensionalized vector is used:

$$\boldsymbol{\eta} = \begin{pmatrix} \eta_1 \\ \eta_2 \\ \eta_3 \\ \eta_4 \\ \eta_5 \\ \eta_6 \end{pmatrix} = \begin{pmatrix} y_1/R^2 \\ y_2/R^2 \\ y_3/\pi G \bar{\rho}_0 R^3 \\ y_4/\pi G \bar{\rho}_0^2 R^3 \\ y_5/\pi G \bar{\rho}_0^2 R^3 \\ y_6/\bar{\rho}_0 R^2 \end{pmatrix}. \quad (2.517)$$

where $\tilde{\mathbf{T}}$, $\tilde{\mathbf{K}}$ and $\tilde{\mathbf{S}}$ are the nondimensionalized matrices (2.293) – (2.295), given by

$$\tilde{\mathbf{T}} = \begin{pmatrix} \frac{1}{x} \frac{8\mu - 3\kappa}{4\mu + 3\kappa} & \frac{\sqrt{\ell(\ell+1)}}{x} \frac{3\kappa - 2\mu}{3\kappa + 4\mu} & 0 \\ -\frac{\sqrt{\ell(\ell+1)}}{x} & \frac{2}{x} & 0 \\ -4\frac{\rho_0}{\bar{\rho}_0} & 0 & -\frac{\ell}{x} \end{pmatrix}, \quad (2.518)$$

$$\tilde{\mathbf{K}} = \begin{pmatrix} \frac{3\pi G \bar{\rho}_0^2 R^2}{3\kappa + 4\mu} & 0 & 0 \\ 0 & \frac{\pi G \bar{\rho}_0^2 R^2}{\mu} & 0 \\ 0 & 0 & 4 \end{pmatrix}, \quad (2.519)$$

$$\tilde{\mathbf{S}} = \begin{pmatrix} \frac{4(\gamma - \rho_0 g_0 R x)}{\pi G (\bar{\rho}_0 R x)^2} - \frac{\rho_0}{\bar{\rho}_0} \Omega^2 & S_{21} & S_{31} \\ \frac{\sqrt{\ell(\ell+1)}}{\pi G (\bar{\rho}_0 R x)^2} (Q_0 g_0 R x - 2\gamma) & \frac{\ell(\ell+1)(\gamma + \mu) - 2\mu}{\pi G (\bar{\rho}_0 R x)^2} - \frac{\rho_0}{\bar{\rho}_0} \Omega^2 & S_{32} \\ -\frac{\rho_0}{\bar{\rho}_0} \frac{(\ell+1)}{x} & \frac{\rho_0}{\bar{\rho}_0} \frac{\sqrt{\ell(\ell+1)}}{x} & 0 \end{pmatrix}, \quad (2.520)$$

where $\gamma = 3\mu\kappa \left(\kappa + \frac{4\mu}{3} \right)^{-1}$ and $\tilde{\mathbf{S}}$ is symmetric. In the case a polytropic equation of state is used, the average density $\bar{\rho}_0$ follows from equation (2.38).

Since solid cores are not considered in this study, one extra starting value (2.339) at the core-crust boundary is needed. The nondimensionalized form $\eta^{(3)}$ of this starting value is:

$$\eta_2^{(3)} = 1, \quad (2.521)$$

with all other components zero. At the free surface $x = 1$ it follows from section 2.3.6 that $\eta_4 = \eta_5 = \eta_6 = 0$.

2.7.5 Elastic solid in the Cowling approximation

To nondimensionalize equations (2.296) – (2.301), the following vector η containing the independent variables is used:

$$\eta = \begin{pmatrix} \eta_1 \\ \eta_2 \\ \eta_4 \\ \eta_5 \end{pmatrix} = \begin{pmatrix} y_1/R^2 \\ y_2/R^2 \\ y_4/\pi G \bar{\rho}_0^2 R^3 \\ y_5/\pi G \bar{\rho}_0^2 R^3 \end{pmatrix}. \quad (2.522)$$

where $\tilde{\mathbf{T}}$, $\tilde{\mathbf{K}}$ and $\tilde{\mathbf{S}}$ are the nondimensionalized matrices (2.299) – (2.301), given by

$$\tilde{\mathbf{T}} = \begin{pmatrix} \frac{1}{x} \frac{8\mu-3\kappa}{4\mu+3\kappa} & \frac{\sqrt{\ell(\ell+1)}}{x} \frac{3\kappa-2\mu}{3\kappa+4\mu} \\ -\frac{\sqrt{\ell(\ell+1)}}{x} & \frac{2}{x} \end{pmatrix}, \quad (2.523)$$

$$\tilde{\mathbf{K}} = \begin{pmatrix} \frac{3\pi G \bar{\rho}_0^2 R^2}{3\kappa+4\mu} & 0 \\ 0 & \frac{\pi G \bar{\rho}_0^2 R^2}{\mu} \end{pmatrix}, \quad (2.524)$$

$$\tilde{\mathbf{S}} = \begin{pmatrix} \frac{4(\gamma-\varrho_0 g_0 R x)}{\pi G (\bar{\rho}_0 R x)^2} - \frac{\varrho_0}{\bar{\rho}_0} \Omega^2 + 4 \left(\frac{\varrho_0}{\bar{\rho}_0} \right)^2 & S_{21} \\ \frac{\sqrt{\ell(\ell+1)}}{\pi G (\bar{\rho}_0 R x)^2} (\varrho_0 g_0 R x - 2\gamma) & \frac{\ell(\ell+1)(\gamma+\mu)-2\mu}{\pi G (\bar{\rho}_0 R x)^2} - \frac{\varrho_0}{\bar{\rho}_0} \Omega^2 \end{pmatrix}, \quad (2.525)$$

where $\gamma = 3\mu\kappa \left(\kappa + \frac{4\mu}{3} \right)^{-1}$ and $\tilde{\mathbf{S}}$ is symmetric. In the case a polytropic equation of state is used, the average density $\bar{\rho}_0$ follows from equation (2.38). Like in the case where the Cowling approximation is not applied, one extra starting value (2.339) at the core-crust boundary is needed. The nondimensionalized form $\eta^{(3)}$ of this starting value is:

$$\eta_2^{(3)} = 1, \quad (2.526)$$

with all other components zero. At the free surface $x = 1$ it follows from section 2.3.6 that $\eta_4 = \eta_5 = 0$.

2.7.6 Relativistic elastic solid in the Cowling approximation

In order to nondimensionalize equations (2.474) – (2.482), the following nondimensionalized vector is defined:

$$\boldsymbol{\eta} = \begin{pmatrix} \eta_1 \\ \eta_2 \\ \eta_4 \\ \eta_5 \end{pmatrix} = \begin{pmatrix} y_1/R^2 \\ y_2/R^2 \\ y_4/\pi G \bar{\rho}_0^2 R^3 \\ y_5/\pi G \bar{\rho}_0^2 R^3 \end{pmatrix}, \quad (2.527)$$

where R is the radius of the fluid sphere and $\bar{\rho}_0$ is the average density. The nondimensional analogues of matrices (2.477) – (2.479) are given by $\tilde{\mathbf{T}}$, $\tilde{\mathbf{K}}$ and $\tilde{\mathbf{S}}$:

$$\tilde{\mathbf{T}} = \begin{pmatrix} \frac{1}{x} \frac{8\mu-3\kappa}{4\mu+3\kappa} & \frac{\sqrt{\ell(\ell+1)}}{x} \frac{3\kappa-2\mu}{3\kappa+4\mu} \\ -e^{2\lambda} \frac{\sqrt{\ell(\ell+1)}}{x} & \frac{d\lambda}{dx} + \frac{2}{x} \end{pmatrix}, \quad (2.528)$$

$$\tilde{\mathbf{K}} = e^{\lambda-\nu} \begin{pmatrix} \frac{3\pi G \bar{\rho}_0^2 R^2}{3\kappa+4\mu} & 0 \\ 0 & e^{2\lambda} \frac{\pi G \bar{\rho}_0^2 R^2}{\mu} \end{pmatrix}, \quad (2.529)$$

$$\tilde{\mathbf{S}} = \begin{pmatrix} \tilde{S}_{11} & \tilde{S}_{12} \\ \tilde{S}_{21} & \tilde{S}_{22} \end{pmatrix}, \quad (2.530)$$

and $\tilde{\mathbf{S}}$ is symmetric, with components:

$$\tilde{S}_{11} = \frac{4\gamma e^{\nu-\lambda}}{\pi G (\bar{\rho}_0 R x)^2} + \frac{(\varrho_0 c^2 + P_0)}{\pi G (\bar{\rho}_0 R x)^2} \left(x^2 e^\nu \frac{d}{dx} \left(\frac{e^{-\lambda}}{x^2} \frac{d\nu}{dx} \right) - \frac{\pi G \bar{\rho}_0 R^2}{c^2} \Omega^2 e^{\lambda-\nu} \right), \quad (2.531)$$

$$\tilde{S}_{12} = \frac{e^{\nu-\lambda} \sqrt{\ell(\ell+1)}}{\pi G \bar{\rho}_0^2 R^2 x} \left(\frac{d\nu}{dx} (\varrho_0 c^2 + P_0) - \frac{2\gamma}{x} \right), \quad (2.532)$$

$$\tilde{S}_{21} = S_{12}, \quad (2.533)$$

$$\tilde{S}_{22} = (\ell(\ell+1)(\gamma+\mu) - 2\mu) \frac{e^{\nu-\lambda}}{\pi G (\bar{\rho}_0 R x)^2} - \frac{(\varrho_0 c^2 + P_0)}{\bar{\rho}_0 c^2} e^{-(\nu+\lambda)} \Omega^2, \quad (2.534)$$

where $\gamma = 3\mu\kappa \left(\kappa + \frac{4\mu}{3} \right)^{-1}$ and $\tilde{\mathbf{S}}$ is symmetric. In case a polytropic equation of state is used, equations (2.76) and (2.77) are useful expressions to calculate parameters such as $\frac{\pi G \bar{\rho}_0 R^2}{c^2}$.

Like in the Newtonian elastic case, one starting value (2.339) at the core-crust boundary is needed. The nondimensionalized form $\boldsymbol{\eta}^{(3)}$ of this starting value is:

$$\eta_2^{(3)} = 1, \quad (2.535)$$

with all other components zero. At the free surface $x = 1$ it follows from section 2.6.2 that $\eta_4 = \eta_5 = 0$.

Chapter 3

Numerical methods

In the previous chapter, it was shown that the differential equations that govern the configuration of dynamical equilibrium and the oscillations of a neutron star could be reduced to a problem involving a set of nondimensionalized first-order differential equations

$$\frac{d\boldsymbol{\eta}(x)}{dx} = \tilde{\mathbf{A}}(\Omega, x)\boldsymbol{\eta}(x), \quad (3.1)$$

in terms of a vector $\boldsymbol{\eta}$ containing the independent variables as a function of radial position x and a matrix $\tilde{\mathbf{A}}$ containing functions of equilibrium model parameters.

These equations can only be solved if boundary conditions are specified. The way the boundary conditions are formulated, determines how the problem is solved numerically. Boundary conditions are formulated in two different ways: in *initial value problems*, the value of all independent variables is given at one point $r = r_A$. In *boundary value problems*, the boundary conditions are specified at more than one point, i.e. some of the conditions need to be satisfied at r_A and others at r_B .

Both type of problems occur in the study of neutron star oscillations. The problem of finding the equilibrium configuration of a neutron star forms an initial value problem. The equations for oscillations form a boundary value problem. This chapter contains a brief description of the numerical methods that are used in this study. Section 3.1 gives a description of the way in which the differential equations are integrated to give solutions, and in which way the boundary conditions are implemented. In section 3.2 the algorithm is described which is used to find the oscillation eigenfrequencies. The chapter is concluded with section 3.3 on the description of the algorithm that is used to calculate eigenfunctions.

3.1 Numerical analysis of first order ordinary differential equations

The underlying idea of all algorithms that are used to numerically solve ordinary differential equations is Euler's method: the infinitely small differentials $d\boldsymbol{\eta}$ and dx in equation (3.1) are replaced by finite differentials $\Delta\boldsymbol{\eta}$ and Δx . Given an initial value $\boldsymbol{\eta}(x_A)$ at position x_A , the solution at the next point $x_A + \Delta x$ is given by

$$\boldsymbol{\eta}(x_A + \Delta x) = \boldsymbol{\eta}(x_A) + \Delta\boldsymbol{\eta} = \boldsymbol{\eta}(x_A) + \mathbf{A}(x_A)\boldsymbol{\eta}(x_A)\Delta x. \quad (3.2)$$

In practice, using this method literally is not advised, because it turns out to be both unstable and inefficient. In this study, the Runge-Kutta method is used, which is a spin-off of Euler's method. In the Runge-Kutta method, the information from a number of Euler type numerical integrations is used to find a Taylor series of the solution to some order in x around the starting point x_A . This Taylor series is used to propagate the solution from x_A to $x_A + \Delta x$.

It turns out that an estimate can be made of the error due to truncation of the Taylor series. This allows for implementing a variable stepsize Δx which is adjusted every integration step such that a predetermined value for the estimate of the truncation error is not exceeded. In this way, an accurate integration is possible at low computational cost: when the situation allows it, a large stepsize is used to stride quickly through smooth parts of the integration domain. When things get rough, small stepsizes are used.

It is beyond the scope of this study to give a detailed review on the Runge-Kutta method. A very useful and practical review is given in chapter 16 of (Press et. al., 1992) on the integration of ordinary differential equations.

3.1.1 Initial value problems

Once the Runge-Kutta algorithm for integration of the differential equations from x to $x + \Delta x$ is implemented, the solution of an initial value problem is relatively straightforward. For differential equation (3.1), the initial values $\boldsymbol{\eta}(x_s)$ at $x = x_A$ are repetitively integrated for steps that lead to an acceptable truncation error, until the endpoint x_B is reached. Solutions for $\boldsymbol{\eta}$ are stored at intermediate values of x .

This method is applied to both the Newtonian and relativistic equations that describe the equilibrium model of a neutron star. The numerical results are given in section 4.1.1 and 4.1.2.

3.1.2 Boundary value problems

Boundary value problems distinguish themselves from initial value problems because, unlike for initial value problems, the boundary conditions at the starting point of integration x_A do not uniquely define the solution at x_A . Instead, there are multiple linearly independent solutions that satisfy the boundary conditions at x_A . The integration of a random linear combination of these solutions will almost certainly not satisfy the boundary conditions at $x = x_B$. The art of solving boundary value problems is to find the starting values for integration that will lead to solutions that will satisfy the boundary conditions at $x = x_B$.

In general, iterative methods are used to solve this problem. However, in the case of a linear problem, like in the case of the linearized equations of motion for neutron star oscillations, a modification of the algorithm for initial value problems leads to an efficient algorithm to solve the boundary value problem. By exploiting that a linear combination of solutions yields a new solution, a linear combination of linear independent solutions that satisfies the boundary conditions at x_A is picked in such a way that the boundary conditions at x_B are also satisfied. This algorithm is explained in section 3.3.

3.2 Calculation of eigenfrequencies

In sections 2.3.5.1 and 2.6.1 on boundary conditions in Newtonian and relativistic theory respectively, it was shown that for each frequency ω , a set of two linearly independent solutions exist that satisfy the boundary conditions at the center of the fluid neutron star model. In case the Cowling approximation is applied, this reduces the number of independent solutions at the center to one. As explained in sections 2.3.5.2 and 2.6.1.1, if a crust is added to the model, an extra independent solution is added at the core-crust boundary. The nondimensionalized starting solutions as defined in section 2.7 are integrated for a given nondimensionalized eigenfrequency \mathcal{Q} through the fluid part of the neutron star model using a variable stepsized fourth order Runge-Kutta method, as given in chapter 16 of Press et. al. (1992). In case a solid crust is present, an extra starting solution is integrated along from the base of the crust onwards. This results in three (in the Cowling-approximated case two) independent solutions at the free surface. If \mathcal{Q} is an eigenfrequency, a linear combination of these solutions must exist that satisfies the boundary conditions. This implies that for a model with a crust, a linear combination of the solutions $\boldsymbol{\eta}^{(1)}$,

$\eta^{(2)}$ and $\eta^{(3)}$

$$C_1 \begin{pmatrix} \eta_4^{(1)} \\ \eta_5^{(1)} \\ \eta_6^{(1)} \end{pmatrix} + C_2 \begin{pmatrix} \eta_4^{(2)} \\ \eta_5^{(2)} \\ \eta_6^{(2)} \end{pmatrix} + C_3 \begin{pmatrix} \eta_4^{(3)} \\ \eta_5^{(3)} \\ \eta_6^{(3)} \end{pmatrix}, \quad (3.3)$$

is equal to zero at the free surface, with C_1 , C_2 and C_3 constants. This is equivalent with the condition that the determinant

$$D(\Omega) = \begin{vmatrix} \eta_4^{(1)} & \eta_4^{(2)} & \eta_4^{(3)} \\ \eta_5^{(1)} & \eta_5^{(2)} & \eta_5^{(3)} \\ \eta_6^{(1)} & \eta_6^{(2)} & \eta_6^{(3)} \end{vmatrix}, \quad (3.4)$$

is zero at the free surface. For a completely fluid model, $\eta_5 = 0$ and the boundary condition reduces to

$$D(\Omega) = \begin{vmatrix} \eta_4^{(1)} & \eta_4^{(2)} \\ \eta_6^{(1)} & \eta_6^{(2)} \end{vmatrix} = 0, \quad (3.5)$$

at the free surface. In the case the Cowling approximation is applied, η_6 is no longer an independent parameter and the condition at the free surface of a model with a solid crust reduces to

$$D(\Omega) = \begin{vmatrix} \eta_4^{(1)} & \eta_4^{(3)} \\ \eta_5^{(1)} & \eta_5^{(3)} \end{vmatrix} = 0. \quad (3.6)$$

For a completely fluid model in the Cowling approximation, there is only one linearly independent solution left, hence the condition at the free surface is simplified further to

$$D(\Omega) = \eta_4^{(1)} = 0. \quad (3.7)$$

Because at the free surface the equations have a regular singularity, in practice the integration is stopped at a distance ϵ just before the surface to avoid a division by zero. It turns out that when ϵ is chosen to be sufficiently small, this does not influence the results, except for high frequency overtones, where the value of ϵ influences the eigenfrequencies by a few tenths of a percent. In this study, ϵ is always chosen to be a number ≤ 0.001 .

The eigenfrequencies of oscillations are found in all cases by integrating the equations repetitively for a range of frequencies Ω . This results in a function of the determinant $D(\Omega)$, of which the roots give the eigenfrequencies. The determinant functions are calculated for various Newtonian and relativistic neutron star models and presented in chapter 4.

3.3 Calculation of eigenfunctions

In the case of a fluid model, two linearly independent solutions exist that satisfy the boundary conditions in the center. Because the differential equations are all linear, linear combinations of the two linearly independent solutions are also solutions. This fact can be exploited to find an eigenfunction that satisfies one of the two boundary conditions at the free surface, by making a clever linear combination of the two linearly independent solutions that satisfies one boundary condition. If the eigenfrequencies of the system are known, eigenfunctions are calculated by making such a linear combination to satisfy one boundary condition. The second boundary condition is then automatically satisfied when the equations are integrated for an eigenfrequency, hence an eigenfunction has been found.

Take the two linearly independent starting solutions $\eta^{(1)}(x_1)$ and $\eta^{(2)}(x_1)$ at a small radius x_1 . These starting solutions are integrated to find two linearly independent solutions that satisfy the boundary conditions in the center of the model, but in general not the boundary conditions at the free surface $x = 1$. From these two solutions, a new starting solution is constructed by making a particular linear combination of $\eta^{(1)}$ and $\eta^{(2)}$, which is possible because of the linearity of the differential equations involved:

$$\eta^{\text{eig}}(x_1) = \eta^{(2)}(x_1) - \frac{\eta^{(2)}(x_1) - \eta^{(1)}(x_1)}{1 - \eta_4^{(1)}(1)/\eta_4^{(2)}(1)}. \quad (3.8)$$

The value of η_4^{eig} is now zero at $x = 1$, hence η^{eig} satisfies one of the two boundary conditions at the surface and will satisfy the second boundary condition as well if the equations are integrated for an eigenfrequency. Hence η^{eig} will be an eigenfunction.

In the case of an elastic model, three linearly independent solutions exist that satisfy the boundary conditions in the center, but not at the surface. Again linearity of the differential equations makes it possible to make a particular linear combination which yields a solution that satisfies two of the three boundary conditions at the free surface.

Take the three linearly independent solutions $\eta^{(1)}$, $\eta^{(2)}$ and $\eta^{(3)}$. Using the first two and the same construction as for the fluid case, an auxiliary starting solution $\eta^{\text{aux}(1)}(x_1)$ is constructed:

$$\eta^{\text{aux}(1)}(x_1) = \eta^{(2)}(x_1) - \frac{\eta^{(2)}(x_1) - \eta^{(1)}(x_1)}{1 - \eta_4^{(1)}(1)/\eta_4^{(2)}(1)}. \quad (3.9)$$

The same is done with the pair $\boldsymbol{\eta}^{(1)}$ and $\boldsymbol{\eta}^{(3)}$:

$$\boldsymbol{\eta}^{\text{aux}(2)}(x_1) = \boldsymbol{\eta}^{(3)}(x_1) - \frac{\boldsymbol{\eta}^{(3)}(x_1) - \boldsymbol{\eta}^{(1)}(x_1)}{1 - \eta_4^{(1)}(1)/\eta_4^{(2)}(1)}. \quad (3.10)$$

The linearly independent solutions $\boldsymbol{\eta}^{\text{aux}(1)}(x_1)$ and $\boldsymbol{\eta}^{\text{aux}(2)}(x_1)$ now both satisfy the boundary condition $\eta_4^{\text{aux}(1)} = \eta_4^{\text{aux}(2)} = 0$ at $x = 1$. On these two functions the same trick is again applied to find a function $\boldsymbol{\eta}^{\text{eig}}$ with both $\eta_4^{\text{eig}}(1) = \eta_5^{\text{eig}}(1) = 0$:

$$\boldsymbol{\eta}^{\text{eig}}(x_1) = \boldsymbol{\eta}^{\text{aux}(2)}(x_1) - \frac{\boldsymbol{\eta}^{\text{aux}(2)}(x_1) - \boldsymbol{\eta}^{\text{aux}(1)}(x_1)}{1 - \eta_5^{\text{aux}(1)}(1)/\eta_5^{\text{aux}(2)}(1)}. \quad (3.11)$$

This function now satisfies two of the three boundary conditions at the free surface and will satisfy the third boundary condition as well if the equations are integrated for an eigenfrequency. Hence $\boldsymbol{\eta}^{\text{eig}}$ will be an eigenfunction. The eigenfunctions calculated with this algorithm for various Newtonian and relativistic neutron star models are presented in the next chapter.

Chapter 4

Results

In this chapter, the outcome of this numerical study on the nonradial oscillations of neutron star models is presented.

Here, the nondimensionalized differential equations given in sections 2.1.2, 2.1.3 and 2.7 that govern the configuration of dynamical equilibrium and the oscillations of neutron star models are numerically solved using the algorithms presented in chapter 3.

The oscillation frequency spectrum for a fluid neutron star model is evenly spaced, starting with the lowest frequency of the fundamental mode. When an elastic crust is added to the model, the spectrum becomes irregular and many new oscillation eigenfrequencies appear. Only when the corresponding eigenfunctions are calculated, the apparent irregularity of the spectrum is resolved because it turns out that two types of mode can be recognized, which are both evenly spaced and together make up the apparent irregular spectrum.

The first mode type is very similar to the oscillatory modes that occur in a fluid. These are the acoustic modes, primarily driven by pressure perturbations in the neutron star. The second mode type is the shear mode, characterized by motion confined to the crust, in which angular movement is much larger than radial movement. These modes are highly dependent on the shear modulus μ in the crust.

To classify the oscillations, the same nomenclature that is used in McDermott, Van Horn and Hansen (1988) is employed. The fundamental mode is denoted by f and the acoustic modes of the k th overtone are denoted as p_k . These modes are present in both the fluid and solid neutron star models. The shear modes are denoted by s_k .

In section 4.1, various nonrelativistic and relativistic polytropic neutron star models are presented.

The oscillation spectra of the models discussed in section 4.1 are determined next. In section 4.2, the oscillation spectra of fluid polytropic neutron star models are analyzed in the Newtonian and relativistic gravity, following Robe (1968) in the Newtonian case and Ipser and Lindblom (1992) and Yoshida and Kojima (1997) in the Cowling-approximated relativistic case. The determinant functions (3.5) and (3.7) are given and the eigenfunction U , which describes radial oscillatory motion, is calculated. The effect of general relativity on the spectrum is investigated by analyzing four increasingly more relativistic models. In the nonrelativistic case, the accuracy of the Cowling approximation is assessed.

In section 4.3, the oscillation spectra of fluid neutron star models with an elastic crust are analyzed in Newtonian and relativistic context. A comparison is made between the spectra for three models with different crustal properties. The determinant functions (3.4) and (3.6) are given and the eigenfunctions U and V , which describe radial oscillatory motion, are shown. The relativistic effects are quantified by calculating spectra for four, increasingly more relativistic models. In the Newtonian case, the accuracy of the Cowling approximation is studied by comparing exact and approximated spectra.

4.1 The equilibrium model

The configuration of dynamic equilibrium of a polytropic fluid star is found by solving the the Lane-Emden equation. In the nonrelativistic case, the Lane-Emden equation is restated as two first order differential equations (2.28) and (2.29) with boundary conditions (2.30). In the relativistic case the problem is stated as the set of equations (2.68) and (2.69) with boundary conditions (2.70).

Solutions are found by using the methods given in section 3.1.1. The analytical solution of equation (2.26) for $n = 1$ will be used for the nonrelativistic models in this study. In the next section, outcomes of nonrelativistic calculations are presented.

Numerical solutions for the relativistic Lane-Emden equations were first found by Tooper (1964) and serve as a benchmark for the numerical solutions to the relativistic Lane-Emden equations used in this study. The numerical approach is identical to the Newtonian case. The numerical solution for a relativistic $n = 1$ polytrope will be used for the relativistic calculations in this study. An example result for a relativistic $n = 1$ polytropic stellar model with $\frac{GM}{c^2 R} = 0.1$ is given in section 4.1.2.

4.1.1 Solutions of the Newtonian Lane-Emden equation

The analytical solution to the Newtonian Lane-Emden equation (2.26) for $n = 1$ that will be used throughout this study is found by assuming a power series solution and by figuring out the expansion coefficients. This yields the solution

$$\vartheta(\xi) = \frac{\sin \xi}{\xi}, \quad (4.1)$$

with the free surface at $\xi = \xi_1 = \pi$. For general n , the Lane-Emden equation (2.26) is restated as a set of two coupled first order differential equations (2.28, 2.29) with boundary conditions given by (2.30). Using the numerical method described in 3.1.1 a solution for ϑ is found, yielding the model parameters (pressure, density and gravitational acceleration) from equations (2.23) – (2.36).

Using solution (4.1) for a $n = 1$ polytrope, equations (2.23) – (2.36) reduce to:

$$\varrho_0 = \varrho_c \frac{\sin \pi x}{\pi x}, \quad (4.2)$$

$$P_0 = \frac{2G\varrho_c^2 R^2}{\pi} \left(\frac{\sin \pi x}{\pi x} \right)^2, \quad (4.3)$$

$$g_0 = \frac{4GR\varrho_c}{\pi x} \left(\frac{\sin \pi x}{\pi x} - \cos \pi x \right), \quad (4.4)$$

where x is a nondimensional radial parameter, $x = 0$ corresponds to the center of the model, $x = 1$ corresponds to the free surface. The numerical results for a $n = 1$ polytropic neutron star model are given in figure 4.1.

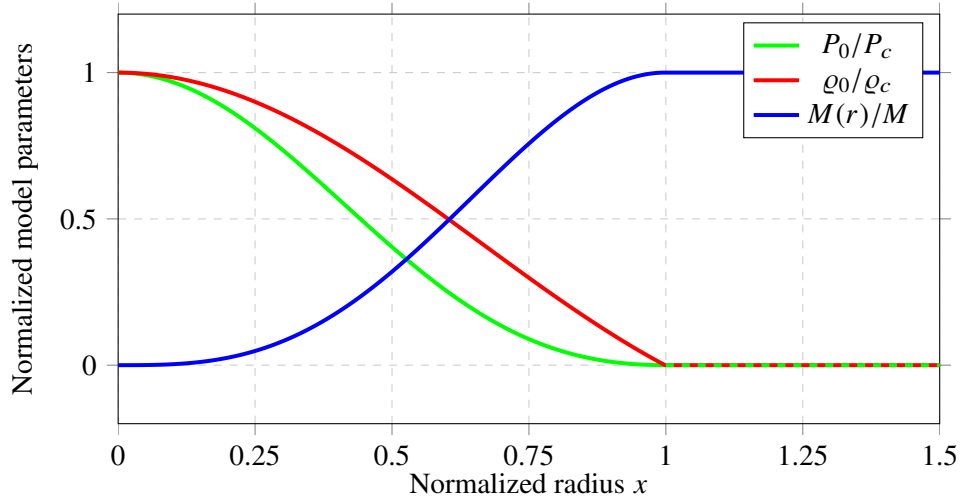


Figure 4.1: Solution of equilibrium model parameters for a $n = 1$ polytropic sphere in dynamical equilibrium.

The numerical results are an exact match with the analytical solutions (4.2) – (4.4) that serve as a benchmark for the numerical method. The numerical results for $n = 2, 3$ polytropic models are presented in figure 4.2.

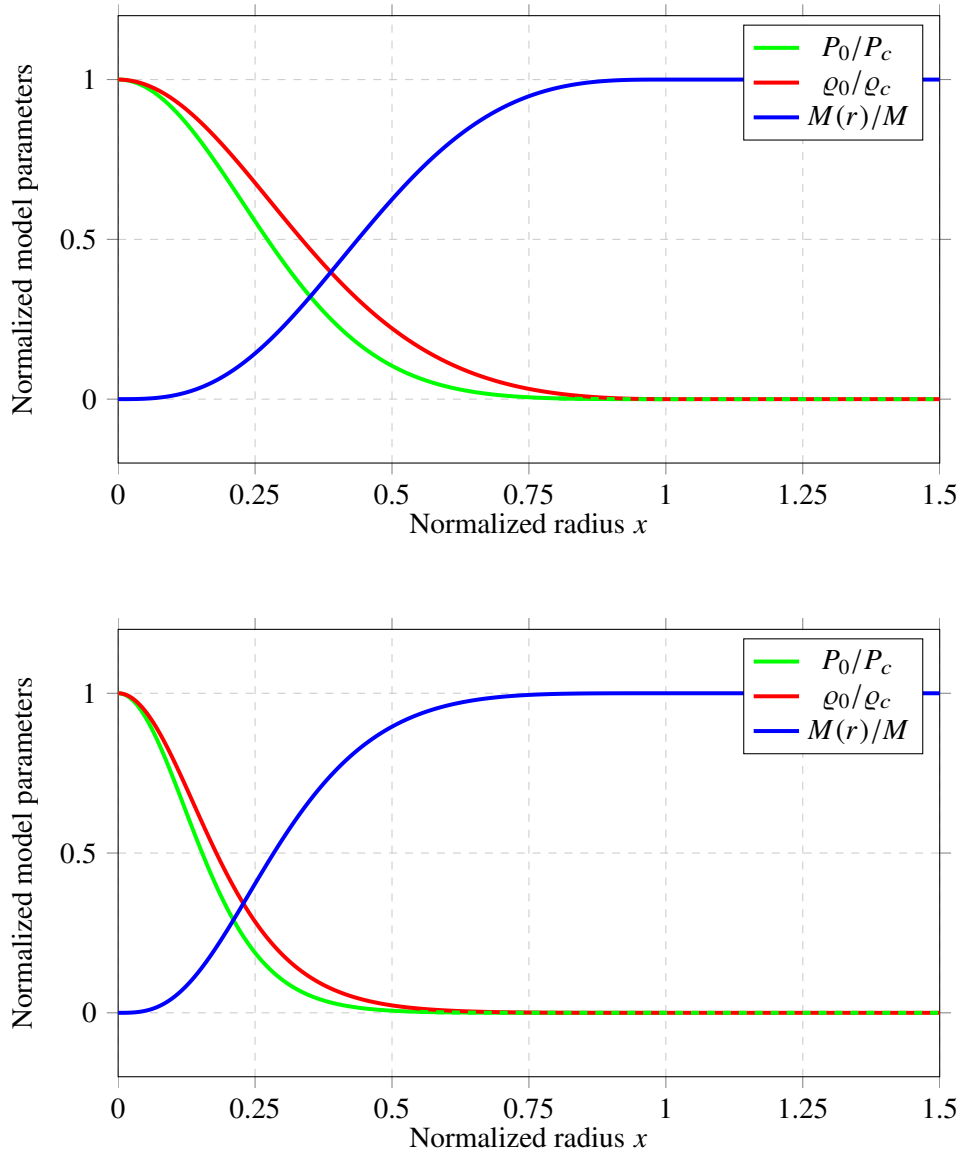


Figure 4.2: Top: solution of equilibrium model parameters for a Newtonian $n = 2$ polytropic sphere in dynamical equilibrium. Bottom: solution for $n = 3$.

4.1.2 Solutions of the relativistic Lane-Emden equations

The relativistic Lane-Emden equations are a set of two coupled, first order differential equations, given by equations (2.68) and (2.69) for ϑ and w with boundary conditions (2.70). Like in the Newtonian case, these equations have the polytropic index n , as a parameter. In the relativistic case however, an additional parameter $\sigma = P_c/\rho_c c^2$ is also present in the differential equations. This parameter determines the magnitude of relativistic effects in the calculation, with $\sigma = 0$ corresponding to the non-relativistic limit $c \rightarrow \infty$.

The relativistic Lane-Emden equations are solved numerically, using the same algorithm as in the Newtonian case. Having solved for ϑ , the model parameters as a function of $x = \xi/\xi_1$ follow from identities (2.80) – (2.86). The limiting values of these model parameters for $x = 0$ are given in (2.87) – (2.91). The model parameters for $x > 1$ (outside the neutron star model) are given by (2.92) – (2.95).

The numerical results for a relativistic $n = 1$ polytropic neutron star model with $\sigma = 0.0657452$ are given in figure 4.3. Equation (2.73), shows that this value for σ corresponds to a model with $\frac{GM}{c^2 R} = 0.1$. This is one of the neutron star models of which the oscillation spectrum will be determined.

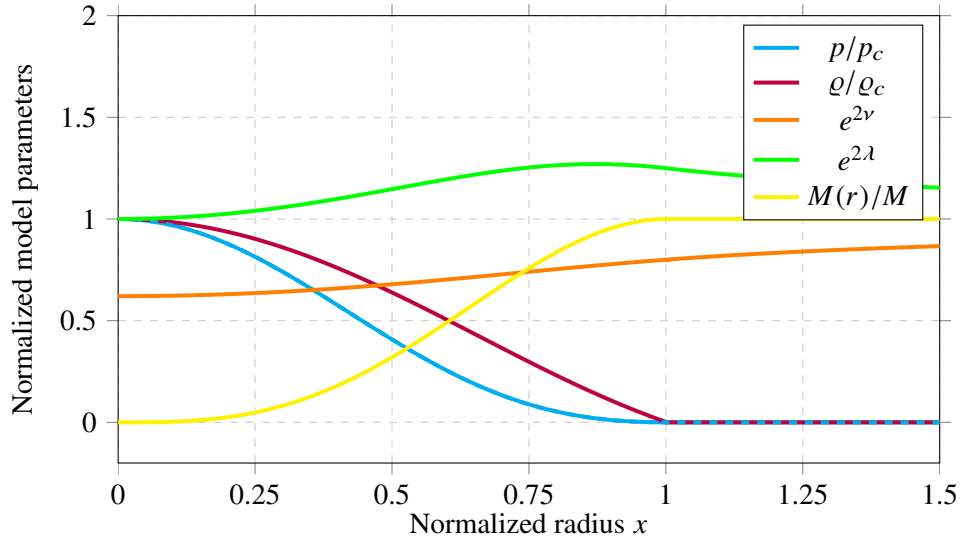


Figure 4.3: Numerical solution for the state of mechanical equilibrium of a relativistic $n = 1$ polytropic fluid star model.

4.2 Oscillation spectra of polytropic fluid stellar models

In this section, all results for the oscillation spectra of fluid stars are presented. Section 4.2.1 describes how the numerical method that is used is benchmarked. Section 4.2.2 gives the oscillation spectrum of a polytropic fluid sphere using Newtonian equations of motion. Section 4.2.3 gives the oscillation spectrum of the corresponding relativistic problem.

4.2.1 Benchmarks of the numerical algorithm

The correctness of the numerical algorithm used to solve for the oscillation spectrum of Newtonian fluid neutron star models is assessed by comparing the results of the code with the analytical solutions (2.275) – (2.286) in combination with (2.288) that exist for a uniform fluid sphere. By choosing the analytical solutions as starting values at radius r_1 and integrating the solution numerically through a uniform model, the accuracy is checked by comparing the numerical result at radius r_2 with the analytical result. The numerical algorithm is very precise and if the maximum truncation error that was allowed is lowered, the difference between the numerical and analytical solutions can be diminished to an almost arbitrarily small value. The results for spectra of polytropic stellar models obtained by Robe (1968) are also reproduced for confirmation.

Unfortunately, there is no analytical result for the oscillation spectrum of the corresponding Cowling-approximated relativistic problem to use as a benchmark. However, the limiting case of $\sigma \rightarrow 0$ of the relativistic algorithm is compared with the Cowling-approximated Newtonian results and they coincide, as expected. Instead of an analytical benchmark, a comparison with existing results is possible. In the work of Ipser and Lindblom (1992) and Yoshida and Kojima (1997) spectra for relativistic polytropic neutron star models have been calculated. There is no difference between their results and the spectrum calculated in this study, which further corroborates the results for relativistic oscillation spectra obtained in this study.

4.2.2 Oscillation spectra in Newtonian gravity

In this section, the frequency spectra and radial displacement eigenfunctions of the $\ell = 2$ modes for a $n = 1$ polytropic neutron star model are presented. The oscillations are assumed to be adiabatic, with adiabatic index $\Gamma_1 = 5/3$, which determines the bulk modulus (2.98) throughout the neutron star model.

This spectrum has been calculated earlier by Robe (1968), where a comparison was made between the exact and Cowling-approximated results. Here, the exact frequency spectrum of oscillations is obtained by using the method described in section 3.2. Two linearly independent solutions $\boldsymbol{\eta}^{(1)}$ and $\boldsymbol{\eta}^{(2)}$ to the differential equations are found. It follows that for eigenfrequencies, the determinant $D(\Omega)$ of the vectors containing the boundary conditions at the free surface is zero:

$$D(\Omega) = \begin{vmatrix} \eta_4^{(1)} & \eta_6^{(1)} \\ \eta_4^{(2)} & \eta_6^{(2)} \end{vmatrix} = 0 \text{ if } \Omega \text{ is an eigenfrequency.} \quad (4.5)$$

When the Cowling approximation is applied, one starting solution $\boldsymbol{\eta}^{(1)}$ remains and the eigenfrequencies are determined by the roots of $D(\Omega)$:

$$D(\Omega) = \eta_4^{(1)} = 0 \text{ if } \Omega \text{ is an eigenfrequency.} \quad (4.6)$$

The determinant as a function of the frequency Ω is plotted in figure 4.4, for both the exact calculation and the Cowling-approximated calculation. The eigenfrequencies are given in table 4.1.

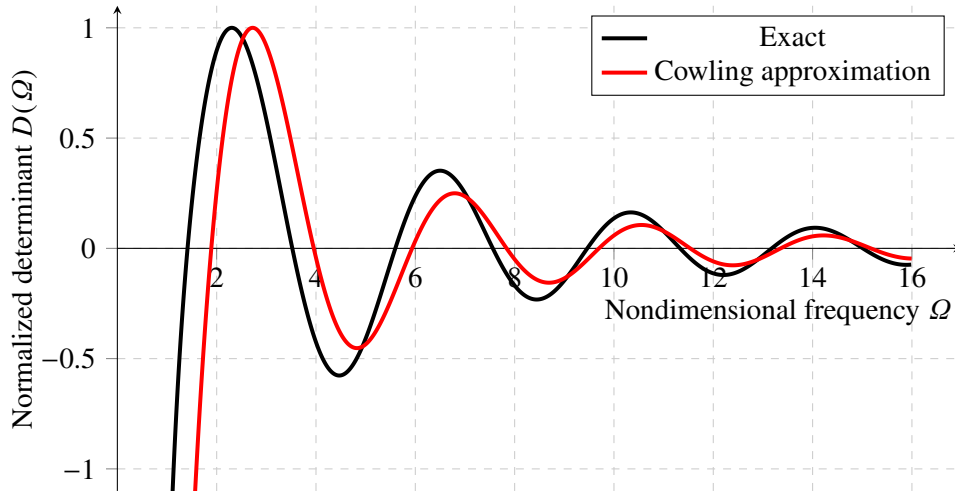


Figure 4.4: Determinant (normalized to have unit value at the first peak) for a $n = 1$ polytropic fluid model, with $\Gamma_1 = 5/3$. The eigenfrequencies, which are the zeros of the determinant, are given in table 4.1.

The results coincide with the results obtained by Robe (1968).

	f	p_1	p_2	p_3	p_4	p_5	p_6	p_7
Ω_E	1.413	3.523	5.597	7.560	9.458	11.320	13.159	14.982
Ω_C	1.892	3.955	5.934	7.835	9.692	11.523	13.338	15.142

Table 4.1: Oscillation spectra corresponding to the graphs in figure 4.4. Since the eigenfrequencies are normalized, they are given in units of $\sqrt{\pi G \bar{\rho}_0}$. Exact frequencies are given by Ω_E , Cowling-approximated frequencies are given by Ω_C .

For each frequency, there is a corresponding radial displacement eigenfunction U . Since the differential equations are linear, the eigenfunction can be scaled. This freedom is used to normalize U to be of unit value at the surface. The method described in section 3.3 is used to get the eigenfunction U in the exact case. For the Cowling-approximated case, the eigenfunction is obtained directly from $\eta_1(x)$. Unlike in the exact calculation, no special algorithm for this is needed, since there is one integration, and a special linear combination needed earlier and described in section 3.3 need not be taken. Plots of these eigenfunctions is given in figure 4.5.

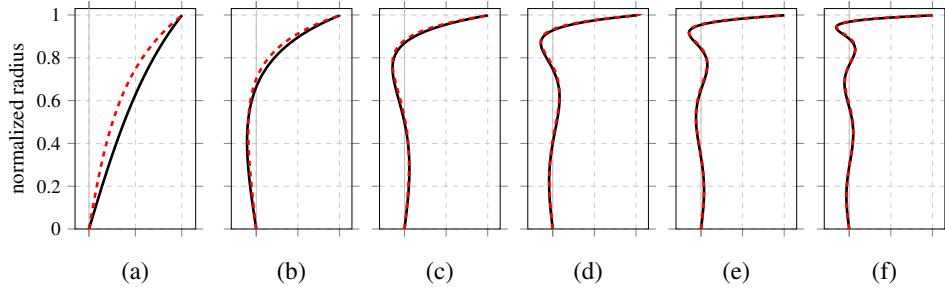


Figure 4.5: Normalized radial displacement eigenfunctions U . From left to right the fundamental mode and first to fifth overtones of the $\ell = 2$ mode. In black the exact results, in red the results in the relativistic Cowling approximation.

4.2.3 Spectra in the relativistic Cowling approximation

In this section, the frequency spectra and radial displacement eigenfunctions of the $\ell = 2$ modes for a $n = N = 1$ relativistic polytrope will be calculated, for models with increasingly relativistic configurations, following Yoshida and Kojima (1997). The parameter N determines the bulk modulus κ through definition (2.98).

Fundamental mode frequencies for $\ell = 2, 3, 4$ and 5 for a $n = N = 1$ model with $GM/c^2R = 0.145$ are calculated first. The resulting eigenfrequencies are given in table 4.2 and coincide with the eigenfrequencies obtained by Ipser and Lindblom (1992).

$\ell =$	2	3	4	5
$GM/c^2R = 0.145$	1.67568	2.01353	2.29377	2.53879

Table 4.2: Eigenfrequencies of the model with $GM/c^2R = 0.145$ for various values of ℓ . The frequencies are given in units of $\sqrt{\pi G \bar{\rho}_0}$.

The frequency spectra for the models considered by Yoshida and Kojima (1997) are found by finding the roots of the determinant $D(\Omega) = \eta_4(x = 1)$. The determinant function is calculated for four increasingly relativistic models, starting with a nonrelativistic calculation with $GM/c^2R = 0$. The resulting determinant functions as a function of Ω and the results are given in figure 4.6. The corresponding eigenfrequencies for the $\ell = 2$ mode are given in table 4.3. The results coincide with Yoshida and Kojima (1997).

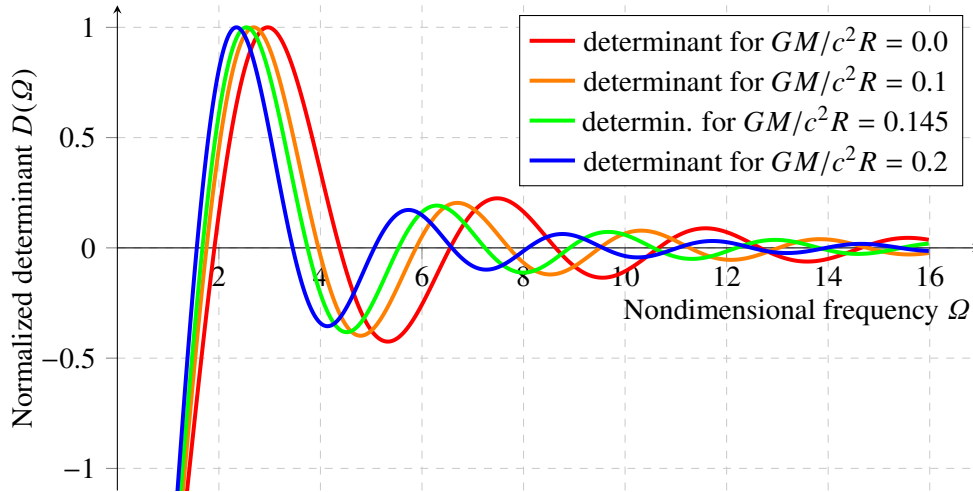


Figure 4.6: Determinant for a $n = 1$ polytropic fluid model in the relativistic Cowling approximation, with $\Gamma_1 = 2$. The zeros of the determinant are given in table 4.3.

For each frequency, there is a corresponding radial displacement eigenfunction U . Like in the Newtonian case, these are normalized to be unit value at the surface. The eigenfunctions are directly calculated from the eigenfunction $\eta_1(x)$ for a given eigenfrequency. The eigenfunctions are given in figure 4.7.

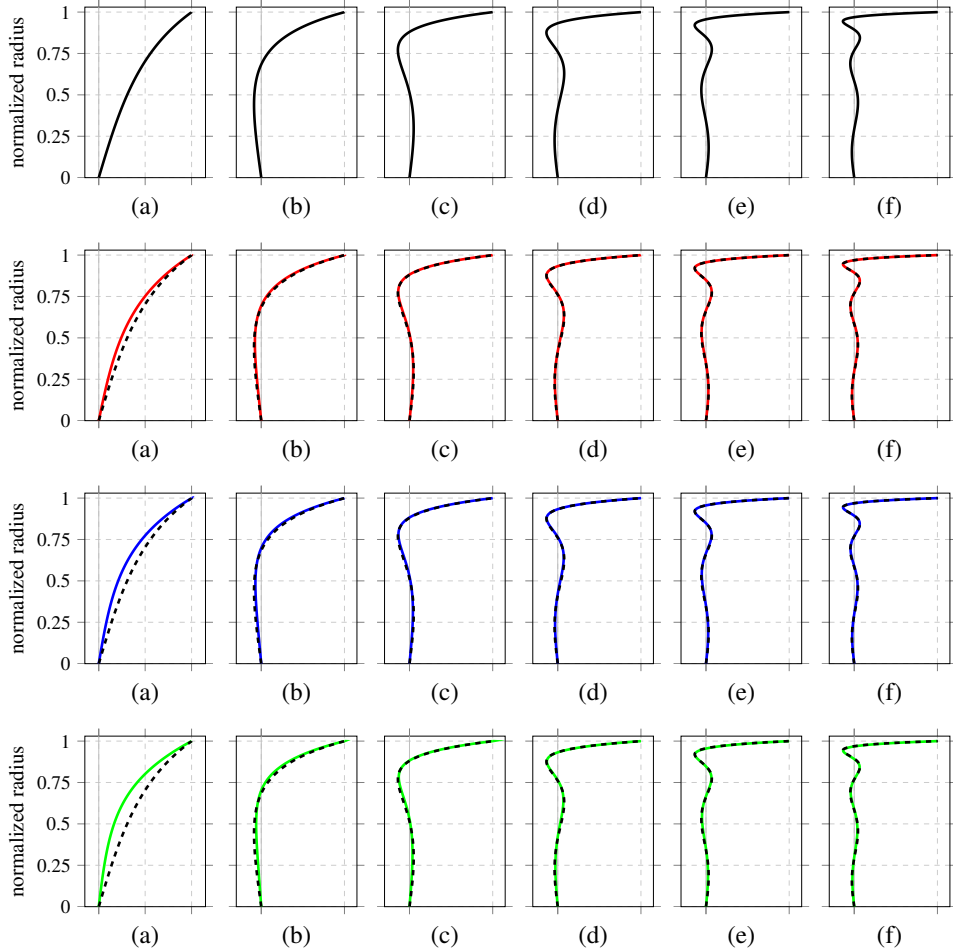


Figure 4.7: Normalized radial displacement eigenfunctions U . From left to right the fundamental mode and first to fifth overtones of the $\ell = 2$ mode for the nonrelativistic Cowling approximation (black), the relativistic case with $GM/c^2 R = 0.1$ (red), $GM/c^2 R = 0.145$ (blue) and $GM/c^2 R = 0.2$ (green). The nonrelativistic result is given (dashed) for comparison.

GM/c^2R	0.0	0.1	0.145	0.2
f	1.91171	1.75631	1.67568	1.56444
p_1	4.37813	3.96050	3.74682	3.45384
p_2	6.55474	5.88186	5.53686	5.06149
p_3	8.63157	7.71327	7.24167	6.58995
p_4	10.6600	9.50323	8.90860	8.08560
p_5	12.6612	11.2706	10.5554	9.56466
p_6	14.6455	13.0242	12.1902	11.0342

Table 4.3: Oscillation spectra corresponding to the graphs in figure 4.6. The frequencies are given in units of $\sqrt{\pi G \bar{\rho}_0}$.

4.3 Oscillation of fluid star models with a solid crust

In this section, all results for the oscillation spectra of stellar models with an elastic crust are presented. Section 4.3.1 describes how the numerical method that is used is benchmarked. Section 4.3.2 gives the oscillation spectrum of a polytropic fluid sphere with an elastic crust using Newtonian equations of motion. Section 4.3.3 gives the oscillation spectrum of the corresponding relativistic problem.

4.3.1 Benchmarks of the numerical algorithm

The correctness of the numerical algorithm used to solve for the oscillation spectrum of nonrelativistic elastic neutron star models is assessed by comparing the results of the code with the analytical solutions (2.275) – (2.286) in combination with (2.256) that exist for a uniform elastic sphere in the same way as for a fluid. Just like in the case of a fluid model, the numerical algorithm is almost arbitrarily precise.

Unfortunately, there is no analytical result for the oscillation spectrum of the corresponding Cowling-approximated relativistic problem to use as a benchmark. Analogously to a calculation for a fluid model however, the limiting case of $\sigma \rightarrow 0$ of the relativistic algorithm is compared with the Cowling-approximated nonrelativistic results and they coincide, as expected.

4.3.2 Oscillation spectra in Newtonian gravity

In this section, the frequency spectra and radial and angular displacement eigenfunctions of the $\ell = 2$ modes for a $n = 1$ polytrope with a bulk modulus κ defined by equation (2.98) for adiabatic oscillations with $N = \frac{3}{2}$ are presented. The model has an elastic crust in the interval $x = [0.7, 1.0]$.

The calculations have been done for three different values for the shear modulus μ in the crust: $\mu = \frac{3}{5}\kappa$, $\mu = \frac{3}{25}\kappa$ and $\mu = \frac{3}{50}\kappa$. As is described in section 3.2, the calculation procedure in the fluid core is identical to the procedure of fluid models leading to two linearly independent solutions $\boldsymbol{\eta}^{(1)}$ and $\boldsymbol{\eta}^{(2)}$, except that an extra solution $\boldsymbol{\eta}^{(3)}$ is integrated from the core-crust boundary onwards, which is located at $x = 0.7$.

The boundary conditions on the free surface at $x = 1$ are summarized as:

$$D(\Omega) = \begin{vmatrix} \eta_4^{(1)} & \eta_5^{(1)} & \eta_6^{(1)} \\ \eta_4^{(2)} & \eta_5^{(2)} & \eta_6^{(2)} \\ \eta_4^{(3)} & \eta_5^{(3)} & \eta_6^{(3)} \end{vmatrix} = 0 \text{ if } \Omega \text{ is an eigenfrequency.} \quad (4.7)$$

In case the Cowling approximation is applied, $\boldsymbol{\eta}^{(2)}$ is no longer linearly independent and the boundary conditions at $x = 1$ reduce to:

$$D(\Omega) = \begin{vmatrix} \eta_4^{(1)} & \eta_5^{(1)} \\ \eta_4^{(3)} & \eta_5^{(3)} \end{vmatrix} = 0 \text{ if } \Omega \text{ is an eigenfrequency.} \quad (4.8)$$

The determinant as a function of the frequency Ω is plotted in figures 4.8, 4.11 and 4.14, for the crustal models with $\mu = \frac{3}{5}\kappa$, $\mu = \frac{3}{25}\kappa$ and $\mu = \frac{3}{50}\kappa$ respectively, for both the exact and the Cowling-approximated calculation. The eigenfrequencies are given in table 4.4, 4.5 and 4.6.

Each eigenfrequency has corresponding radial and angular eigenfunctions. The f and p -mode eigenfunctions U and V for the three crustal models are given in figures 4.9, 4.12 and 4.16 respectively. These eigenfunctions are normalized, such that $U = 1$ at the surface. The eigenfunctions for the s -modes are given in figures 4.10, 4.13 and 4.15 respectively. Since in these modes, V dominates the oscillations, the solutions have been normalized such that $V = 1$ at the free surface.

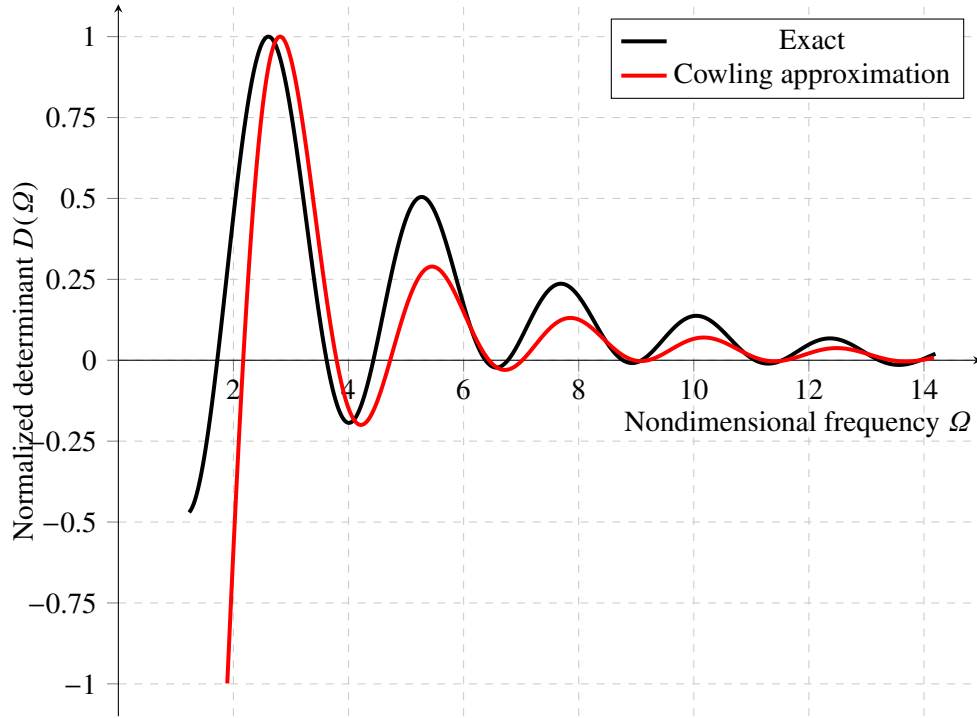


Figure 4.8: Determinant for a $n = 1$ polytropic model with $N = \frac{3}{2}$ and $\ell = 2$, and a solid crust with shear modulus $\mu = \frac{3}{5}\kappa$. Exact results are given in black, Cowling-approximated results in red. The zeros of the determinant are given in table 4.4.

	f	p_1	p_2	p_3	p_4	p_5
Ω_E	1.720	3.620	6.380	8.770	11.066	13.222
Ω_C	2.170	3.793	6.442	8.963	11.228	13.440
	s_1	s_2	s_3	s_4	s_5	
Ω_E	4.432	6.770	9.093	11.537	13.933	
Ω_C	4.724	7.020	9.205	11.588	13.938	

Table 4.4: Oscillation spectra corresponding to the graph in figure 4.8. The frequencies are given in units of $\sqrt{\pi G \bar{\rho}_0}$. The exact frequency is given by Ω_E , the frequency in the Cowling approximation is given by Ω_C .

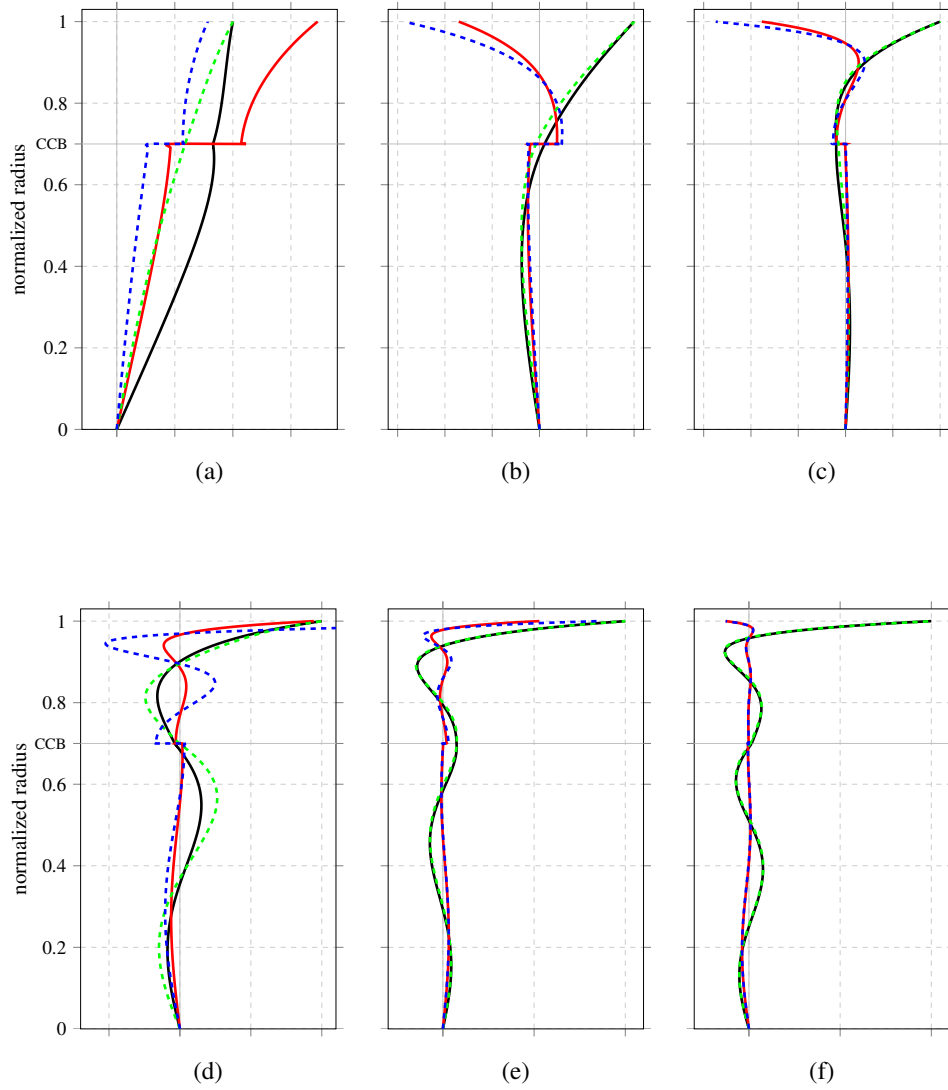


Figure 4.9: Eigenfunctions of f - and p -modes with $\ell = 2$ for the $n = 1$ polytropic fluid model with a crust with shear modulus $\mu = \frac{3}{5}\kappa$, $N = \frac{3}{2}$. Normalized radial (black for exact calculation and green for Cowling approximation) and angular (red for exact calculation and blue for Cowling approximation) displacement eigenfunctions U and V . Figure (a) contains the results for the fundamental (f) mode, figures (b) – (f) contain the results for the p -modes. The boundary between core and crust is indicated by CCB.

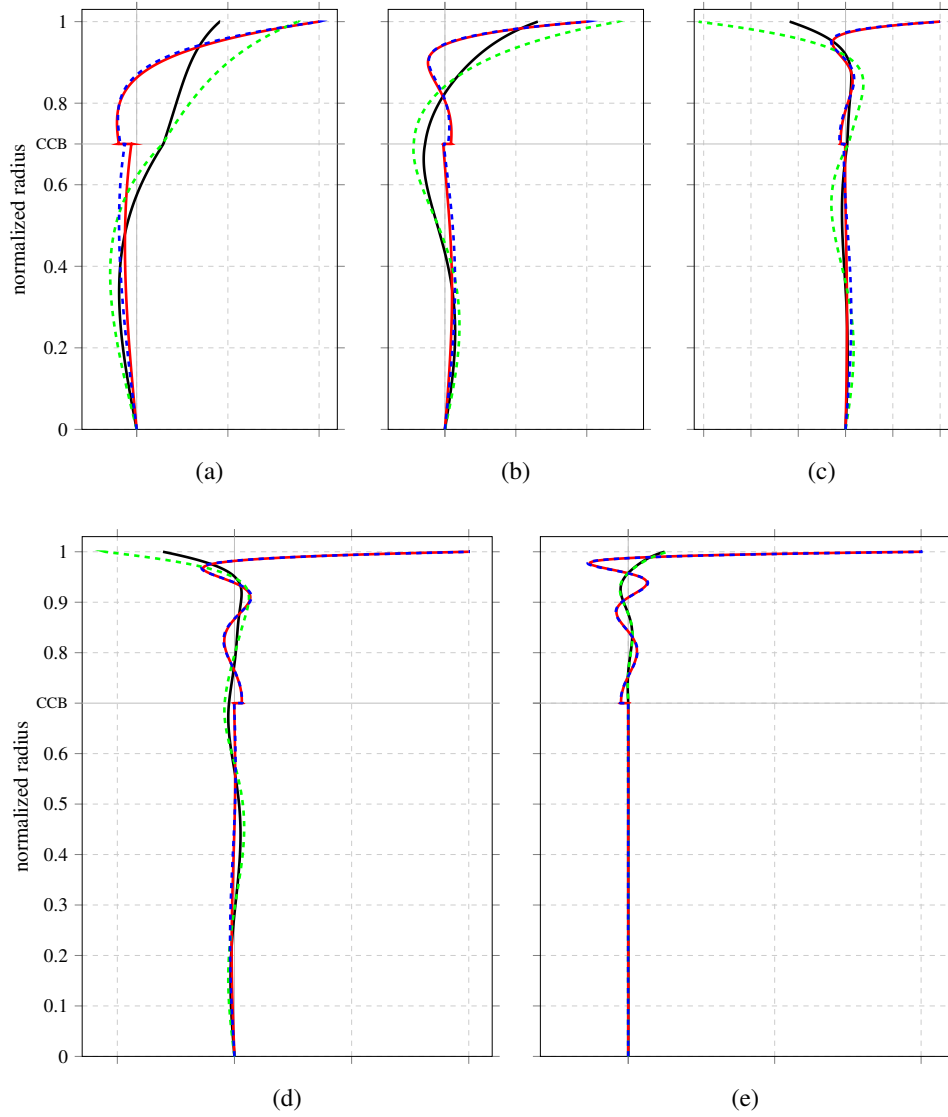


Figure 4.10: Eigenfunctions of s -modes with $\ell = 2$ for the $n = 1$ polytropic fluid model with a crust with shear modulus $\mu = \frac{3}{5}\kappa$, $N = \frac{3}{2}$. Normalized radial (black for exact calculation and green for Cowling approximation) and angular (red for exact calculation and blue for Cowling approximation) displacement eigenfunctions U and V . Figures (a) – (e) contain the results for the s -modes, ascending in overtone number. The boundary between core and crust is indicated by CCB.

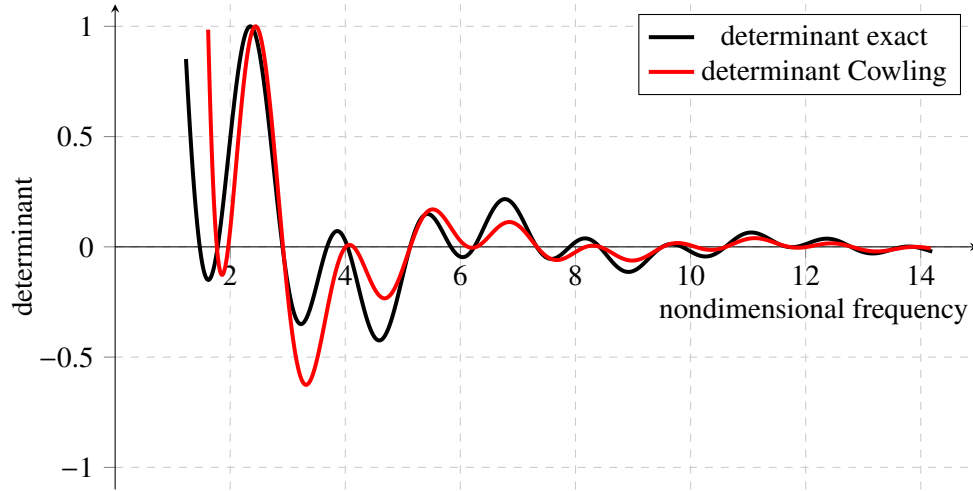


Figure 4.11: Determinant for a $n = 1$ polytropic model with $N = \frac{3}{2}$ and $\ell = 2$, and a solid crust with shear modulus $\mu = \frac{3}{25}\kappa$. The exact results are given in black, Cowling-approximated results in red. The zeros of the determinant are given in table 4.5.

	f	p_1	p_2	p_3	p_4	p_5	p_6
Ω_E	1.470	3.683	5.834	7.901	9.853	11.830	13.702
Ω_C	1.966	4.142	6.131	8.180	10.083	12.029	13.876
	s_1	s_2	s_3	s_4	s_5	s_6	s_7
Ω_E	1.781	2.909	4.040	5.126	6.241	7.326	8.418
Ω_C	1.768	2.917	4.007	5.129	6.278	7.330	8.425
	s_8	s_9	s_{10}	s_{11}	s_{12}		
Ω_E	9.507	10.604	11.691	12.786	13.879		
Ω_C	9.517	10.616	11.708	12.806	13.912		

Table 4.5: Oscillation spectra corresponding to the graphs in figure 4.11. The frequencies are given in units of $\sqrt{\pi G \bar{\rho}_0}$. The exact frequency is given by Ω_E , the frequency in the Cowling approximation is given by Ω_C .

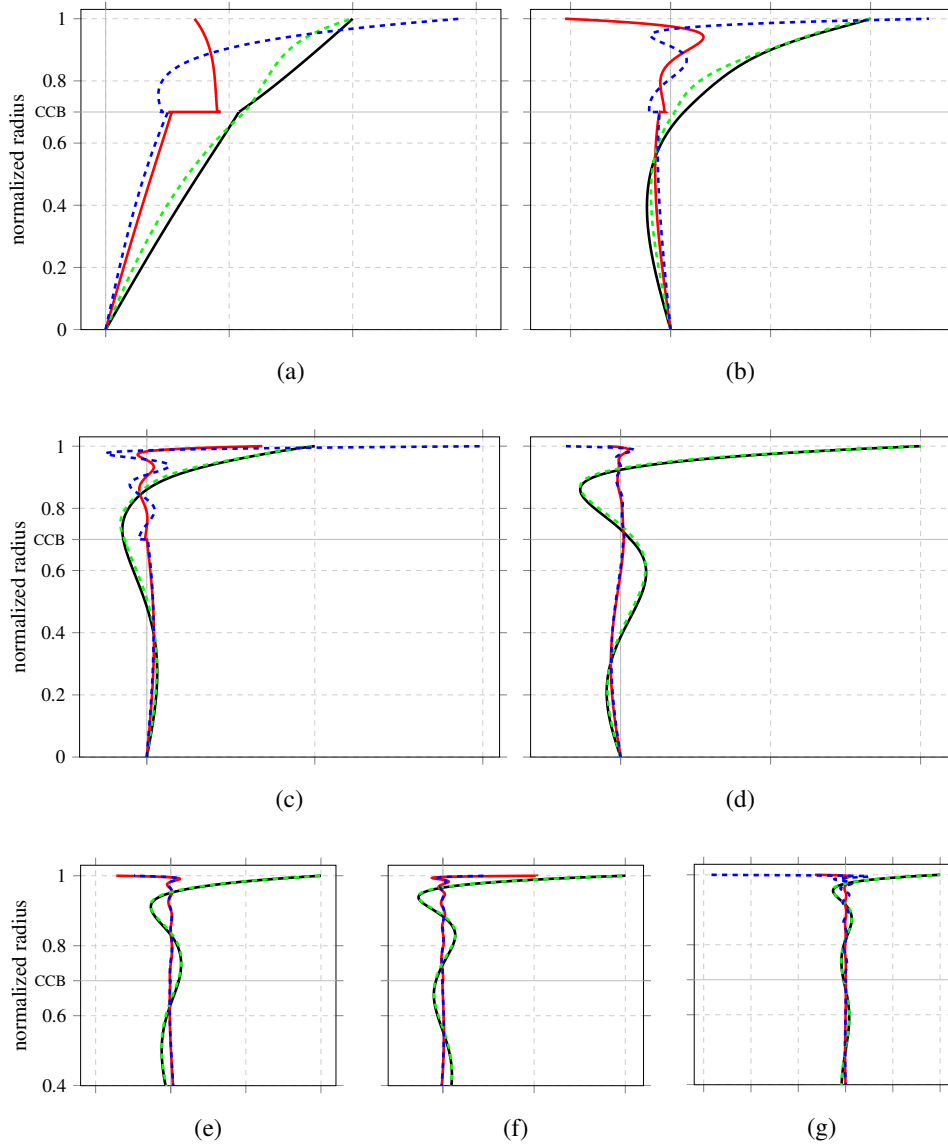


Figure 4.12: Eigenfunctions of f - and p -modes with $\ell = 2$ for the $n = 1$ polytropic fluid model with a crust with shear modulus $\mu = \frac{3}{25}\kappa$, $N = \frac{3}{2}$. Normalized radial (black for exact calculation and green for Cowling approximation) and angular (red for exact calculation and blue for Cowling approximation) displacement eigenfunctions U and V . Figure (a) contains the results for the fundamental (f) mode, figures (b) – (g) contain the results for the p -modes. The boundary between core and crust is indicated by CCB.

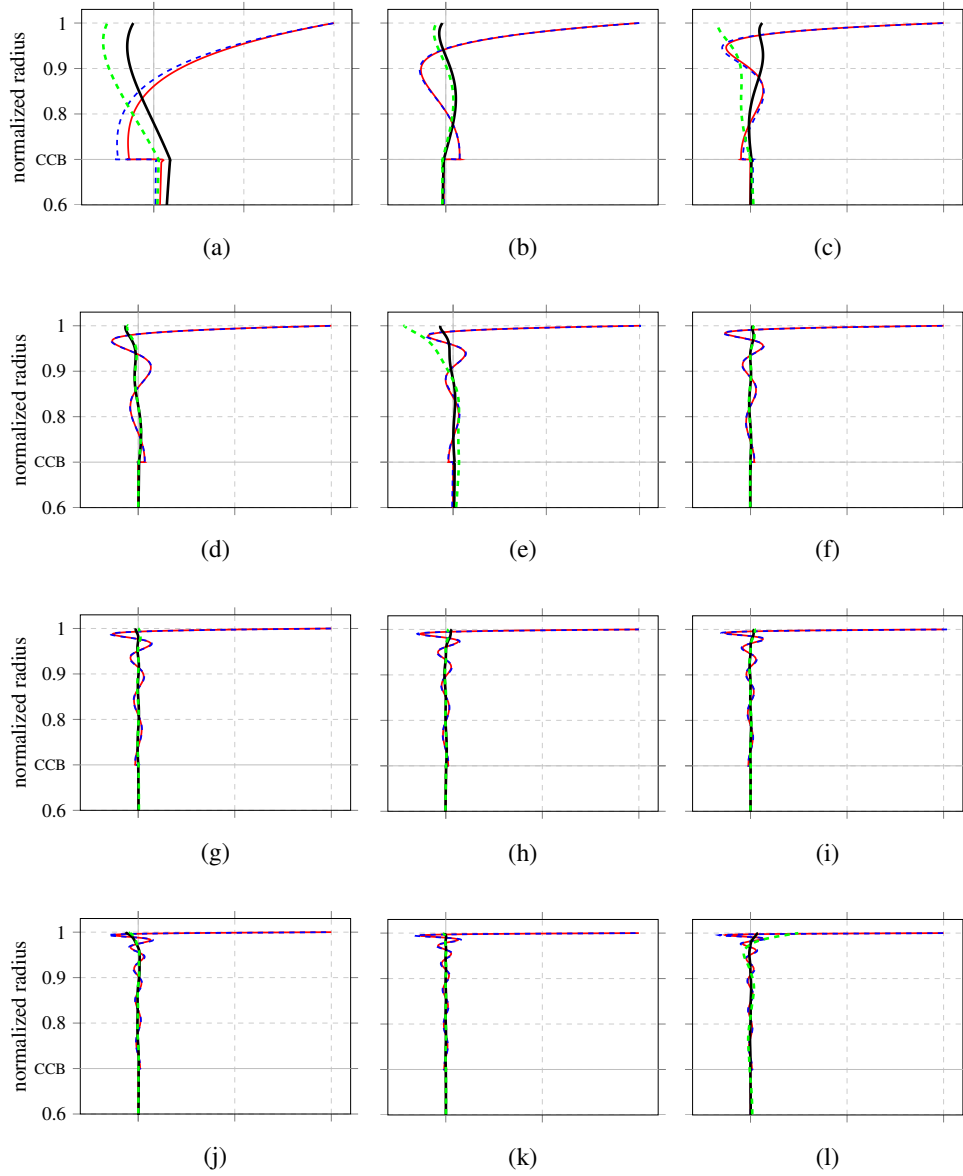


Figure 4.13: Eigenfunctions of s -modes with $\ell = 2$ for the $n = 1$ polytropic fluid model with a crust with shear modulus $\mu = \frac{3}{25}\kappa$, $N = \frac{3}{2}$. Normalized radial (black for exact calculation and green for Cowling approximation) and angular (red for exact calculation and blue for Cowling approximation) displacement eigenfunctions U and V . Figures (a) – (l) contain the results for the s -modes, ascending in overtone number. The boundary between core and crust is indicated by CCB.

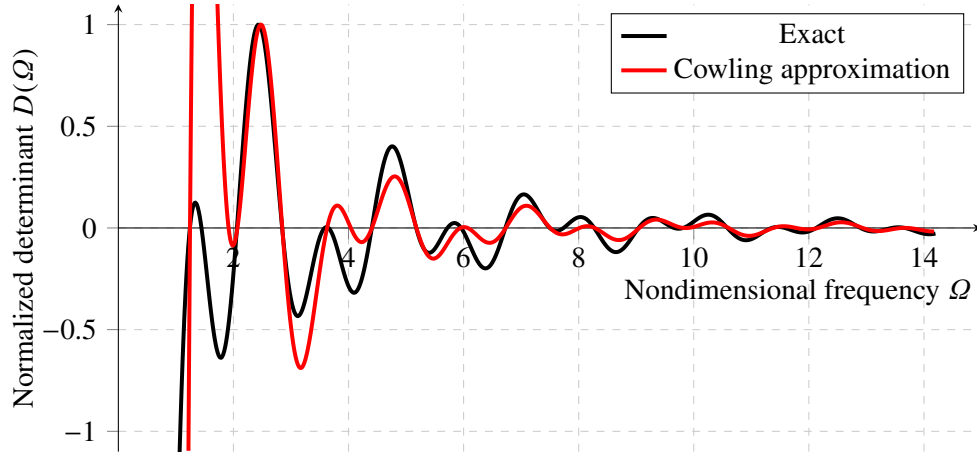
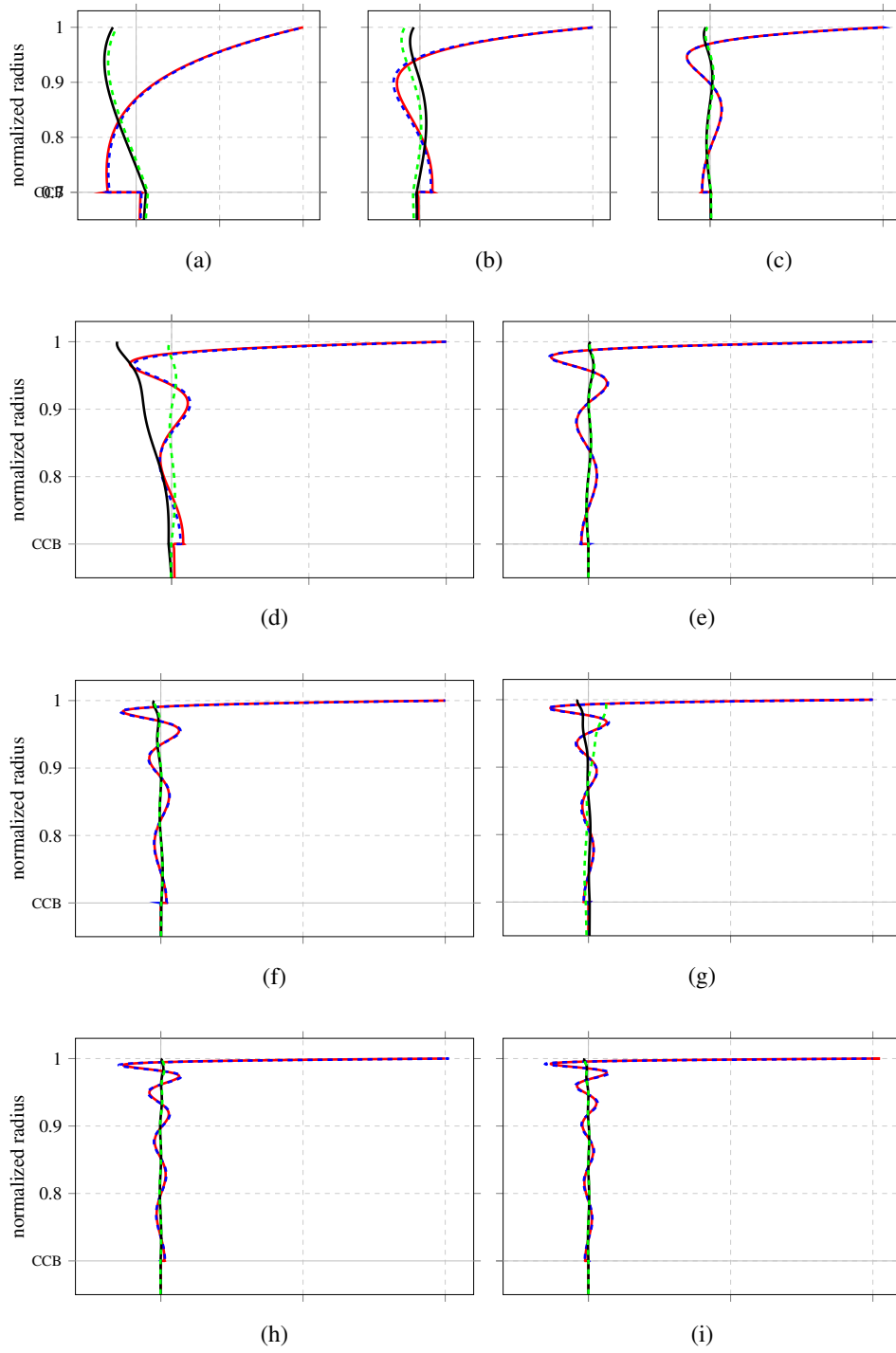


Figure 4.14: Determinant for a $n = 1$, $N = \frac{3}{2}$ polytropic model with $\ell = 2$, and a solid crust with shear modulus $\mu = \frac{3\kappa}{50}$. Exact results are given in black, Cowling-approximated results in red. The roots of the determinant are given in table 4.6.

	f	p_1	p_2	p_3	p_4	p_5	p_6
Ω_E	1.445	3.585	5.719	7.736	9.658	11.582	13.443
Ω_C	1.916	4.040	6.070	8.014	9.899	11.783	13.625
	s_1	s_2	s_3	s_4	s_5	s_6	s_7
Ω_E	1.243	2.061	2.847	3.652	4.404	5.177	5.958
Ω_C	1.245	2.070	2.849	3.628	4.406	5.180	5.945
	s_8	s_9	s_{10}	s_{11}	s_{12}	s_{13}	s_{14}
Ω_E	6.726	7.497	8.269	9.041	9.814	10.584	11.354
Ω_C	6.732	7.505	8.281	9.055	9.827	10.607	11.383
	s_{15}	s_{16}	s_{17}				
Ω_E	12.126	12.900	13.668				
Ω_C	12.161	12.938	13.716				

Table 4.6: Oscillation spectra corresponding to the graphs in figure 4.14. The frequencies are given in units of $\sqrt{\pi G \bar{\rho}_0}$. The exact frequency is given by Ω_E , the frequency in the Cowling approximation is given by Ω_C .



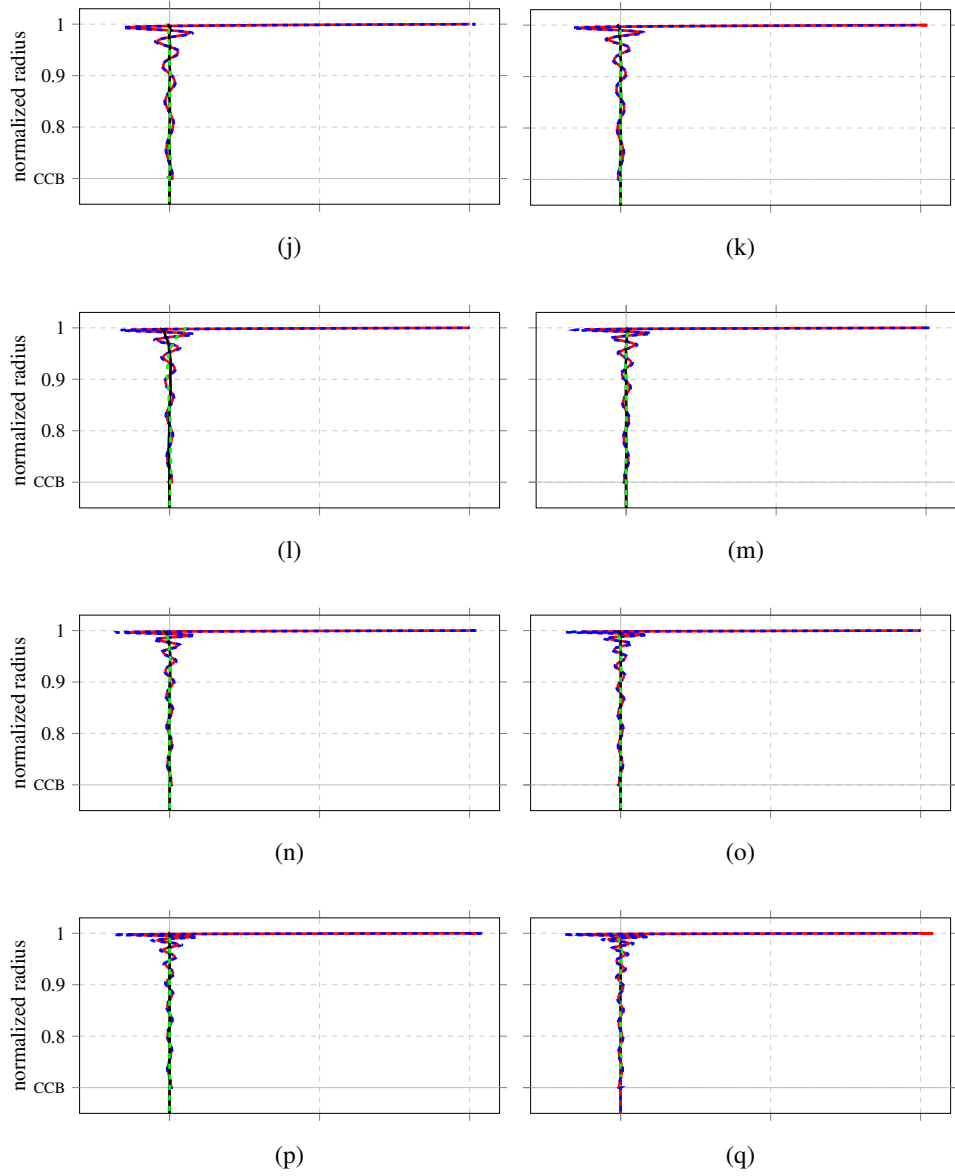


Figure 4.15: Eigenfunctions of s -modes with $\ell = 2$ for the $n = 1$ polytropic fluid model with a crust with shear modulus $\mu = \frac{3}{50}\kappa$, $N = \frac{3}{2}$. Normalized radial (black for exact calculation and green for Cowling approximation) and angular (red for exact calculation and blue for Cowling approximation) displacement eigenfunctions U and V . Figures (a)-(q) contain the results for the s -modes, ascending in overtone number. The boundary between core and crust is indicated by CCB.

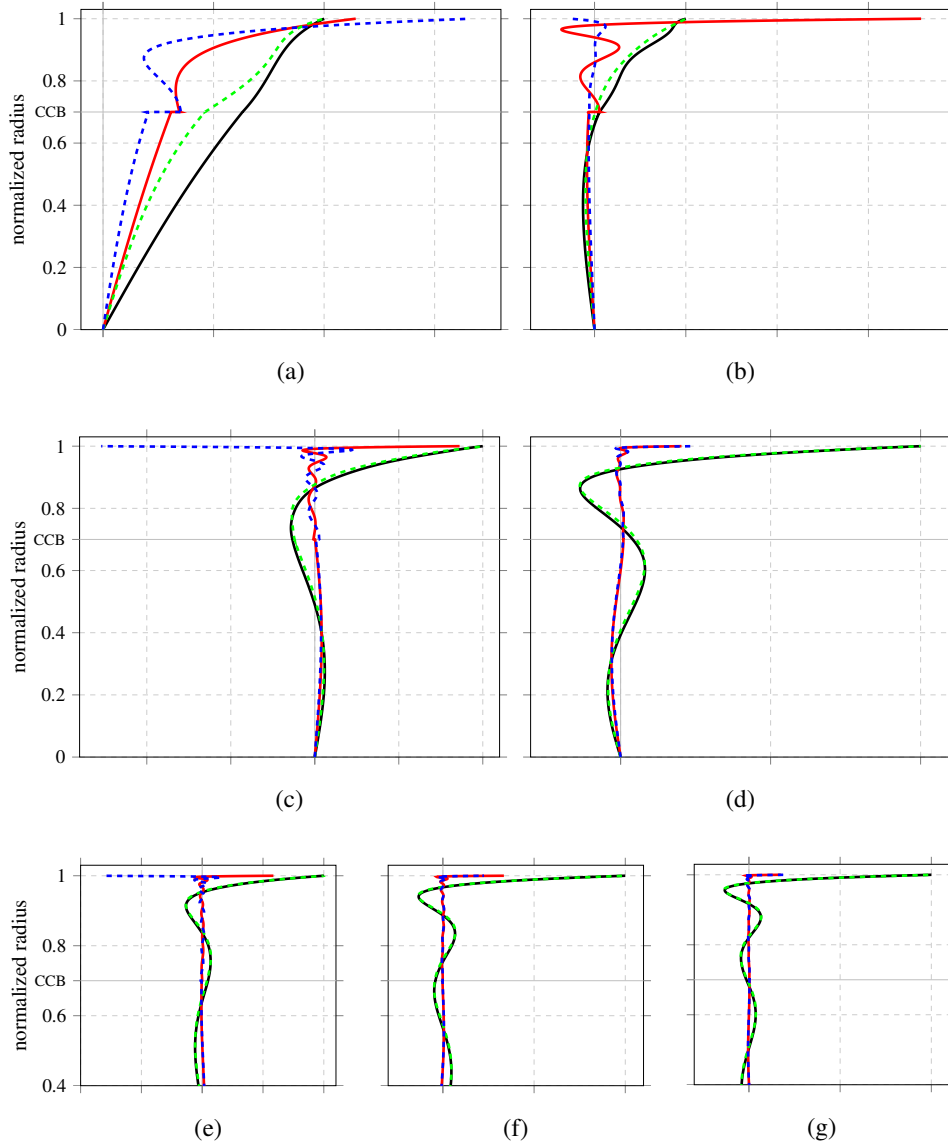


Figure 4.16: Eigenfunctions of f - and p -modes with $\ell = 2$ for the $n = 1$, $N = \frac{3}{2}$ polytropic fluid model with a crust with shear modulus $\mu = \frac{3\kappa}{50}$. Normalized radial (black for exact calculation and green for Cowling approximation) and angular (red for exact calculation and blue for Cowling approximation) displacement eigenfunctions U and V . Figure (a) contains the results for the fundamental (f) mode, figures (b) – (g) contain the results for the p -modes. The boundary between core and crust is indicated by CCB.

4.3.3 Spectra in Cowling-approximated general relativity

In this section, the frequency spectra and radial displacement eigenfunctions of the $\ell = 2$ modes for a $n = N = 1$ relativistic polytrope with a bulk modulus κ defined by equation (2.98) are presented, for three different models with a crust with shear modulus $\mu = \frac{3}{5}\kappa$, $\mu = \frac{13}{40}\kappa$ and $\mu = \frac{3}{50}\kappa$.

The calculations are done for four increasingly relativistic models, starting with a nonrelativistic calculation.

As is described in section 3.2, the Cowling-approximated calculation procedure in the fluid core is identical to the procedure of fluid models leading to a solution $\boldsymbol{\eta}^{(1)}$, except that an extra solution $\boldsymbol{\eta}^{(3)}$ is integrated from the core-crust boundary onwards, which is located at $x = 0.7$.

Since the Cowling approximation is applied, at the free surface, the boundary conditions are formulated as:

$$D(\Omega) = \begin{vmatrix} \eta_4^{(1)} & \eta_5^{(1)} \\ \eta_4^{(3)} & \eta_5^{(3)} \end{vmatrix} = 0 \text{ if } \Omega \text{ is an eigenfrequency.} \quad (4.9)$$

The determinants for the increasingly more relativistic models with $GM/c^2R = 0.0, 0.1, 0.145$ and 0.2 are plotted as a function of the frequency Ω in figures 4.17, 4.20 and 4.23, for the crustal models with $\mu = \frac{3}{5}\kappa$, $\mu = \frac{13}{40}\kappa$ and $\mu = \frac{3}{50}\kappa$ respectively.

The eigenfrequencies for the fundamental mode and p -modes are given in table 4.7, 4.9 and 4.11. The eigenfrequencies for the s -modes are given in table 4.8, 4.10 and 4.12.

Each eigenfrequency has corresponding radial and angular eigenfunctions. The f - and p -mode eigenfunctions for the three crustal models are given in figures 4.18, 4.21 and 4.24 respectively. These eigenfunctions are normalized such that U has unit value at the free surface. The eigenfunctions for the s -modes are given in figures 4.19, 4.22 and 4.25 respectively, and are normalized such that $V = 1$ at the free surface, since these modes are dominated by angular motion.

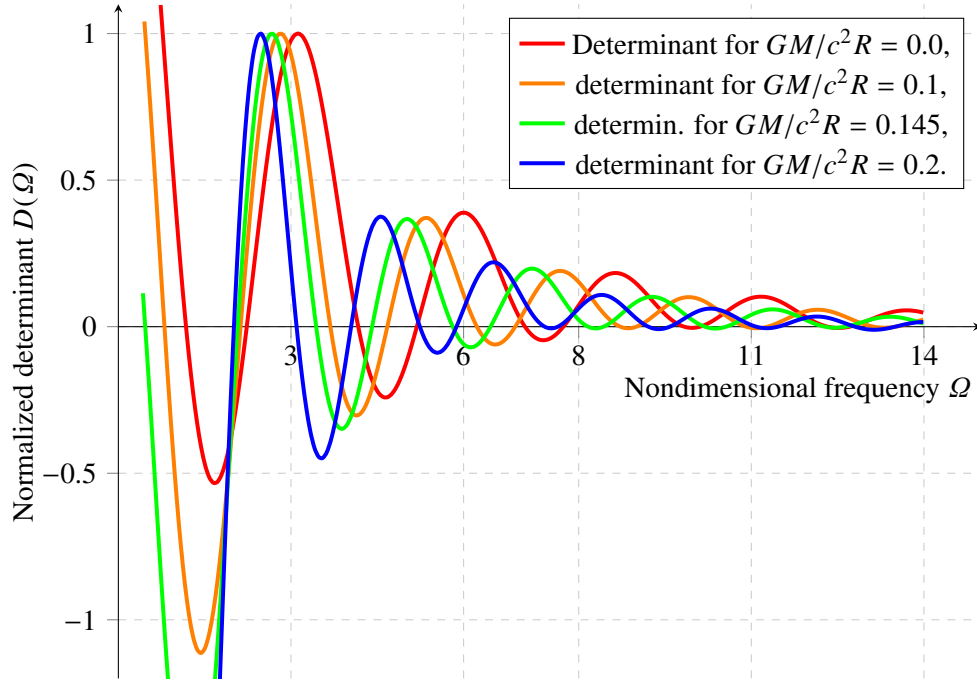


Figure 4.17: Determinant for a $n = N = 1$ relativistic polytropic model with $\ell = 2$, and a solid crust with shear modulus $\mu = \frac{3}{5}\kappa$. Calculations for four increasingly relativistic models are given. The zeros of the determinants are given in tables 4.7 and 4.8 for the f - and p -modes and s -modes respectively.

GM/c^2R	0.0	0.1	0.145	0.2
f	2.232	2.124	2.074	2.009
p_1	5.188	4.674	4.410	4.045
p_2	7.734	6.898	6.468	5.876
p_3	10.109	9.003	8.432	7.639
p_4	12.326	10.911	10.193	9.210
p_5		13.125	12.277	11.085
p_6				12.802

Table 4.7: Oscillation spectra for f - and p -modes corresponding to figure 4.17. The frequencies are given in units of $\sqrt{\pi G \bar{\rho}_0}$.

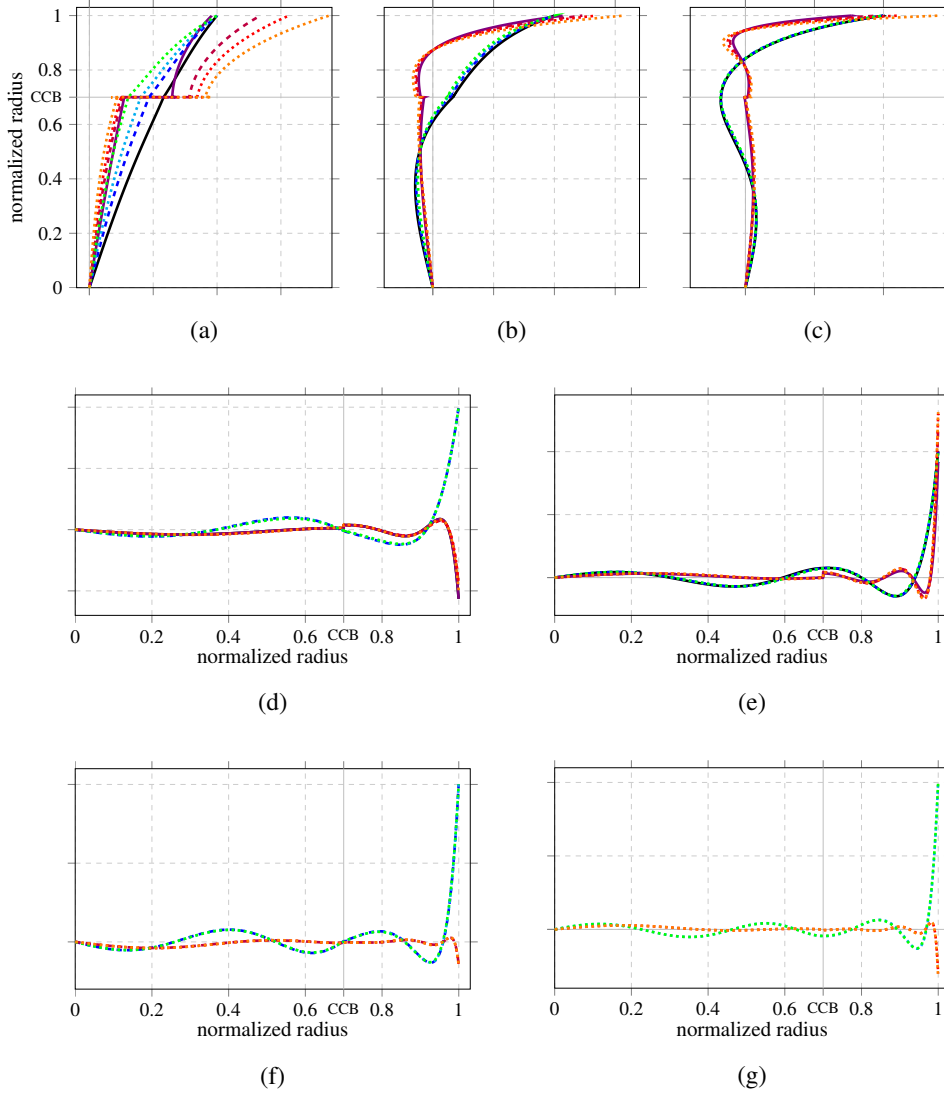


Figure 4.18: Eigenfunctions of f - and p -modes with $\ell = 2$ for the $n = N = 1$ polytropic relativistic fluid model with a crust with shear modulus $\mu = \frac{3}{5}\kappa$. Normalized radial (black for nonrelativistic calculation and blue, cyan and green for relativistic calculations with $GM/c^2R = 0.1, 0.145$ and 0.2 respectively) and angular (violet for nonrelativistic calculation and purple, red and orange for the relativistic calculations for ascending GM/c^2R) displacement eigenfunctions U and V . Figure (a) contains the results for the fundamental (f) mode, figures (b) – (g) contain the results for the p -modes. The boundary between core and crust is indicated by CCB.

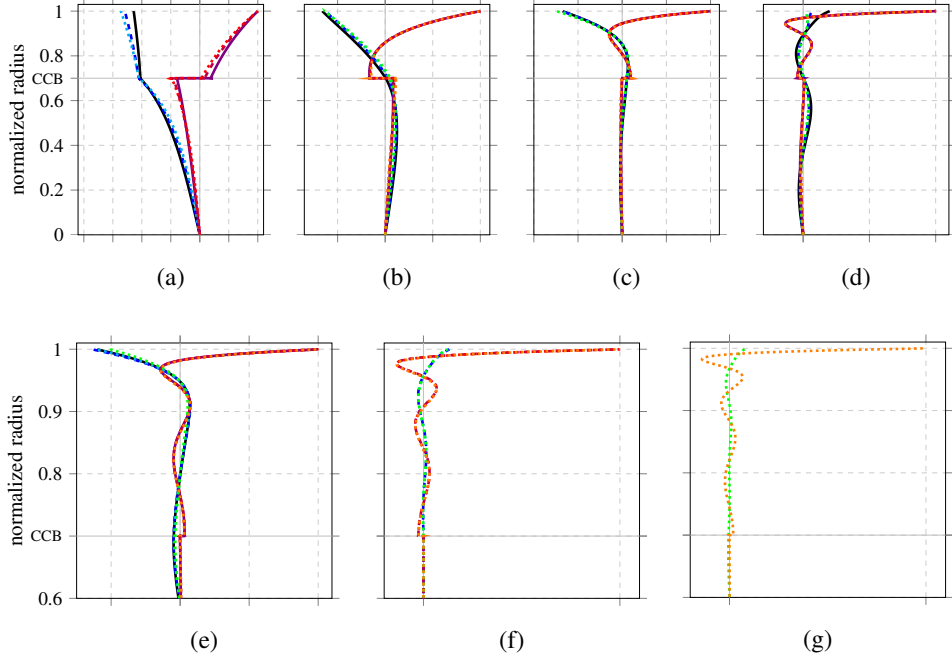


Figure 4.19: Eigenfunctions of s -modes with $\ell = 2$ for the $n = N = 1$ polytropic relativistic fluid model with a crust with shear modulus $\mu = \frac{3}{5}\kappa$. Colors as in figure 4.18. Figures (a) – (g) contain the results for the s -modes. The boundary between core and crust is indicated by CCB.

GM/c^2R	0.0	0.1	0.145	0.2
s_1	1.176	0.801	0.467	
s_2	4.169	3.685	3.438	3.098
s_3	7.067	6.231	5.811	5.240
s_4	9.834	8.723	8.164	7.408
s_5	12.708	11.283	10.563	9.584
s_6		13.511	12.635	11.465
s_7				13.501

Table 4.8: Oscillation spectra for s -modes corresponding to figure 4.17. The frequencies are given in units of $\sqrt{\pi G \bar{\rho}_0}$.

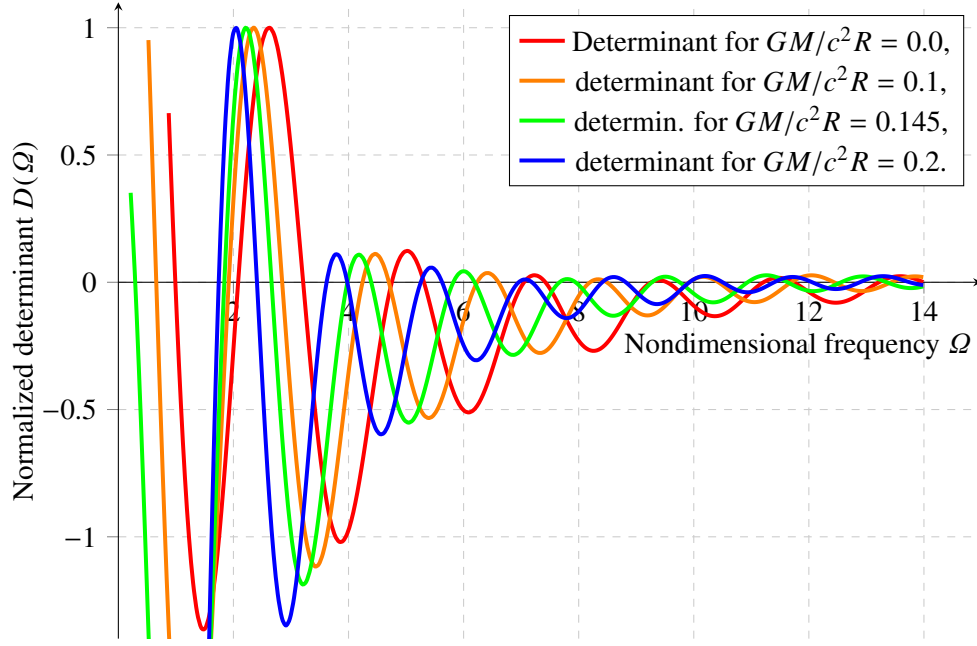
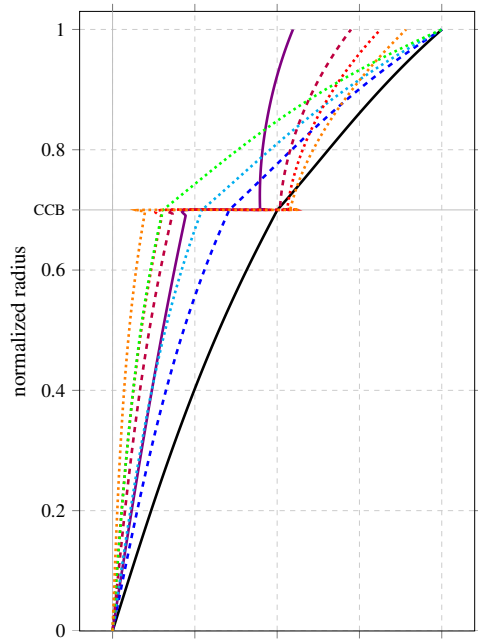


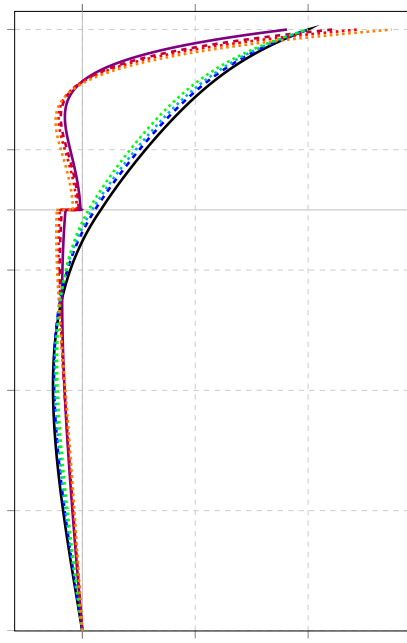
Figure 4.20: Determinants for a $n = N = 1$ relativistic polytropic model with $\ell = 2$, and a solid crust with shear modulus $\mu = \frac{13}{40}\kappa$. Calculations for four increasingly relativistic models are given. The zeros of the determinants are given in tables 4.9 and 4.10 for the f - and p -modes and s -modes respectively.

GM/c^2R	0.0	0.1	0.145	0.2
f	2.082	1.918	1.842	1.745
p_1	4.752	4.243	3.981	3.619
p_2	7.051	6.235	5.821	5.256
p_3	9.532	8.487	7.945	7.187
p_4	11.735	10.428	9.754	8.819
p_5	13.996	12.438	11.630	10.502
p_6			13.355	12.058
p_7				13.752

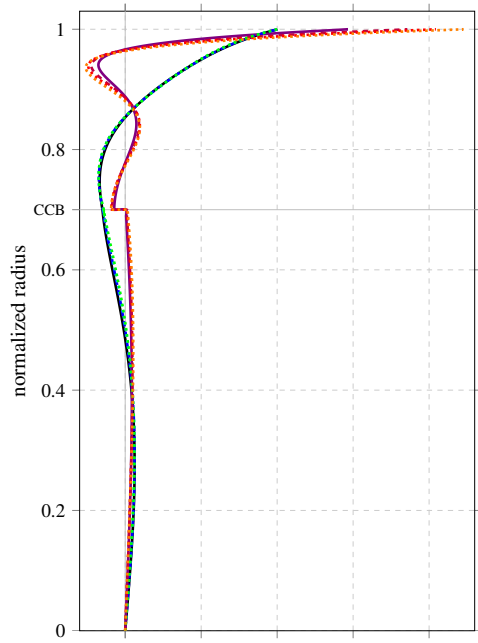
Table 4.9: Oscillation spectra for f - and p -modes corresponding to figure 4.20. The frequencies are given in units of $\sqrt{\pi G \bar{\rho}_0}$.



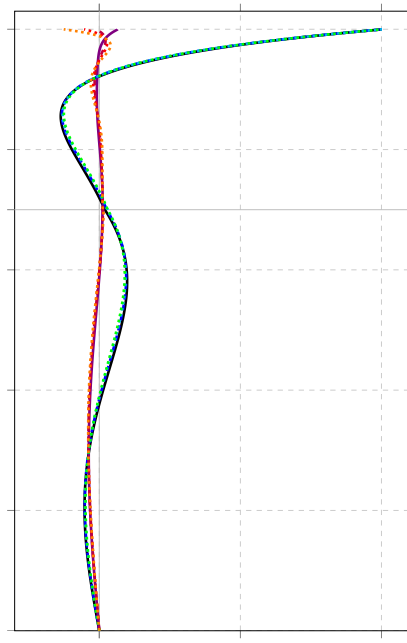
(a)



(b)



(c)



(d)

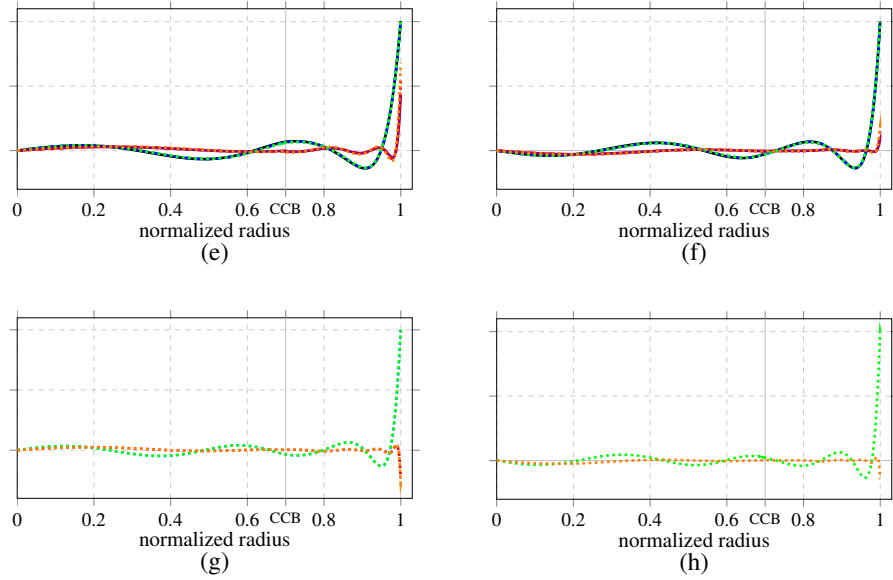


Figure 4.21: Eigenfunctions of f - and p -modes with $\ell = 2$ for the $n = N = 1$ polytropic relativistic fluid model with a crust with shear modulus $\mu = \frac{13}{40}\kappa$. Colors as in figure 4.18. Figure (a) contains results for the f -mode, figures (b)–(h) contain results for the p -modes. The boundary core-crust boundary is indicated by CCB.

GM/c^2R	0.0	0.1	0.145	0.2
s_1	0.990	0.659	0.293	
s_2	3.212	2.847	2.662	2.409
s_3	5.311	4.702	4.395	3.979
s_4	7.421	6.605	6.191	5.627
s_5	9.261	8.197	7.666	6.957
s_6	11.211	9.918	9.273	8.410
s_7	13.218	11.694	10.936	9.924
s_8		13.433	12.561	11.396
s_9				12.886

Table 4.10: Oscillation spectra for s -modes corresponding to figure 4.20. The frequencies are given in units of $\sqrt{\pi G \bar{\rho}_0}$.

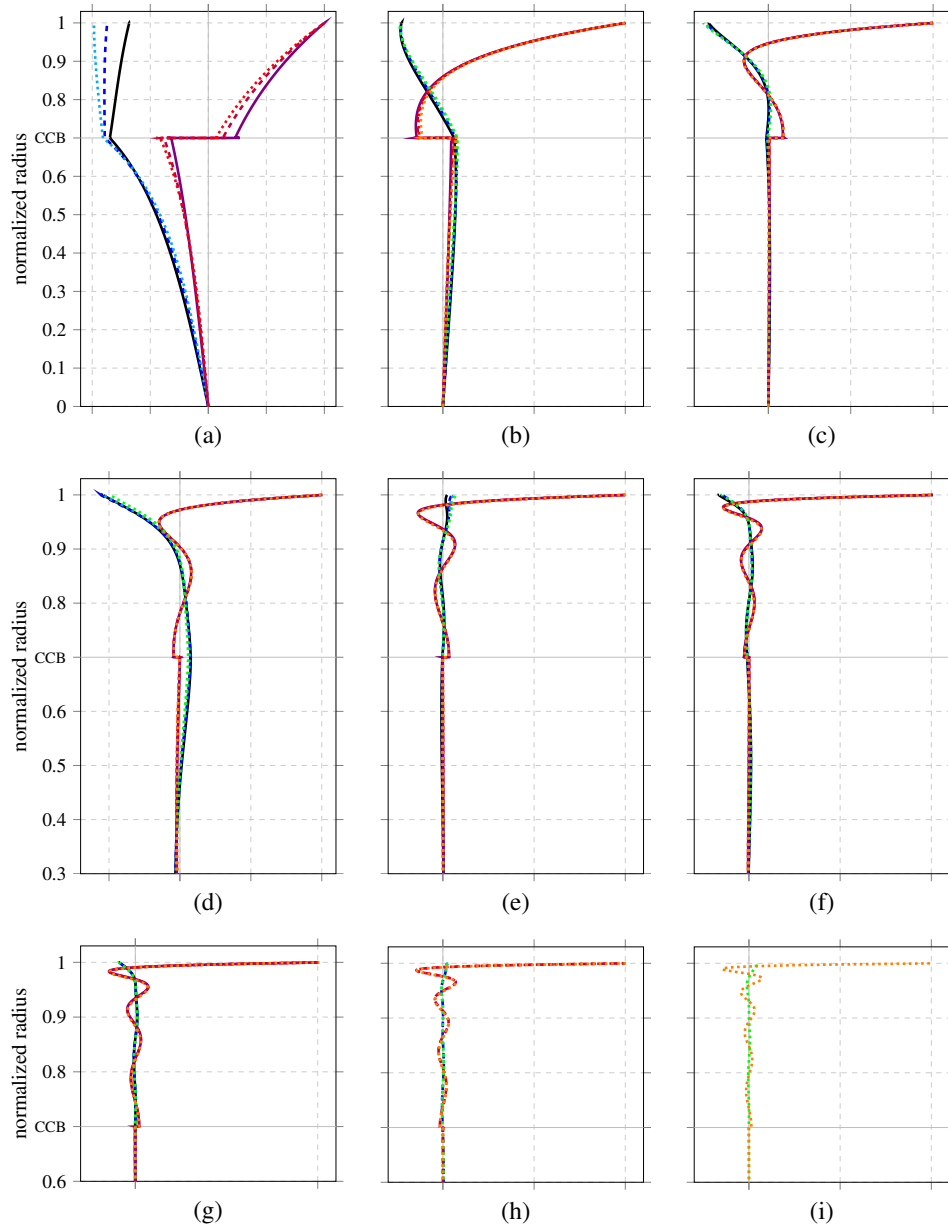


Figure 4.22: Eigenfunctions of s -modes with $\ell = 2$ for the $n = N = 1$ polytropic relativistic fluid model with a crust with shear modulus $\mu = \frac{3}{25}\kappa$. Colors as in figure 4.18. Figures (a) – (i) contain the results for the s -modes in ascending overtone number. The boundary between core and crust is indicated by CCB.

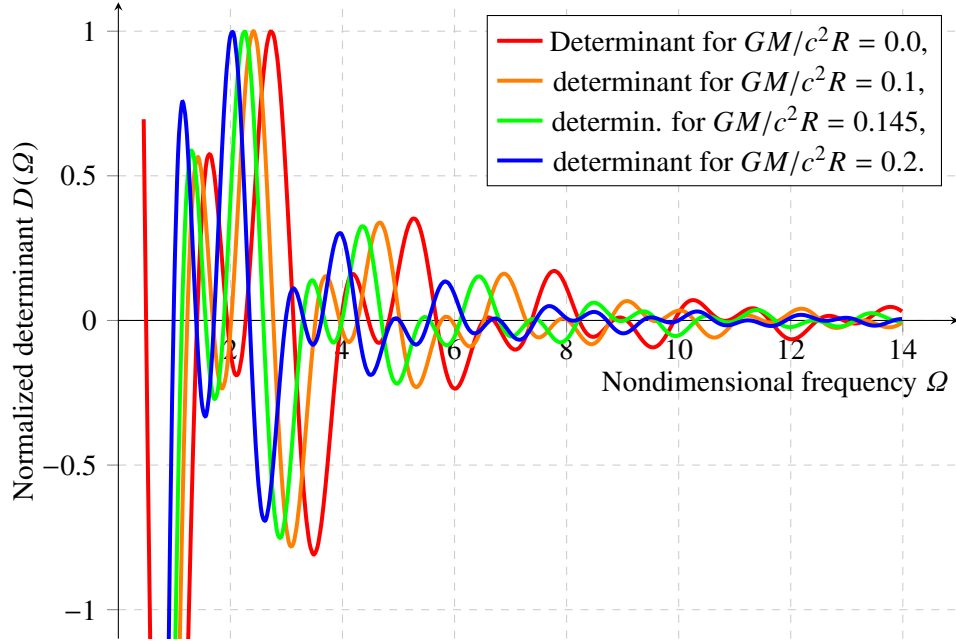


Figure 4.23: Determinants for a $n = N = 1$ relativistic polytropic model with $\ell = 2$, and a solid crust with shear modulus $\mu = \frac{3}{50}\kappa$. Calculations for four increasingly relativistic models are given. The zeros of the determinants are given in tables 4.11 and 4.12 for the f - and p -modes and s -modes respectively.

GM/c^2R	0.0	0.1	0.145	0.2
f	1.941	1.686	1.556	1.389
p_1	4.465	3.949	3.682	3.310
p_2	6.699	5.948	5.559	5.017
p_3	8.826	7.845	7.338	6.632
p_4	10.884	9.665	9.036	8.161
p_5	12.944	11.492	10.743	9.702
p_6		13.277	12.410	11.203
p_7			14.080	12.710

Table 4.11: Oscillation spectra for f - and p -modes corresponding to figure 4.23. The frequencies are given in units of $\sqrt{\pi G \bar{\rho}_0}$.

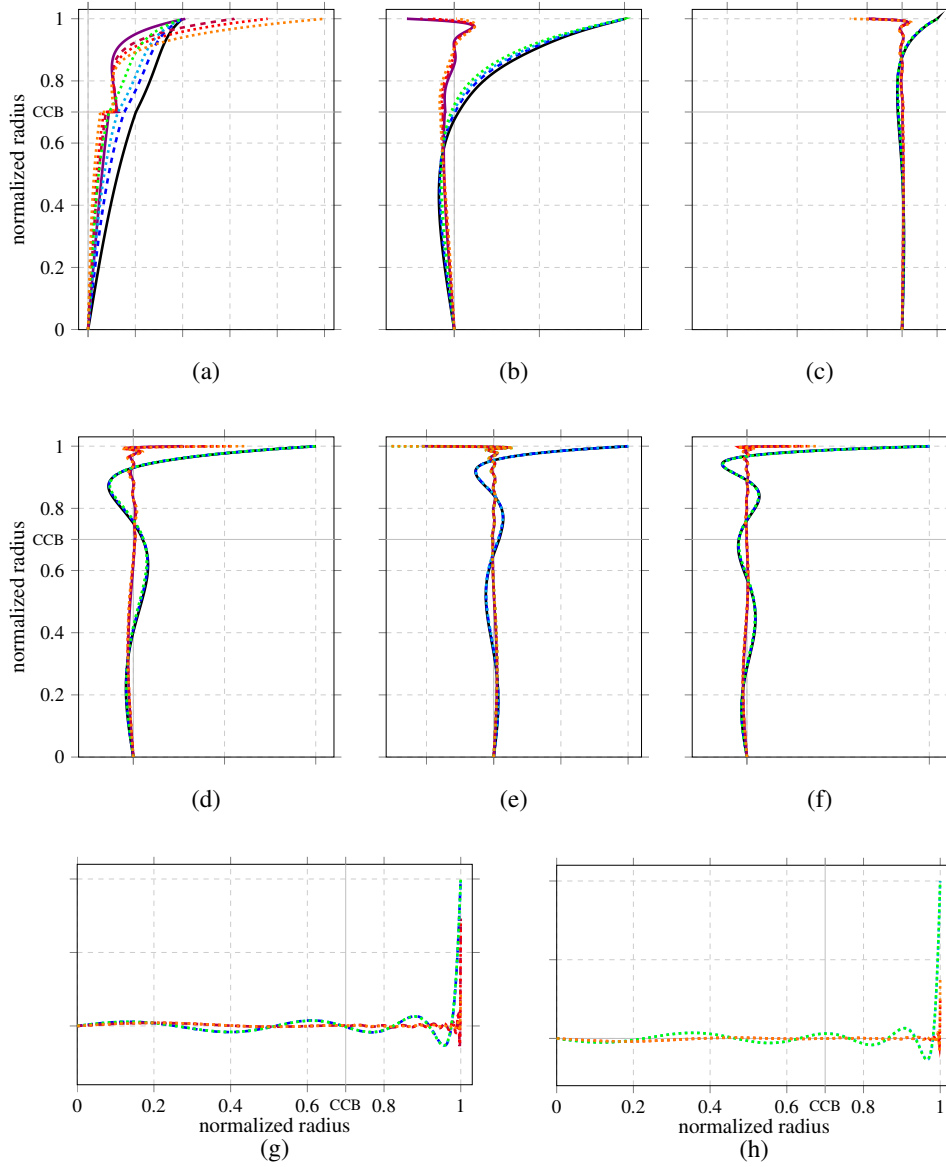
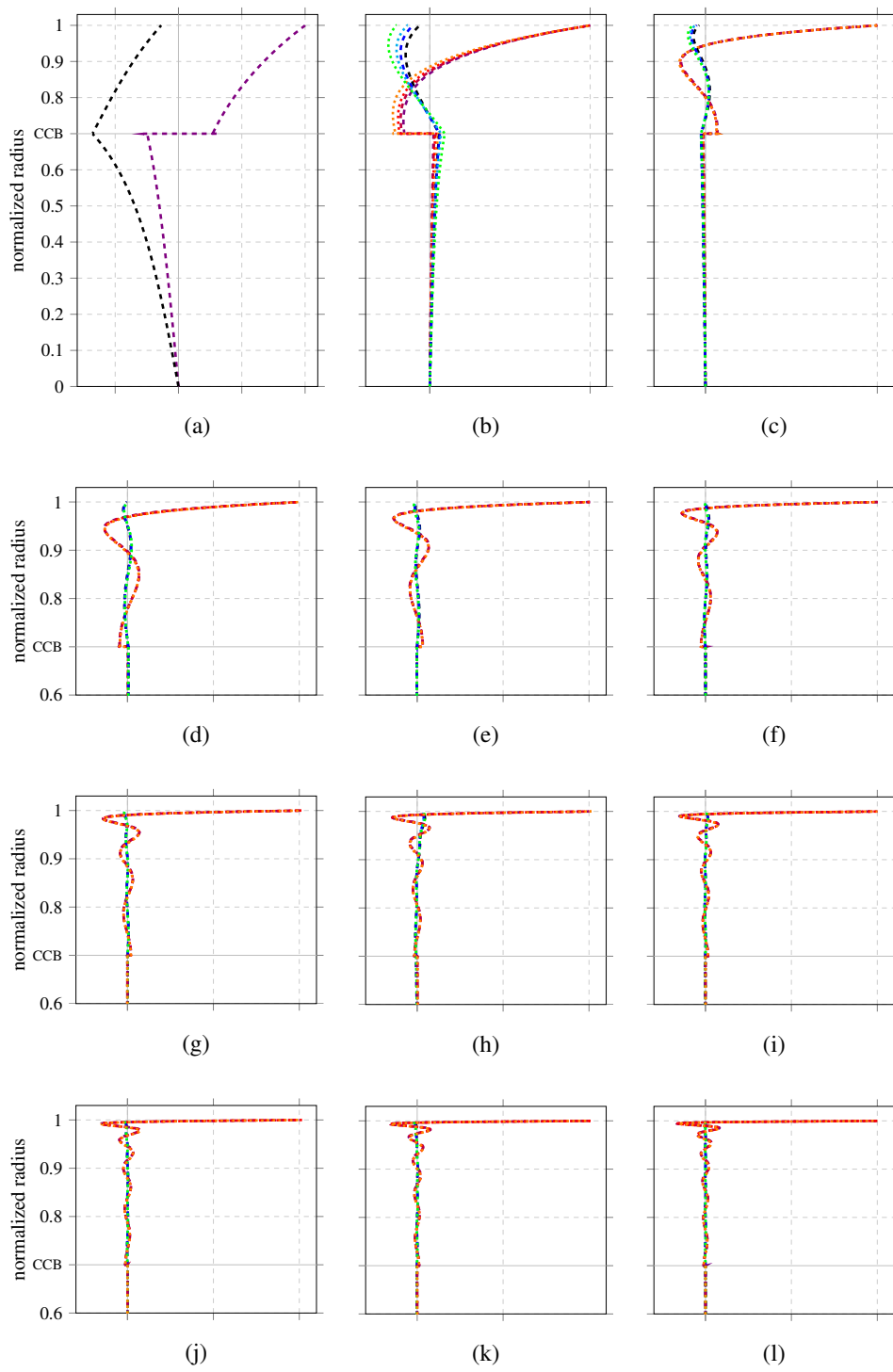


Figure 4.24: Eigenfunctions of f - and p -modes with $\ell = 2$ for the $n = N = 1$ polytropic relativistic fluid model with a crust with shear modulus $\mu = \frac{3}{50}\kappa$. Colors as in figure 4.18. Figure (a) contains the results for the fundamental (f) mode, figures (b) – (h) contain the results for the p -modes.

GM/c^2R	0.0	0.1	0.145	0.2
s_1	0.495			
s_2	1.406	1.230	1.133	0.985
s_3	2.273	2.014	1.884	1.707
s_4	3.125	2.766	2.586	2.345
s_5	3.976	3.518	3.290	2.985
s_6	4.828	4.271	3.994	3.623
s_7	5.676	5.021	4.695	4.260
s_8	6.518	5.765	5.390	4.888
s_9	7.377	6.525	6.102	5.536
s_{10}	8.224	7.274	6.802	6.171
s_{11}	9.074	8.026	7.505	6.810
s_{12}	9.923	8.776	8.206	7.445
s_{13}	10.772	9.527	8.907	8.080
s_{14}	11.625	10.280	9.611	8.719
s_{15}	12.477	11.033	10.314	9.356
s_{16}	13.331	11.788	11.020	9.996
s_{17}		12.541	11.724	10.634
s_{18}		13.296	12.429	11.273
s_{19}		14.050	13.134	11.912
s_{20}			13.839	12.551
s_{21}				13.193
s_{22}				13.834

Table 4.12: Oscillation spectra for s -modes corresponding to figure 4.23. The frequencies are given in units of $\sqrt{\pi G \bar{\rho}_0}$.



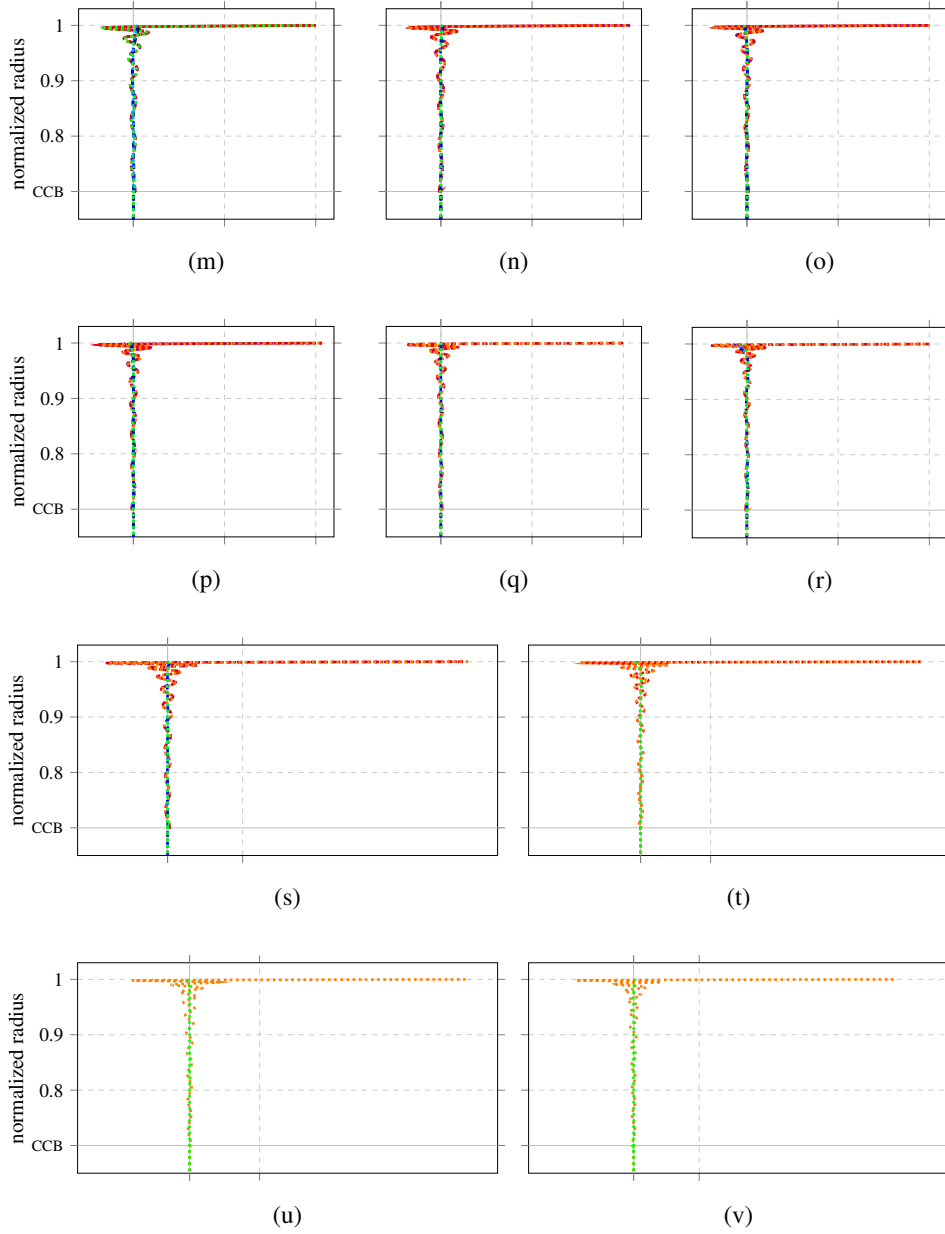


Figure 4.25: Eigenfunctions of s -modes with $\ell = 2$ for the $n = N = 1$ polytropic relativistic fluid model with a crust with shear modulus $\mu = \frac{3}{50}\kappa$. Colors as in figure 4.18. Figures (a) – (v) contain the results for the s -modes in ascending overtone number. The boundary between core and crust is indicated by CCB.

Chapter 5

Discussion and conclusion

The findings presented in this thesis show that the Cowling-approximated equations of motion governing relativistic neutron star oscillations for fluid and elastic models can be put as a set of coupled first order differential equations

$$\frac{d\mathbf{y}(r)}{dr} = \mathbf{A}(\omega, r)\mathbf{y}(r), \quad (5.1)$$

where \mathbf{y} is a vector with functions representing perturbations of the stellar model as a function of the radial position r in the model; \mathbf{A} is a matrix of which the components are functions dependent on equilibrium model parameters and the oscillation frequency ω . The matrix \mathbf{A} has the form of a Hamiltonian matrix:

$$\mathbf{A} = \begin{pmatrix} \mathbf{T} & \mathbf{K} \\ \mathbf{S} & -\mathbf{T}^T \end{pmatrix}, \quad (5.2)$$

where \mathbf{T} , \mathbf{K} and \mathbf{S} are matrices and \mathbf{K} and \mathbf{S} are symmetric. Oscillation spectra for various Newtonian and relativistic polytropic stellar model have been calculated to prove the practical applicability of this new formulation of the equations of motion.

Further, it is shown that the Cowling approximation, in which the perturbation of gravitational potential is neglected, has very little effect on s -modes of neutron star models, when analyzed in the context of Newtonian gravity.

The fact that the relativistic oscillations of stars are expressible as (5.1) – (5.2) is noteworthy, because it opens the way to the application of the ‘minors’ method discovered by Gilbert and Backus (1966) and (1969) to the equations (5.1) – (5.2) in a way Woodhouse (1988) has done in the context of terrestrial seismology.

This technique solves two problems that are present in normal mode seismology. Firstly it makes it possible to check in an efficient way whether all eigenfrequencies in a given frequency interval are found, which is useful since the oscillation spectrum for a neutron star model with a crust contains many irregularly spaced eigenfrequencies. Secondly, for moderately high frequencies the differential equations in the form (5.1) – (5.2) are numerically unstable, which is not the case anymore if the ‘minors’ method is applied. Although it is not the objective of this study to implement the ‘minors’ method in relativistic neutron star seismology, the first step to this end is taken by showing that the Cowling-approximated relativistic equations possess the structure of the form (5.1) – (5.2).

The fact that the Cowling approximation has very little effect on the s -mode spectrum of oscillations in the context of Newtonian gravity is an expected result, since s -modes are dominated by angular motion and hence do not significantly effect the mass distribution and consequently the neglect of gravitational potential perturbation is not expected to have a big influence on the results. The numerical confirmation of this expectation is important however, since s -modes play an important role in neutron star seismology. Since starquakes originate in the crust, these modes are excited in particular and an accurate theoretical description of the modes is needed to correctly interpret measurements of oscillation spectra. Further, this suggests that for the relativistic calculations, the Cowling-approximated s -mode spectrum is a good benchmark for a numerical algorithm solving the fully relativistic oscillation spectrum.

The numerical findings obtained by using the formulation (5.1) – (5.2) of the equations of motion for neutron star oscillations coincide with results for the spectrum obtained in different studies. Firstly, for the calculations in the context of Newtonian gravitational theory, the spectra for uniform spherical models obtained by Love (1911) are reproduced for both a fluid and an elastic sphere. The spectra obtained by Robe (1968) for polytropic fluid stellar models with and without applying the Cowling approximation are also reproduced. The results for Cowling-approximated oscillation spectra obtained by McDermott, Van Horn and Hansen (1988), agree qualitatively with the results obtained in this study. There is no quantitative agreement, since another (non-polytropic) equation of state is used in their equilibrium neutron star model. Both results do agree in the sense that important qualitative observations such as the existence of the f - p - and s -modes in the spectrum, coincide. Secondly, for relativistic Cowling-approximated calculations, the spectra for polytropic fluid stellar models obtained by Ipser and Lindblom (1992) and Yoshida and Kojima (1997) are reproduced. The calculations for neutron star models with a crust agree qualitatively with Yoshida and Lee (2002).

One important limitation in this study is the apparent instability of the numerical methods at very low frequencies. Whereas McDermott, Van Horn and Hansen (1988) and Yoshida and Lee (2002) report the existence of interfacial *i*-modes and buoyancy driven *g*-modes at frequencies lower than that of the *f*-mode, these are not found in this study, since for very low frequencies the spectrum could not be resolved.

An interesting phenomenon occurs when eigenfrequencies of different mode types almost coincide. The eigenfunctions of these two modes are usually very different. But when their corresponding eigenfrequencies are close, both modes are mixed. This phenomenon is called avoided mode crossing, and is observed by McDermott, Van Horn and Hansen (1988) and Yoshida and Lee (2002) between *i*-modes and by Levin and Ushomirsky (2001) between rotational *r*-mode and higher order toroidal modes in the crust.

The results presented in this study suggest that avoided mode crossing also takes place between *p*- and *s*-modes. When the eigenfrequencies of *p*- and *s*-modes are close, both modes get a mixed character, resulting in two modes with $U \sim V$ that are difficult to distinguish.

This is, for example, clearly visible in figures 4.15 and 4.16, which are the *p*- and *s*-mode eigenfunctions for the Newtonian calculations with a crust having a shear modulus of $\mu = \frac{3}{50}\kappa$. In these two images, it is clearly visible that the fact that the Cowling approximation is applied, makes little difference on the form of the eigenfunctions, except in some cases, where significant deviations between the Cowling-approximated and exact results occur. In figure 4.16 for the *p*-modes, this is the case for subfigures (b), (c) and (e), for the p_1 , p_2 and p_4 modes. In figure 4.15 for the *s*-modes, this is the case for subfigures (d), (g) and (l), for the s_4 , s_7 and s_{12} modes. Unlike for the other modes, a clear distinction between the Cowling-approximated and exact eigenfunctions exists. This is explained by examining the frequencies of the *s*-modes in table 4.6. Clearly, the exact eigenfrequencies of the p_1 and s_4 modes are very close, whereas the corresponding Cowling-approximated frequencies are further apart. This means that the exact result for the p_1 and s_4 mode should be of a more mixed character than its Cowling approximated counterpart. This is indeed the case, since in both cases, the amplitudes of the oscillations are shifted more toward $U \sim V$. In the case of the p_2 , s_4 and p_4 , s_7 pairs of modes, the opposite is the case: now the Cowling-approximated eigenfrequencies of both pairs are very close, whereas their exact counterparts are not. Hence the opposite effect is observed: the Cowling-approximated eigenfunctions are of a more mixed character.

Another interesting observation can be made by comparing the spectra for different crustal neutron star models. Since the square of the shear wave speed $v_s^2 = \mu/\rho$ is linearly related to the shear modulus, it is expected that the squared oscillation frequencies of s -modes are also linearly related to the shear modulus. It turns out that this relation indeed exists, which is shown by taking the squared eigenfrequencies for different crustal models from the results section. These values are summarized in table 5.1 and plotted in figure 5.1.

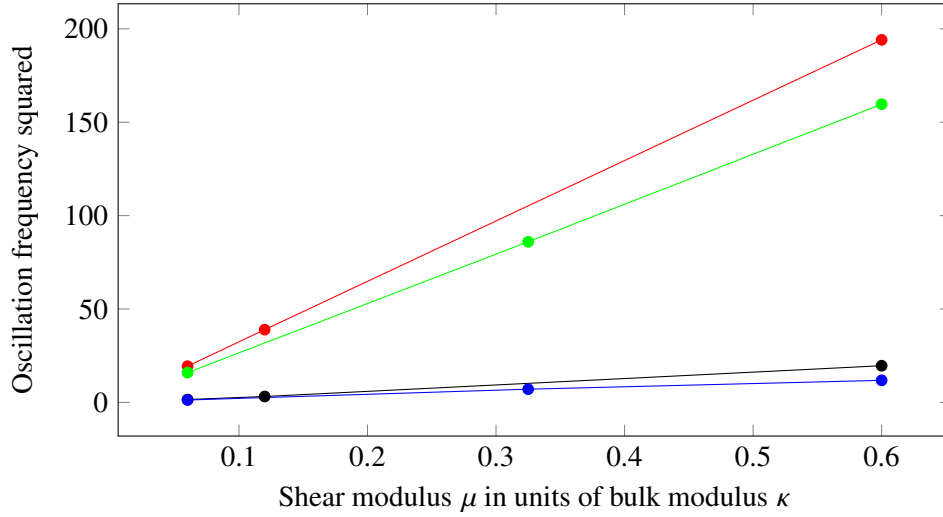


Figure 5.1: Linear relation between squared eigenfrequency and shear modulus.

(a)	$\mu = \frac{3}{50}\kappa$	$\mu = \frac{3}{25}\kappa$	$\mu = \frac{3}{5}\kappa$
s_1	1.545	3.172	19.643
s_5	19.395	38.950	194.128
(b)	$\mu = \frac{3}{50}\kappa$	$\mu = \frac{13}{40}\kappa$	$\mu = \frac{3}{5}\kappa$
s_2	1.284	7.086	11.820
s_6	15.952	85.989	159.643

Table 5.1: Squared frequencies for shear modes for (a): a Newtonian model with various crustal models, and for (b): a relativistic model with $GM/c^2R = 0.145$ for various crustal models. The values are squared frequencies taken from tables 4.4, 4.5, 4.6 and tables 4.8, 4.10, 4.12 respectively.

Whereas the exact relativistic oscillation spectrum of a completely fluid neutron star has been found (Detweiler and Lindblom, 1985), until now the relativistic Cowling approximation has always been applied when nonradial relativistic oscillations of a neutron star model with a solid crust are studied numerically, even though the equations of motion for the exact relativistic problem have been derived by Finn (1990). An interesting direction of further research would be to take these equations of motion and to see whether they can be formulated in the form (5.1) – (5.2). Subsequently, numerical solutions of this problem could be obtained. A further step would be to implement the ‘minors’ method, which would allow very accurate calculations of the exact relativistic oscillation spectrum of neutron stars up to very high frequencies. In these calculations, the Cowling-approximated results for s -modes found in this study could serve as a benchmark.

It is hypothesized, see Weber (2005) for a review, that the core of neutron stars may consist of quark matter. Rajagopal and Sharma (2006) have shown that it is reasonable to suppose that the entire quark matter core could be in a crystalline color superconducting phase. The Earth also has a solid core and in terrestrial seismology, there is one mode of particular interest, which is not yet observed: the Slichter mode (Rieutord, 2002). This is an oscillatory mode with a very low frequency, in which the inner core makes translational oscillations around the center of the earth, moving in the fluid outer core. It could be an interesting direction of further research to see what the influence of a solid core on the oscillation spectrum of a neutron star is and whether a potentially observable relativistic analogue of the Slichter mode exists for neutron stars.

As was mentioned, the differential equations have a regular singularity at the free surface, because the bulk modulus and shear modulus vanishes there. In this study, this problem was addressed by stopping integration just underneath the free surface. A more neat way to treat this problem has yet to be found.

In conclusion, in this study I tried to bring the fields of terrestrial and stellar seismology a little bit closer together. By introducing a formulation with symplectic structure of the equations of motion for the Earth in relativistic neutron star seismology, relativistic neutron star seismology gains access to methods used in terrestrial seismology to calculate the oscillation spectrum of the Earth accurately up to very high frequencies. This brings the final goal of neutron star seismology a little closer: to find out about the inside of one of the most extreme astronomical objects in our universe.

Bibliography

- Al-Attar, David and Woodhouse, John H.; 2008. Calculation of seismic displacement fields in self-gravitating earth models – applications of minors vectors and symplectic structure; *Geophysical Journal International*; 175; 3; 1176 – 1208.
- Alterman, Z., Jarosch, H. and Pekeris, C.L.; 1959. Oscillations of the Earth; *Proceedings of the Royal Society of London. Series A, Mathematical and Physical sciences*; Vol. 252; No. 1268; 80 – 95.
- Andersson, Nils and Kokkotas, Kostas D.; 1998. Towards gravitational wave asteroseismology; *Mon. Not. R. Astron. Soc.*; 299; 1059 – 1068.
- Carter, B. and Quintana, H.; 1972. Foundations of General Relativistic High-Pressure Elasticity Theory; *Proceedings of the Royal Society of London*; Series A; 331; 1584; 57 – 83.
- Chandrasekhar, S.; 1957. An introduction to the study of Stellar Structure; *Dover Publications Inc.*; New York.
- Chapman, C.H., Woodhouse, J.H.; 1981. Symmetry of the wave equation and excitation of body waves; *Geophysical Journal of the Royal Astronomical Society*; 65; 3; 777 – 782.
- Cowling, Thomas G.; 1941. The non-radial oscillations of polytropic stars; *Monthly Notices of the Royal Astronomical Society*; 101; 367 – 375.
- Crossley, D.J.; 1974. The Free-Oscillation Equations at the Centre of the Earth; *Geophysical Journal of the Royal Astronomical Society*; 41; 2; 153 – 163.
- Dahlen, F.A. and Tromp, J.; 1998. Theoretical Global Seismology; *Princeton University Press*.

- Detweiler, S.L. and Lindblom, L.; 1985. On the nonradial pulsations of general relativistic stellar models; *Astrophysical Journal*, Part 1, Vol. 292, 12 – 15.
- Euler, Leonhard; 1757. Principes generaux du mouvement des fluides; *Mémoires de l'académie des sciences de Berlin*; 11; 274 – 315.
- Finn, Lee Samuel; 1990. Non-radial pulsations of neutron stars with a crust; *Mon. Not. R. astr. Soc.*; 245, 82 – 91.
- Gilbert, F., Backus, G. E.; 1966. Propagator matrices in elastic wave and vibration problems; *Geophysics*; 31; 326 – 333.
- Gilbert, F., Backus, G. E.; 1969. A computational problem encountered in a study of the Earth's normal modes. *Proc. December 9-11, 1968 Fall Joint Computer Conference*, part II, 1273 – 1277.
- Haensel, P, Potekhin, A.Y., and Yakovlev, D.G.; 2007. Neutron stars 1: Equation of state and structure, *Springer*, chapter 3.7.1, 156 – 159.
- Hansen, Carl J. and van Horn, Hugh M.; 1979. White dwarf seismology; *The Astrophysical Journal*; 233; 253 – 258.
- Hurley, K. et. al.; 1999. A giant periodic flare from the soft big gamma-ray repeater SGR1900+14; *Nature*; 397; 41 – 43.
- Hurley, K. et. al.; 2005. An exceptionally bright flare from SGR 1806–20 and the origins of short-duration big gamma-ray bursts; *Nature*; 434; 1098 – 1103.
- Hurley, Margaret, Roberts, P.H., Wright, K.; 1966. The oscillations of Gas Spheres; *The Astrophysical Journal*; 143; 535 – 551.
- Ipsier, James R. and Lindblom, Lee; 1992. On the pulsations of relativistic accretion disks and rotating stars: the Cowling approximation; *Astrophysical Journal*; 389; 392 – 399.
- Israel, G.L., Belloni, T., Stella, L., et. al.; 2005. Discovery of rapid X-ray oscillations in the tail of the SGR 1806-20 hyperflare; *Astrophysical Journal*; 628, L53.
- Jeffreys, Sir Harold, and Swirles, Bertha (Lady Jeffreys); 1956. Methods of Mathematical Physics, third edition; *Cambridge University Press*; Chapter 3.03; 87 – 89.
- Kojima, Y.; Two Families of Normal Modes in Relativistic Stars; *Progress of Theoretical Physics*; 79; 665 – 675.

- Kokkotas, K.D. and Schutz, B.F.; 1986. Normal modes of a model radiating system; *General Relativity and Gravitation*; 18; 913 – 921.
- Kokkotas, K.D. and Schutz, B.F.; 1992. W-modes - A new family of normal modes of pulsating relativistic stars; *Monthly Notices of the Royal Astronomical Society*; 255; 119 – 128.
- Lamb, H.; 1882. On the vibrations of an elastic sphere, *Proc. Lond. Math. Soc.*; 13; 189 – 212.
- Leins, M.; 1994. PhD Thesis, *Univ. Tübingen*.
- Levin, Y. and Ushomirsky, G.; 2001. Crust–core coupling and r-mode damping in neutron stars: a toy model; *Mon. Not. R. Astron. Soc.*; 324; 917– 922.
- Lindblom, L. and Detweiler, S.L.; 1983. The quadrupole oscillations of neutron stars; *Astrophysical Journal Supplement Series*; 53; 73 – 92.
- Love, Augustus E. H.; 1911. Some Problems of Geodynamics; *Cambridge University Press*.
- Martinec, Z.; 1984. Free oscillations of the Earth; *Travaux geophysiques*, 591, XXXII, 117–236.
- Mazets, E.P. et. al.; A flaring X-ray pulsar in Dorado; *Pis'ma Astron. Zh.*; 5; 307 – 312.
- Mazets, E.P. et. al.; Observations of a flaring X-ray pulsar in Dorado; *Nature*; 282; 578 – 589.
- McDermott, P.N., Van Horn, H.M., Hansen, C.J.; 1988. Nonradial Oscillations of Neutron Stars; *The Astrophysical Journal*, 325; 725 – 748.
- McDermott, P. N., Van Horn, Hugh M. and Scholl, J. F.; 1983. Nonradial g-mode oscillations of warm neutron stars; *The Astrophysical Journal*; 268; 837 – 848.
- Navier, Claude L. M. H.; 1823. Mémoire sur les lois du mouvement des fluides; *Mém. Acad. Sci. Inst. France*; 6; 389 – 440.
- Negele, J.W., and Vautherin, D.; 1973. Neutron star matter at sub-nuclear densities; *Nuclear Physics A*; 207; 2; 298 – 320.
- Ogata, Shuji and Ichimaru, Setsuo; 1990. First-principles calculations of shear moduli for Monte Carlo-simulated Coulomb solids; *Physical review A*; 42; 8; 4867 – 4870.

- Pekeris, Chaim L.; 1938. Nonradial Oscillation of Stars; *Astrophysical Journal*; 88; 189 – 199.
- Poisson, S. D.; 1829. Mémoire sur l'équilibre et le mouvement des corps élastiques; *Mém. Acad. Roy. Sci. Inst. France*; 8; 357 – 370.
- Press, William H.; Teukolsky, Saul A.; Vetterling, William T.; Flannery, Brian P.; 1992. Numerical Recipes in Fortran 77, Second Edition, *Cambridge University Press*.
- Rajagopal, K. and Sharma, R.; 2006. Crystallography of three-flavor quark matter; *Physical Review D*; 74; 094019.
- Rieutord, M.; 2002. Slichter modes of the Earth revisited; *Physics of the Earth and Planetary Interiors*; 131, 269 – 278.
- Robe, H.; 1968. Les oscillations non radiales des polytropes; *Annales d' Astrophysique*; 31; 475 – 482.
- Schumaker, Bonny L., Thorne, Kip S.; 1983. Torsional oscillations of neutron stars; *Mon. Not. R. astr. Soc.*; 203, 457 – 489.
- Schwarzschild, Karl; 1916. Über das Gravitationsfeld einer Kugel aus inkompressibler Flüssigkeit; *Reimer, Berlin* 1916; pp. 424-434 (Sitzungsberichte der Königlich-Preussischen Akademie der Wissenschaften)
- Thomson, William; 1863. Dynamical problems regarding elastic spheroidal shells and spheroids of incompressible liquid; *Phil. Trans. Roy. Soc. Lond.*; 153; 583 – 616.
- Thorne, Kip S.; Campolattaro, Alfonso; 1967. Non-Radial Pulsation of General-Relativistic Stellar Models. I. Analytic Analysis for $L \geq 2$; *Astrophysical Journal*, vol 149, 591 – 611.
- Tooper, Robert F.; 1964. General Relativistic Polytropic Fluid Spheres; *Astrophysical Journal*, vol. 140; 434 – 459.
- Weber, F.; 2005. Strange quark matter and compact stars; *Progress in Particle and Nuclear Physics*; 54; 1; 193 – 288.
- Woodhouse, J.; 1978. Lecture notes obtained from Prof. Dr. Jeannot Trampert.
- Woodhouse, J. H.; 1988. The calculation of the eigenfrequencies and eigenfunctions of the free oscillations of the Earth and the Sun, In: D. J. Doornbos, ed., *Seismological Algorithms*; *Academic Press*; 321 – 370.

- Yoshida, Shijun and Kojima, Yasufumi; 1997. Accuracy of the relativistic Cowling approximation in slowly rotating stars; *Mon. Not. R. Astron. Soc.*; 289; 117 – 122.
- Yoshida, S., Lee, U.; 2002. Nonradial oscillations of neutron stars with a solid crust; *Astronomy and Astrophysics*; 395; 201 – 208.

Appendix A

Vector calculus

A.1 Identities

A few identities from vector calculus have been listed below. Proofs of these identities are readily found in introductory text books on vector calculus. In the identities below, f is a scalar function, \mathbf{v} is a vector field and \mathbf{T} is a tensor field. The \times -sign denotes a cross product, the central dot a dot product. The superscript T denotes transposition.

Curl of the gradient:

$$\nabla \times \nabla f = 0. \quad (\text{A.1})$$

Divergence of the curl:

$$\nabla \cdot \nabla \times \mathbf{v} = 0. \quad (\text{A.2})$$

Gradient of the divergence:

$$\nabla (\nabla \cdot \mathbf{v}) = \nabla \cdot [(\nabla \mathbf{v})^T]. \quad (\text{A.3})$$

Curl of the curl:

$$\nabla \times \nabla \times \mathbf{v} = \nabla (\nabla \cdot \mathbf{v}) - \nabla \cdot \nabla \mathbf{v}. \quad (\text{A.4})$$

Product rule I:

$$\nabla (fg) = f\nabla g + g\nabla f. \quad (\text{A.5})$$

Product rule II:

$$\nabla \cdot (f\mathbf{T}) = f\nabla \cdot \mathbf{T} + (\nabla f) \cdot \mathbf{T}. \quad (\text{A.6})$$

Product rule III:

$$\nabla \cdot (f\mathbf{v}) = f\nabla \cdot \mathbf{v} + \mathbf{v} \cdot \nabla f. \quad (\text{A.7})$$

Product rule IV:

$$\nabla \times (f\mathbf{v}) = f\nabla \times \mathbf{v} - \mathbf{v} \times \nabla f. \quad (\text{A.8})$$

Definition of the Laplacian operator ∇^2 :

$$\nabla \cdot \nabla f = \nabla^2 f. \quad (\text{A.9})$$

A.2 Spherical coordinates

The spherical coordinate system that is used has radial coordinate r , polar coordinate θ and azimuthal coordinate ϕ . Expressions for the gradient, curl, divergence and Laplacian in spherical coordinates are listed below. These expressions are mainly used to obtain equations of motion for neutron star oscillations in spherical coordinates. Proofs can be found in introductory text books on vector analysis.

The gradient of a scalar function f in spherical coordinates is:

$$\nabla f = \hat{r} \frac{\partial}{\partial r} + \hat{\theta} \frac{1}{r} \frac{\partial}{\partial \theta} + \hat{\phi} \frac{1}{r \sin \theta} \frac{\partial}{\partial \phi}. \quad (\text{A.10})$$

The Laplacian of a scalar function f in spherical coordinates is:

$$\nabla^2 f = \frac{1}{r^2} \frac{\partial}{\partial r} \left(r^2 \frac{\partial f}{\partial r} \right) + \frac{1}{r^2 \sin \theta} \frac{\partial}{\partial \theta} \left(\sin \theta \frac{\partial f}{\partial \theta} \right) + \frac{1}{r^2 \sin^2 \theta} \frac{\partial^2 f}{\partial \phi^2}. \quad (\text{A.11})$$

The curl of a vector field \mathbf{v} is:

$$\begin{aligned} \nabla \times \mathbf{v} = & \frac{1}{r \sin \theta} \left(\frac{\partial}{\partial \theta} (v_\phi \sin \theta) - \frac{\partial v_\theta}{\partial \phi} \right) \hat{r} + \\ & + \frac{1}{r} \left(\frac{1}{\sin \theta} \frac{\partial v_r}{\partial \phi} - \frac{\partial}{\partial r} (r v_\phi) \right) \hat{\theta} + \frac{1}{r} \left(\frac{\partial}{\partial r} (r v_\theta) - \frac{\partial v_r}{\partial \theta} \right) \hat{\phi}. \end{aligned} \quad (\text{A.12})$$

The divergence of a vector field \mathbf{v} is:

$$\nabla \cdot \mathbf{v} = \frac{1}{r^2} \frac{\partial}{\partial r} (r^2 v_r) + \frac{1}{r \sin \theta} \left(\frac{\partial}{\partial \theta} (v_\theta \sin \theta) + \frac{\partial v_\phi}{\partial \phi} \right). \quad (\text{A.13})$$

The Laplacian of a vector field \mathbf{v} is:

$$\begin{aligned}\nabla^2 \mathbf{v} = & \left(\nabla^2 v_r - \frac{2}{r^2 \sin \theta} \left(v_r \sin \theta + \frac{\partial}{\partial \theta} (v_\theta \sin \theta) + \frac{\partial v_\phi}{\partial \phi} \right) \right) \hat{r} + \\ & + \left(\nabla^2 v_\theta - \frac{1}{r^2 \sin^2 \theta} \left(v_\theta + 2 \cos \theta \frac{\partial v_\phi}{\partial \phi} \right) + \frac{2}{r^2} \frac{\partial v_r}{\partial \theta} \right) \hat{\theta} + \\ & + \left(\nabla^2 v_\phi + \frac{2}{r^2 \sin^2 \theta} \left(\cos \theta \frac{\partial v_\theta}{\partial \phi} + \frac{\partial v_r}{\partial \phi} - \frac{v_\phi}{2} \right) \right) \hat{\phi}. \quad (\text{A.14})\end{aligned}$$

The gradient of a vector field \mathbf{v} is:

$$(\nabla \mathbf{v})_{ij} = \begin{pmatrix} (\nabla \mathbf{v})_{rr} & (\nabla \mathbf{s})_{r\theta} & (\nabla \mathbf{v})_{r\phi} \\ (\nabla \mathbf{v})_{\theta r} & (\nabla \mathbf{v})_{\theta\theta} & (\nabla \mathbf{v})_{\theta\phi} \\ (\nabla \mathbf{v})_{\phi r} & (\nabla \mathbf{v})_{\phi\theta} & (\nabla \mathbf{v})_{\phi\phi} \end{pmatrix}, \quad \text{where} \quad (\text{A.15})$$

$$\begin{aligned}(\nabla \mathbf{v})_{rr} &= \frac{\partial v_r}{\partial r}, & (\nabla \mathbf{v})_{r\theta} &= \frac{\partial v_\theta}{\partial r}, \\ (\nabla \mathbf{v})_{r\phi} &= \frac{\partial v_\phi}{\partial r}, & (\nabla \mathbf{v})_{\theta r} &= \frac{1}{r} \left(\frac{\partial v_r}{\partial \theta} - v_\theta \right), \\ (\nabla \mathbf{v})_{\theta\theta} &= \frac{1}{r} \left(v_r + \frac{\partial v_\theta}{\partial \theta} \right), & (\nabla \mathbf{v})_{\theta\phi} &= \frac{1}{r} \frac{\partial v_\phi}{\partial \theta}, \\ (\nabla \mathbf{v})_{\phi r} &= \frac{1}{r \sin \theta} \left(\frac{\partial v_r}{\partial \phi} - v_\phi \sin \theta \right), & (\nabla \mathbf{v})_{\phi\theta} &= \frac{1}{r \sin \theta} \left(\frac{\partial v_\theta}{\partial \phi} - v_\phi \cos \theta \right), \\ (\nabla \mathbf{v})_{\phi\phi} &= \frac{1}{r \sin \theta} \left(v_r \sin \theta + v_\theta \cos \theta + \frac{\partial v_\phi}{\partial \phi} \right).\end{aligned}$$

The divergence of a second order tensor \mathbf{T} is, in components:

$$\begin{aligned}(\nabla \cdot \mathbf{T})_r &= \frac{\partial T_{rr}}{\partial r} + \\ & + \frac{1}{r} \left(\frac{\partial T_{\theta r}}{\partial \theta} + \csc \theta \frac{\partial T_{\phi r}}{\partial \phi} + 2T_{rr} + \cot \theta T_{\theta r} - T_{\theta\theta} - T_{\phi\phi} \right), \quad (\text{A.16})\end{aligned}$$

$$\begin{aligned}(\nabla \cdot \mathbf{T})_\theta &= \frac{\partial T_{r\theta}}{\partial r} + \\ & + \frac{1}{r} \left(\frac{\partial T_{\theta\theta}}{\partial \theta} + \csc \theta \frac{\partial T_{\phi\theta}}{\partial \phi} + 2T_{r\theta} + T_{\theta r} + \cot \theta (T_{\theta\theta} - T_{\phi\phi}) \right), \quad (\text{A.17})\end{aligned}$$

$$\begin{aligned}(\nabla \cdot \mathbf{T})_\phi &= \frac{\partial T_{r\phi}}{\partial r} + \\ & + \frac{1}{r} \left(\frac{\partial T_{\theta\phi}}{\partial \theta} + \csc \theta \frac{\partial T_{\phi\phi}}{\partial \phi} + 2T_{r\phi} + T_{\phi r} + \cot \theta (T_{\theta\phi} + T_{\phi\theta}) \right). \quad (\text{A.18})\end{aligned}$$

Appendix B

Spherical harmonics

Spherical harmonics are the angular part of a set of solutions of the Laplace equation. They are defined by:

$$Y_\ell^m(\theta, \phi) = (-)^m \sqrt{\frac{(2\ell + 1)(\ell - m)!}{4\pi(\ell + m)!}} P_\ell^m(\cos \theta) e^{im\phi}, \quad (\text{B.1})$$

where $P_\ell^m(x)$ are the associated Legendre functions:

$$P_\ell^m(x) = \frac{1}{2^\ell \ell!} (1 - x^2)^{m/2} \frac{d^{\ell+m}}{dx^{\ell+m}} (x^2 - 1)^\ell. \quad (\text{B.2})$$

Spherical harmonics form a complete set of orthonormal functions on the unit sphere. Square integrable functions f on the unit sphere are hence expressible as a linear combination of spherical harmonics Y_ℓ^m . Hence for a function $f(\theta, \phi)$ it holds that

$$f(\theta, \phi) = \sum_{\ell=0}^{\infty} \sum_{m=-\ell}^{\ell} F_\ell^m Y_\ell^m(\theta, \phi), \quad (\text{B.3})$$

where F_ℓ^m are the expansion coefficients. Spherical harmonics obey the following identity:

$$\hat{\nabla}_1^2 Y_\ell^m(\theta, \phi) = -\ell(\ell + 1) Y_\ell^m(\theta, \phi), \quad (\text{B.4})$$

where

$$\hat{\nabla}_1^2 = \partial_\theta^2 + \cot \theta \partial_\theta + \csc^2 \theta \partial_\phi^2, \quad (\text{B.5})$$

is the surface Laplacian on the unit sphere.

Vector spherical harmonics are an extension of spherical harmonics to use for expansion of vector fields $\mathbf{v}(\theta, \phi)$.

$$\mathbf{v} = \hat{r} V_1 + \hat{\nabla}_1 V_2 - \hat{r} \times \hat{\nabla}_1 V_3, \quad (\text{B.6})$$

where $\hat{\nabla}_1$ is the tangential derivative operator on the unit sphere:

$$\hat{\nabla}_1 = \hat{\theta} \partial_\theta + \hat{\phi} \csc \theta \partial_\phi, \quad (\text{B.7})$$

and V_1 , V_2 and V_3 are given by:

$$V_1 = \sum_{\ell=0}^{\infty} \sum_{m=-\ell}^{\ell} V_{1,\ell}^m Y_\ell^m(\theta, \phi), \quad (\text{B.8})$$

$$V_2 = \sum_{\ell=0}^{\infty} \sum_{m=-\ell}^{\ell} V_{2,\ell}^m Y_\ell^m(\theta, \phi), \quad (\text{B.9})$$

$$V_3 = \sum_{\ell=0}^{\infty} \sum_{m=-\ell}^{\ell} V_{3,\ell}^m Y_\ell^m(\theta, \phi), \quad (\text{B.10})$$

where $V_{1,\ell}^m$, $V_{2,\ell}^m$ and $V_{3,\ell}^m$ are expansion coefficients.

Appendix C

Solutions to some differential equations

The radial part of the Laplace equation in spherical coordinate for a function $f = f(r)$ is:

$$\frac{d}{dr} \left(r^2 \frac{df}{dr} \right) = \ell(\ell + 1)f. \quad (\text{C.1})$$

By substituting $r = e^t$, the solution to this equation follows:

$$f(r) = Ar^\ell + Cr^{-\ell-1}. \quad (\text{C.2})$$

Similarly, the differential equation

$$\frac{d^2}{dr^2} (r^2 f) = \ell(\ell + 1)f, \quad (\text{C.3})$$

is also solved by substitution of $r = e^t$ and has solution

$$f(r) = Ar^{-\ell-2} + Br^{\ell-1}. \quad (\text{C.4})$$

The spherical Bessel differential equation for a function $f = f(r)$ is:

$$\left(\mathcal{L}^2 + k^2 \right) f = 0, \quad (\text{C.5})$$

With k a constant and

$$\mathcal{L}^2 = \frac{d^2}{dr^2} + \frac{2}{r} \frac{d}{dr} - \frac{\ell(\ell + 1)}{r^2}. \quad (\text{C.6})$$

The general solution of Bessel's differential equation is a linear combination of Bessel's spherical functions of the first and second kind,

$$j_\ell(x) = J_{\ell+\frac{1}{2}} \sqrt{\frac{\pi}{2x}}, \quad y_\ell(x) = Y_{\ell+\frac{1}{2}} \sqrt{\frac{\pi}{2x}}. \quad (\text{C.7})$$

where $x = kr$ and $J_\alpha(x)$ is Bessel's function of the first kind that can be defined by its Taylor series around $x = 0$:

$$J_\alpha(x) = \sum_{m=0}^{\infty} \frac{(-1)^m}{m! \Gamma(m + \alpha + 1)} \left(\frac{x}{2}\right)^{2m+\alpha}. \quad (\text{C.8})$$

The Bessel function of the second kind $Y_\alpha(x)$ is defined by:

$$Y_\alpha(x) = \frac{J_\alpha(x) \cos(\alpha\pi) - J_{-\alpha}(x)}{\sin(\alpha\pi)}. \quad (\text{C.9})$$

Hence the solution $f(x) = f_\ell(x)$ to the spherical Bessel differential equation is:

$$f(x) = C_1 j_l(x) + C_2 y_l(x), \quad (\text{C.10})$$

where C_1 and C_2 are constants. The following recurrent formulae hold for f :

$$f_{l-1}(x) + f_{l+1}(x) = \frac{2l+1}{x} f_l(x), \quad (\text{C.11})$$

$$l f_{l-1}(x) - (l+1) f_{l+1}(x) = (2l+1) \frac{df_l(x)}{dx}, \quad (\text{C.12})$$

$$\frac{d}{dx} [x^{l+1} f_l(x)] = x^{l+1} f_{l-1}(x), \quad (\text{C.13})$$

$$\frac{d}{dx} [x^{-l} f_l(x)] = -x^{-l} f_{l+1}(x). \quad (\text{C.14})$$

When solving the equations of motion for a uniform elastic sphere, a differential equation related to Bessel's spherical differential equation occurs:

$$(\mathcal{L}^2 + k_1^2) (\mathcal{L}^2 + k_2^2) g(r) = 0. \quad (\text{C.15})$$

The solution for this equation is found by using the solution to the spherical Bessel differential equation. The solution is:

$$g(r) = D_1 f(k_1 r) + D_2 f(k_2 r), \quad (\text{C.16})$$

where D_1 and D_2 are constants.

Appendix D

Eulerian and Lagrangian perturbations

If small oscillations of an object are considered, the most straightforward approach is to perturb the variables that describe the dynamics of the object around some equilibrium value and analyze the equations of motion for the perturbations of the dynamical variable up to linear order. However, there are different ways to do perturbations in continuum mechanics. Two types of perturbations are very common and they are related to the Eulerian and Lagrangian (or material) derivative that will be introduced later, in appendix F.1.1.

Consider a dynamical variable $\psi = \psi(\mathbf{x}, t)$ which is a function of position \mathbf{x} and time t . Suppose there exists an equilibrium value of ψ denoted by $\psi_0 = \psi_0(\mathbf{x})$. An Eulerian perturbation, denoted with δ , is a perturbation at a constant position \mathbf{p} in space. Hence:

$$\psi(\mathbf{p}, t) = \psi_0(\mathbf{p}) + \delta\psi(\mathbf{p}, t), \quad (\text{D.1})$$

or shorthand,

$$\psi = \psi_0 + \delta\psi. \quad (\text{D.2})$$

A Lagrangian perturbation, denoted by Δ , is a perturbation at the position of a material particle $\mathbf{x}(\mathbf{X}, t)$, located at \mathbf{X} at $t = 0$. Hence:

$$\psi(\mathbf{x}(\mathbf{X}, t), t) = \psi_0(\mathbf{X}) + \Delta\psi(\mathbf{x}(\mathbf{X}, t), t), \quad (\text{D.3})$$

or shorthand,

$$\psi = \psi_0 + \Delta\psi. \quad (\text{D.4})$$

The relation between an Eulerian and Lagrangian perturbation is found by plugging in the position of a material particle at a particular time t_p as a constant position in the equation for an Eulerian perturbation (D.1):

$$\psi(\mathbf{x}(\mathbf{X}, t_p), t_p) = \psi_0(\mathbf{x}(\mathbf{X}, t_p)) + \delta\psi(\mathbf{x}(\mathbf{X}, t_p)). \quad (\text{D.5})$$

If the displacement \mathbf{s} as defined in (G.33) is used, the first term on the right hand side has a Taylor expansion, which yields to first order in \mathbf{s} :

$$\psi_0(\mathbf{x}(\mathbf{X}, t_p)) = \psi_0(\mathbf{X}) + \mathbf{s}(\mathbf{X}, t_p) \cdot \nabla\psi_0(\mathbf{X}). \quad (\text{D.6})$$

This equation gives, in combination with equations (D.3) and (D.5), the relationship between an Eulerian and Lagrangian perturbation, to first order in \mathbf{s} , for arbitrary t :

$$\Delta\psi(\mathbf{x}(\mathbf{X}, t), t) = \delta\psi(\mathbf{x}(\mathbf{X}, t)) + \mathbf{s}(\mathbf{X}, t) \cdot \nabla\psi_0(\mathbf{X}), \quad (\text{D.7})$$

or shorthand,

$$\Delta\psi = \delta\psi + \mathbf{s} \cdot \nabla\psi_0. \quad (\text{D.8})$$

The argument presented here holds for vector or tensor valued functions ψ as well.

Appendix E

Gravity

In this study, gravitational effects are analyzed in Newtonian gravity and general relativity. This appendix gives a short recapitulation of the important equations in both gravitational theories.

E.1 Newtonian gravity

Newton's inverse square law of gravitation states that for two objects with mass m and M and a separation distance r , the mutual attractive force F_g is given by

$$F_g = \frac{GMm}{r^2}, \quad (\text{E.1})$$

where G is the gravitational constant. Since gravity is a conservative force, a potential φ exists, such that the negative gradient of the potential gives the gravitational acceleration. It follows that Newton's inverse square law is equivalent to the following differential equation for the gravitational potential $\varphi = \varphi(x)$ at a point x :

$$\nabla^2 \varphi = 4\pi G \varrho, \quad (\text{E.2})$$

where $\varrho = \varrho(x)$ is the density at x .

E.2 General relativity

It is not the objective of this section to give a review of general relativity. Some concepts that are used in this thesis are recapitulated.

E.2.1 World lines and proper time

The proper time τ that passes on a clock that travels through spacetime with metric $g_{\mu\nu}$ depends on the trajectory of the clock \mathbf{x} through four-dimensional spacetime parameterized by λ . Proper time is defined by:

$$\tau = \int_{\lambda_1}^{\lambda_2} \sum_{\mu,\nu} \sqrt{g_{\mu\nu} \frac{dx^\mu}{d\lambda} \frac{dx^\nu}{d\lambda}} d\lambda. \quad (\text{E.3})$$

Hence the history of each object traces a curve in four dimensional spacetime. This curve is called a worldline and can also be parameterized by τ .

E.2.2 Four-velocity

The four-velocity \mathbf{u} is a tangent vector to a worldline. More specifically, it is defined as:

$$\mathbf{u} = \frac{d\mathbf{x}}{d\tau}. \quad (\text{E.4})$$

The magnitude of the four-velocity is always equal to the speed of light:

$$\sum_{\mu} u_{\mu} u^{\mu} = c^2. \quad (\text{E.5})$$

E.2.3 Covariant derivative

When manifolds, or more specifically curved spacetimes or curvilinear coordinate systems such as the spherical coordinate system are considered, the partial derivative does not behave as a tensor and it turns out to be convenient to introduce a differential operator that does behave as a tensor. The covariant derivative, denoted by a subscript semicolon, has this property and occurs frequently in general relativity.

It is not within the scope of this appendix to give an explanation of the concept of a covariant derivative. Instead, the definitions used in this study will be stated. More detailed explanations can be found in books on general relativity or differential geometry. Its definition, when applied to a vector \mathbf{v} , is:

$$v^\alpha{}_{;\beta} = \partial_\beta v^\alpha + \sum_\gamma \Gamma^\alpha{}_{\beta\gamma} v^\gamma, \quad (\text{E.6})$$

where $\Gamma^\alpha{}_{\beta\gamma}$ are the Christoffel symbols, defined by:

$$\Gamma^\alpha{}_{\beta\gamma} = \sum_\delta \frac{g^{\alpha\delta}}{2} \left(\frac{\partial g_{\delta\beta}}{\partial x^\gamma} + \frac{\partial g_{\delta\gamma}}{\partial x^\beta} - \frac{\partial g_{\beta\gamma}}{\partial x^\delta} \right), \quad (\text{E.7})$$

where $g^{\alpha\delta}$ is the inverse of the metric $g_{\alpha\delta}$. The covariant derivative, applied to a covector \mathbf{w} is:

$$w_{\alpha;\beta} = \partial_\beta w_\alpha - \sum_\gamma \Gamma^\gamma{}_{\alpha\beta} w_\gamma. \quad (\text{E.8})$$

When applied to a scalar function, the covariant derivative reduces to the partial derivative. It follows that the divergence of a vector \mathbf{v} is:

$$\sum_\mu v^\mu{}_{;\mu} = \sum_\mu \frac{1}{\sqrt{-\|g\|}} \partial_\mu \left(\sqrt{-\|g\|} v^\mu \right), \quad (\text{E.9})$$

where $\|g\|$ is the determinant of the metric. When applied to a general tensor \mathbf{T} , the covariant derivative is:

$$\begin{aligned} T^{a_1 \dots a_r}{}_{b_1 \dots b_s;c} &= \frac{\partial}{\partial x^c} T^{a_1 \dots a_r}{}_{b_1 \dots b_s} + \sum_d \left\{ \Gamma^{a_1}{}_{dc} T^{d \dots a_r}{}_{b_1 \dots b_s} + \dots + \right. \\ &+ \Gamma^{a_r}{}_{dc} T^{a_1 \dots a_{r-1}d}{}_{b_1 \dots b_s} - \Gamma^d{}_{b_1c} T^{a_1 \dots a_r}{}_{d \dots b_s} - \dots \\ &\left. - \Gamma^d{}_{b_sc} T^{a_1 \dots a_r}{}_{b_1 \dots b_{s-1}d} \right\}. \quad (\text{E.10}) \end{aligned}$$

E.2.4 Curvature and Einstein field equations

The Einstein field equations are a set of ten equations that relate the curvature at a point in spacetime to the energy and momentum in that point. The solutions to the Einstein field equations are given by the components $g_{\alpha\beta}$ of the metric tensor. The Einstein field equations can be stated as:

$$R_{\alpha\beta} - \frac{1}{2} g_{\alpha\beta} R = \frac{8\pi G}{c^4} T_{\alpha\beta}, \quad (\text{E.11})$$

where $R_{\alpha\beta}$ is the Ricci curvature tensor

$$R_{\alpha\beta} = \sum_{\rho} [\partial_{\rho} \Gamma_{\beta\alpha}^{\rho} - \partial_{\beta} \Gamma_{\rho\alpha}^{\rho}] + \sum_{\rho,\lambda} [\Gamma_{\rho\lambda}^{\rho} \Gamma_{\beta\alpha}^{\lambda} - \Gamma_{\beta\lambda}^{\rho} \Gamma_{\rho\alpha}^{\lambda}], \quad (\text{E.12})$$

and R is the Ricci scalar, which is the trace of the Ricci curvature tensor:

$$R = \sum_{\alpha} R^{\alpha}_{\alpha} = \sum_{\alpha,\beta} g^{\alpha\beta} R_{\alpha\beta}. \quad (\text{E.13})$$

The left hand side of the Einstein field equations expresses the curvature of spacetime. The right hand side of the Einstein field equations is given by the stress-energy tensor, which gives the density and flux of energy and momentum at a given point in spacetime.

E.2.5 Spherically symmetric metric

Some analytical solutions to the Einstein field equations exist for spacetimes that exhibit symmetry. The most general metric for a spherically symmetric spacetime is:

$$ds^2 = e^{2\nu} c^2 dt^2 - e^{2\lambda} dr^2 - r^2 (d\theta^2 + \sin^2 \theta d\phi^2), \quad (\text{E.14})$$

By solving the Einstein field equations for a metric of this form, the solution for the parameters λ and ν are found for spherically symmetric stellar models. In the case the Einstein field equations are solved for a vacuum, it follows that the unique solution is given by the Schwarzschild metric:

$$ds^2 = \left(1 - \frac{2GM}{rc^2}\right) dt^2 - \left(1 - \frac{2GM}{rc^2}\right)^{-1} dr^2 - r^2 (d\theta^2 + \sin^2 \theta d\phi^2), \quad (\text{E.15})$$

where M is the mass of an object located at the center of the spherically symmetric spacetime. The result that this is an unique solution to the Einstein field equations is also known as Birkhoff's theorem.

E.2.6 Conservation of energy-momentum

It can be shown that the divergence of the left hand side of the Einstein field equations is zero. This follows from the so-called Bianchi identities. This leads to the following conservation law for energy-momentum:

$$\sum_{\nu} T_{\mu;\nu}^{\nu} = 0. \quad (\text{E.16})$$

Appendix F

Fluid mechanics

Fluid mechanics is a branch in physics concerned with the static, kinematic and dynamic behaviour of fluids and gases. Fluid statics studies the properties of fluids at rest. Fluid kinematics is concerned with the behaviour of fluid in motion and fluid dynamics is the study of the effect of forces on a fluid.

F.1 Nonrelativistic fluid mechanics

Like any other scientific theory, fluid mechanics explains the behaviour of nature in a certain domain of validity that is constrained by the foundational assumptions of the theory. In fluid mechanics, there are four basic assumptions:

1. The continuum hypothesis. The continuum hypothesis requires matter to be continuous, that is: parameters as the density, fluid velocity or temperature vary continuously throughout the material. The fact that matter consists of discrete molecules is ignored. This assumption is typically valid if the typical length scale of the problem is much larger than the mean free path length of the molecules of which the fluid consists.
2. Mass conservation.
3. Newton's Second Law, or momentum conservation.
4. The First Law of Thermodynamics, or energy conservation.

Sometimes one or two additional assumptions are made:

5. No internal friction in the fluid: Inviscid flow.
6. Incompressibility.

From assumptions (1–5), a number of fundamental equations for a so called perfect fluid follow. These equations are due to Euler (1757). Assumption (5) leads to adiabatic flow, since if internal friction is absent, no heat exchange occurs. If assumption (5) is dropped and a viscous mechanism is assumed where viscous forces are proportional to the gradient of the velocity field, a more general set of equations is obtained, which is due to Navier (1823). Throughout this thesis, inviscid fluids are assumed. Sometimes the assumption of incompressibility will also be made. This appendix will give a review on the concepts of fluid mechanics that are relevant to understand stellar oscillations. Equations of motion for continuous fluid systems are derived.

F.1.1 Material derivative

Consider a scalar function $\psi(\mathbf{x}, t)$, where \mathbf{x} is the position and t is time. The (total) derivative of ψ with respect to time is:

$$\frac{d\psi}{dt} = \frac{\partial\psi}{\partial t} + \frac{d\mathbf{x}}{dt} \cdot \nabla\psi \quad (\text{F.1})$$

Two different choices for the position \mathbf{x} are commonly used. The first is a constant position. Then the total derivative reduces to a partial derivative. In the context of fluid mechanics, this is called the Eulerian derivative. The second is the position of a fluid parcel $\mathbf{x}(t)$. In this case the derivative (F.1) reduces to the material derivative or Lagrangian derivative, denoted with a capital D and $d\mathbf{x}/dt$ becomes the fluid velocity \mathbf{v} :

$$\frac{D\psi}{Dt} = \frac{\partial\psi}{\partial t} + \mathbf{v} \cdot \nabla\psi \quad (\text{F.2})$$

This concept can be illustrated by the following example. Imagine yourself floating in a lake, very early in the morning. There are currents in the lake, but you are safely attached to a rope that is fixed at the bottom of the lake, hence you stand completely still. The water is still cold, but the sun starts to heat it. You feel that the temperature of the water is rising. The change in temperature in this case is given by the Eulerian derivative of the temperature function at your fixed position. Now suppose the next morning you are in for more adventure. You cut yourself

loose from the rope and now you are moving along with the currents in the lake. Again the temperature in the lake is rising, but now you notice another change on top of this effect. The currents have moved you in a very warm and pleasant part of the lake that is heated by geothermal energy. The change in temperature is in this case given by the material or Lagrangian derivative. The material derivative gives the change of a function along the trajectory of a fluid parcel.

F.1.2 Reynolds' transport theorem

Take an arbitrary volume V in a fluid. The boundary of this volume ∂V moves along with the fluid, hence both V and ∂V are functions of time. Now take the volumetric density q of some arbitrary quantity Q in the fluid. The rate of change of the total amount of Q in V is given by:

$$\frac{dQ}{dt} = \frac{d}{dt} \int_{V(t)} q dV = \int_{V(t)} \frac{\partial q}{\partial t} dV + \int_{\partial V(t)} q \mathbf{v} \cdot \hat{\mathbf{n}} dS. \quad (\text{F.3})$$

The first term is the change in Q due to local changes of the density distribution in time. The second is the change due to flux through ∂V . Gauss' theorem is applied on the second term on the left hand side of the equation, yielding:

$$\frac{dQ}{dt} = \frac{d}{dt} \int_{V(t)} q dV = \int_{V(t)} \left\{ \frac{\partial q}{\partial t} + \nabla \cdot (q \mathbf{v}) \right\} dV. \quad (\text{F.4})$$

This is called Reynolds' transport theorem. In fact, there is no restriction on what kind of quantity Q might be. It can be a scalar, vector or arbitrary tensor.

This result can also be illustrated by an example. Consider a fishing net that encloses a certain volume of water in the ocean and flows along with the ocean current. A certain type of algae lives in the ocean. To calculate the change in the number of algae in the net, two effects have to be considered. The first one is that the algae may die or multiply within the net, which causes a change in the local algae density. This is the effect that is calculated in the first term on the right hand side of equation (F.3). The second effect is that algae may 'swim' in or out the net, hence the total algae flux needs to be integrated over the net, which corresponds to the second term on the right hand side of equation (F.3).

F.1.3 Mass conservation and incompressibility

The assumption of mass conservation postulates that the material derivative of the total mass M within $V(t)$ is zero. Hence:

$$\frac{dM}{dt} = \frac{d}{dt} \int_{V(t)} \varrho dV = 0, \quad (\text{F.5})$$

where $\varrho = \varrho(\mathbf{x}, t)$ is the density of the fluid. Reynolds' transport theorem directly yields for mass conservation:

$$\int_{V(t)} \left\{ \frac{\partial \varrho}{\partial t} + \nabla \cdot (\varrho \mathbf{v}) \right\} dV = 0. \quad (\text{F.6})$$

Since this holds for any comoving volume the integrand must be zero, hence:

$$\frac{\partial \varrho}{\partial t} + \nabla \cdot (\varrho \mathbf{v}) = 0. \quad (\text{F.7})$$

This equation is called the *continuity equation*. If incompressibility is assumed, the material derivative of the density is zero, since the density of a fluid parcel followed along the flow will remain unchanged. Hence:

$$\frac{D\varrho}{Dt} = \frac{\partial \varrho}{\partial t} + \mathbf{v} \cdot \nabla \varrho = 0. \quad (\text{F.8})$$

Combined with equation (F.7), this yields:

$$\nabla \cdot \mathbf{v} = 0. \quad (\text{F.9})$$

Hence for incompressible fluids, the divergence of the velocity field is zero.

F.1.4 Alternate form of Reynolds' transport theorem

If mass conservation is assumed, Reynolds' transport theorem can be recast in an alternate form. Redefine q in equation (F.3) in the following way:

$$q = \varrho \chi. \quad (\text{F.10})$$

Here, χ is the density per unit mass (rather than per unit volume) of some quantity. Using the continuity equation (F.7) in the previous form of Reynolds' transport theorem (F.4) the alternate form follows:

$$\frac{dQ}{dt} = \frac{d}{dt} \int_{V(t)} \varrho \chi dV = \int_{V(t)} \varrho \frac{D\chi}{Dt} dV. \quad (\text{F.11})$$

It is clear that in this formulation, mass conservation is assumed, because $\chi = 1$ implies $Q = M$ and gives a zero right hand side of equation (F.11).

F.1.5 Momentum equation

Newton's second law for a fluid parcel is:

$$\sum F = \frac{d\mathbf{p}}{dt} = \frac{d}{dt} \int_{V(t)} \varrho \mathbf{v} dV, \quad (\text{F.12})$$

where the left hand side contains the sum of all forces acting on the fluid parcel contained in $V(t)$. The momentum of the fluid parcel is given by \mathbf{p} . The left hand side of the equation can consist of two types of forces. The first type is called a *surface force*, which is a force acting on the boundary of the surface $\partial V(t)$. The second type of force is called a *body force*, which acts on all particles in $V(t)$. In standard fluid dynamics, the surface force is given by pressure and the body force is given by gravity. Of course, different forces can be considered as well. For example, if the fluid is conducting, electromagnetic body forces need to be considered as well, leading to the magnetohydrodynamic (MHD) equations. This is a relevant concept in theoretical astrophysics. However, in this thesis only pressure and gravity are considered. Then Newton's second law (F.12) becomes:

$$\frac{d}{dt} \int_{V(t)} \varrho \mathbf{v} dV = - \int_{\partial V(t)} p dS - \int_{V(t)} \varrho \nabla \varphi dV. \quad (\text{F.13})$$

The pressure term has a negative sign because pressure works in the inward direction on the fluid parcel, hence the direction of the force is opposite to the direction of the normal vector on the surface. The gravity term also has a minus sign, because the gravitational acceleration has been written as minus the gradient of the gravitational potential φ . Gauss' theorem on the first term on the right hand side in combination with the alternate form of Reynolds' transport theorem (F.11) on the left hand side yields:

$$\int_{V(t)} \left\{ \varrho \frac{D\mathbf{v}}{Dt} + \nabla p + \varrho \nabla \varphi \right\} dV = 0 \quad (\text{F.14})$$

This equation is for an arbitrary volume $V(t)$ hence the integrand must be zero. Explicitly using expression (F.2) for the material derivative then yields:

$$\varrho \left(\frac{\partial \mathbf{v}}{\partial t} + (\mathbf{v} \cdot \nabla) \mathbf{v} \right) = -\nabla p - \varrho \nabla \varphi. \quad (\text{F.15})$$

This is the form of the momentum equation that is used for fluids in this study.

F.2 Relativistic fluid mechanics

For relativistic calculations of stellar dynamical equilibrium configurations and oscillations, a relativistic analogue of fluid mechanics is needed. This appendix gives a short review. In this appendix, the covariant derivative denoted by a semicolon is used, which is defined in equation (E.10).

F.2.1 Law of Baryon conservation

Unlike in nonrelativistic fluid mechanics, mass is no longer necessarily conserved in the relativistic context. Mass and energy are equivalent, which means mass is convertible into energy, violating mass conservation. However, a more fundamental conservation law exists, which is the law of baryon conservation:

$$\frac{dn}{d\tau} = -n \sum_{\mu} u^{\mu}{}_{;\mu}, \quad (\text{F.16})$$

where n is the baryon number density and \mathbf{u} is the velocity field in the continuum.

F.2.2 Relativistic Euler equation

Analogously to the nonrelativistic case, where equations of motion for fluids are found by considering momentum conservation, in the relativistic case equations of motion for relativistic fluids are found by using the law of conservation of energy-momentum (E.16), applied on the stress-energy tensor for a perfect fluid, which is:

$$T_{\alpha\beta} = \left(\varrho + \frac{P}{c^2}\right) u_{\alpha} u_{\beta} - P g_{\alpha\beta}, \quad (\text{F.17})$$

in which P is the pressure of the perfect fluid and ϱ is the rest frame mass density. Conservation of energy-momentum $\sum_{\mu} T^{\mu\nu}{}_{;\mu} = 0$ gives:

$$\sum_{\mu} \left\{ (\partial_{\mu} \varrho) u^{\mu} u^{\nu} + \varrho (u^{\mu}{}_{;\mu}) u^{\nu} + \varrho u^{\mu} u^{\nu}{}_{;\mu} + (\partial_{\mu} P) \frac{u^{\mu} u^{\nu}}{c^2} + \right. \\ \left. + \frac{P}{c^2} (u^{\mu}{}_{;\mu}) u^{\nu} + \frac{P}{c^2} u^{\mu} u^{\nu}{}_{;\mu} - \partial_{\mu} P g^{\mu\nu} \right\} = 0. \quad (\text{F.18})$$

After recollecting terms, it is found that:

$$\sum_{\mu} (\varrho + \frac{P}{c^2}) u^{\mu} u^{\nu}{}_{;\mu} = \partial^{\nu} P - \sum_{\mu} \left[(\varrho + \frac{P}{c^2}) (u^{\mu}{}_{;\mu}) u^{\nu} + (\partial_{\mu} P) \frac{u^{\mu} u^{\nu}}{c^2} + (\partial_{\mu} \varrho) u^{\mu} u^{\nu} \right]. \quad (\text{F.19})$$

By taking the inner product with u_{ν} and by recognizing that $\sum_{\mu,\nu} u_{\nu} u^{\mu} u^{\nu}{}_{;\mu} = \frac{1}{2} \sum_{\mu,\nu} u^{\mu} (u_{\nu} u^{\nu}){}_{;\mu} = 0$ because $\sum_{\mu} u_{\mu} u^{\mu} = c^2$ it is found that:

$$\sum_{\mu} \left[(\varrho + \frac{P}{c^2}) u^{\mu}{}_{;\mu} + (\partial_{\mu} \varrho) u^{\mu} \right] = \sum_{\mu} \left[(\varrho + \frac{P}{c^2}) u^{\mu}{}_{;\mu} + \frac{\partial \varrho}{\partial \tau} \right] = 0. \quad (\text{F.20})$$

Using this in equation (F.19) yields the relativistic Euler equation:

$$\sum_{\mu} (\varrho + \frac{P}{c^2}) u^{\mu} u_{\nu}{}_{;\mu} = \partial_{\nu} P - \sum_{\mu} \frac{u_{\nu} u^{\mu}}{c^2} (\partial_{\mu} P). \quad (\text{F.21})$$

Appendix G

Elasticity

Solid materials deform when stress is applied. Some materials remain permanently deformed when stress is removed, while other materials assume their original shape. For the latter category, elastic materials, internal stress due to interatomic or intermolecular forces remains present when the external stress that causes the deformation is removed. This internal stress brings the material to its original shape. Neutron stars are assumed to have a solid crust. To understand the oscillations of neutron star crusts, an understanding is needed of elastic materials. This appendix gives a short review on nonrelativistic and relativistic elasticity.

G.1 Nonrelativistic elasticity

In this section, a review of the concepts deformation, stress and the equations of motion for a solid will be given.

G.1.1 Deformation

Consider an undeformed body B contained in a volume V with surface S . The curvilinear coordinates (for example, spherical polar coordinates) in terms of which the position vector \mathbf{X} is given in the undeformed body, are given by $\{X^K\}$, where $K = 1, 2, 3$. Each vector \mathbf{X} labels a unique material point. Therefore, $\{X^K\}$ are usually called *material coordinates*. The body is deformed into a body b with volume v and surface s . The deformation is a function of time t . In the deformed

body, the position \mathbf{x} is expressed in curvilinear coordinates $\{x^k\}$, where $k = 1, 2, 3$. These coordinates are usually called *spatial coordinates*. The deformation can be seen as a mapping from B to b taking a material point \mathbf{X} in the undeformed body to different positions \mathbf{x} in the deformed body as a function of t . Another, equivalent, perspective is that at each point \mathbf{x} different material points \mathbf{X} are passing by as a function of t .

$$\mathbf{X} = \mathbf{X}(\mathbf{x}, t), \quad \mathbf{x} = \mathbf{x}(\mathbf{X}, t). \quad (\text{G.1})$$

It is demanded that the mapping is continuously differentiable and that the Jacobian determinant of the mapping j is not zero, which, by using the inverse function theorem, implies that the mapping has an inverse.

$$j = \det \frac{\partial \mathbf{x}}{\partial \mathbf{X}} \neq 0. \quad (\text{G.2})$$

Physically, this prohibits deformations in which two different points are deformed into a single point. Also, the motion is impenetrable. This means that for example crack formation, kinking or tearing of the material cannot be described by this mapping.

Capital letters will always be used to indicate that a given quantity is considered in the undeformed body, while lowercase letters will be used for quantities in the deformed body. The same holds for the indices used to denote vector or tensor components, where capital letters indicate that the component is with respect to basis vectors in the material coordinate frame. Lower-case letters indicate that the component is with respect to basis vectors in the spatial coordinate frame.

Since curvilinear coordinates have basis vectors which in general depend on the position, it is convenient to express positions \mathbf{X} in B and \mathbf{x} in b in Cartesian coordinates $\{Y^K\}$ and $\{y^k\}$ as well, because Cartesian basis vectors are constant:

$$\mathbf{X} = \sum_K Y^K \hat{\mathbf{e}}_K, \quad \mathbf{x} = \sum_k y^k \hat{\mathbf{e}}_k, \quad (\text{G.3})$$

where $\hat{\mathbf{e}}_K$ and $\hat{\mathbf{e}}_k$ are unit base vectors for the Cartesian coordinate systems of the deformed and undeformed body. Just like in a Cartesian coordinate system, the base vectors in a curvilinear coordinate system are defined to be a tangent vector to a coordinate line. Using the notion of Cartesian coordinates, base vectors in the curvilinear coordinate system $\mathbf{G}_K(\mathbf{X})$ and $\mathbf{g}_k(\mathbf{x})$ are:

$$\mathbf{G}_K(\mathbf{X}) = \frac{\partial \mathbf{X}}{\partial X^K} = \sum_M \frac{\partial Y^M}{\partial X^K} \hat{\mathbf{e}}_M, \quad \mathbf{g}_k(\mathbf{x}) = \frac{\partial \mathbf{x}}{\partial x^k} = \sum_m \frac{\partial y^m}{\partial x^k} \hat{\mathbf{e}}_m. \quad (\text{G.4})$$

The notion of these base vectors will aid in the definition of a metric tensor. Consider a differential $d\mathbf{X}$ at point \mathbf{X} and $d\mathbf{x}$ at point \mathbf{x} :

$$d\mathbf{X} = \sum_K \frac{\partial \mathbf{X}}{\partial X^K} dX^K = \sum_K \mathbf{G}_K dX^K, \quad d\mathbf{x} = \sum_k \frac{\partial \mathbf{x}}{\partial x^k} dx^k = \sum_k \mathbf{g}_k dx^k. \quad (\text{G.5})$$

The square infinitesimal lengths dS^2 and ds^2 are the scalar product of the vectors $d\mathbf{X}$ and $d\mathbf{x}$ respectively:

$$dS^2 = d\mathbf{X} \cdot d\mathbf{X} = \sum_{K,L} G_{KL} dX^K dX^L, \quad ds^2 = d\mathbf{x} \cdot d\mathbf{x} = \sum_{k,l} g_{kl} dx^k dx^l, \quad (\text{G.6})$$

where G_{KL} and g_{kl} are metric tensors, defined as:

$$G_{KL}(\mathbf{X}) = \mathbf{G}_K \cdot \mathbf{G}_L = \sum_{M,N} \frac{\partial Y^M}{\partial X^K} \frac{\partial Y^N}{\partial X^L} \delta_{MN}, \quad (\text{G.7})$$

$$g_{kl}(\mathbf{x}) = \mathbf{g}_k \cdot \mathbf{g}_l = \sum_{m,n} \frac{\partial y^m}{\partial x^k} \frac{\partial y^n}{\partial x^l} \delta_{mn}, \quad (\text{G.8})$$

where δ is the Kronecker delta symbol. Metric G measures distances in the undeformed body. Metric g does this in the deformed body. *Reciprocal base vectors* \mathbf{G}^K and \mathbf{g}^k are defined by equations

$$\mathbf{G}^K \cdot \mathbf{G}_L = \delta_L^K, \quad \mathbf{g}^k \cdot \mathbf{g}_l = \delta_l^k. \quad (\text{G.9})$$

The solution of these equations is of the following form

$$\mathbf{G}^K = G^{KL} \mathbf{G}_L, \quad \mathbf{g}^k = g^{kl} \mathbf{g}_l, \quad (\text{G.10})$$

where G^{KL} and g^{kl} are the inverses of G_{KL} and g_{kl} respectively. The tensors g and G can be used to define a way to raise and lower indices of tensor components by using equations (G.10). For example, take a vector \mathbf{p} :

$$\mathbf{p} = \sum_k p^k \mathbf{g}_k(\mathbf{x}) = \sum_{k,l} p^k g_{kl} \mathbf{g}^l(\mathbf{x}) \equiv \sum_l p_l \mathbf{g}^l(\mathbf{x}). \quad (\text{G.11})$$

Hence

$$p_l \equiv \sum_k p^k g_{kl}. \quad (\text{G.12})$$

This definition is generalized, such that contraction with the metric tensor can raise and lower indices of any vector or tensor.

Up until now, no way has been introduced to project vectors or tensors from B to b and vice versa. However, it is in physical situations necessary to project vectors and tensors from the undeformed state into the deformed state and vice versa. Therefore, shift vector \mathbf{p} located at \mathbf{x} to point \mathbf{X} . If p^K are the components of the shifted vector \mathbf{p} expressed in curvilinear basis vectors \mathbf{G}_K at \mathbf{X} , then

$$\mathbf{p} = p^K \mathbf{G}_K(\mathbf{X}) = p^k \mathbf{g}_k(\mathbf{x}). \quad (\text{G.13})$$

Taking the scalar product with \mathbf{G}^L and \mathbf{g}^l yields

$$p^K = \sum_k g_k^K p^k, \quad p^k = \sum_K g_K^k p^K, \quad (\text{G.14})$$

where

$$g_k^K(\mathbf{X}, \mathbf{x}) = \mathbf{G}^K(\mathbf{X}) \cdot \mathbf{g}_k(\mathbf{x}), \quad g_K^k(\mathbf{X}, \mathbf{x}) = \mathbf{g}^k(\mathbf{x}) \cdot \mathbf{G}_K(\mathbf{X}), \quad (\text{G.15})$$

are two-point tensors, i.e. tensors which transform as a tensor with respect to X^K and x^k for the tensor indices K and k . These tensors project a vector in the deformed coordinate space into the undeformed coordinate space and vice versa. In the same manner, other forms of the two-point tensor g are possible. For example:

$$g_{Kk}(\mathbf{X}, \mathbf{x}) = g_{kK}(\mathbf{X}, \mathbf{x}) = \mathbf{g}_k(\mathbf{x}) \cdot \mathbf{G}_K(\mathbf{X}), \quad (\text{G.16})$$

$$g^{Kk}(\mathbf{X}, \mathbf{x}) = g^{kK}(\mathbf{X}, \mathbf{x}) = \mathbf{g}^k(\mathbf{x}) \cdot \mathbf{G}^K(\mathbf{X}), \quad (\text{G.17})$$

These tensors also lower or raise indices, but on top of that, lower-case indices are replaced by capital indices and vice versa.

G.1.2 Deformation gradient

Until now, no way has been introduced to compare the difference in distance between two material points during deformation. The first step to find the way to do this, is to consider the relationship between differentials $d\mathbf{x}$ and $d\mathbf{X}$:

$$dx^k = \sum_K \frac{\partial x^k}{\partial X^K} dX^K, \quad (\text{G.18})$$

$$dX^K = \sum_k \frac{\partial X^K}{\partial x^k} dx^k. \quad (\text{G.19})$$

The tensor $F_K^k \equiv \frac{\partial x^k}{\partial X^K}$ is called the *deformation gradient* tensor. Because of demand (G.2) this tensor has an inverse $(F^{-1})_k^K = \frac{\partial X^K}{\partial x^k}$. Explicitly, this inverse is given by:

$$\frac{\partial X^K}{\partial x^k} = \frac{1}{2j} e^{KLM} e_{klm} \frac{\partial x^l}{\partial X^L} \frac{\partial x^m}{\partial X^M}, \quad (\text{G.20})$$

where e_{klm} and e^{KLM} are Levi-Civita symbols. Using the deformation gradient tensor in equation (G.6) alternative expressions for differential length in the undeformed and deformed state of the material follow:

$$dS^2 = \sum_{k,l} c_{kl}(\mathbf{x}, t) dx^k dx^l, \quad ds^2 = \sum_{K,L} C_{KL}(\mathbf{X}, t) dX^K dX^L, \quad (\text{G.21})$$

in which the differential length in the undeformed state is given as a function of the position in the deformed state and vice versa, which makes comparison between the deformed and undeformed state possible. In these expressions c and C are given by

$$c_{kl}(\mathbf{x}, t) = \sum_{K,L} G_{KL}(\mathbf{X}(\mathbf{x}, t)) \frac{\partial X^K}{\partial x^k} \frac{\partial X^L}{\partial x^l} \quad (\text{G.22})$$

$$C_{KL}(\mathbf{X}, t) = \sum_{k,l} g_{kl}(\mathbf{x}(\mathbf{X}, t)) \frac{\partial x^k}{\partial X^K} \frac{\partial x^l}{\partial X^L} \quad (\text{G.23})$$

Because of the symmetry of G and g , tensors C and c are symmetric as well.

New base vectors in the deformed state are defined as follows:

$$\mathbf{c}_k(\mathbf{x}, t) = \frac{\partial \mathbf{X}}{\partial x^k} = \sum_K \frac{\partial \mathbf{X}}{\partial X^K} \frac{\partial X^K}{\partial x^k} = \sum_K \mathbf{G}_K(\mathbf{X}(\mathbf{x}, t)) \frac{\partial X^K}{\partial x^k} \quad (\text{G.24})$$

$$\mathbf{C}_K(\mathbf{X}, t) = \frac{\partial \mathbf{x}}{\partial X^K} = \sum_k \frac{\partial \mathbf{x}}{\partial x^k} \frac{\partial x^k}{\partial X^K} = \sum_k \mathbf{g}_k(\mathbf{x}(\mathbf{X}, t)) \frac{\partial x^k}{\partial X^K} \quad (\text{G.25})$$

These base vectors are defined such, that differentials $d\mathbf{X}$ and $d\mathbf{x}$ can be expressed in terms of dx^k and dX^K respectively. Hence:

$$d\mathbf{X} = \sum_k \mathbf{c}_k dx^k \quad (\text{G.26})$$

$$d\mathbf{x} = \sum_K \mathbf{C}_K dX^K \quad (\text{G.27})$$

Also, it follows that $c_{kl} = \mathbf{c}_k \cdot \mathbf{c}_l$ and $C_{KL} = \mathbf{C}_K \cdot \mathbf{C}_L$.

Infinitesimal distances dS and ds are now expressed in spatial and material coordinates respectively:

$$dS^2 = \sum_{K,L} G_{KL}(\mathbf{X}) dX^K dX^L = \sum_{k,l} c_{kl}(\mathbf{x}, t) dx^k dx^l \quad (\text{G.28})$$

$$ds^2 = \sum_{k,l} g_{kl}(\mathbf{x}) dx^k dx^l = \sum_{K,L} C_{KL}(\mathbf{X}, t) dX^K dX^L \quad (\text{G.29})$$

Hence c can be seen as a metric tensor, giving the length in the undeformed state of an infinitesimal line element in the deformed state. Similarly C gives the length in the deformed state of an infinitesimal line element in the undeformed state.

G.1.3 Strain

The Lagrangian strain tensor E and Eulerian strain tensor e are defined as:

$$E_{KL} = \frac{1}{2} [C_{KL}(\mathbf{X}, t) - G_{KL}(\mathbf{X})], \quad (\text{G.30})$$

$$e_{kl} = \frac{1}{2} [g_{kl}(\mathbf{x}) - c_{kl}(\mathbf{x}, t)]. \quad (\text{G.31})$$

These expressions, combined with (G.28) and (G.29) yield the following important relation:

$$ds^2 - dS^2 = 2 \sum_{K,L} E_{KL}(\mathbf{X}, t) dX^K dX^L = 2 \sum_{k,l} e_{kl}(\mathbf{x}, t) dx^k dx^l. \quad (\text{G.32})$$

Deformation in a material is characterized by a change in distance between arbitrary points in a material. The strain tensor fully characterizes such changes in distance, because it determines $ds^2 - dS^2$. Hence it gives a measure of deformation of the body.

Instead of using the metric tensor, the strain tensors can also be expressed in terms of the displacement vector \mathbf{s} , which is defined as:

$$\mathbf{s} = \mathbf{x} - \mathbf{X} + \mathbf{b}, \quad (\text{G.33})$$

where \mathbf{b} is a vector connecting the origin of the material coordinate frame $\{X^K\}$ with the origin of the spatial coordinate frame $\{x^k\}$. The displacement vector \mathbf{s} can be represented in material or spatial vector components,

$$\mathbf{s} = \sum_K S^K \mathbf{G}_K = \sum_k s^k \mathbf{g}_k. \quad (\text{G.34})$$

The Lagrangian strain tensor in terms of the displacement vector is:

$$\begin{aligned}
E_{KL} &= \frac{1}{2} \left(\sum_{k,l} g_{kl} \frac{\partial x^k}{\partial X^K} \frac{\partial x^l}{\partial X^L} - G_{KL} \right), \\
&= \frac{1}{2} \left(\frac{\partial \mathbf{x}}{\partial X^K} \cdot \frac{\partial \mathbf{x}}{\partial X^L} - G_{KL} \right), \\
&= \frac{1}{2} \left(\left(\frac{\partial \mathbf{s}}{\partial X^K} + \mathbf{G}_K \right) \cdot \left(\frac{\partial \mathbf{s}}{\partial X^L} + \mathbf{G}_L \right) - G_{KL} \right), \\
&= \frac{1}{2} \left(S_{K;L} + S_{L;K} + \sum_M S_{M;K} S_{M;L} \right), \tag{G.35}
\end{aligned}$$

where $\partial \mathbf{s} / \partial X^K = \sum_M S_{M;K} \mathbf{G}^M$ and the semi-colon indicates a covariant derivative, defined in appendix E.2.3. For curvilinear coordinates, the covariant derivative arises because the derivative of curvilinear basis vectors is nonzero. Below, the argument is given for curvilinear basisvector \mathbf{g}_k , but the argument also holds for basisvector \mathbf{G}_K .

$$\frac{\partial \mathbf{g}_k}{\partial x^l} = \frac{\partial}{\partial x^l} \left(\frac{\partial \mathbf{x}}{\partial x^k} \right) = \sum_m \frac{\partial^2 y^m}{\partial x^k \partial x^l} \hat{\mathbf{e}}_m. \tag{G.36}$$

The Cartesian unit vector $\hat{\mathbf{e}}_m$ is expressed in terms of the curvilinear unit vector \mathbf{g}_k by inverting relation (G.4). This leads to:

$$\sum_m \frac{\partial^2 y^m}{\partial x^l \partial x^k} \hat{\mathbf{e}}_m = \sum_{n,m} \frac{\partial^2 y^m}{\partial x^k \partial x^l} \frac{\partial x_n}{\partial y^m} \hat{\mathbf{g}}_n. \tag{G.37}$$

By using equation (G.8), it is found that:

$$\frac{\partial \mathbf{g}_k}{\partial x^l} = \sum_m \Gamma^m_{kl} \mathbf{g}_m, \tag{G.38}$$

where Γ^m_{kl} are the Christoffel symbols defined by (E.7). The Eulerian strain tensor is derived and expressed in a similar way as the Lagrangian strain tensor:

$$e_{kl} = \frac{1}{2} \left(s_{k;l} + s_{l;k} - \sum_m s_{m;k} s^m_{;l} \right). \tag{G.39}$$

G.1.4 Stress

As was discussed earlier, two type of forces exist that act on a continuum: body forces and surface forces. In an inviscid fluid, the surface force is given in terms

of a scalar field: the pressure field. Consequently, the pressure force in the fluid is independent of the orientation of the surface in the fluid, on which the pressure force acts. However, if the fluid is viscous, or if elastic materials are considered, the material can withstand shear forces. Therefore more general surface forces need to be considered, which depend on the orientation of the surface, on which the force acts.

The surface force per unit area in the deformed body will be denoted by the stress vector $\mathbf{t}_{(\mathbf{n})}$, where \mathbf{n} denotes the normal vector on the surface on which the force acts. The stress vector which acts on the k th coordinate surface is denoted by \mathbf{t}_k , its l th component will be denoted by t_{kl} , a matrix representation of the *stress tensor*:

$$\mathbf{t}_k = t_{kl} \mathbf{g}^l \quad (\text{G.40})$$

The relationship between the stress vector $\mathbf{t}_{(\mathbf{n})}$ and the matrix representation of the stress tensor t_{kl} is found by using the condition of mechanical equilibrium of an infinitesimal tetrahedron, of which three sides are parallel to coordinate surfaces and one side has normal vector \mathbf{n} . Analysis of this so-called *Cauchy tetrahedron* leads to:

$$\mathbf{t}_{(\mathbf{n})} = \sum_{k,l} t_{kl} n^k \mathbf{g}^l, \quad (\text{G.41})$$

in which n^k are the components of the unit normal vector on the surface. Moreover, conservation of angular momentum leads to the fact that the stress tensor is symmetric. Hence a symmetric, second order stress tensor fully describes the state of stress of the material, since it can give the stress vector acting on any surface.

G.1.5 Momentum equation for an elastic solid

Compared to the case of an inviscid fluid, the equations of motion for an elastic material are qualitatively the same. The continuity equation (F.7) still holds, since, compared to a fluid, mass is still conserved in exactly the same way. However, some changes need to be taken into account in the momentum equation (F.15). The term representing surface force changes. In the case of an elastic material, the pressure term in momentum equation (F.13) needs to be replaced with a term containing the stress vector integrated over the surface. The following, more general equation is obtained:

$$\frac{d}{dt} \int_{V(t)} \rho \mathbf{v} dV = \int_{\partial V(t)} \mathbf{t}_{(\mathbf{n})} dS - \int_{V(t)} \rho \nabla \varphi dV. \quad (\text{G.42})$$

Using Gauss' theorem, generalized for a second order tensor field, on the first term on the right hand side gives

$$\frac{d}{dt} \int_{V(t)} \varrho \mathbf{v} dV = \int_{V(t)} \nabla \cdot \mathbf{t} dV - \int_{V(t)} \varrho \nabla \varphi dV, \quad (\text{G.43})$$

where $\mathbf{t} = t_{kl} \mathbf{g}^k \mathbf{g}^l$ is the second order stress tensor and $\mathbf{t}_{(n)} = \mathbf{t} \cdot \mathbf{n}$. Applying the alternate form of Reynolds' theorem on the first term, yields:

$$\int_{V(t)} \varrho \frac{D\mathbf{v}}{Dt} dV = \int_{V(t)} \nabla \cdot \mathbf{t} dV - \int_{V(t)} \varrho \nabla \varphi dV, \quad (\text{G.44})$$

Since this equation holds for an arbitrary volume, the equation also holds for the integrands. Hence, the momentum equation for an elastic body is:

$$\varrho \left(\frac{\partial \mathbf{v}}{\partial t} + (\mathbf{v} \cdot \nabla) \mathbf{v} \right) = \nabla \cdot \mathbf{t} - \varrho \nabla \varphi. \quad (\text{G.45})$$

This is the form of the momentum equation that will be used for elastic solids in the remainder of this thesis.

G.1.6 Isotropic linear elasticity

In linearly elastic materials, the Lagrangian perturbation of the stress tensor is linearly related to the deformation. This is a good approximation if small deformations are considered, and the linear approximation is precise enough. The most general linear relation between the Lagrangian perturbation of the stress tensor $\Delta \mathbf{t}$ and strain tensor \mathbf{e} is given through a fourth order elasticity tensor \mathbf{c} :

$$(\Delta t)_{ij} = \sum_{k,l} c_{ij}{}^{kl} e_{kl}, \quad (\text{G.46})$$

where the linearized strain tensor e_{kl} is found from equation (G.39) and given by:

$$e_{kl} = \frac{1}{2} (s_{k;l} + s_{l;k}). \quad (\text{G.47})$$

Since \mathbf{c} is a fourth order tensor, it has $3^4 = 81$ components. In an isotropic elastic medium, the elasticity tensor has no preferential direction: regardless of the orientation of the medium, a certain amount of applied stress will always give the same strain. If such a medium is considered, the number of independent components reduces to two (Jeffreys and Jeffreys, 1956). The elasticity tensor then takes the form:

$$c_{ijkl} = \kappa \delta_{ij} \delta_{kl} + \mu (\delta_{ik} \delta_{jl} + \delta_{il} \delta_{jk} - \frac{2}{3} \delta_{ij} \delta_{kl}), \quad (\text{G.48})$$

where κ is the bulk modulus, which measures resistance against compression and μ is the shear modulus, which measures resistance against shear forces. When this form of the elasticity tensor is used, the relation between the Lagrangian stress perturbation and the displacement \mathbf{s} takes the form:

$$\Delta \mathbf{t} = 2\mu \mathbf{e} + \left(\kappa - \frac{2\mu}{3} \right) \Theta \mathbf{I}, \quad (\text{G.49})$$

where Θ is the trace of the linearized strain tensor \mathbf{e} and \mathbf{I} is the identity matrix.

G.2 Relativistic elasticity

For a linearly elastic solid, the stress-energy tensor is more general than the tensor (F.17) for a fluid. Since in an elastic solid, shear stress can be present, the stress-energy tensor has an added term Σ , which is the shear tensor (Schumaker and Thorne, 1983). This leads to the stress-energy tensor for an elastic solid:

$$T_{\alpha\beta} = \left(\varrho_0 + \frac{P_0}{c^2} \right) u_\alpha u_\beta - P_0 g_{\alpha\beta} + 2\mu \Sigma_{\alpha\beta}. \quad (\text{G.50})$$

The shear tensor as a function of the displacement is found by using the general relativistic formulation of linear elasticity, which is formulated by Carter and Quintana (1972). The linear approximation of the shear tensor is calculated from:

$$\Sigma_{\mu\nu} = e^\nu \int_0^t \sigma_{\mu\nu} dt', \quad (\text{G.51})$$

where $\sigma_{\mu\nu}$ is the rate of shear, defined as:

$$\sigma_{\mu\nu} = \frac{1}{2} \sum_\alpha \left(P_\mu^\alpha u_{\nu;\alpha} + P_\nu^\alpha u_{\mu;\alpha} \right) - \frac{1}{3} \sum_\alpha P_{\mu\nu} u^\alpha{}_{;\alpha}, \quad (\text{G.52})$$

where the projection tensor $P_{\mu\nu}$ is defined as

$$P_{\mu\nu} = g_{\mu\nu} - u_\mu u_\nu / c^2. \quad (\text{G.53})$$

The relativistic Euler equation is then found by adding an extra term due to elastic effects to the relativistic Euler equation (F.21) for a fluid. This leads to:

$$\sum_\mu (\varrho + p) u^\mu u_{\nu;\mu} = \partial_\nu P - \sum_\mu u_\nu u^\mu (\partial_\mu P) - \sum_\mu (2\mu \Sigma_\nu^\mu{}_{;\mu}). \quad (\text{G.54})$$